frontiers | Research Topics

Low-temperature plasma for biomedical applications

Edited by
Mounir Laroussi, Michael Keidar and Vladimir I. Kolobov

Published in
Frontiers in Physics

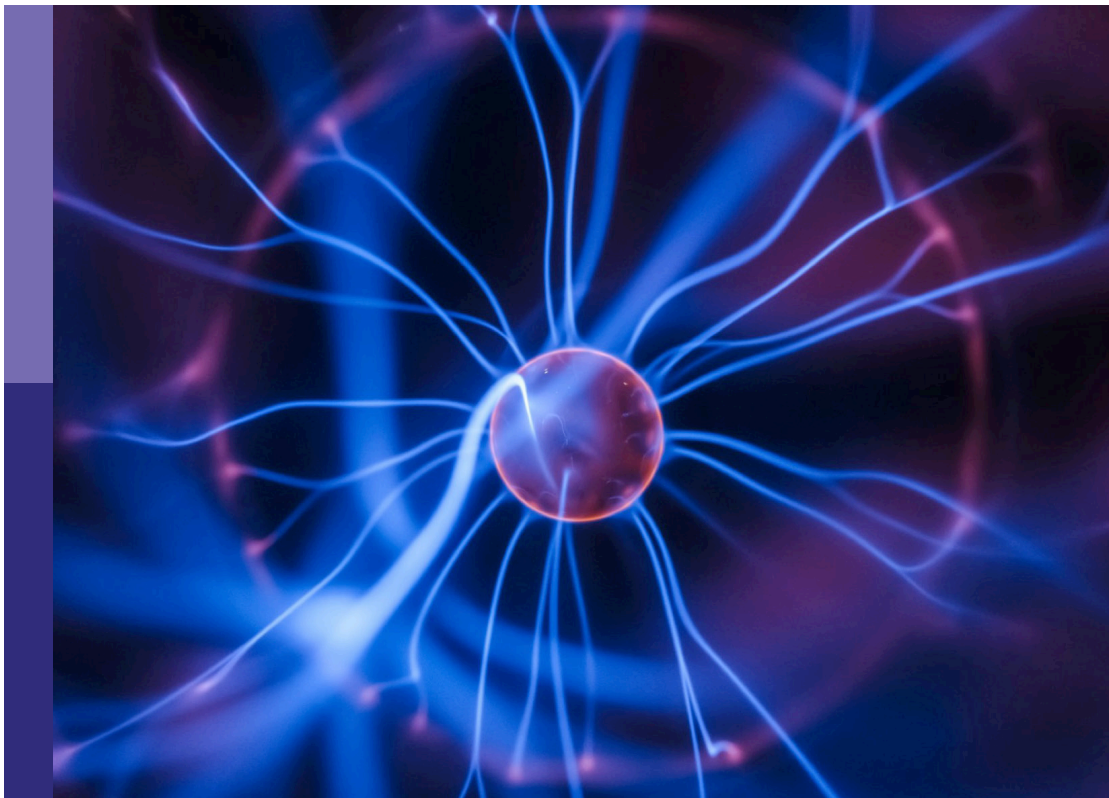

ISSN 1664-8714
ISBN 978-2-8325-3874-6
DOI 10.3389/978-2-8325-3874-6

About Frontiers

Frontiers is more than just an open access publisher of scholarly articles: it is a pioneering approach to the world of academia, radically improving the way scholarly research is managed. The grand vision of Frontiers is a world where all people have an equal opportunity to seek, share and generate knowledge. Frontiers provides immediate and permanent online open access to all its publications, but this alone is not enough to realize our grand goals.

Frontiers journal series

The Frontiers journal series is a multi-tier and interdisciplinary set of open-access, online journals, promising a paradigm shift from the current review, selection and dissemination processes in academic publishing. All Frontiers journals are driven by researchers for researchers; therefore, they constitute a service to the scholarly community. At the same time, the *Frontiers journal series* operates on a revolutionary invention, the tiered publishing system, initially addressing specific communities of scholars, and gradually climbing up to broader public understanding, thus serving the interests of the lay society, too.

Dedication to quality

Each Frontiers article is a landmark of the highest quality, thanks to genuinely collaborative interactions between authors and review editors, who include some of the world's best academicians. Research must be certified by peers before entering a stream of knowledge that may eventually reach the public - and shape society; therefore, Frontiers only applies the most rigorous and unbiased reviews. Frontiers revolutionizes research publishing by freely delivering the most outstanding research, evaluated with no bias from both the academic and social point of view. By applying the most advanced information technologies, Frontiers is catapulting scholarly publishing into a new generation.

What are Frontiers Research Topics?

Frontiers Research Topics are very popular trademarks of the *Frontiers journals series*: they are collections of at least ten articles, all centered on a particular subject. With their unique mix of varied contributions from Original Research to Review Articles, Frontiers Research Topics unify the most influential researchers, the latest key findings and historical advances in a hot research area.

Find out more on how to host your own Frontiers Research Topic or contribute to one as an author by contacting the Frontiers editorial office: frontiersin.org/about/contact

Low-temperature plasma for biomedical applications

Topic editors

Mounir Laroussi — Old Dominion University, United States
Michael Keidar — George Washington University, United States
Vladimir I. Kolobov — CFD Research Corporation, United States

Citation

Laroussi, M., Keidar, M., Kolobov, V. I., eds. (2023). *Low-temperature plasma for biomedical applications*. Lausanne: Frontiers Media SA.
doi: 10.3389/978-2-8325-3874-6

Table of contents

frontiers in Physics

MINI REVIEW
published: 20 March 2020
doi: 10.3389/fphy.2020.00074

Cold Plasma in Medicine and Healthcare: The New Frontier in Low Temperature Plasma Applications

*Mounir Laroussi**

Electrical and Computer Engineering Department, Old Dominion University, Norfolk, VA, United States

Low temperature plasmas that can be generated at atmospheric pressure and at temperatures below 40°C have in the past couple of decades opened up a new frontier in plasma applications: biomedical applications. These plasma sources produce agents, such as reactive species (radicals and non-radicals), charged particles, photons, and electric fields, which have impactful biological effects. Investigators have been busy elucidating the physical and biochemical mechanisms whereby low temperature plasma affects biological cells on macroscopic and microscopic scales. A thorough understanding of these mechanisms is bound to lead to the development of novel plasma-based medical therapies. This mini review introduces the reader to this exciting multidisciplinary field of research.

Keywords: plasma discharge, cold plasma, plasma jet, plasma medicine, cells, tissues, bacteria, cancer

OPEN ACCESS

Edited by:
Gianpiero Colonna,
Italian National Research Council, Italy

Reviewed by:
Milan Simek,
Institute of Plasma Physics (ASCR), Czechia
Kazuo Takahashi,
Kyoto Institute of Technology, Japan

***Correspondence:**
Mounir Laroussi
mlarouss@odu.edu

Specialty section:
This article was submitted to Plasma Physics, a section of the journal Frontiers in Physics

Received: *19 January 2020*
Accepted: *03 March 2020*
Published: *20 March 2020*

Citation:
Laroussi M (2020) Cold Plasma in Medicine and Healthcare: The New Frontier in Low Temperature Plasma Applications. Front. Phys. 8:74. doi: 10.3389/fphy.2020.00074

INTRODUCTION

Plasma medicine is about using low temperature atmospheric pressure plasmas to generate controllable amounts of specific chemically reactive species that are transported to react with biological targets including cells and tissues. The remarkable achievement of this plasma application is that it took only about 25 years to take it from initial discovery, to fundamental scientific investigation stage, and finally to applications on actual patients. How did this happen in a relatively short time? A brief answer to this question is that although the field started in a rather modest and unexpected way, it did not take long for the plasma physics community to realize its great potential and its revolutionary promise. This was accentuated by the recruitment of health science experts (biochemists, microbiologists, etc.) who joined the various research endeavors and greatly advanced the ongoing research. Up until the present the mechanisms of action of plasma on cells and tissues are still not fully understood but the body of knowledge has been steadily growing and our understanding has expanded significantly to include a relatively good grasp on the physical and biochemical pathways whereby plasma impacts biological matter.

The field started in the mid-1990s by few proof of principle experiments which showed that low temperature plasma (LTP) possesses efficient bactericidal property [1–5]. It was realized from the very beginning that the reactive species generated by LTP, which include reactive oxygen species (ROS) and reactive nitrogen species (RNS) played a pivotal role in the observed biological outcomes [1, 6]. It also became quickly apparent that LTP can not only be used to inactivate pathogens, such as bacteria, on abiotic surfaces but it can also be used to disinfect biological tissues and therefore can be employed for wound healing. In due time these early bold ideas, backed by some preliminary experimental data, resonated strongly within the LTP research community, which by then (around 2005) realized what these new, promising but not fully explored applications meant and joined

this emerging research field in droves. Consequently, advances and new milestones were reached at relatively "break neck" speed, and by the beginning of the second decade of the 2000s clinical trials on chronic wounds were conducted with some success [7]. In addition small doses of LTP were found to selectively kill cancer cells without harming healthy ones. This opened up another research avenue sometimes referred to as "plasma oncology." Investigators from research labs around the world reported promising *in vitro* and *in vivo* results on the killing of various cancer cell lines (see review [8] and references therein). The cell lines included those associated with leukemia, carcinoma, breast cancer, brain cancer, prostate cancer, colorectal cancer, etc. [8]. In addition, more recently, cold plasma was used in Germany in limited preliminary trials as a palliative therapy for head and neck cancer patients [9]. The above described various efforts finally culminated in the US Food & Drug Administration (FDA) approval of the first clinical trials in the USA in 2019. This constitutes yet another major milestone for the efforts to develop novel LTP-based cancer therapies.

In this mini review, descriptions of LTP sources used in plasma medicine is first given, then some major medical applications are briefly described.

COLD ATMOSPHERIC PRESSURE PLASMA SOURCES

Two types of plasma discharges have been used extensively in biomedical applications: The dielectric barrier discharge (DBD) and the non-equilibrium atmospheric pressure plasma jet (N-APPJ). **Figure 1** illustrates two photographs showing a DBD ignited in argon gas (left photo) and the plasma plume emanating from a N-APPJ operated with helium (right photo).

Dielectric Barrier Discharge (DBD)

Dielectric Barrier Discharges are ideal for the generation of large volume non-equilibrium atmospheric pressure diffuse plasma. Extensive investigations allowed for a good understanding and improvement of their operation [10–23]. DBDs use a dielectric material, such as glass or alumina, to cover at least one of the electrodes. The electrodes are driven by high AC voltages in the kV range and at frequencies in the kHz. Plasmas generated by DBDs have been used for ozone generation, for material surface modification, as flow control actuators, etc. DBDs most recent domain of application has been in biomedicine after their successful early use in the mid-1990s to inactivate bacteria [1]. Today they are used in various biomedical applications including wound healing and the destruction of cancer cells and tumors [24–27].

Sinusoidal voltages with amplitudes in the kV range and frequencies of few the kHz were originally used to power DBDs. However, since the early 2000s it was found that repetitive high voltage short pulses (ns - μs) offered a more efficient way to enhance the chemistry of such discharges [28–30]. DBDs are able to maintain the non-equilibrium state of the plasma due surface charge accumulation on the dielectric surface as soon as a discharge is ignited. This creates an electrical potential that counteracts the externally applied voltage and results in a self-limited pulsed current waveform.

The electron energy distribution function (EEDF) defines/controls the chemistry in the plasma. Short repetitive high voltage pulses allow for preferential heating of the electrons population and therefore an increase of ionization and excitation [29]. Pulses with widths less than the characteristic time of the onset of the glow-to-arc transition maintain stable non-equilibrium low temperature plasma [29, 30].

To extend the operating frequency range below the kHz few methods were proposed. For example, Okazaki and co-workers used a dielectric wire mesh electrode to generate a discharge at a frequency of 50 Hz [16]. Laroussi and co-workers used a high resistivity layer/film to cover one of the electrodes in a device they referred to as the Resistive Barrier Discharge (RBD) [31]. The RBD can be operated with low frequencies extending all the way to DC. The film barrier usually has a resistivity of few MΩ.cm. The high resistivity film plays the role of a distributed resistive ballast which inhibits the discharge from localizing and the current from reaching high values.

Non-equilibrium Atmospheric Pressure Plasma Jets (N-APPJ)

Although plasma jets were previously employed for material processing applications [32, 33] biotolerant plasma jets developed specifically for plasma medicine have been in use only since the mid-2000s [34, 35]. These jets can emit low temperature plasma plumes in the surrounding air. Because they can maintain

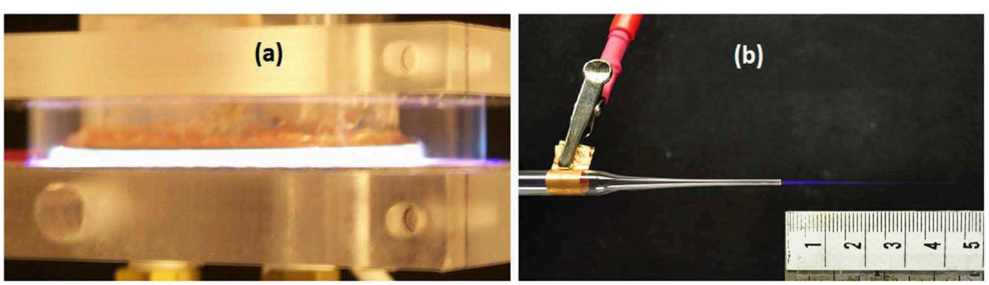

FIGURE 1 | Two sources of low temperature atmospheric pressure plasma: Dielectric Barrier Discharge in argon driven by repetitive short duration (ns - μs) high voltage pulses **(a)**; A micro-jet using helium as operating gas, generating a cold plasma plume about 2.5 cm in length **(b)**.

temperatures below 40°C, they can come in touch with soft matter, including biological tissues, without causing thermal damage. These plasma sources proved to be very useful for various applications including biomedical applications [26, 34, 35]. Because the plasma propagates away from the high voltage electrodes and into a region free from high voltage the plasma does not cause electrical shock/damage to the target cells or tissues. However, the plasma plume does exhibit a very high instantaneous and local electric field at its tip. This field plays a role in the propagation of the plasma plume and can also affect the treated target.

Investigators discovered that the plasma plumes generated by N-APPJs are not continuous volumes of plasma but discrete plasma packets/bullets propagating at high velocities, up to 10^5 m/s [36, 37]. The mechanisms governing the generation and propagation of these plasma bullets were reported by both experimental and modeling investigations [38–49]. A photoionization model was proposed by Lu and Laroussi who first investigated the dynamics of the plasma bullet [37]. Further investigations also showed that the high electrical field at the head of the plume plays a role in the propagation process. The average strength of this electric field was experimentally measured to be in the 10–30 kV/cm range [50–52].

The low temperature plasma sources described above produce chemically reactive species including reactive oxygen species (ROS) and reactive nitrogen species (RNS), which are known from redox biology to play important biological roles [53]. Other agents generated by these plasma sources are also suspected to play active roles in biological applications. These include charges particles (electrons and ions), UV and VUV radiation, and electric fields. For example the electric field can cause electroporation of cell membranes, allowing molecules (including ROS and RNS) to enter the cells and cause damage to the cell's internal organelles (including mitochondria) and macromolecules such as lipids, proteins, and DNA. To learn more about the physics and design of LTP sources the reader is referred to the following references [23, 27, 54–57].

APPLICATIONS OF COLD PLASMA IN BIOLOGY AND MEDICINE

The early groundbreaking experiments using low temperature atmospheric pressure plasma for biomedical applications were conducted in a decade spanning from 1995 to 2004 [1–6, 58–60]. The earliest experiments involved the use of dielectric barrier discharge to inactivate bacteria on surfaces and in liquids [1, 58] and to generate pulsed plasma in saline solutions for surgical applications [61, 62]. Works on using cold plasma for the disinfection of wounds, enhancement of proliferation of fibroblasts, and cell detachment soon followed [25, 59, 60]. Eventually these seminal works attracted the interest of the low temperature plasma research community and the field witnessed a substantial growth in the years following 2005 and until the present. Applications in wound healing, dentistry, cancer treatment, etc. have since then been pursued in various laboratories and research centers around the world leading to a remarkable increase in the number of journal manuscripts on the topic and to the publication of several books [63–66].

The ability of cold atmospheric plasma to inactivate bacteria recently gained more relevance because modern society has been facing several serious healthcare challenges. Amongst these are: (1) Antibiotic resistant strains of bacteria such as Methicillin Resistant Staphylococcus aureus (MRSA) and Clostridium difficile (C-diff) are sources of hospital acquired infection (HAI), which can be fatal to patients with a compromised immune system; (2) Chronic wounds, such as diabetic ulcers, do not heal easily or at all, and one of the problems is the high level of infection caused by a spectrum of bacteria. The inability of conventional methods to satisfactorily deal with these problems necessitated the need for novel approaches based on new technologies. Cold atmospheric plasma has been shown to effectively inactivate bacteria such as MRSA and to greatly reduce the bioburden in infected chronic wounds, making it a very attractive technology that can be used to help overcome the challenges listed above. In 2010, the first clinical trials on the treatment of chronic wounds with cold atmospheric plasma took place and yielded encouraging results [7]. Today there are several plasma devices on the market which have been licensed as medical instruments and which can be used in medicine, including the treatment of various dermatological diseases.

LTP can be applied in two different ways. The first is what is referred to as "direct" exposure. In this mode of application the plasma comes in direct contact with the biological target and therefore all plasma-produced agents act on the cells/tissues. The second mode is what is referred to as "indirect" exposure. In this case only the afterglow of the plasma is used or the plasma is first used to activate a liquid medium then the plasma-activated liquid is applied on top of cells/tissues. One of the advantages of the latter is that the plasma activated liquid (PAL) can be stored and used at a later time, giving a degree of flexibility that direct exposure does not offer.

Direct Exposure

As mentioned earlier under direct exposure the biological target is subjected to all plasma agents including charged particles, photons, electric field, and reactive species. These agents act alone and/or in synergy to produce certain biological outcomes. In the case of bacteria inactivation, all the above agents were reported to play a role. Lysing of vegetative cells as well spores were reported after direct exposure to LTP, but cell death without lysis was reported as well for gram-positive bacteria [67, 68].

The inactivation of bacteria by LTP has several applications ranging from sterilization of heat sensitive medical tools, to the destruction of biofilms, to disinfection of wounds, to decontamination of liquids, food, and agricultural products.

Direct exposure has also been used in a non-lethal way to affect eukaryotic cell functions, by modulating cell signaling pathways [69], and in a lethal way for the destruction of cancer cells and tumors [70–74]. Experiments using various cell lines have been reported which showed that under a certain exposure dose LTP can kill cancer cells in a selective manner [70–74]. Investigators reported that LTP exposure leads to an increase in intracellular ROS concentrations. Since cancer cells are under high oxidative

stress, the increase in ROS leads to severe redox imbalance, which can lead to one or more of the following: DNA damage, mitochondrial dysfunction, caspase activation, advanced state of oxidation of proteins, etc. Such acute stress ultimately leads to cancer cells death.

Indirect Exposure

In this section we limit the discussion to the case of plasma activated liquids (PAL). In this mode of exposure only long lived chemical species that diffuse and solvate into the aqueous state play a role. This eliminates the effects of photons, electric field, short lived species, and heat. Liquids that have been used include water to make plasma activated water (PAW) and biological culture media to make plasma activated media (PAM). The following discussion focuses on the use of PAM to destroy cancer cells. Over the past few years investigators have reported encouraging results on the use of PAM *in vitro* and *in vivo* to kill cancer cells and reduce tumors [75–81]. The anticancer characteristic of PAM has been attributed to the long lived species produced in the liquid phase after LTP exposure. These species include hydrogen peroxide, H_2O_2, nitrite, NO_2^-, nitrate, NO_3^-, peroxynitrite, $ONOO^-$, and organic radicals.

The making of PAM involves the exposure of a liquid medium to an LTP source, most frequently the plasma plume of a plasma jet, for a certain length of time. Media used include Eagle's Minimum Essential Medium (EMEM), Dulbecco's Modified Eagle Medium (DMEM), Ringer's Lactate solution (RL), Roswell Park Memorial Institute medium (RPMI), with additives such as serum (e.g., bovine serum), glutamine, and antibiotics (e.g., mix of Penicillin/Streptomycin). As an example of producing PAM, a 24-well plate can be used where a few ml of fresh cell culture media is added to each well. Each well can be treated by LTP for a certain length of time, this way producing different PAMs with different "strengths." To illustrate the effects of PAM on cancer cells the following work done at the author's laboratory is summarized [81].

In this experiment, to make PAM, 1 ml of fresh cell culture media (MEM) was added to each well of a 24 well plate. Each well was exposed to the plume of the plasma pencil (a pulsed plasma jet) for a designated time. After exposure, the media on top of cells grown in a 96-well plate was replaced by 100 μl of PAM. After PAM application, cells were stored at 37°C in a humidified incubator with 5% CO_2. Media not exposed by LTP was used for the control sample. The cancer cell line used was SCaBER (ATCC® HTB3™) cell line from a urinary bladder tissue with squamous cell carcinoma. Cell viability was quantified at different times of incubations using The CellTiter 96® AQueous One Solution Cell Proliferation Assay (MTS) (Promega, Madison, MI, USA). To quantify the MTS assay results trypan blue exclusion assay was used [81]. **Figure 2** shows the results.

As can be seen in **Figure 2**, PAM that was created by longer LTP treatment times causes a greater cell kill. PAM created with an exposure time greater than 3 min induces more than 90% cell reduction. However, for the 2 min case, over time the proliferation of live cells overtakes the destruction of cells and therefore an increase in viability at 24 and 48 h was observed. To investigate the role of the reactive species in the killing of SCaBER cells measurements of hydrogen peroxide, H_2O_2, produced in PAM were made. It was found that the concentration of H_2O_2 in PAM increased with exposure time and correlated well with the reduction in cell viability of SCaBER [81]. This was in agreement with works of various investigators which have shown the key role H_2O_2 plays in the anticancer efficacy of PAM. Recently Bauer proposed the hypothesis that H_2O_2 and nitrite lead to the generation of singlet oxygen ($^1O_2$) which causes inactivation of catalase [82]. Catalase, which is normally expressed on the membrane of cancer cells, protects them from intercellular ROS/RNS signaling. With enough inactivation of catalase an influx of H_2O_2 via aquaporin occurs. Therefore the inactivation of the protective catalase causes ROS mediated signals that lead to apoptosis of malignant cells. Since healthy cells do not express catalase on their surface they are subject to an influx of ROS such as H_2O_2 or peroxynitrite. So if they are exposed to very high ROS concentrations they also can be damaged. Therefore, the applied dose of ROS/RNS has to be below a certain threshold to achieve selective killing of cancer cells.

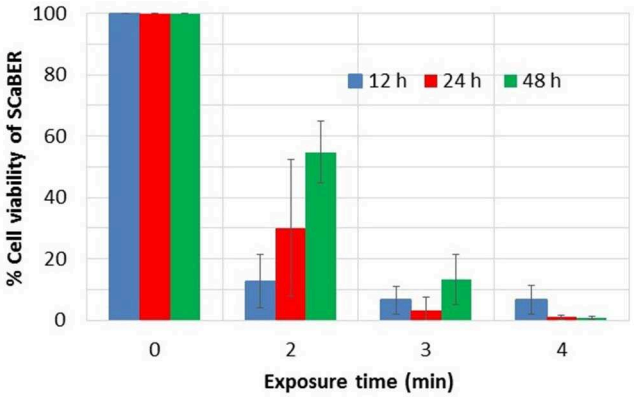

FIGURE 2 | Viability of SCaBER cells after PAM treatment, using MTS assay. Exposure time indicates the time the liquid media was exposed to plasma to make PAM. Measurements were made after 12, 24, and 48 h of PAM application. Data is based on three independent experiments using two replications each. This figure is plotted based on data previously published in Mohades et al. [81].

CONCLUSION

The application of low temperature atmospheric pressure plasma in biomedicine opened up new frontiers in science and technology. On a scientific level, new fundamental knowledge (albeit still incomplete) regarding the interaction of plasma with soft matter has been created. Before the mid-1990s basic scientific understanding of the physical and biochemical effects of plasma on cells and tissues was simply missing. Today, 25 years later and after extensive and hectic scientific investigations, our knowledge has greatly grown and many of the mechanisms involved have been elucidated on the cellular and sub-cellular levels. This allowed remarkable advances in the quest of developing novel plasma-based therapies to overcome

various healthcare challenges. The recent approval of the US Food & Drug Administration of clinical trials using plasma for cancer treatment is a critical milestone and a sign that low temperature plasma may be on its way to be accepted as a promising and exciting healthcare technology. To learn more about the future directions of the field the reader is referred to references [83, 84]. In addition, low temperature plasma has obvious merits as a viable technology for space medicine. As deep-space long-duration space travel becomes a reality it is crucial to have available adequate methods to meet medical emergencies in space. In this context plasma offers a practical "energy-based" and "dry" technology that can replace perishable drugs.

AUTHOR CONTRIBUTIONS

The author confirms being the sole contributor of this work and has approved it for publication.

REFERENCES

1. Laroussi M. Sterilization of contaminated matter with an atmospheric pressure plasma. *IEEE Trans Plasma Sci.* (1996) **24**:1188–91. doi: 10.1109/27.533129
2. Kelly-Wintenberg K, Montie TC, Brickman C, Roth JR, Carr AK, Sorge K, et al. Room temperature sterilization of surfaces and fabrics with a one atmosphere uniform glow discharge plasma. *J Indust Microbiol Biotechnol.* (1998) **20**:69–74. doi: 10.1038/sj.jim.2900482
3. Laroussi M, Saylor G, Glascock B, McCurdy B, Pearce ME, Bright NG, et al. Images of biological samples undergoing sterilization by a glow discharge at atmospheric pressure. *IEEE Trans Plasma Sci.* (1999) **27**:34–5. doi: 10.1109/27.763016
4. Herrmann HW, Henins I, Park J, Selwyn GS. Decontamination of Chemical and Biological Warfare (CBW) agents using an atmospheric pressure plasma jet. *Phys Plasmas.* (1999) **6**:2284–9. doi: 10.1063/1.873480
5. Laroussi M, Alexeff I, Kang W. Biological decontamination by non-thermal plasmas. *IEEE Trans Plasma Sci.* (2000) **28**:184–8. doi: 10.1109/27.842899
6. Laroussi M. Non-Thermal decontamination of biological media by atmospheric pressure plasmas: review, analysis, and prospects. *IEEE Trans Plasma Sci.* (2002) **30**:1409–15. doi: 10.1109/TPS.2002.804220
7. Isbary G, Morfill G, Schmidt HU, Georgi M, Ramrath K, Heinlin J, et al. A first prospective randomized controlled trial to decrease bacterial load using cold atmospheric argon plasma on chronic wounds in patients. *Br J Dermatol.* (2010) **163**:78. doi: 10.1111/j.1365-2133.2010.09744.x
8. Laroussi M. From killing bacteria to destroying cancer cells: twenty years of plasma medicine. *Plasma Process Polym.* (2014) **11**:1138–41. doi: 10.1002/ppap.201400152
9. Metelmann HR, Nedrelow DS, Seebauer C, Schuster M, von Woedtke T, Weltmann K-D, et al. Head and neck cancer treatment and physical plasma. *Clin Plasma Med.* (2015) **3**:17–23. doi: 10.1016/j.cpme.2015.02.001
10. Bartnikas R. Note on discharges in helium under AC conditions. *J Appl Phys D Appl Phys.* (1968) **1**:659. doi: 10.1088/0022-3727/1/5/417
11. Donohoe KG. *The development and characterization of an atmospheric pressure nonequilibrium plasma chemical reactor.* (Ph.D Thesis). California Institute of Technology, Pasadena, CA, United States (1976).
12. Kanazawa S, Kogoma M, Moriwaki T, Okazaki S. Stable glow at atmospheric pressure. *J Phys D Appl Phys.* (1988) **21**:838. doi: 10.1088/0022-3727/21/5/028
13. Yokoyama T, Kogoma M, Moriwaki T, Okazaki S. The mechanism of the stabilized glow plasma at atmospheric pressure. *J Phys D Appl Phys.* (1990) **23**:1128. doi: 10.1088/0022-3727/23/8/021
14. Massines F, Mayoux C, Messaoudi R, Rabehi A, Ségur P. Experimental study of an atmospheric pressure glow discharge application to polymers surface treatment. In: *Proceeding of GD-92*, Vol. 2. Swansea (1992). p. 730–3.
15. Roth JR, Laroussi M, Liu C. Experimental generation of a steady-state glow discharge at atmospheric pressure. In: *Proceeding of IEEE International Confrence Plasma Science*. Tampa, FL (1992). p. 170−1.
16. Okazaki S, Kogoma M, Uehara M, Kimura Y. Appearance of a stable glow discharge in air, argon, oxygen and nitrogen at atmospheric pressure using a 50 Hz source. *J Phys D Appl Phys.* (1993) **26**:889. doi: 10.1088/0022-3727/26/5/025
17. Massines F, Rabehi A, Decomps P, Gadri RB, Ségur P, Mayoux C. Experimental and theoretical study of a glow discharge at atmospheric pressure controled by a dielectric barrier. *J Appl Phys.* (1998) **8**:2950. doi: 10.1063/1.367051
18. Gherardi N, Gouda G, Gat E, Ricard A, Massines F. Transition from glow silent discharge to micro-discharges in nitrogen gas. *Plasma Sources Sci Technol.* (2000) **9**:340. doi: 10.1088/0963-0252/9/3/312
19. Gheradi N Massines F. Mechanisms controlling the transition from glow silent discharge to streamer discharge in nitrogen. *IEEE Trans Plasma Sci.* (2001) **29**:536. doi: 10.1109/27.928953
20. Shi JJ, Deng XT, Hall R, Punnett JD, Kong M. Three modes in a radio frequency atmospheric pressure glow discharge. *J Appl Phys.* (2003) **94**:6303. doi: 10.1063/1.1622110
21. Massines F, Gherardi N, Naude N, Segur P. Glow and townsend dielectric barrier discharge in various atmosphere. *Plasma Phys Contrl Fusion.* (2005) **47**:B557. doi: 10.1088/0741-3335/47/12B/S42
22. Kogelschatz U. Silent discharges for the generation of ultraviolet and vacuum ultraviolet excimer radiation. *Pure Appl Chem.* (1990) **62**:1667. doi: 10.1351/pac199062091667
23. Kogelschatz U, Eliasson B, Egli W. Dielectric-Barrier discharges: principle and applications. *J Physique IV.* (1997) **7**:47. doi: 10.1051/jp4:1997405
24. Fridman G, Friedman G, Gutsol A, Shekhter AB, Vasilets VN, Fridman A. Applied plasma medicine. *Plasma Process Polym.* (2008) **5**:503. doi: 10.1002/ppap.200700154
25. Laroussi M. Low temperature plasmas for medicine? *IEEE Trans Plasma Sci.* (2009) **37**:714. doi: 10.1109/TPS.2009.2017267
26. Weltmann KD, Kindel E, von Woedtke T, Hähnel M, Stieber M, Brandenburg R. Atmospheric-pressure plasma sources: prospective tools for plasma medicine. *Pure Appl Chem.* (2010) **82**:1223. doi: 10.1351/PAC-CON-09-10-35
27. Laroussi M, Lu XP, Keidar M. Perspective: the physics, diagnostics, and applications of atmospheric pressure low temperature plasma sources used in plasma medicine. *J. Appl Phys.* (2017) **122**:020901. doi: 10.1063/1.4993710
28. Mildren RP, Carman RJ. Enhanced performance of a dielectric barrier discharge lamp using short-pulsed excitation. *J Phys D Appl Phys.* (2001) **34**:3378. doi: 10.1088/0022-3727/34/1/101
29. Stark R, Schoenback KH. Electron heating in atmospheric pressure glow discharges. *J Appl Phys.* (2001) **89**:3568. doi: 10.1063/1.1351546
30. Laroussi M, Lu XP, Kolobov V, Arslanbekov R. Power consideration in the pulsed dbd at atmospheric pressure. *J Applied Phys.* (2004) **6**:3028. doi: 10.1063/1.1777392
31. Laroussi M, Alexeff I, Richardson JP, Dyer FF. The resistive barrier discharge. *IEEE Trans Plasma Sci.* (2002) **30**:158. doi: 10.1109/TPS.2002.1003972
32. Koinuma H, Ohkubo H, Hashimoto T. Development and application of a microbeam plasma generator. *Appl Phys Lett.* (1992) **60**:816. doi: 10.1063/1.106527
33. Janca J, Klima M, Slavicek P, Zajickova L. HF plasma pencil – new source for plasma surface processing. *Surf Coating Technol.* (1999) **116–119**:547–51. doi: 10.1016/S0257-8972(99)00256-X
34. Laroussi M, Lu XP. Room temperature atmospheric pressure plasma plume for biomedical applications. *Appl Phys Letts.* (2005) **87**:113902. doi: 10.1063/1.2045549
35. Laroussi M, Akan T. Arc-free atmospheric pressure cold plasma jets: a review. *Plasma Process Polym.* (2007) **4**:777–88. doi: 10.1002/ppap.200700066

36. Teschke M, Kedzierski J, Finantu-Dinu EG, Korzec D, Engemann J. High-Speed photographs of a dielectric barrier atmospheric pressure plasma jet. *IEEE Trans Plasma Sci*. (2005) **33**:310. doi: 10.1109/TPS.2005.845377
37. Lu XP, Laroussi M. Dynamics of an atmospheric pressure plasma plume generated by submicrosecond voltage pulses. *J Appl Phys*. (2006) **100**:063302. doi: 10.1063/1.2349475
38. Mericam-Bourdet N, Laroussi M, Begum A, Karakas E. Experimental investigations of plasma bullets. *J Phys D Appl Phys*. (2009) **42**:055207. doi: 10.1088/0022-3727/42/5/055207
39. Sands BL, Ganguly BN, Tachibana K. A streamer-like atmospheric pressure plasma jet. *Appl Phys Lett*. (2008) **92**:151503. doi: 10.1063/1.2909084
40. Walsh JL, Kong MG. Contrasting characteristics of linear-field and cross-field atmospheric plasma jets. *Appl Phys Lett*. (2008) **93**:111501. doi: 10.1063/1.2982497
41. Xiong Q, Lu XP, Liu J, Xian Y, Xiong Z, Zou F, et al. Temporal and spatial resolved optical emission behaviors of a cold aatmospheric pressure plasma jet. *J Appl Phys*. (2009) **106**:083302. doi: 10.1063/1.3239512
42. Karakas E, Koklu M, Laroussi M. Correlation between helium mole fraction and plasma bullet propagation in low temperature plasma jets. *J Phys D Appl Phys*. (2010) **43**:155202. doi: 10.1088/0022-3727/43/15/155202
43. Naidis GV. Modeling of plasma bullet propagation along a helium jet in ambient air. *J Phys D Appl Phys*. (2011) **44**:215203. doi: 10.1088/0022-3727/44/21/215203
44. Naidis GV. Modeling of streamer propagation in atmospheric pressure helium plasma jets. *J Phys D Appl Phys*. (2010) **43**:402001. doi: 10.1088/0022-3727/43/40/402001
45. Yousfi M, Eichwald O, Merbahi N, Jomma N. Analysis of ionization wave dynamics in low-temperature plasma jets from fluid modeling supported by experimental investigations. *Plasma Sources Sci Technol*. (2012) **21**:045003. doi: 10.1088/0963-0252/21/4/045003
46. Boeuf JP, Yang L, Pitchford L. Dynamics of guided streamer (plasma bullet) in a helium jet in air at atmospheric pressure. *J Phys D Appl Phys*. (2013) **46**:015201. doi: 10.1088/0022-3727/46/1/015201
47. Karakas E, Laroussi M. Experimental studies on the plasma bullet propagation and its inhibiton. *J Appl Phys*. (2010) **108**:063305. doi: 10.1063/1.3483935
48. Jarrige J, Laroussi M, Karakas E. Formation and dynamics of the plasma bullets in a non-thermal plasma jet: influence of the high voltage parameters on the plume characteristics. *Plasma Sources Sci Technol*. (2010) **19**:065005. doi: 10.1088/0963-0252/19/6/065005
49. Sakiyama Y, Graves DB, Jarrige J, Laroussi M. Finite element analysis of ring-shaped emission profile in plasma bullets. *Appl Phys Lett*. (2010) **96**:041501. doi: 10.1063/1.3298639
50. Begum A, Laroussi M, Pervez MR. Atmospheric pressure helium/air plasma jet: breakdown processes and propagation phenomenon. *AIP Adv*. (2013) **3**:062117. doi: 10.1063/1.4811464
51. Stretenovic GB, Krstic IB, Kovacevic VV, Obradovic AM, Kuraica MM. Spatio-temporally resolved electric field measurements in helium plasma jet. *J Phys D Appl Phys*. (2014) **47**:102001. doi: 10.1088/0022-3727/47/10/102001
52. Sobota A, Guaitella O, Garcia-Caurel E. Experimentally obtained values of electric field of an atmospheric pressure plasma jet impinging on a dielectric surface. *J Phys D Appl Phys*. (2013) **46**:372001. doi: 10.1088/0022-3727/46/37/372001
53. Lu X, Naidis GV, Laroussi M, Reuter S, Graves DB, Ostrikov K. Reactive species in non-equilibrium atmospheric pressure plasma: generation, transport, and biological effects. *Phys Rep*. (2016) **630**:1–84. doi: 10.1016/j.physrep.2016.03.003
54. Lietz, AM, Kushner MJ. Molecular admixtures and impurities in atmospheric pressure plasma jets. *J Appl Phys*. (2018) **124**:153303. doi: 10.1063/1.5049430
55. Winter J, Brandenburg R, Weltmann KD. Atmospheric pressure plasma jets: an overview of devices and new directions. *Plasma Sources Sci Technol*. (2015) **24**:054001. doi: 10.1088/0963-0252/24/6/064001
56. Becker KH, Shoenbach KH, Eden JG. Microplasmas and applications. *J Phys D Appl Phys*. (2006) **39**:R55. doi: 10.1088/0022-3727/39/3/R01
57. Lietz, AM, Kushner MJ. Electrode configurations in atmospheric pressure plasma jets: production of reactive species. *Plasma Sources Sci Technol*. (2018) **27**:105020. doi: 10.1088/1361-6595/aadf5b
58. Laroussi M. Sterilization of liquids using a plasma glow discharge. US Patent # 5,876,663 (1999).
59. Shekhter AB, Kabisov RK, Pekshev AV, Kozlov NP, Perov Yu L. Experimental and clinical validation of plasmadynamic therapy of wounds with nitric oxide. *Bull Exp Biol Med*. (1998) **126**:829–34. doi: 10.1007/BF02446923
60. Stoffels E, Flikweert AJ, Stoffels WW, Kroesen GMW. Plasma needle: a non-destructive atmospheric plasma source for fine surface treatment of biomaterials. *Plasma Sources Sci Technol*. (2002) **11**:383–88. doi: 10.1088/0963-0252/11/4/304
61. Stalder KR, Woloszko K, Brown IG, Smith CD. Repetitive plasma discharges in saline solutions. *Appl Phys Lett*. (2001) **79**:4503. doi: 10.1063/1.1429752
62. Woloszko K, Stalder KR, Brown IG. Plasma characteristics of repetitively-pulsed electrical discharges in saline solutions used for surgical procedures. *IEEE Trans Plasma Sci*. (2002) **30**:1376–83. doi: 10.1109/TPS.2002.801612
63. Laroussi M, Kong M, Morfill G, Stolz W. *Plasma Medicine: Applications of Low-Temperature Gas Plasmas in Medicine and Biology*. Cambridge: Cambridge Univ. Press. (2012).
64. Fridman A, Friedman G. *Plasma Medicine*. New York, NY: Wiley (2013).
65. Metelmann HR, von Woedtke T, Weltmann KD. *Comprehensive Clinical Plasma Medicine*. Berlin: Springer (2018).
66. Toyokuni S, Ikehara Y, Kikkawa F, Hori M. *Plasma Medical Science*. Cambridge, MA: Academic Press (2018).
67. Laroussi M, Richardson JP, Dobbs FC. Effects of non-equilibrium atmospheric pressure plasmas on the heterotrophic pathways of bacteria and on their cell morphology. *Appl Phys Lett*. (2002) **81**:772–4. doi: 10.1063/1.1494863
68. Laroussi M, Mendis DA, Rosenberg M. Plasma interaction with microbes. *N J Phys*. (2003) **5**:41.1–10. doi: 10.1088/1367-2630/5/1/341
69. Barekzi N, Laroussi M. Fibropblasts cell morphology altered by low temperature atmospheric pressure plasma. *IEEE Trans Plasma Sci*. (2014) **42**:2738. doi: 10.1109/TPS.2014.2315787
70. Keidar M, Walk R, Shashurin A, Srinivasan P, Sandler A, Dasgupta S, et al. Cold plasma selectivity and the possibility of paradigm shift in cancer therapy. *Br J Cancer*. (2011) **105**:1295. doi: 10.1038/bjc.2011.386
71. Barekzi N, Laroussi M. Effects of low temperature plasmas on cancer cells. *Plasma Process Polym*. (2013) **10**:1039. doi: 10.1002/ppap.201300083
72. Keidar M, Shashurin A, Volotskova O, Stepp MA, Srinivasan P, Sandler A, et al. Cold atmospheric plasma in cancer therapy. *Phys Plasmas*. (2013) **20**:057101. doi: 10.1063/1.4801516
73. Köritzer J, Boxhammer V, Schäfer A, Shimizu T, Klämpfl TG, Li YF, et al. Restoration of sensitivity in chemo-resistant glioma cells by cold atmospheric plasma. *PLoS ONE*. (2013) **8**:e64498. doi: 10.1371/journal.pone.0064498
74. Vandamme M, Robert E, Pesnele S, Barbosa E, Dozias S, Sobilo J, et al. Antitumor effects of plasma treatment on U87 glioma xenografts: preliminary results. *Plasma Process Polym*. (2010) **7**:264–73. doi: 10.1002/ppap.200900080
75. Tanaka H, Mizuno M, Ishikawa K, Nakamura K, Kajiyama H, Kano H, et al. Plasma-activated medium selectively kills glioblastoma brain tumor cells by down-regulating a survival signaling molecule, AKT kinase. *Plasma Med*. (2011) **1**:265. doi: 10.1615/PlasmaMed.2012006275
76. Utsumi F, Kjiyama H, Nakamura K, Tanaka H, Mizuno M, Ishikawa K, et al. Effect of indirect nonequilibrium atmospheric pressure plasma on anti-proliferative activity against chronic chemo-resistant ovarian cancer cells *in vitro* and *in vivo*. *PLoS ONE*. (2013) **8**:e81576. doi: 10.1371/journal.pone.0081576
77. Tanaka H, Mizuno M, Ishikawa K, Takeda K, Nakamura K, Utsumi F, et al. Plasma medical science for cancer therapy: toward cancer therapy using nonthermal atmospheric pressure plasma. *IEEE Trans Plasma Sci*. (2014) **42**:3760. doi: 10.1109/TPS.2014.2353659
78. Mohades S, Barekzi N, Laroussi M. Efficacy of low temperature plasma against scaber cancer cells. *Plasma Process Polym*. (2014) **11**:1150–55. doi: 10.1002/ppap.201400108
79. Laroussi M, Mohades S, Barekzi N. Killing of adherent and non-adherent cancer cells by the plasma pencil. *Biointerphases*. (2015) **10**:029410. doi: 10.1116/1.4905666
80. Mohades S, Laroussi M, Sears J, Barekzi N, Razavi H. Evaluation of the effects of a plasma activated medium on cancer cells. *Phys Plasmas*. (2015) **22**:122001. doi: 10.1063/1.4933367
81. Mohades S, Barekzi N, Razavi H, Maramuthu V, Laroussi M. Temporal evaluation of antitumor efficiency of plasma activated media. *Plasma Process Polym*. (2016) **13**:1206. doi: 10.1002/ppap.201600118

82. Bauer, G. Cold atmospheric plasma and plasma activated medium: antitumor cell effects with inherent synergistic potential. *Plasma Med*. (2019) **9**:57–88. doi: 10.1615/PlasmaMed.2019029462
83. Weltmann KD, Kolb JF, Holub M, Uhrlandt D, Šimek M, Ostrikov K, et al. The future of plasma science and technology. *Plasma Process Polym*. (2019) **16**:e1800118. doi: 10.1002/ppap.201800118
84. Bekeschus S, Favia P, Robert E, von Woedtke T. White paper on plasma for medicine and hygiene: future in plasma health sciences. *Plasma Process Polym*. (2019) **16**:e1800033. doi: 10.1002/ppap.201800033

Conflict of Interest: The author declares that the research was conducted in the absence of any commercial or financial relationships that could be construed as a potential conflict of interest.

frontiers in Physics

ORIGINAL RESEARCH
published: 30 July 2020
doi: 10.3389/fphy.2020.00242

The Effect of Air-Water-Plasma-Jet-Activated Water on *Penicillium*: The Reaction of HNO_2 and H_2O_2 Under Acidic Condition

Kun Liu, Shi-ting Liu and Cong-fu Ran*

The State Key Laboratory of Power Transmission Equipment & System Security and New Technology, Chongqing University, Chongqing, China

Plasma-activated water (PAW) is produced by microhollow cathode discharge (MHCD), where air is the working gas used. The treatment effect of PAW against *Penicillium* is expressed by the germination inhibition rate and the sporoderm-breakage rate. The maximum values of the germination inhibition rate and the sporoderm-breakage rate are 82.31 and 66.91%, respectively. In this paper, the importance of the reaction of HNO_2 and H_2O_2 in *Penicillium* inactivation is illustrated, which is most likely due to its product—ONOOH. The effective impact of ONOOH on inactivation beyond its theoretical lifetime is indirectly reflected by the treatment efficiency, and the complexity of peroxynitrite chemistry may be responsible for prolonging this effect. Moreover, according to the difference of concentration magnitude between HNO_2 and H_2O_2, and the reaction of them under acidic conditions, a method to increase the H_2O_2 production is demonstrated, which can contribute to improving the yield of ONOOH.

Keywords: ONOOH, plasma activated-water, *Penicillium*, sporoderm-breakage rate, water containing

OPEN ACCESS

Edited by:
Mounir Laroussi,
Old Dominion University, United States

Reviewed by:
Jayr Amorim,
Aeronautics Institute of Technology (ITA), Brazil
Eugen Stamate,
Technical University of Denmark, Denmark

****Correspondence:***
Kun Liu
liukun@cqu.edu.cn

Specialty section:
This article was submitted to Plasma Physics, a section of the journal Frontiers in Physics

Received: *01 April 2020*
Accepted: *03 June 2020*
Published: *30 July 2020*

Citation:
Liu K, Liu S and Ran C (2020) The Effect of Air-Water-Plasma-Jet-Activated Water on Penicillium: The Reaction of HNO_2 and H_2O_2 Under Acidic Condition. Front. Phys. 8:242. doi: 10.3389/fphy.2020.00242

INTRODUCTION

Recently, the demand for food with low preservatives and low processing levels has increased, and the requirements for food quality have also improved. How to quickly and effectively kill pathogens on food surfaces without affecting its quality is one a key issue in the field of food safety and preservation. In order to overcome these problems, plasma-activated water (PAW) is being rapidly developed. It has an outstanding inactivation ability and can efficiently inactivate a wide variety of micro-organisms [1–5]. Compared with using the plasma directly, the main advantage of PAW is its harmlessness. The dangers of the electric field, charged particles, and thermal damage to tissue can be avoided by the PAW treatment with only reactive species [6]. PAW that is generated by treating water with plasma differs from the conventional disinfection method, which uses chemicals, and represents an environmentally friendly and cost-effective bactericide. Based on the above advantages, PAW has been widely used and has made satisfactory progress in many fields, especially in the food industry [7, 8].

Air plasma that is generated by dielectric barrier discharge (DBD), gliding arc, or corona discharge adjacent to water creates an acidic solution that contains hydrogen peroxide (H_2O_2), nitrate (NO_3^-), and nitrite (NO_2^-) anions, along with other long-lived secondary products [9–14].

These species may be partly responsible for the extended biological effects of PAW. Additional effects are exerted by short-lived reactive species, especially the post-discharge evolution of these species. $^{\cdot}OH$, O, HO_2, ONOOH, and O_2NOOH have been reported to be present in PAW [15–18]. ONOOH is considered by many researchers to be of substantial significance in PAW inactivation. For example, Brisset and Hnatiuc [15] and Brisset and Pawlat [17] presumed that ONOOH is likely to be an intermediate in acidic solutions and analyzed its formation pathway. Lukes et al. [19] provided evidence of the formation of ONOOH in PAW through a pseudo-second-order post-discharge reaction of H_2O_2 and HNO_2. However, these studies are all analytical and do not explain the importance of ONOOH from an experimental perspective. Theoretically, the lifetime of ONOOH is very short [20]. In addition, it requires a period of time after being obtained to be adopted for PAW, which is at least on the order of seconds. It is unknown whether PAW remains effective in practical applications beyond the lifetime of ONOOH, namely, whether the inactivation efficiency is affected by ONOOH. Very few experiments have been conducted to investigate this. To resolve this uncertainty, in this study, the behaviors of ONOOH in the process are analyzed, namely its biological effects. Furthermore, it was proven in a previous study that adding water into the working gas can increase the content of OH radicals in the plasma [21–23] and, subsequently, increase the yield of H_2O_2. Is there a way to improve the production of ONOOH if it does have an important role in the application? To address the issue, in this paper, air-water microhollow cathode discharge (MHCD) plasma-jet-activated water is generated for the study of the treatment efficiency.

Fungi are ubiquitous in nature and closely related to human life. Most fungi are saprophytic and not pathogenic, and even play significant roles in various fields. However, a few fungal species present a threat to agricultural production by causing diseases such as rice blast, [24] wheat rust, [25], and citrus rot [26]. Hence, the research on fungi is of substantial importance. However, in previous studies, attention was rarely paid to the effects of PAW against fungi. Furthermore, the treatment effect of fungi is reflected by the germination inhibition rate, which is a typical parameter for an evaluation method that is used in biology [27]. Hence, the fungi do not germinate for a period of time. This does not mean that they are actually inactivated and can no longer germinate, but just that they are inhibited, and these spores may continue to germinate during the extended incubation time. Thus, the germination inhibition rate is not equal to the inactivation rate. Then, how many fungi have actually been inactivated? And is it possible to conduct a more in-depth investigation? In this study, the treatment effect of PAW on *Penicillium*, which is used to represent typical fungi, is investigated more thoroughly, thereby resulting in sufficient analysis of the relevant mechanisms.

MATERIALS AND METHODS

Penicillium Preparation

The Italicum Sacc, which is a species of *Penicillium*, was obtained from the Chinese Academy of Agricultural Sciences Citrus Research Institute,. The P. digitatum was inoculated using potato dextrose agar medium and incubated for 5–7 days at 25°C. Then, the most viable spores were selected for the treatment, diluted with sterilized water to 2.0 × 107 per milliliter, and kept in the refrigerator at 4°C. For plasma treatment, 3 mL of sterilized water was injected into petri dishes 35 mm in diameter, and the distance from the equipment nozzle to the suspension surface was ∼4 mm. Then, 150 μL of PAW was added to 60 μL of the spore suspension. It was necessary to vibrate the spore suspension for 1 min to mix it homogeneously prior to treatment. After a period of time, 600 μL of the medium was added and placed in a constant-temperature incubator shaker for 16 h to germinate the spores of P. digitatum. The temperature was set to 25°C and the rotating speed was set to 220 r min^{-1}.

Experimental Setup

The experimental setup is schematically illustrated in **Figure 1**. Plasma activated water used in this study is generated by treating water with a microhollow cathode discharge (MHCD) jet device at atmospheric pressure. The MHCD jet is set above the surface of the water, which is a common method to produce PAW [4, 8]. The reactor consisted of two metal molybdenum electrodes and a sapphire insulator, where the cathode and anode were made of metal molybdenum and had diameters of 15 and 30.5 mm, respectively. The sapphire between two electrodes acted as the dielectric layer, which was 30.5 mm in diameter and 0.6 mm thick. These dimensions were designed to effectively avoid surface discharge between the two electrodes. All three layers had a microhole with a diameter of 0.5 mm in the center. By adjusting the coaxial alignment of the three microholes during assembly, the gas flowed through the micropore and formed the discharge channel. To ensure the safety of the operator, a clamping device that was made of Teflon was used to prevent high-voltage shock. As illustrated in **Figure 1**, the power supply to the microhollow cathode discharge device was provided by a negative HVDC power supply (Xi'an Zhaofu Electronic Company: 0–30 and 2 kW), and its output voltage range was 0 to −30 kV and power was 2 kW. A 400 kΩ resistor was connected in series between the negative high-voltage output of the power supply and the cathode of the MHCD device, with the objectives of limiting the current and ensuring the stable operation of the plasma jet. The gas flow consisted of two parts: the bottle air flow Q_A, which was almost dry air, and the humid air flow Q_W, which was obtained by passing through the homemade Monteggia bottle that contained the secondary distilled water. The water content in the working gas was precisely adjusted by two mass flow controllers (MFCs) of model Sevenstar D07-7 and could be varied in a well-defined way (from 2.53 to 9.57 mg L^{-1}) by changing the settings of the gas flowmeters of the two parts. The relationship between water ratio and water content was evaluated by the Karl Fischer titration method. The main advantage of the gas-liquid mixing method that is used in this experiment was that the particles of water vapor in the obtained working gas were sufficiently small for distributing equably in the gas flow to realize a stable condition. The pure bottle air that was used in this study was provided by Wangmiao Industrial Trading Company in Chongqing, and its water content was <1 ppm.

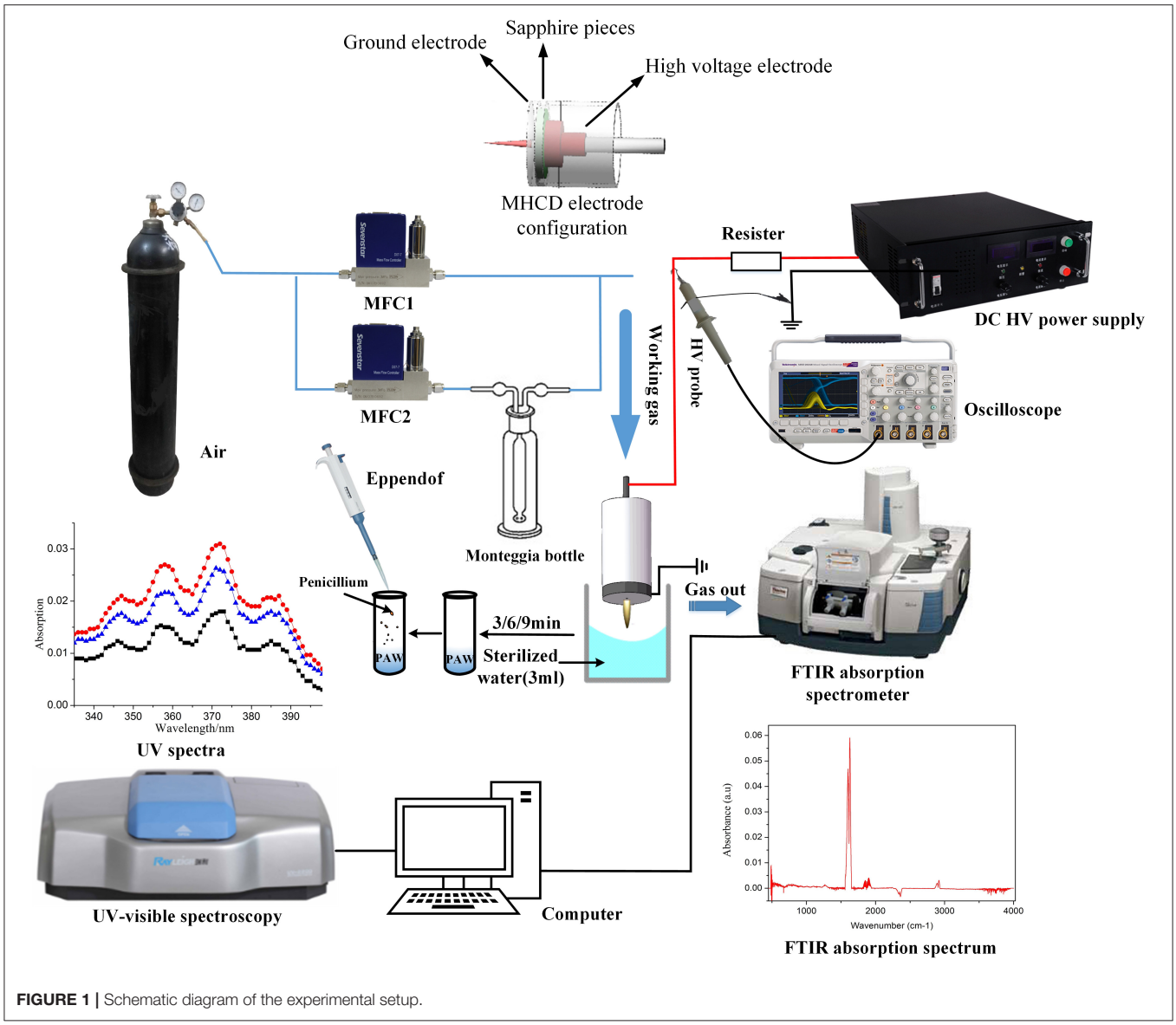

FIGURE 1 | Schematic diagram of the experimental setup.

Measurement Methods

To identify the gas-phase active components that were produced by the MHCD jet, FTIR spectroscopy in the spectral range from 400 to 4,000 cm^{-1} was used, which was conducted in a poly tetra fluoro ethylene (PTFE) cell using a Nicolet iS50 with a spectral resolution of 2 cm^{-1}. The cell consisted of two KBr windows, each with a diameter of 4 cm, which were positioned at each end of the tube, while the gas inlet and outlet were fixed sideways along its length of 10 cm. A vacuum pump was used to evacuate the gas-phase product from the cell to obtain a more accurate result. Furthermore, the ultraviolet-visible spectrophotometer (Beijing BeiFen RayLeigh Company, UV 2200) was adopted to measure the active species in PAW, such as NO_2^- and NO_3^-. The measurement was done by placing the PAW in a cuvette and then placing the cuvette in the spectrophotometer. And the content of H_2O_2 that was generated by the air–water MHCD in the phosphate buffer saline (PBS) buffer was detected via electrochemical measurement.

RESULTS AND DISCUSSION

Germination Inhibition by Plasma-Activated Water

In this study, to explore the ability of plasma-activated water (PAW) to inactivate *Penicillium*, a series of experiments are conducted under various parameter conditions and the treatment efficiency of the air-water MHCD plasma jet is evaluated in terms of the germination inhibition rate of the spores, which is calculated via **Equation 1**. In this formula, S_c and S_t represent the rates at which spores are germinated in the control group and the treatment group, respectively, where the germination

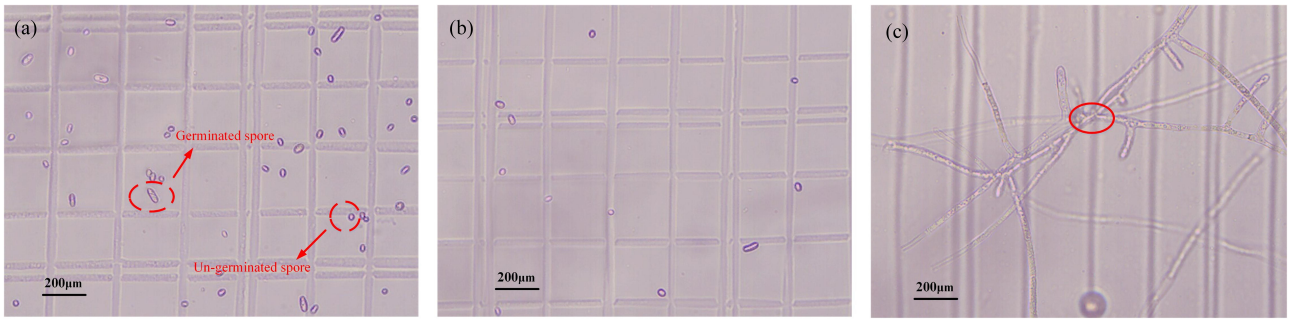

FIGURE 2 | Spore germination of *Penicillium* (at a magnification of 400 times). **(a)** The control group, **(b)** after PAW treatment, and **(c)** spores that grew into hyphae after prolonged cultivation.

rate is obtained by dividing the number of germinated spores by the total number in each group. The main advantage of this approach is that is excludes some of the spores that are not originally germinated. During the experiment, we are surprised to find that the total number of spores in the treated group is significantly reduced compared with the control group under various conditions. For example, as shown in **Figure 2**, which presents the spore germination figure of *Penicillium* at the applied voltage of −6 kV and treatment time of 9 min, the total number of spores decreases to 106 in the treatment group (**Figure 2b**) compared with 350 in the control group (**Figure 2a**). When preparing the solution, its concentration in the experimental group is the same as that in the control group; hence, the numbers of spores should be approximately equal. However, now there is a large difference in the total number of spores, which could be related to sporoderm breakage caused by PAW. Then, the commonly used method for calculating the germination inhibition rate (Equation 1) is no longer applicable. Since the number of broken spores is not known, we use the total number of spores in the control group as that of the experimental group to reduce the error. Therefore, **Equation 2** is adopted. It expresses that, based on Equation 1, the total number of spores in the experimental group is equal to that in the control group, in which the inhibition effect of PAW on the spores can be identified.

Equation 1:

$$\text{Spore germination inhibition (\%)} = \frac{S_c - S_t}{S_c} \times 100$$

where S_c and S_t are the rates of spore germination in the control group and the treatment group, respectively.

Equation 2:

$$\text{Spore germination inhibition (\%)} = \frac{N_c - N_t}{N_c} \times 100$$

where N_c and N_t are the numbers of spores that were germinated in the control group and the treatment group, respectively.

In this experiment, the cultivation time is set to 16 h. Within a limited time, it is easy to distinguish the germinated and the ungerminated spores; however, it is difficult to distinguish the spores after long-term cultivation. Since some spores grew into hyphae and intertwined with each other after prolonged cultivation, those fungi are impossible to recognize under a microscopic view. In the red circle in **Figure 2c**, we cannot determine whether there is one bifurcated spore or two intertwined spores. Hence, via experiments, we selected 16 h as the cultivation time.

In the experiment, it is demonstrated that the inhibition efficiency is strongly affected by the applied voltage, processing time, and storage time. Treatment time, response time, and storage time, respectively, refers to the treatment of water by the jet, the treatment of fungi spores solution by PAW, and the period of time after being obtained to be adopted for PAW. First, the change laws of the germination inhibition rate of PAW with the applied voltage and the treatment time are investigated when the response time is set at 10 min, the water content is 9.57 mg L^{-1}, and the storage time is 5 min, as plotted in **Figure 3**. From the result, we find that the inhibition efficiency increases with the increase of the applied voltage, namely, the plasma-activated water at a high voltage is favorable for inhibiting *Penicillium*. When the treatment time is 3 min and the applied voltage is −3 kV, the corresponding germination inhibition rate is 41.40%. Then, the inhibition rate increases to 72.91% as the voltage is increased to −6 kV. This behavior is also suitable for other treatment times. **Figure 3** shows the change in the inhibition rate with the treatment time. According to **Figure 3**, the inhibition efficiency increases with the treatment time when the other conditions remain unchanged. For example, under the −6 kV condition, when the treatment time is set at 3 min, the inhibition efficiency of the plasma-activated water against *Penicillium* is 72.91%. When the treatment time increases to 9 min, the corresponding germination inhibition rate increases to 82.31%. This behavior is similar to that under other voltage conditions. Thus, increasing the applied voltage or treatment time improves the inhibition efficiency of PAW.

Figure 4 plots the change curves of the inhibition efficiency under various response times when the treatment time is 6 min, storage time is 5 min, and the water content is 9.57 mg L^{-1}. The reaction time is measured from the addition of PAW into the

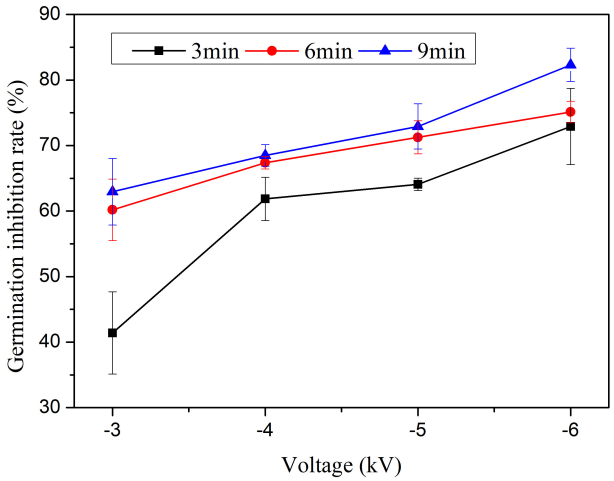

FIGURE 3 | Changes in the inhibition efficiency with the treatment time at various voltages when the water content is 9.57 mg L^{-1}, the response time is 10 min, and the storage time is 5 min.

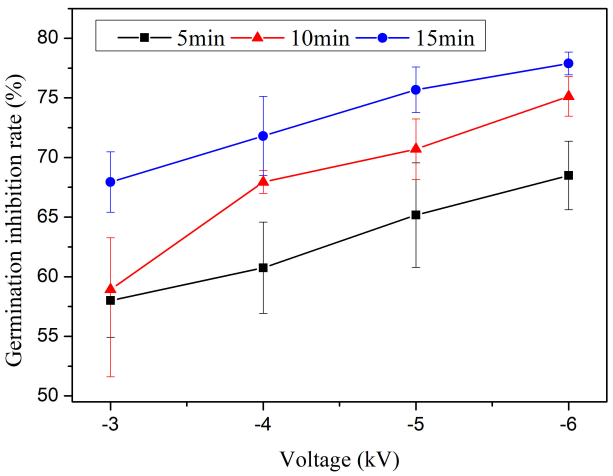

FIGURE 4 | Changes in the germination inhibition efficiency with the response time when the treatment time is 6 min, the storage time is 5 min, and the water content is 9.57 mg L^{-1}.

Penicillium suspension to the addition of a large amount of the medium to the mixture (to prevent PAW from continuing to act on *Penicillium*) [14]. The results prove that the germination inhibition rate against *Penicillium* increases substantially when the response time increases from 5 to 15 min. **Figure 5** plots the variation of the germination inhibition efficiency with the storage time. The germination inhibition rate significantly decreases with the increase in the delay time. The PAW that has been stored for 24 h remains effective for the treatment of *Penicillium*; however, its efficiency is reduced ∼2 times. For example, in the case of −3 kV voltage and 9.57 mg L^{-1} water content, when the storage time is set to 0 min, the germination inhibition rate is 63.52%, and it decreases to 33.11% as the storage time increases to 24 h. The behavior at the −6 kV condition is similar. Among all the experimental conditions, the germination inhibition rate attains its highest value of 82.31% at −6 kV applied voltage when the treatment time and water content are 9 min and 9.57 mg L^{-1}, respectively. Moreover, according to **Figure 5**, there was no significant difference in inhibition efficiency within the first 15 min. The fastest relative reduction occurs in the time range from 15 to 30 min. Hence, the active species that are generated in the liquid are sufficiently stable to continue acting within a limited time, while the inhibition efficiency of the liquids decreases substantially upon a longer delay.

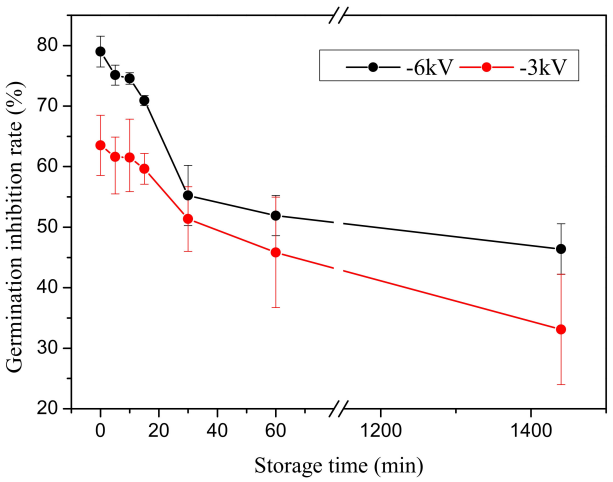

FIGURE 5 | Changes in the germination inhibition efficiency with the storage time in the case of 6 min treatment time, 9.57 mg L^{-1} water content, and 10 min response time.

Measurements of the Sporoderm-Breakage Rate

The total number of spores rapidly decreases, as shown in **Figure 2**. Hence, the sporoderms of some spores are directly broken with the application of PAW. The strong inactivation effect of PAW is also observed here. The spores that are broken are inactivated and no longer germinate. If we can quantify the proportion of spores that are broken, it will be useful for studying the properties of PAW. Hence, the sporoderm-breakage rate is measured. DNA is present in cells, and each spore contains DNA. If the sporoderm is broken, the DNA spills out of the cell and is destroyed; hence, the number of spores that remain in the solution is reflected by the DNA content. DNA, namely, deoxyribonucleic acid, is similar to other substances, such as proteins and nitric acid, that have high absorbance at distinct wavelengths. Therefore, it can be measured by a spectrometer. The method is described as follows: Destruction of the cytoderm is a prerequisite for DNA extraction [28]. Therefore, we apply the method of grinding with liquid nitrogen to destroy the cytoderm. To prevent insufficient milling, lywallzyme (Beijing TianGen Company, RT410) is added to further degrade the sample. After that, a mixture of various substances is obtained, which mainly

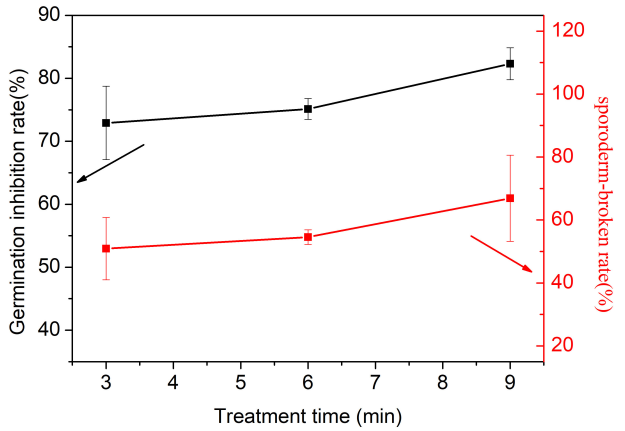

FIGURE 6 | Variations of the germination inhibition rate and sporoderm-breakage rate with the treatment time under 9.57 mg L^{-1} water content, −6 kV voltage, 10 min response time, and 5 min storage time.

include sugars, proteins, and DNA. Then, the Plant Genomic DNA Kit (Beijing TianGen Company, DP305) is used to perform targeted extraction of the DNA from the mixture, and the content of DNA is measured via spectrophotometry. In **Figure 6**, the variation of the sporoderm-breakage rate with the treatment time is plotted. As the treatment time increases, the sporoderm-breakage rate increases. For instance, when the voltage and water content are fixed at −6 kV and 9.57 mg L^{-1}, respectively, the sporoderm-breakage rate is 50.9% at 3 min treatment time, and when the treatment time is 9 min, the corresponding sporoderm-breakage rate is 66.9%. The results demonstrate that the spores are completely inactivated due to the sporoderm being broken.

The inactivated *Penicillium* spores are divided into two parts: those with a broken sporoderm and those that have been inactivated but not broken. The latter are still present in PAW and do not germinate under longer culture. Since other spores grew into hyphae and entangle with each other after prolonged cultivation, as shown in **Figure 2**, we cannot judge those spores that are inactivated but not broken. Therefore, the consideration of both the germination inhibition rate and the sporoderm-breakage rate will be the most comprehensive method for evaluating the treatment effect of PAW on the fungi.

Detection and Analysis of Products in PAW

To obtain additional insight into the process, liquid analytics are necessary. Therefore, we use an ultraviolet spectrophotometer to detect active species in PAW. The existence of both NO_3^- and NO_2^- is obtained from the UV-VIS spectra, as shown in **Figure 7**. A group of 5 peaks in the range of 330–395 nm is a characteristic profile of NO_2^- [29]. The peak at 302 nm is mainly attributed to NO_3^- [30]. The measured absorbance values are converted to absolute concentrations through a standard curve. The experimental results demonstrate that the concentration of NO_3^- increases whereas that of NO_2^- decreases upon longer exposure to plasma, where a transformation between them is observed. As expressed in reactions (1) - (2), the disproportionation of

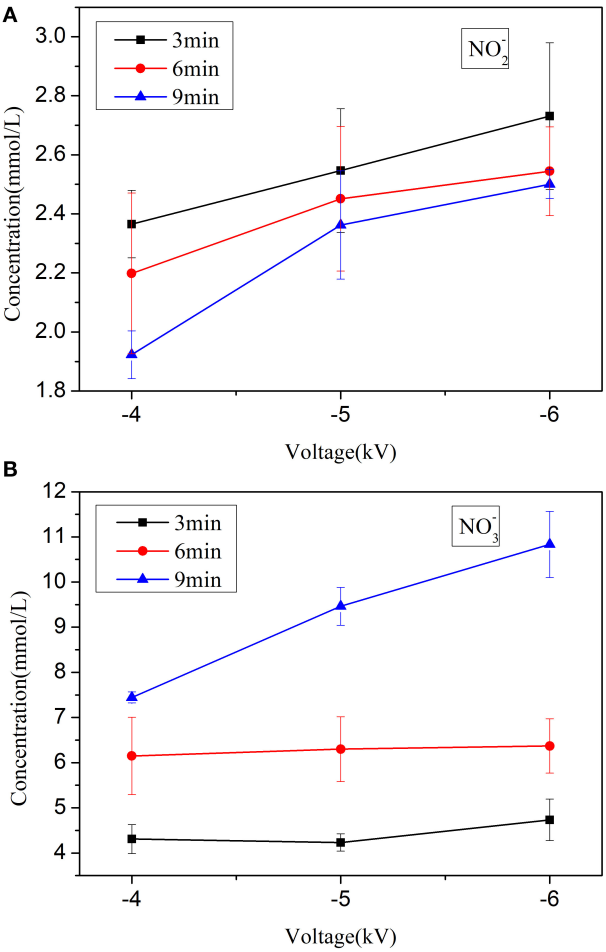

FIGURE 7 | UV absorbance: **(A)** NO_2^- and **(B)** NO_3^- at various voltages and treatment times.

nitrites in acidic medium and the reaction with OH may be partly responsible for this result. In addition, the yields of NO_2^- and NO_3^- both increase with the applied voltage. For example, when the applied voltage and treatment time are set at −4 kV and 9 min, respectively, the concentration of NO_3^- is 7.45 mmol/L and that of NO_2^- is 1.92 mmol/L. As the voltage increases to −6 kV, the corresponding concentrations are 10.83 and 2.5 mmol/L. The behaviors of NO_2^- and NO_3^- are consistent with our results of germination inhibition and indicate that those in the solution may play an important role in the inactivation properties of PAW.

$$3NO_2^- + 2H^+ \rightarrow NO_3^- + 2NO^{\cdot} + H_2O \quad (1)$$

$$\cdot OH + HNO_2 \rightarrow NO_2^{\cdot} + H_2O \quad (2)$$

According to previous studies, products in PAW may include O_3, NO_2^-, NO_3^-, H_2O_2. However, neither O_3 nor H_2O_2 is detected in this study.

To assess these processes comprehensively, liquid analytics must be combined with plasma diagnostic investigations. Thus, the gas products of a plasma jet are observed via an FTIR absorption measurement. The variations of two infrared spectral regions with the voltage and water content are plotted in **Figure 8**, in which the main products are nitrogen oxides such as NO_2, NO, and N_2O, without the absorption of O_3. The experimental results demonstrate that the products in the plasma jet are strongly affected by the applied voltage. For instance, when the flow rate and water content are set at 2.5 L min^{-1} and 2.53 mg L^{-1}, respectively, the peak value of NO increases with the applied voltage. The main reason for this is related to reactions (3)-(5). With respect to NO_2, when the water content is fixed at 2.53 mg L^{-1}, as the applied voltage increases from 3 to 6 kV, its peak value increases, which is mainly due to reactions (6)-(8). Therefore, combined with reactions (9)-(10), this indicates that these products, as precursors of the liquid products, contribute to the changes in HNO_2 and HNO_3 in PAW. In addition, the behaviors of the gas products as functions of the voltage are consistent with our results from the obtained UV spectra. Since the gaseous products in this system do not include O_3, almost no O_3 is detected in the PAW within the detection limit; instead, products of further reaction of nitrogen oxides are detected. Most likely, due to the small-hole discharge, inside of which is a small arc, the local temperature is high, thereby resulting in O_3 not being detected. However, since the gas in the small holes blows the arc, the arc is cooled; hence, the blowing temperature is not high. For H_2O_2, the reaction (11) is widely recognized [31–33]. In the case of excess HNO_2, H_2O_2 is completely reacted, thereby resulting in its absence from PAW.

$$N + O_2 \rightarrow NO + O \quad (3)$$
$$O + NO_2 \rightarrow NO + O_2 \quad (4)$$
$$N + NO_2 \rightarrow NO + NO \quad (5)$$
$$O + NO_3 \rightarrow O_2 + NO_2 \quad (6)$$
$$NO_3 + H \rightarrow OH + NO_2 \quad (7)$$
$$N_2O_5 + M \rightarrow NO_2 + NO_3 + M \quad (8)$$
$$2NO_2 + H_2O \rightarrow NO_2^- + NO_3^- + 2H^+ \quad (9)$$
$$NO + OH + M \rightarrow HNO_2 + M \quad (10)$$
$$NO_2^- + H_2O_2 + H^+ \rightarrow O = NOOH + H_2O \quad (11)$$

Significance and Lifetime of ONOOH in PAW

To determine whether the treatment effect of PAW is realized only by the mixture of HNO_2 and HNO_3, we mixed HNO_2 and HNO_3 solutions in which the two species are in the same concentration as PAW. We found that the inhibition effect is non-significant and the germination inhibition rate is only 8.48%. Furthermore, at concentrations of nearly 10^2 times the initial concentrations, an inhibition rate of 60.71% was realized, which is similar to the treatment effect of PAW. In the case of such a low germination inhibition rate, the sporoderm-breakage rate must be much lower. Hence, the combination of HNO_2 and HNO_3 does not play a central role in the process, and it should not be the main factor for sporoderm-breakage of *Penicillium*. Therefore, the additional species or products that are generated from the plasma treatment play an important or synergistic role in the inhibition properties of PAW.

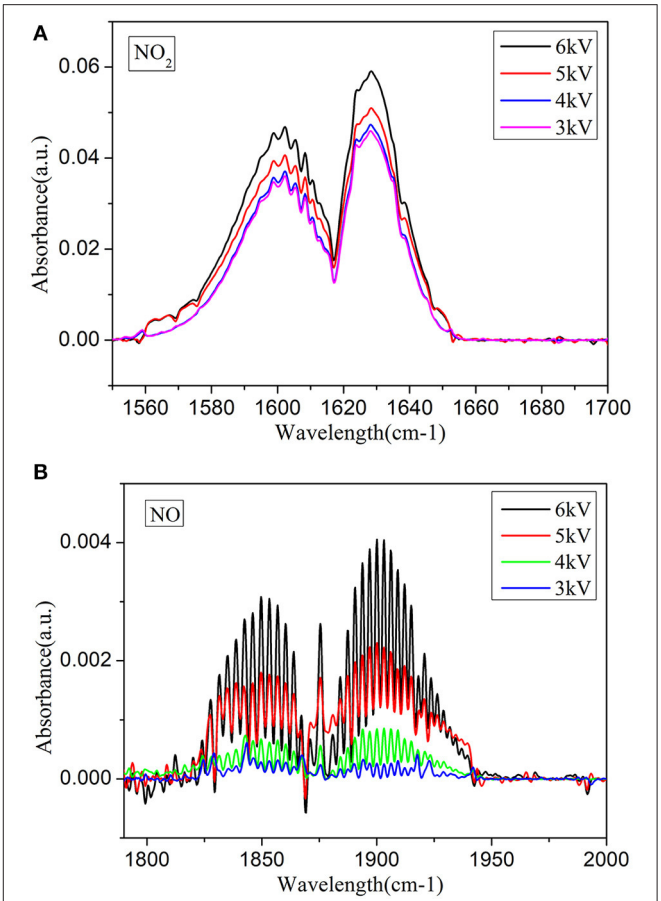

FIGURE 8 | Gas-phase FTIR spectra: **(A)** NO_2, **(B)** NO of varying voltage.

Considering the reaction of nitrites (HNO_2) with hydrogen peroxide (H_2O_2) to form peroxynitrous acid (ONOOH) under acidic conditions, it is speculated that ONOOH plays an important role in the application of PAW. Due to the overlapping spectra of HNO_3 and ONOOH as isomers, ONOOH cannot be detected in PAW. However, this does not mean that it is not present. Thus, we adopt the method of mixing H_2O_2 and HNO_2 to obtain a solution with the same concentrations as in PAW, and we further investigate the treatment effect of ONOOH. To conduct the experiment, we determine the amount of H_2O_2 that is produced in PAW. In this experiment, the content of H_2O_2 that is generated by treating phosphate buffer saline (PBS) buffer using the MHCD is detected via electrochemical measurement. Under this condition, the reaction between HNO_2 and H_2O_2 is prevented. The method was described in detail in previous papers [21, 34, 35].

Figure 9 plots the variations of the concentration of H_2O_2 with the voltage and treatment time when the water content is 9.57 mg L^{-1} and the flow rate is 2.5 L min^{-1}. The experiment

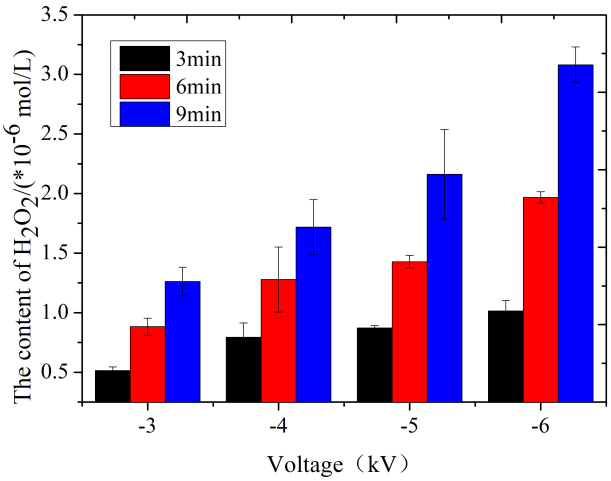

FIGURE 9 | Effect of the treatment time of the air-water jet on the content of H_2O_2 at four applied voltages.

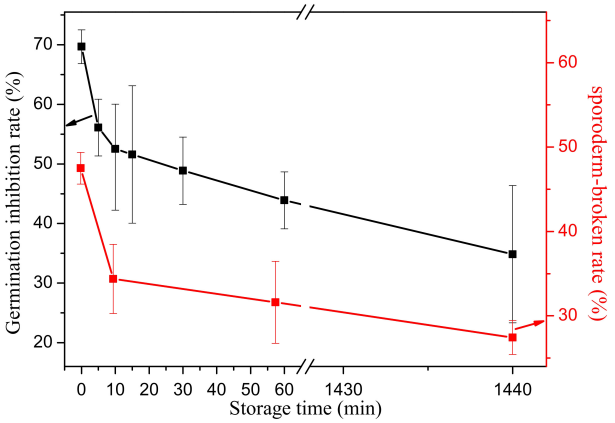

FIGURE 10 | Variations of the germination inhibition rate and the sporoderm-breakage rate with the storage time for a mixed solution.

results demonstrate that the concentration of H_2O_2 that is produced increases with the applied voltage. For example, when the treatment time is set at 9 min, the concentration of H_2O_2 ranges from 1.26 μmol L^{-1} at −3 kV up to 3.08 μmol L^{-1} at −6 kV. In addition, the H_2O_2 content that is produced in the PBS buffer increases with the treatment time. For example, in the case of an applied voltage of −6 kV and a water content of 9.57 mg L^{-1}, when the jet processing time is 3 min, the generated H_2O_2 concentration is 1.02 μmol L^{-1}. If the processing time increases to 9 min, the corresponding H_2O_2 concentration is 3.08 μmol L^{-1}. The behaviors at other applied voltages (−3, −4, and −5 kV) is similar. The variation of H_2O_2 accords with that of the germination inhibition rate in the presence of sufficient HNO_2, thereby suggesting that the intermediate products of ONOOH that are generated by the reaction between H_2O_2 and HNO_2 may play a synergistic role in this process.

Combined with the results for H_2O_2 that are presented above, the relationship between the contents of $\cdot OH$ radicals and H_2O_2 is analyzed. H_2O_2 may be generated via reactions (12-16) when the voltage is <-4.5 kV, where some of the H_2O_2 is detected. As the parameters are increased, more $\cdot OH$ radicals are produced, which increases the number of pathways for generating H_2O_2, as expressed in reactions (17) and (18).

$$O + H_2O \rightarrow H + HO_2 \quad (12)$$
$$O_2 + H_2O \rightarrow OH + HO_2 \quad (13)$$
$$HO_2 + HO_2 \rightarrow H_2O_2 + O_2 \quad (14)$$
$$HO_2 + H_2O \rightarrow H_2O_2 + OH \quad (15)$$
$$H_2O + O_2 \rightarrow H_2O_2 + O \quad (16)$$
$$HO_2 + OH \rightarrow H_2O_2 + O \quad (17)$$
$$\cdot OH + \cdot OH \rightarrow H_2O_2 \quad (18)$$

To further explore whether or not ONOOH plays an important role in the process, H_2O_2 is added into the mixture of HNO_3 and HNO_2, namely, mixture solutions with the same concentrations of HNO_3, HNO_2, and H_2O_2 as in the PAW that is produced under −6 kV voltage, 6 min treatment time, 10 min response time, and 9.57 mg L^{-1} water content are prepared. Then, these mixtures are treated with *Penicillium*. According to **Figure 10,** the inhibition effect of the solution is significantly improved and is close to that of PAW at the corresponding concentrations. The inhibition effect is ∼8 times as strong compared with the solution to which only HNO_3 and HNO_2 have been added. This indicates that in addition to HNO_2 and HNO_3, the product ONOOH generated by the reaction of H_2O_2 and HNO_2 is involved, and it enhances the treatment effect. Due to the strong increase in the treatment efficiency, the sporoderm-breakage rate is measured to determine whether it is related to ONOOH. According to the results, the maximum sporoderm-breakage rate is attained at 47.49%, which is even higher than the germination inhibition rate under the condition that H_2O_2 is not added. It is demonstrated that ONOOH is generated by the reaction of HNO_2 and H_2O_2 under acidic conditions and plays an important role in improving the germination inhibition rate and the sporoderm-breakage rate.

ONOOH is a transient substance, and its lifetime is very short. The germination inhibition rate of PAW that has been aged for 24 h is still almost 6 times that of the HNO_2 and HNO_3 mixture. Is this caused by ONOOH? And is the high efficiency of PAW attributable to the important role that is played by ONOOH? To answer these questions, the variation of the treatment efficiency with the storage time for the HNO_3, HNO_2, and H_2O_2 mixture is studied. According to **Figure 10**, although both the sporoderm-breakage rate and the germination inhibition rate for the mixture decrease with the increase of the storage time, we find that the mixture is also effective after being stored for 1,440 min and the magnitude of the reduction with the storage time is ∼30%, which is similar to that of PAW. In addition, the treatment effect of NO_2^- in an acidic environment is largely intensified by H_2O_2, namely, it is proven that ONOOH has a substantial impact on

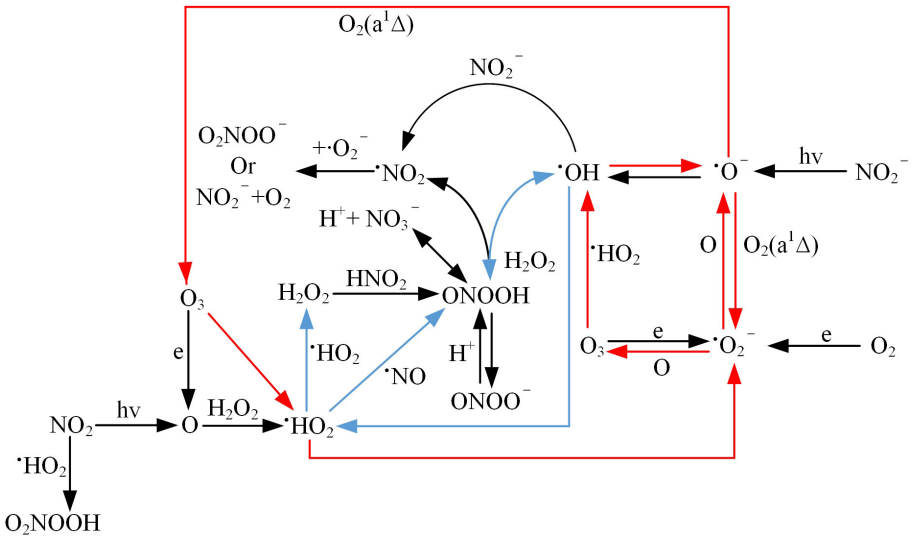

FIGURE 11 | Schematic diagram of several chemical reactions that occur in PAW.

inactivation beyond its theoretical lifetime. Since ONOOH and HNO_3 are isomers, it is not possible to detect ONOOH via UV spectroscopy, Raman spectroscopy, or mass spectroscopy. However, in this study, we detect the presence of ONOOH. Moreover, the reason why a transient substance can age for 24 h is analyzed as follows: Approximately 30% of the ONOOH, which is a short-lived substance, is decomposed into $\cdot OH$ and NO_2^- radicals [reaction (19)], while the remainder transforms to nitric acid, which is immediately followed by dissociation into NO_3^- and H^+ [reaction (20)] [36, 37]. However, due to Le Chatelier's principle, in the case of a high HNO_3 concentration, the latter reaction is expected to be significantly weakened. Hence, ONOOH may be present when the HNO_3 concentration is high. In addition, ONOOH may be present in the cyclic reaction to prolong its effect in a short period of time, as indicated in blue in **Figure 11**. Nevertheless, as time goes on, complex chemical kinetics are not sufficient to maintain it, and ONOOH is gradually dissipated, thereby resulting in reduced inactivation efficiency. Overall, the complexity of the peroxynitrite chemistry is related to the prolonged treatment phenomena of PAW.

$$2HNO_2 \rightarrow NO^{\cdot} + NO_2^{\cdot} + H_2O \quad (19)$$

$$ONOOH \rightarrow HNO_3 \quad (20)$$

$$ONOOH \rightarrow NO_2^{\cdot} + \cdot OH \sim 30\% \quad (21)$$

$$ONOOH \rightarrow HNO_3 \rightarrow NO_3^- + H^+ \sim 70\% \quad (22)$$

Moreover, although the addition of H_2O_2 into the mixture of HNO_3 and HNO_2 significantly improves the treatment efficiency against *Penicillium*, it is not as effective as PAW with the same concentration, even if it is used immediately after mixing. Therefore, in addition to ONOOH, other substances are involved in the cyclic kinetic process and enhance the treatment effect. We posit that O_2^- and O^- are also useful. A species such as O_2^- cannot be obtained by mixing HNO_3, HNO_2, and H_2O_2; however, it could be generated by the collision of electrons with O_2 or O_3 in the plasma discharge region. The strong performance of O_2^- in medical inactivation has been proven in previous research. O^- can be acquired by NO_2^- or $\cdot OH$ in the discharge area. As transient substances, their lifetimes are very short. However, combined with the cyclic reactions of O^-- O_3- HO_2 – O_2^- and OH – O^- – O_2^- – O_3, which are marked in red in **Figure 11**, it is reasonably speculated that O_2^- and O^- remain effective beyond their longevity, thereby contributing to the stronger effect of PAW than the mixture. Their behaviors and the roles that are played by these species in the process merit further exploration in the future.

Possible Ways to Increase the Yield of ONOOH

According to the analysis above, an indirect indication of the important role of ONOOH is proposed; hence, increasing the yield of ONOOH will have a positive effect on the treatment of *Penicillium*. According to the data that are presented above, the productions of HNO_2 and H_2O_2 differ by an order of magnitude, namely, the yield of HNO_2 is much larger than that of H_2O_2. Therefore, according to the reaction of H_2O_2 and HNO_2 under acidic conditions, more H_2O_2 can contribute to more ONOOH being produced. Thus, we studied a method for improving H_2O_2 production. **Figure 12** plots the variation curve of the concentration of H_2O_2 with the water content when the treatment time is 9 min and the flow rate is 2.5 L min^{-1}. The experimental results demonstrate that, with increasing water content, the concentration of H_2O_2 increases substantially. For instance, when the applied voltage and the treatment time are fixed at −6 kV and 9 min, respectively, the H_2O_2 content increases to 3.08 μmol L^{-1} at 9.57 mg L^{-1} water content from 1.03 μmol L^{-1} at 2.53 mg L^{-1} water content. Therefore,

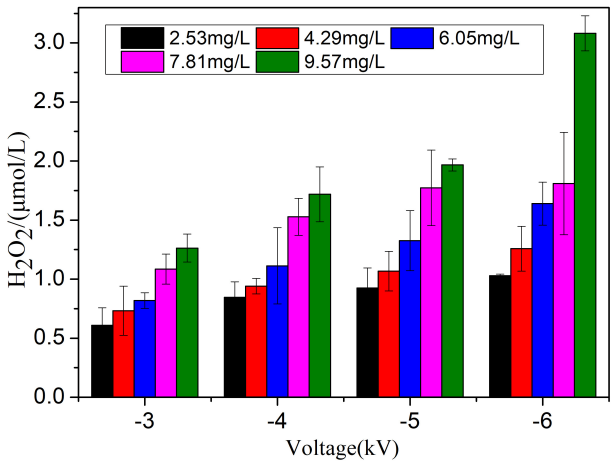

FIGURE 12 | Variation of the H_2O_2 content with the water content.

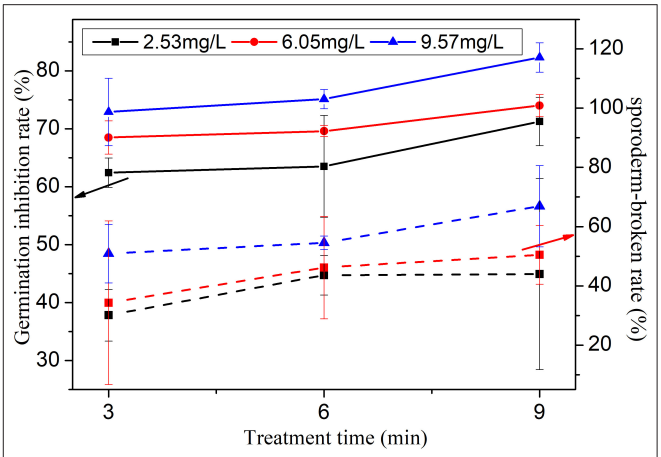

FIGURE 13 | Variations of the germination inhibition rate and the sporoderm-breakage rate with the water content and the treatment time under −6 kV voltage, 10 min response time, and 5 min storage time.

increasing the water content in the working gas contributes to the formation of H_2O_2.

To verify our assumption, the variations of the germination inhibition rate and the sporoderm-breakage rate of PAW with the water content are investigated when the response time is set at 10 min, the voltage is −6 kV, and the storage time is 5 min, as shown in **Figure 13**. It is confirmed that the inhibition efficiency is strongly affected by the water content, namely, when the water content is increased, the germination inhibition rate increases substantially. For example, under the treatment time of 6 min, when the water content is 2.5 L min^{-1}, the germination inhibition rate is 63.52%, which increases to 75.12% when the water content reaches 9.57 mg L^{-1}. At the same time, according to **Figure 13**, the sporoderm-breakage rate increases when increasing the water content of the working gas. For example, under the condition of 9 min treatment time, when the water content is fixed at 9.57 mg L^{-1}, the corresponding sporoderm-breakage rate is 43.96%, which increases to 66.91% as the water content increases to 9.57 mg L^{-1}. This behavior is also observed for other treatment times.

According to the experimental results, the germination inhibition rate and the sporoderm-breakage rate effectively increase as the water content in the working gas increases, which is most likely attributable to the increase in ONOOH production through the reaction between HNO_2 and H_2O_2. Thus, adding water into the working gas of the MHCD jet may be an effective approach for increasing the concentration of ONOOH in PAW. It also indirectly indicates the important role of ONOOH in the application of PAW.

CONCLUSION

In this paper, for the application of PAW to *Penicillium* inactivation, the general formula for calculating the germination inhibition rate is modified to minimize the experimental errors as much as possible. In addition, the sporoderm-breakage rate is utilized to assess the treatment effect of PAW on fungi, which is the most comprehensive method. We find that the maximum values of the germination inhibition rate and the sporoderm-breakage rate are 82.31 and 66.91%, respectively. The high treatment efficiency of PAW is demonstrated not only for bacteria but also for fungi. This result is meaningful because the topic of plasma agriculture is very hot, and fungi are abundant in agriculture. Moreover, we artificially prepare a solution with the corresponding concentrations of H_2O_2, HNO_3, and HNO_2 in PAW. It is demonstrated from the results that the reaction of H_2O_2 and HNO_2 is involved in inactivating *Penicillium*, and its product ONOOH may play an important role in the process. Furthermore, the effective impact of ONOOH on inactivation beyond the theoretical lifetime is indirectly reflected by the treatment efficiency, and the complexity of peroxynitrite chemistry is responsible for prolonging its effect. Moreover, according to the difference of concentration magnitude between HNO_2 and H_2O_2, and the reaction of them under acidic conditions, a method to increase the H_2O_2 production is demonstrated, which can contribute to improving the yield of ONOOH. It can reflect on the germination inhibition rate and the sporoderm-breakage rate.

DATA AVAILABILITY STATEMENT

The raw data supporting the conclusions of this article will be made available by the authors, without undue reservation.

AUTHOR CONTRIBUTIONS

KL and SL: designed experiments and wrote the manuscript. SL and CR: carried out the experiments. KL, SL, and CR: analyzed experimental results. All authors: contributed to the article and approved the submitted version.

FUNDING

This work was supported by National Natural Science Foundation of China (NSFC) under Grants No. 51877021, and sponsored by Natural Science Foundation of Chongqing under Grants No. cstc2018jcyjAX0449, Fundamental Research Funds for the Central Universities under Grants No. 2018CDQYDQ0004, and Key Research and Development Plan of Science & Technology Department of Sichuan Province under Grants No. 2017GZ0094.

REFERENCES

1. Kamgang-Youbi G, Herry JM, Brisset JL, Bellon-Fontaine MN, Doubla A, Naïtali M. Impact on disinfection efficiency of cell load and of planktonic/adherent/detached state: case of Hafnia alvei inactivation by plasma activated water. *Appl Microbiol Biot*. (2008) **81**:449–57. doi: 10.1007/s00253-008-1641-9
2. Naïtali M, Kamgang-Youbi G, Herry JM, Bellon-Fontaine MN, Brisset JL. Combined Effects of long-living chemical species during microbial inactivation using atmospheric plasma-treated water. *Appl Environ Microb*. (2010) **76**:7662−4. doi: 10.1128/AEM.01615-10
3. Kamgang-Youbi G, Herry JM, Meylheuc T, Brisset JL, Bellon-Fontaine MN, Doubla A, et al. Microbial inactivation using plasma-activated water obtained by gliding electric discharges. *Appl Microbiol*. (2009) **48**:13–18. doi: 10.1111/j.1472-765X.2008.02476.x
4. Zhang Q, Liang YD, Feng HQ, Ma RN, Tian Y, Zhang J, et al. A study of oxidative stress induced by non-thermal plasma-activated water for bacterial damage. *Appl Phys Lett*. (2013) 1**02**:203701. doi: 10.1063/1.4807133
5. Oehmigen K, Hähnel M, Brandenburg R, Wilke CH, Weltmann KD, Woedtke TV. the role of acidification for antimicrobial activity of atmospheric pressure plasma in liquids. *Plasma Process Polym.* **7**:250–7. doi: 10.1002/ppap.200900077
6. Ercan UK, Wang H, Ji H, Fridman G, Brooks AD, Joshi SG. Nonequilibrium plasma-activated antimicrobial solutions are broad-spectrum and retain their efficacies for extended period of time. *Plasma Process Polym*. (2013) **10**:544–55. doi: 10.1002/ppap.201200104
7. Patange A, Lu P, Boehm D, Cullen PJ, Bourke P. Efficacy of cold plasma functionalised water for improving microbiological safety of fresh produce and wash water recycling. *Food Microbiol.* (2019) **84**:103226. doi: 10.1016/j.fm.2019.05.010
8. Ma RN, Yu S, Tian Y, Wang K, Sun CD, Li X, et al. Effect of non-thermal plasma-activated water on fruit decay and quality in postharvest Chinese bayberries. *Food Bioprocess Tech.* (2016) **9**:1825–34. doi: 10.1007/s11947-016-1761-7
9. Liu ZC, Liu DX, Chen C, Li D, Yang AJ, Rong MZ, et al. Physicochemical processes in the indirect interaction between surface air plasma and deionized water. *J Phys D Appl Phys*. (2015) **48**:495201. doi: 10.1088/0022-3727/48/49/495201
10. Moussa D, Abdelmalek F, Benstaali B, Addou A, Hnatiuc E, Brisset JL. Acidity control of the gliding arc treatments of aqueous solutions: application to pollutant abatement and biodecontamination. *Eur Phys J Appl Phys*. (2005) **29**:189–99. doi: 10.1051/epjap:2004211
11. Kozakova Z, Klimova EJ, Obradovic BM, Dojcinovic BP, Krcma F, Kuraica MM, et al. Comparison of liquid and liquid-gas phase plasma reactors for discoloration of azo dyes: Analysis of degradation products. *Plasma Process Polym*. (2018) **15**:e1700178. doi: 10.1002/ppap.201700178
12. Joshi AA, Locke BR, Arce P, Finney WC. Formation of hydroxyl radicals, hydrogen peroxide and aqueous electrons by pulsed streamer corona discharge in aqueous solution. *J Hazard Mater*. (1995) **41**:3–30. doi: 10.1016/0304-3894(94)00099-3
13. Oehmigen K, Winter J, Hähnel M, Wilke C, Brandenburg R, Weltmann KD, et al. Estimation of possible mechanisms of escherichia coli inactivation by plasma treated sodium chloride solution. *Plasma Process Polym*. (2011) **8**:904–13. doi: 10.1002/ppap.201000099
14. Traylor MJ, Pavlovich MJ, Karim S, Hait P, Sakiyama Y, Clark DS, et al. Long-term antibacterial efficacy of air plasma-activated water. *J Phys D Appl Phys*. (2011) **44**:472001. doi: 10.1088/0022-3727/44/47/472001
15. Brisset JL, Hnatiuc E. Peroxynitrite: a re-examination of the chemical properties of non-thermal discharges burning in air over aqueous solutions. *Plasma Chem Plasma*. (2012) **32**:655–74. doi: 10.1007/s11090-012-9384-x
16. Tresp H, Hammer MU, Winter J, Weltmann KD, Reuter S. Quantitative detection of plasma-generated radicals in liquids by electron paramagnetic resonance spectroscopy. *J Phys D Appl Phys*. (2013) **46**:435401. doi: 10.1088/0022-3727/46/43/435401
17. Brisset JL, Pawlat J. Chemical effects of air plasma species on aqueous solutes in direct and delayed exposure modes: discharge, post-discharge and plasma activated water. *Plasma Chem Plasma*. (2016) **36**:355–81. doi: 10.1007/s11090-015-9653-6
18. Machala Z, Tarabova B, Hensel K, Spetlikova E, Sikurova L, Lukes P. Formation of ROS and RNS in water electro-sprayed through transient spark discharge in air and their bactericidal effects. *Plasma Process Polym*. (2013) **10**:649–59. doi: 10.1002/ppap.201200113
19. Lukes P, Dolezalova E, Sisrova I, Clupek M. Aqueous-phase chemistry and bactericidal effects from an air discharge plasma in contact with water: evidence for the formation of peroxynitrite through a pseudo-second-order post-discharge reaction of H_2O_2 and HNO_2. *Plasma Sources Sci Technol*. (2014) **23**:015019. doi: 10.1088/0963-0252/23/1/015019
20. Juliane LF, Sergey AN, Mitchio O, Coleen MR, Joseph SF, Paul OW. Cis-cis and trans-perp HOONO: action spectroscopy and isomerization kinetics. *J Chem Phys*. (2004) **121**:1432–48. doi: 10.1063/1.1760714
21. Liu K, Wang CY, Hu HM, Lei JZ, Han L. Indirect treatment effects of water–air MHCD jet on the inactivation of *penicillium* digitatum suspension. *IEEE T Plasma Sci*. (2016) **44**:2729. doi: 10.1109/TPS.2016.2608926
22. Srivastava N, Wang CJ. Effects of water addition on OH radical generation and plasma properties in an atmospheric argon microwave plasma jet. *J Appl Phys*. (2011) **110**:053304. doi: 10.1063/1.3632970
23. Li L, Nikiforov A, Xiong Q, Britun N, Snyders R, Lu X, et al. OH radicals distribution in an Ar-H_2O atmospheric plasma jet. *Phys Plasmas*. (2013) **20**:093502. doi: 10.1063/1.4820945
24. Dean RA, Talbot NJ, Ebbole DJ. The genome sequence of the rice blast fungus Magnaporthe grisea. *Nature*. (2005) **434**:980–6. doi: 10.1038/nature03449
25. Hovmoller MS, Yahyaoui AH, Milus EA, Justesen FA. Rapid global spread of two aggressive strains of a wheat rust fungus. *Mol Ecol.* (2008) **17**:3818–26. doi: 10.1111/j.1365-294X.2008.03886.x
26. Timmer LW. Preventive and curative trunk treatments for control of phytophthora foot rot of citrus. *Phytopathology*. **67**:1149. doi: 10.1094/Phyto-67-1149
27. He JL, Wu DT, Zhang Q, Chen H, Li HY, Han QH, et al. Efficacy and mechanism of cinnamon essential oil on inhibition of colletotrichum acutatum isolated from 'Hongyang' Kiwifruit. *Front Microbiol.* (2018) **9**:1288. doi: 10.3389/fmicb.2018.01288
28. Dauphin LA, Moser BD, Bowen MD. Evaluation of five commercial nucleic acid extraction kits for their ability to inactivate Bacillus anthracis spores and comparison of DNA yields from spores and spiked environmental samples. *J Microbiol Methods*. (2009) **76**:30–7. doi: 10.1016/j.mimet.2008.09.004
29. Piskarev IM. Effect of spark discharge plasma on water, physiological saline, Hanks' solution. *High Energy Chem.* (2018) **52**:348–54. doi: 10.1134/S0018143918040124
30. Friedman HA, Toth LM, Bell JT. *Method for Selectively Reducing Plutonium Values by a Photochemical Process*. United States Patent. 4131527 (1978).
31. Anbar M, Taube H. Interaction of nitrous acid with hydrogen peroxide and with water. *J Am Chem Soc.* (1954) **76**:6243–47. doi: 10.1021/ja01653a007
32. Tarabová B, Luke P, Hammer MU, Jablonowski H, von Woedtke T, Reuter S, et al. Fluorescent measurement of peroxynitrite /peroxynitrous acid in cold air plasma treated aqueous solutions. *Phys Chem Chem Phys.* (2019) **21**:8883–96. doi: 10.1039/C9CP00871C

33. Takahama U, Tanaka M, Oniki T, Hirota S. Reactions of thiocyanate in the mixture of nitrite and hydrogen peroxide under acidic conditions: Investigation of the reactions simulating the mixture of saliva and gastric juice. *Free Radic Res*. (2007) **41**:627–37. doi: 10.1080/10715760701218566
34. Yu L, Tian Y, Gao A, Shi Z, Liu Y, Li C. Bi-Module sensing device to *in situ* quantitatively detect hydrogen peroxide released from migrating tumor cells. *PLoS ONE*. (2015) **10**:0127610-1. doi: 10.1371/journal.pone.0127610
35. Shi ZZ, Wu XS, Gao L, Tian Y, Yu L. Electrodes/paper sandwich devices for *in situ* sensing of hydrogen peroxide secretion from cells growing in gels-in-paper 3-dimensional matrix. *Anal Methods*. (2014) **6**:4446. doi: 10.1039/C4AY00695J
36. Goldstein S, Lind J, Merenyi G. Chemistry of peroxynitrites as compared to peroxynitrates. *Chem Rev*. (2005) **105**:2457–70. doi: 10.1021/cr0307087
37. van Gils CAJ, Hofmann S, Boekema BKHL, Brandenburg R, Bruggeman PJ. Mechanisms of bacterial inactivation in the liquid phase induced by a remote RF cold atmospheric pressure plasma jet. *J Phys D Appl Phys*. (2013) **46**:175203. doi: 10.1088/0022-3727/46/17/175203

Conflict of Interest: The authors declare that the research was conducted in the absence of any commercial or financial relationships that could be construed as a potential conflict of interest.

frontiers in Physics

ORIGINAL RESEARCH
published: 09 October 2020
doi: 10.3389/fphy.2020.569618

Risk Evaluation of EMT and Inflammation in Metastatic Pancreatic Cancer Cells Following Plasma Treatment

Eric Freund[1,2†], Chiara Spadola[2†], Anke Schmidt[1], Angela Privat-Maldonado[3], Annemie Bogaerts[3], Thomas von Woedtke[1,4], Klaus-Dieter Weltmann[1], Claus-Dieter Heidecke[2], Lars-Ivo Partecke[2,5], André Käding[2] and Sander Bekeschus[1]*

[1] ZIK plasmatis, Leibniz Institute for Plasma Science and Technology (INP), Greifswald, Germany, [2] Department of General, Visceral, Thoracic, and Vascular Surgery, Greifswald University Medical Center, Greifswald, Germany, [3] Plasma Lab for Applications in Sustainability and Medicine - ANTwerp, Department of Chemistry, University of Antwerp, Antwerp, Belgium, [4] Department of Hygiene and Environmental Medicine, Greifswald University Medical Center, Greifswald, Germany, [5] Schleswig Medical Hospital, Schleswig, Germany

OPEN ACCESS

Edited by:
Michael Keidar,
George Washington University,
United States

Reviewed by:
Jayr Amorim,
Aeronautics Institute of Technology (ITA), Brazil
Nagendra Kumar Kaushik,
Kwangwoon University, South Korea

***Correspondence:**
Sander Bekeschus
sander.bekeschus@inp-greifswald.de

[†] These authors have contributed equally to this work

Specialty section:
This article was submitted to Plasma Physics, a section of the journal Frontiers in Physics

Received: 04 June 2020
Accepted: 10 September 2020
Published: 09 October 2020

Citation:
Freund E, Spadola C, Schmidt A, Privat-Maldonado A, Bogaerts A, von Woedtke T, Weltmann K-D, Heidecke C-D, Partecke L-I, Käding A and Bekeschus S (2020) Risk Evaluation of EMT and Inflammation in Metastatic Pancreatic Cancer Cells Following Plasma Treatment. Front. Phys. 8:569618. doi: 10.3389/fphy.2020.569618

The requirements for new technologies to serve as anticancer agents go far beyond their toxicity potential. Novel applications also need to be safe on a molecular and patient level. In a broader sense, this also relates to cancer metastasis and inflammation. In a previous study, the toxicity of an atmospheric pressure argon plasma jet in four human pancreatic cancer cell lines was confirmed and plasma treatment did not promote metastasis *in vitro* and *in ovo*. Here, these results are extended by additional types of analysis and new models to validate and define on a molecular level the changes related to metastatic processes in pancreatic cancer cells following plasma treatment *in vitro* and *in ovo*. In solid tumors that were grown on the chorion-allantois membrane of fertilized chicken eggs (TUM-CAM), plasma treatment induced modest to profound apoptosis in the tissues. This, however, was not associated with a change in the expression levels of adhesion molecules, as shown using immunofluorescence of ultrathin tissue sections. Culturing of the cells detached from these solid tumors for 6d revealed a similar or smaller total growth area and expression of ZEB1, a transcription factor associated with cancer metastasis, in the plasma-treated pancreatic cancer tissues. Analysis of *in vitro* and *in ovo* supernatants of 13 different cytokines and chemokines revealed cell line-specific effects of the plasma treatment but a noticeable increase of, e.g., growth-promoting interleukin 10 was not observed. Moreover, markers of epithelial-to-mesenchymal transition (EMT), a metastasis-promoting cellular program, were investigated. Plasma-treated pancreatic cancer cells did not present an EMT-profile. Finally, a realistic 3D tumor spheroid co-culture model with pancreatic stellate cells was employed, and the invasive properties in a gel-like cellular matrix were investigated. Tumor outgrowth and spread was similar or decreased in the plasma conditions. Altogether, these results provide valuable insights into the effect of plasma treatment on metastasis-related properties of cancer cells and did not suggest EMT-promoting effects of this novel cancer therapy.

Keywords: epithelial-to-mesenchymal transition, kINPen, plasma medicine, plasma sources, reactive oxygen species, ROS

INTRODUCTION

Cancer is the second leading cause of death worldwide after cardiovascular diseases [1]. Cancer incidence is increasing, and the spectrum of regionally dominating tumors and their mutational burden is heterogeneous. Hence, efficient cancer treatment remains challenging and is one of the significant difficulties of today. However, new concepts of cancer therapies are under investigation. This includes immunotherapies [2], target-specific drugs [3, 4], or technological innovations such as photodynamic [5, 6] and cold physical plasma therapy [7]. Cold physical plasmas are partially ionized gases generating a plethora of reactive species (ROS) besides other components such as electric fields, temperature, light of different wavelengths, and charged particles [8, 9]. At sufficient concentrations, these species mediate oxidation-induced damage and death in tumor cells [7]. Plasma treatment was previously shown to control tumor growth in pre-clinical models effectively [10–12]. Moreover, first patients with tumors of the head and neck benefited from this new therapeutic approach and experienced a reduced tumor burden [10, 11].

Today, increased tumor toxicity is only one of the columns of promising new cancer therapies. The other aspects include tolerability (beneficial ratio between anticancer activity and side effects) and safety aspects, for instance. Such risk assessment includes the investigations of whether a new treatment is void of inducing cancer cell detachment and metastasis. Metastasis is one of the greatest challenges in cancer therapies. Disseminated tumor growth induces organ dysfunction and often hinders surgical resection [12–15]. Especially in pancreatic cancer, the disseminated spread into the peritoneal cavity (peritoneal carcinomatosis) hinders successful cancer therapies [16–23]. Therefore, this type of cancer is a challenging but ideal model to investigate the effect of a novel treatment on cellular detachment and metastatic phenotype.

Treatments with the *kINPen* argon plasma jet had been shown to be void of genotoxicity according to OECD-based protocols [24–27] and did not introduce cell detachment through physical irritations (argon gas flow), or biological modulations of adhesion markers [28]. Moreover, the absence of tumor formation after six repetitive treatments of skin was validated in a 1-year follow up study in mice [26]. Also, clinicians that treated patients with the *kINPen* argon plasma jet in similar settings as investigated here (no modulation of feed- or sheath gases), did not report any severe side-effects [29–32]. This study now extends on the previous investigations of four different pancreatic cancer cell lines (MiaPaCa2, PaTuS, PaTuT, and Panc01) and tissue from *in ovo*-grown tumors, to a more detailed analysis of factors that can mediate an altered cell detachment and outgrowth. This includes (i) adhesion molecules, that are responsible for cell-cell and cell-matrix contact being essential to maintain tissue integrity [33–35], (ii) markers of the epithelial-mesenchymal transition (EMT), that are associated with cancer cell polarization and transformation to a more metastatic phenotype [18, 36, 37], and (iii) molecules of inflammation known to drive or limit inflammation-mediated cellular escape from the bulk tumor mass. In a series of experiments, it was demonstrated that the plasma treatment regime using the *kINPen* argon plasma jet was safe with respect to the aspects mentioned above and the model systems employed in this study. There were no hints for the promotion of EMT changes or metastasis and therefore further research in this field is strongly encouraged.

MATERIALS AND METHODS

Cell Cultivation and Plasma Treatment

The experiments were carried out with four human pancreatic cancer cell lines: MiaPaCa2 (ATCC: CRL-1420), PaTuS (DSMZ: ACC-162), PaTuT (DSMZ: ACC-204), and Panc01 (ATCC: CRL-1469). The culturing was performed in Dulbecco's modified Eagle's medium (DMEM; Pan Biotech, Aidenbach, Germany), which was supplemented with 10% fetal bovine serum, 2% glutamine, and 1% penicillin and streptomycin (all Sigma, Steinheim, Germany) in a cell culture incubator (Binder, Tuttlingen, Germany). For co-culture experiments, cells transduced with nuclear fluorescent proteins were used. The pancreatic stellate cell line RLT-PSC (developed at the Faculty of Medicine of the University of Mannheim [38], kindly provided by Prof. Ralf Jesenofsky) was transduced to express nuclear mKate2 (RLT-PSC Red) using a lentiviral vector (Essen BioScience, Essen, Germany). MiaPaCa2 (MiaPaCa2 Green) and Panc01 (Panc01 Green) were transduced to express nuclear green fluorescent protein (Essen BioScience, Essen, Germany). Cells were cultured in DMEM-F12 medium (Gibco, Dreieich, Germany). For experiments, absolute cell counting was performed using an Attune NxT flow cytometer (Thermo Scientific, Waltham, USA), and seeding was done in Roswell Park Memorial Institute medium 1640 (RPMI; Pan Biotech, Aidenbach, Germany) with similar supplements as for DMEM. For FACS experiments, 2×10^4 cells per well were seeded in 96-well flat-bottom plates (Eppendorf, Hamburg, Germany). For three-dimensional tumor spheroids, 3×10^3 cells per well in medium containing 0.24% Methocel (ratio 2:1, 2×10^3 RLT-PSC, 1×10^3 pancreatic cancer cells) were seeded in ultra-low attachment plates (Nunclon Sphera; Thermo Scientific, Waltham, USA). For seeding on the chorion allantois membrane of fertilized chicken eggs (TUM-CAM model), 2×10^6 cells were supplemented with 15 µl Matrigel (Corning, New York, USA). Before plasma treatment, the cells were cultured for an additional 24 h (FACS experiments), 72 h (spheroid experiments), and 96 h (TUM-CAM model). Plasma treatment was done using high-purity (99.999%) argon gas (Air Liquide, Paris, France) at two standard liters per minute running the atmospheric pressure argon plasma jet kINPen (neoplas tools, Greifswald, Germany). The plasma treatment of co-cultured spheroids (in 150 µl PBS and medium exchange 90 min later) was done for 120 s and standardized using an xyz-table (CNC Step, Gelfern, Germany), which fixed the plasma jet and operated the computer-driven treatment protocol.

In ovo Experiments

Specific pathogen-free chicken eggs (Valo BioMedia, Osterholz-Schrambeck, Germany) were incubated in an egg incubator (Thermo de Luxe 250, Hemel, Verl, Germany) at 37.5°C and

65% humidity at constant turning (for the first 6 days). The preparation of the eggs' chorion-allantois membrane (CAM) as well as the treatment was performed as described before [28]. Briefly, the tumor cells were implanted at day 8 of the incubation, and the plasma treatments were performed at days 12 and 14. The cell floaters were detached from the tumors by gently pipetting 150 µl of growth medium (RPMI) up and down and collecting the supernatant after the second plasma treatment. A part of the supernatant was stored for cytokine quantification, and the detached cell floaters were further incubated *in vitro* for the following 6 days (144 h). For this, flat-bottom 96-well cell culture plates (Eppendorf, Hamburg, Germany) were utilized that supply a ring which was filled with water to prevent excessive evaporation of culture medium during that time. After incubation, cells were subjected to imaging and flow cytometry analysis.

Tumor Tissue and Live-Cell Imaging

Tissues from the *in ovo* grown tumors were explanted from the CAM and embedded in OCT medium (Tissue-Tek; Sakura Fintek, Alphen aan de Rijn, Netherlands) before freezing in liquid nitrogen and storage at −80°C. Ultrathin tissue sections were cut (5 µm) and mounted (Dako fluorescence mounting medium; Agilent Technologies, Santa Clara, UA) on microscopy slides. For the quantification of apoptotic cells, the *In situ Cell Death Detection Kit* (TUNEL red; Roche, Basel, Switzerland) was utilized according to the manufacturer's instructions. For nuclear counterstaining, diamide-2-phenylindol (DAPI; BioLegend, San Diego, USA) was used. For the staining of cellular adhesion molecules, the tissue slides were fixed with 4% paraformaldehyde (PFA) and permeabilized with Triton-X (both Sigma Aldrich, St. Louis, USA). Blocking was performed with 5% bovine serum albumin (BSA; Sigma Aldrich, St. Louis, USA) before they were stained with the respective antibodies targeting CD49b conjugated with phycoerythrin (PE; clone: P1E6-C5; BioLegend, San Diego, USA), CD326 conjugated with AlexaFluor (AF) 488 (clone: 9C4; BioLegend, San Diego, USA), and CD324 conjugated with AF647 (clone: EP700Y; Abcam, Cambridge, UK). The images were acquired using a BZ-9000 fluorescence microscope (Keyence, Frankfurt, Germany). The ratio of $TUNEL^+$ cells over the area of the tissue region was quantified utilizing the image analysis software ImageJ.

For the investigation of cultured *ex ovo* tumor cell floaters, and *in vitro* grown three-dimensional tumor and pancreatic stellate cell spheroids, high content imaging was performed utilizing the Operetta CLS imaging system (PerkinElmer, Waltham, USA). The *ex ovo* floaters were fixed and permeabilized as described above and were imaged with a 20 × air objective (NA = 0.4; Carl Zeiss, Jena, Germany) acquiring brightfield as well as fluorescence images at λ_{ex} 365 nm and λ_{em} 430–500 nm for the detection of DAPI, and λ_{ex} 630 nm and λ_{em} 655–760 nm for the detection of Zinc finger E-box-binding homeobox 1 (anti-ZEB1 AF700, clone: 639914, R&D Systems / biotechne, Minneapolis, USA). For the algorithm-driven (Harmony 4.9; PerkinElmer, Waltham, USA) image and cell quantification strategy, a pseudo-fluorescence channel was calculated by merging the fluorescence channels. The total cellular proliferation area resulting from the initial cell floaters added as well as the ZEB1 fluorescence intensity inside that growth area was calculated. The three-dimensional tumor and stellate cell spheroids were imaged 72 h after their treatment with plasma. This was done utilizing a 5 × objective (NA 0.16; Carl Zeiss, Jena, Germany) capturing the brightfield channel, as well as the fluorescence channels for the detection of GFP-expressing tumor cells at λ_{ex} 475 nm and λ_{em} 500–550 nm, and for mKate-expressing stellate cells at λ_{ex} 560 nm and λ_{em} 570–650 nm. The detection of the spheroid area was done by creating a pseudo fluorescence image out of the merged fluorescent channels and an inverted brightfield image, which had the highest intensities in the area of spheroid growth. The cell outgrowth was calculated by determining the number of cells outside the spheroid region. Their distance to the spheroid border region was calculated automatically based on algorithms implemented in the quantitative imaging software.

Flow Cytometry

To quantify the expression of adhesion molecules and markers of the epithelial-to-mesenchymal transition (EMT), the cells were treated in 96-well flat-bottom plates and were harvested 24 h later with accutase (Pan Biotech, Aidenbach, Germany). Subsequently, the cells were transferred to a u-bottom plate (Nunclon; Thermo Scientific, Waltham, USA) and were fixed and permeabilized. The cells were stained with DAPI and antibodies targeting αSMA conjugated with AF594 (clone: 1A4; Abcam, Cambridge, UK), anti-vimentin conjugated with PerCP/Cy5.5 (clone: H84; Santa Cruz Biotechnology Dallas, USA), and anti-ZEB1 conjugated with AF700 (clone: 639914; R&D Systems, Minneapolis, USA). After washing, cells were acquired with a Cytoflex S (Beckman-Coulter, Brea, USA) flow cytometer. The expression of the markers was quantified in viable ($DAPI^-$) cells and normalized to that of untreated cells. Unstained controls were treated like their counterparts and were acquired using the same settings. Data analysis was done using Kaluza 2.1 (Beckman-Coulter, Brea, USA).

Quantitative Polymerase Chain Reaction (qPCR)

The cell lines were cultured in optimal growing conditions before they were harvested with the enzyme accutase, and cell pellets were generated via centrifugation and washing of the cells. Afterward, they were suspended in lysis buffer, and cellular RNA was isolated utilizing an isolation kit according to the manufacturers' instructions (RNA Mini Kit; Bio&SELL, Feucht, Germany). The RNA was quantified using a NanoDrop 2000C (Thermo Scientific, Waltham, MA, USA). Quantitative polymerase chain reaction (qPCR) was then carried out with 1 µg RNA that was synthesized into cDNA using a thermocycler device (Thermo Scientific, Waltham, USA). For these experiments, 96-well v-bottom plates loaded with Sybr Green (BioRad, Munich, Germany) were used to label the mRNA-targets during 50 heat cycles (Light Cycler 480; Roche, Mannheim, Germany). Expression levels were calculated with formulas provided by the $2^{-\Delta\Delta Ct}$ method and in relation to *GAPDH*.

Quantification of Chemokine/Cytokines

Supernatants for chemokine/cytokine analysis of cancer cells were collected 4 h post-treatment of the *in vitro* experiments 96-well plates as well as 30 min after plasma treatment of TUM-CAM with subsequent rinsing of tumors and aspiration of the liquid. Supernatants were stored in 96-well plates at −80°C. For detection of the soluble inflammatory mediators (chemokines/cytokines), the LEGENDplex (BioLegend, San Diego, USA) bead-based immunoassay was utilized. The experiments were carried out according to the manufacturer's instructions. The targets of the assay were the following: interleukin (IL) 1β, IL6, IL8, IL10, and IL12p70, free-active tumor growth factor β (TGFβ), tumor necrosis factor α (TNFα), interferon γ (IFNγ), C-X-C motif chemokine ligand 1(CXCL1), CXCL10, arginase, C-C motif ligand 17 (CCL17/TARC), and vascular endothelial growth factor (VEGF). All 13 targets were quantified simultaneously, each with specific standards and limits of detection. Staining and measurement of samples were done in v-bottom 96-well plates (Eppendorf, Hamburg Deutschland), from which the fluorescent beads were directly acquired with a flow cytometer (CytoFlex; Beckman Coulter, Brea, USA). The discrimination between the 13 different beads was done using differences in forward and side scatter (FSC, SSC) and fluorescent intensity at λ_{ex} 638 nm and λ_{em} 640–680 nm. By analyzing the fluorescence intensity of PE-labeled antibodies (λ_{ex} 561 nm and λ_{em} 564–606 nm) detecting the targets bound to the beads, the absolute concentration of all factors was interpolated using polynomial functions of the 5th degree and dedicated data analysis software (Vigene Tech, Carlisle, USA).

Statistical Analysis

Data are from two to six experiments with several technical replicates. For statistical analysis and graphing, Prism 8.4.2 (GraphPad, San Diego, USA) was utilized. Multiple comparisons

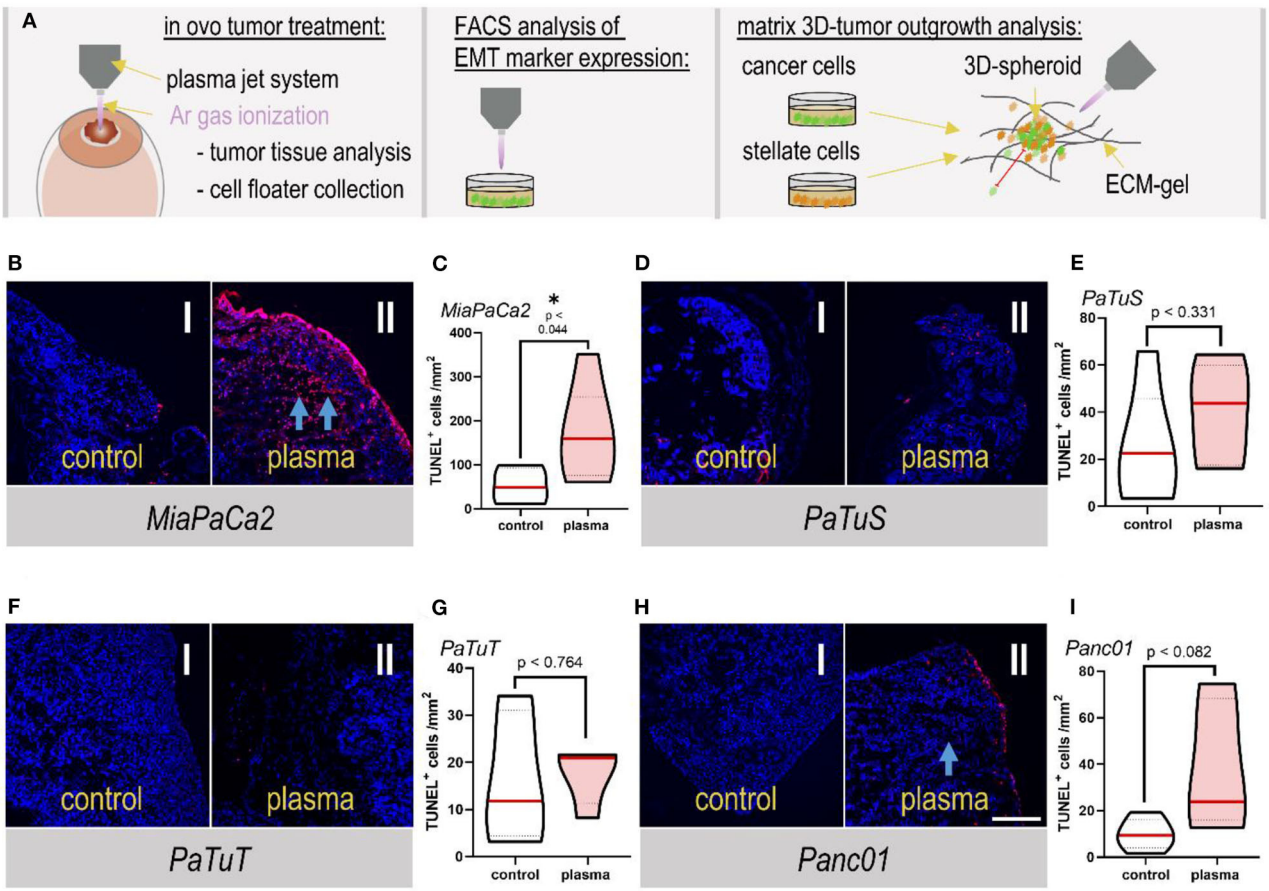

FIGURE 1 | Plasma treatment increased apoptosis in *in ovo*-grown pancreatic tumors. **(A)** Schematic overview of the experimental procedures in this study. **(B)** DAPI and TUNEL-stained tissue from *in ovo*-grown MiaPaCa2 tumors that (I) were left untreated or (II) plasma-treated for 2 × 60 s, and **(C)** quantification of TUNEL$^+$ apoptotic cells per mm^2 of tissue. **(D)** DAPI and TUNEL-stained tissue from *in ovo*-grown PaTuS tumors that (I) were left untreated or (II) plasma-treated for 2 × 60 s, and **(E)** quantification of TUNEL$^+$ apoptotic cells per mm^2 of tissue. **(F)** DAPI and TUNEL-stained tissue from *in ovo*-grown PaTuT tumors that (I) were left untreated or (II) plasma-treated for 2 × 60 s, and **(G)** quantification of TUNEL$^+$ apoptotic cells per mm^2 of tissue. **(H)** DAPI and TUNEL-stained tissue from *in ovo*-grown Panc01 tumors that (I) were left untreated or (II) plasma-treated for 2 × 60 s, and **(I)** quantification of TUNEL$^+$ apoptotic cells per mm^2 of tissue. Arrows in the images indicate a significant (↑↑), and a moderate (↑) increase of apoptosis. The data display the distribution of the values with their mean (red line) as well as 25 and 75% quartiles (dotted lines). The magnification of all images was 20×. The data are from at least 4–5 eggs per group. Scale bar is 500 μm.

were done with ANOVA (with Welch's correction). For comparison between two adjacent groups, the Welch's *t*-test was used. The levels of significance are indicated in the figures as asterisks: $\alpha = 0.05$ (*), $\alpha = 0.01$ (**), and $\alpha = 0.001$ (***).

RESULTS

Plasma Treatment Partly Elicited Apoptosis of Pancreatic Cancer Cells Grown *in ovo*

To test the anticancer efficacy of cold physical plasma generated via the kINPen, different pancreatic cancer cell lines (MiaPaCa2, PaTuS, PaTuT, and Panc01) were seeded on the chorion-allantois membrane of fertilized chicken eggs (TUM-CAM model) to grow solid tumors before these were plasma-treated twice for 60 s on two consecutive days (**Figure 1A**). The induction of apoptosis was different among the cell lines tested. A significant effect ($p < 0.044$) of plasma treatment was observed in MiaPaCa2 tumors (**Figures 1B,C**). An apparent increase in the apoptosis rate (TUNEL$^+$ cells) was visible in the tumor surface region, and to a lower amount also in deep tissue layers (**Figure 1B**). In contrast, PaTuS cells did not show large rates of apoptosis after plasma treatment ($p < 0.764$; **Figures 1D,E**). Similar results were obtained for PaTuT cells ($p < 0.331$) (**Figures 1F,G**). For Panc01 tumors, a modest increase ($p < 0.082$) of apoptotic cells was observed in the plasma treatment conditions, especially at the tumor margins (**Figures 1H,I**).

Plasma Treatment Did Not Affect the Adhesion Marker Profile of *in ovo*-Grown Tumors

Cellular adhesion is a critical factor in tumor metastasis. In addition to the mechanical spread of tumor cells through invasive measures, endogenous metastasis occurs when cells actively detach from their mass and migrate into blood vessels and lymph nodes. Therefore, the expression of adhesion molecules in untreated and plasma-treated tumors was investigated. Tissue sections were prepared, and tissue slides were stained for the cell adhesion markers integrin alpha-2 (CD49b; **Figure 2A**), E-cadherin (CD324; **Figure 2B**), and Ep-CAM (CD326; **Figure 2C**). It was found that CD49b was expressed across all different tumor cell lines, albeit to a different extent. CD324 was highly expressed only in PaTuS but not in the three

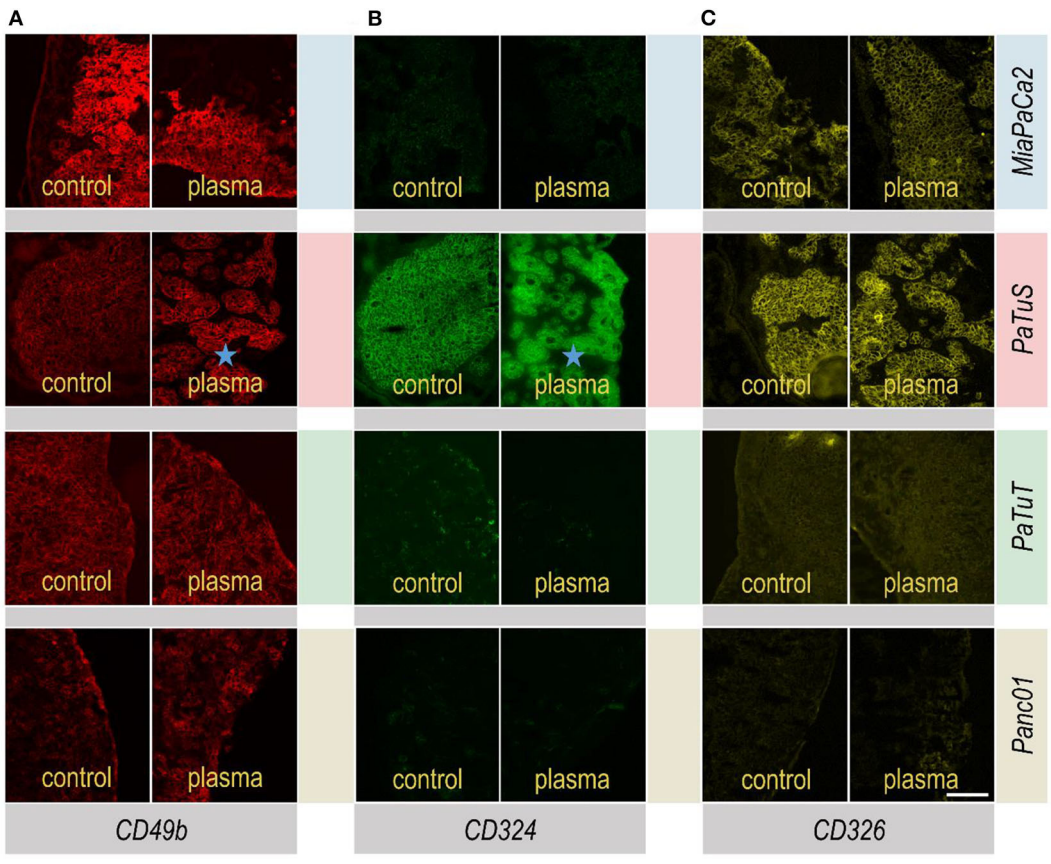

FIGURE 2 | Adhesion marker profile of *in ovo*-grown tumor tissue was unaffected by plasma treatment. **(A)** Tumor tissue from *in ovo*-grown MiaPaCa2, PaTuS, PaTuT, and Panc01 cells that were stained with anti-CD49b (red), **(B)** anti-CD324 (green), **(C)** and anti-CD326 (yellow) antibodies 24 h after 2 × 60 s of plasma treatment. The magnification of all images was 20×. Changes in growth morphology are indicated with stars (★). The images are representatives from at least 4–5 eggs per group carrying one tumor each. Scale bar is 500 μm.

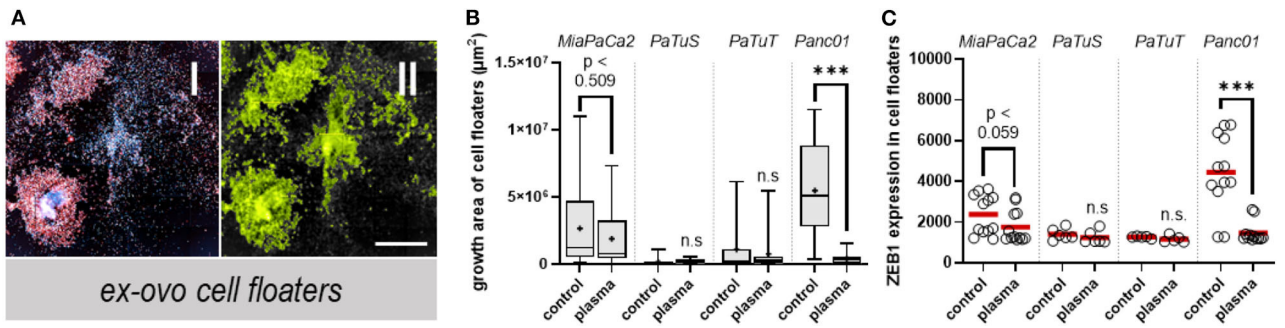

FIGURE 3 | Plasma treatment reduced the growth of *ex ovo* pancreatic cancer cell floaters. **(A)** Representative images of MiaPaCa2 cells that detached from *in ovo*-grown tumors by washing and after seeding them into flat-bottom plates for culture and proliferation in the consecutive 6 days, shown as (I) fluorescence image, and (II) software-processed pseudo-fluorescence image for the quantification of **(B)** the growth area of detached cell floater cultures, and **(C)** the expression of ZEB1 analyzed via high content imaging in these cells. Shown are **(B)** the min-max box-plots and median (black line) and mean (+) and **(C)** the individual values with their mean (red line). The data are technical replicates from at least 4–5 eggs per group. ***$p < 0.001$. Scale bar is 250 µm.

other tumor cell lines. CD326 expression was found in MiaPaCa2 and PaTuS tumors, but only to a negligible extent in PaTuT and Panc01 tumors. Interestingly, the growth pattern of PaTuS tumors was changed following the treatment with plasma to a more glandular, epithelial phenotype. A decrease in E-cadherin and Ep-CAM is a known indicator of pro-metastatic cancer phenotypes, suggesting plasma treatment not to interfere with such processes.

Plasma Treatment Neither Promoted Cell Detachment Nor Expression of ZEB1

After analyzing the toxicity and adhesion-related receptor expression in solid pancreatic cancer tissue, the next question was whether plasma treatment actively engaged the dislodgement of individual cells from the main tumor. This might occur due to, e.g., argon gas pressure, electrical discharges, drying of the outer tumor surface, and ROS-mediated breakage of cell-cell connections. The experiment was done by plasma treatment of the tumors and washing the tumors immediately afterward. The cells that were contained in the washing solution (cell culture medium) were then seeded into cell culture plastic and allowed to grow for 6 days (144 h). This was necessary, as the number of cells retrieved directly in the washing solution was too low to perform intelligent imaging analysis. After 6 days, the cell growth was calculated using a software-based method that was utilizing a filtered image to detect the area of these cell floaters (**Figure 3A**). In MiaPaCa2 cells, it was found that the cell growth non-significantly decreased with plasma treatment, while PaTuS and PaTuT cells contained in the washing liquid overall failed to proliferate significantly *in vitro* (**Figure 3B**). In both cell lines, the growth area was similar or smaller in the plasma treatment condition. This does not suggest that these cells do not grow *in vitro,* but rather the cells detached from the original tumor mass were mostly not viable or too low in numbers. Panc01 cells, in contrast, had a large growth area in the control group, which significantly declined in the plasma treatment group (**Figure 3B**). These results suggest that plasma treatment either did not promote the detachment of pancreatic tumor cells from the bulk tumor mass or that detachment was promoted, but the cells were dead, unable to proliferate, or both. The next question was whether the cells that grew *in vitro* changed their expression levels of the zinc finger e-box binding homeobox 1 (ZEB1) transcription factor, known to be associated with the mesenchymal transition of cancer cells [18]. ZEB1 was detected in the highest amount in MiaPaCa2 and Panc01 cells, and both of these cell lines showed a reduction of ZEB1 expression in the cells initially detached from the plasma-treated bulk tumor mass (**Figure 3C**), suggesting a decreased EMT phenotype.

Plasma Treatment Modulated the Inflammatory Profile *in vitro* and *in ovo*

Inflammation is one key aspect in tumor metastasis, and cytokines and chemokines are the major regulators of inflammation. Therefore, 13 different soluble mediators of inflammation were quantified in supernatants of *in vitro* and *in ovo* experiments (**Figure 4**). All data were normalized to that of untreated controls, while crossed out boxes indicate concentrations above or below the detection limit of the assay. Arrows indicate a 2-fold up or downregulation. Three is an only partial agreement between the *in vitro* and *in vivo results*, exemplifying the need to address research questions in both systems. Panc01 showed a consistent downregulation of almost all cytokines investigated *in vitro and in ovo*, except VEGF and IL8. By contrast, *in vitro* supernatant analysis of MiaPaCa2 and PaTuT revealed only upregulation of cytokines for IL6 and TNFα in both cell lines, and IL1β and TNFα in MiaPaCa2. The results for PaTuS were mainly analogous to those retrieved for PaTuT, except for an increase in CCL17 and a decrease in IL8 and CXCL1. While some of the results were similar to those seen in the *in ovo* samples (e.g., for IL6 and TNFα), some were different either in amplitude or direction of regulation. This was expected, as the CAM provided a nutritious and vascularized tumor microenvironment in which the cells modulate the expression of several genes associated with, e.g., extracellular matrix generation, differentiation, and

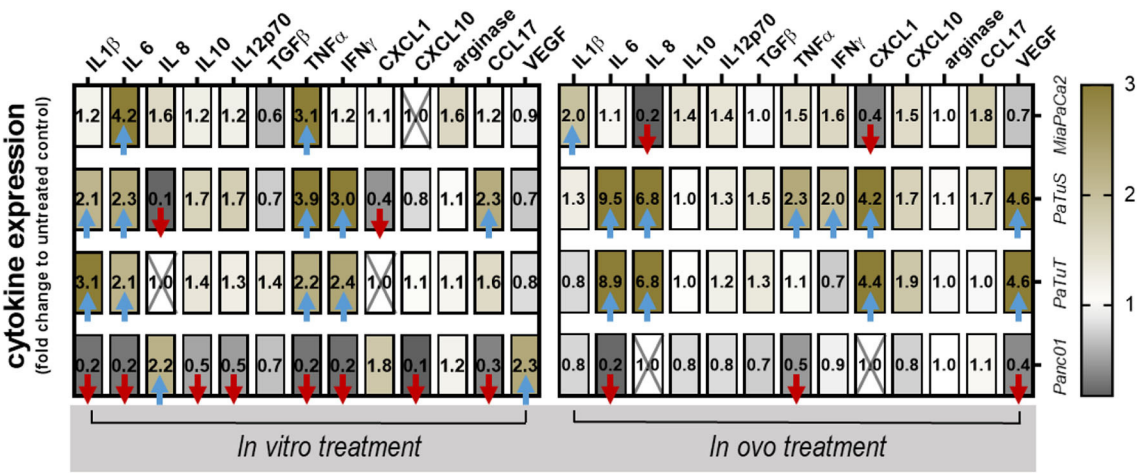

FIGURE 4 | Plasma treatment modulated the chemokine and cytokine profile of pancreatic cancer cells. Quantification of pro and anti-inflammatory cytokines and chemokines 4 h after exposure of the cells to plasma *in vitro*, or after rinsing untreated or plasma-treated tumors on the CAM. The concentrations of the soluble factors were normalized to the respective untreated control, and the fold change of their secretion was blotted in the heat-map, showing the numerical value of the fold change. Decreased cytokine secretion is shown in gray, no change in white, and increased secretion in olive colors. Data are compiled from over 1,000 single data points, and show means of three independent experiments (*in vitro*) and 4–5 eggs per group (*in ovo*) over untreated control = 1. Crossed-out data (X) was at the upper limit of detection of the assay except for CXCL10 in MiaPaCa2, which was at the lower limit of detection. Blue arrows indicate upregulation of >2-fold; red arrows indicate downregulation >2-fold.

angiogenesis. In general, it was observed that PaTuS and PaTuT cells showed a similar pattern in the secretion of IL6, IL8, CXCL1, and VEGF *in vitro* and *in ovo*, which validates their similar nature.

Plasma Treatment Did Not Induce an EMT Phenotype in Pancreatic Cancer Cells *in vitro*

PaTuT and PaTuS cells only showed few cell detachment in the *in ovo* experiments. However, they had the most vital changes in cytokine expression among the tested cancer cell lines. Hence, it was tested if the plasma treatment induced a more invasive mesenchymal phenotype (EMT) that is associated with tumor cell metastasis and growth. The expression of α-smooth-muscle actin (αSMA), was unaffected, while vimentin was slightly increased ($p < 0.1$; **Figures 5A,B**) in PaTuS cells. ZEB1 was not found to be expressed in PaTuS cells (**Figures 5A,B**). In PaTuT cells, α SMA did not show any change in the cells after exposure to plasma (**Figures 5A,C**). Vimentin and ZEB1 gave a modest, non-significant upregulation after plasma treatment (**Figures 5A,C**). Another marker that is protective against tumor invasion and angiogenesis is the Tissue inhibitor of metalloproteinases 2 (TIMP2) [39]. Therefore, the expression of *TIMP2* was investigated among all pancreatic cancer cell lines that were tested in this study. PaTuS cells showed the highest gene expression of *TIMP2*, followed by MiaPaCa2. The expression in both of the cell lines was significantly different compared to PaTuT and Panc01 cells, which had low levels of *TIMP2* (**Figure 5D**).

Plasma Treatment Reduced the Cancer Cell Outgrowth in a Stellate Cell-Matrix-3D-Model

To provide a tumor microenvironment that could be monitored via fluorescence microscopy, a co-culture of human pancreatic stellate and cancer cells was setup. The former are myofibroblasts contributing to matrix formation and remodeling. The 3D tumor spheroid mixtures were exposed to plasma and embedded into a basement membrane matrix (growth factor reduced Matrigel) containing mainly laminin and vimentin collagens providing growth conditions for the cells [34] that allow the analysis of the evasion of the fluorescently labeled cells from the bulk tumor over time using quantitative multicolor fluorescence live-cell microscopy. MiaPaCa2 and Panc01 cells showed the highest release of floaters that had detached from the bulk tumor and grown *in vitro* (**Figure 3B**). Therefore, these two cell lines were used in this model as we expected a high degree of motility. Plasma treatment reduced the size area of the core spheroid in both cancer cell types co-cultured with stellate cells (**Figure 6A**). Interestingly, the stellate cells had a higher capacity of exiting the core spheroid into the extracellular matrix (**Figures 6B,E**, orange cells). Quantification of the absolute number (**Figure 6C**) of evaded cells and absolute distance of evaded cells to the spheroid core (**Figure 6D**) in the stellate cell-MiaPaCa2 spheroid model showed no significant difference for both cell types. By contrast, both the number of cells (**Figure 6F**) as well as their mean migration distance (**Figure 6G**) significantly decreased with plasma treatment of Panc01 cells co-cultured with stellate cells in 3D spheroids.

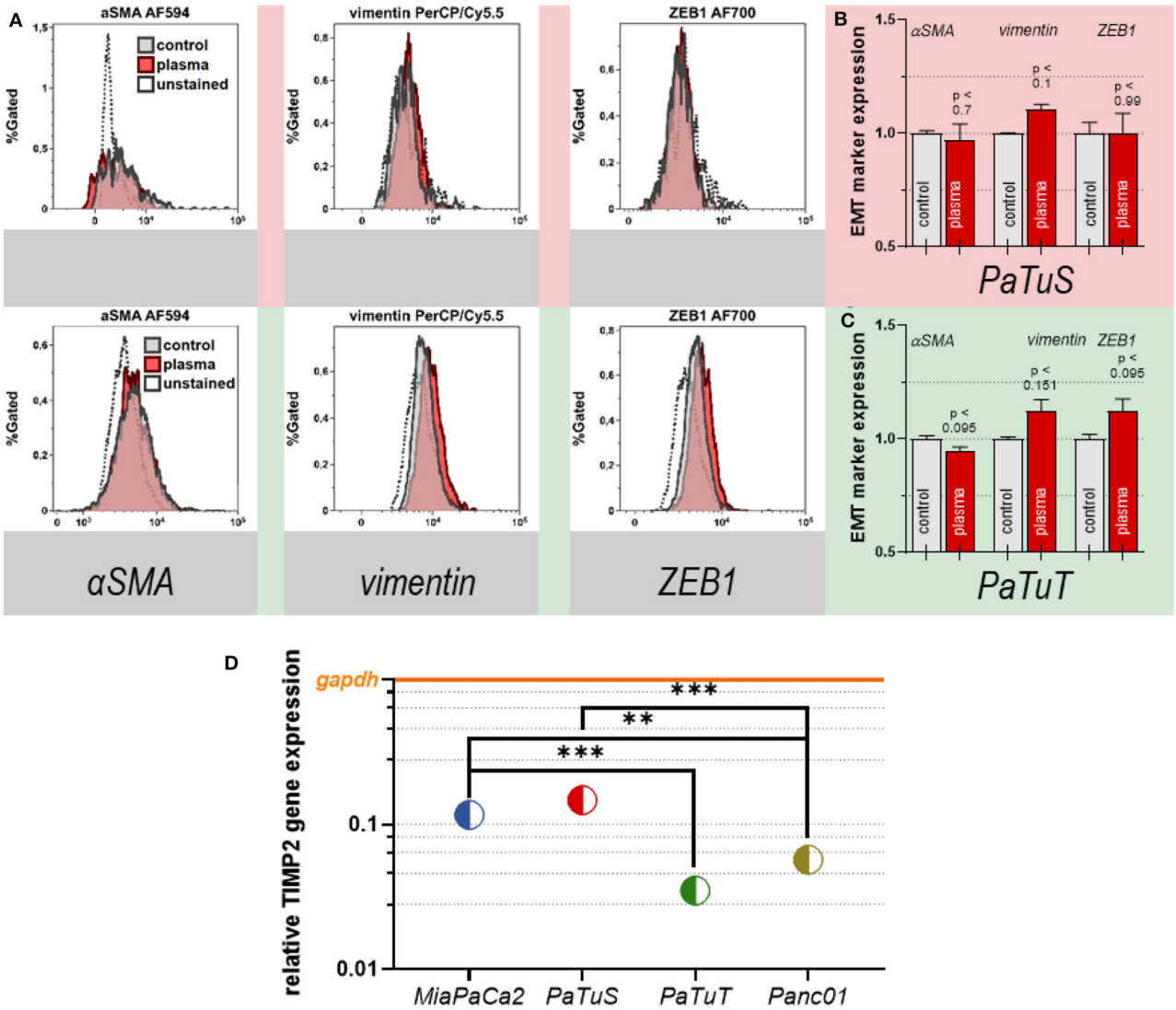

FIGURE 5 | Plasma treatment did not significantly modulate the EMT marker expression profile *in vitro*. **(A)** Overlay of the expression of the EMT marker αSMA, vimentin, and ZEB1 in PaTuS (upper row) and PaTuT cells (lower row) 24 h after their exposure to 60 s of plasma treatment *in vitro*; **(B)** quantification of the expression of EMT markers in PaTuS cells; **(C)** quantification of the expression of EMT markers in PaTuT cells; **(D)** relative expression of *TIMP2* in MiaPaCa2, PaTuS, PaTuT, and Panc01 cells in relation to the housekeeping gene *GAPDH*. Shown is **(B,C)** the mean +SEM, and **(D)** the mean only. The data **(A–C)** are from two independent experiments with 2–3 replicates each. $^{**}p < 0.01$ and $^{***}p < 0.001$, respectively.

DISCUSSION

Pancreatic cancer is an aggressive and fast-growing tumor entity [40, 41]. It is often diagnosed at very late stages after there are already metastases in the liver or lungs. Peritoneal metastases may also be present at this time [41, 42]. Even with surgery in a resectable tumor, the number of R0 resections (no tumor tissue in the respective margins) remains to low [43, 44]. Pancreatic cancer has a poor prognosis, and the importance of cell residuals is outlined by the median survival that drops from 25.1 months (for R0) to only 15.3 months with R1 resection [16]. A combination with plasma treatment might become an additive approach to existing surgical and chemotherapeutic strategies to tackle the tumor cell residuals at the surgical margins of the pancreas. Additional treatment of these cancer cell residuals might be able to decelerate the rapid course of cancer remission observed in most patients. Plasma treatment showed promising effects against pancreatic cancer cells *in vitro* [45–48] and *in vivo* [49–52]. However, the possibility of inducing a more metastatic phenotype in the cells surviving the treatment is underexplored. Early studies with experimental plasma jets showed an increase in cellular detachment [53–55]. Recent investigations did not report any cellular detachment in the TUM-CAM or spheroid model [28, 34], or a lack of EMT marker modulation after cellular exposure to plasma-oxidized medium [23].

In our previous work, it was shown that plasma treatment introduced cellular toxicity *in vitro* and reduced the tumor mass of tumors grown on the chorion-allantois membrane of fertilized

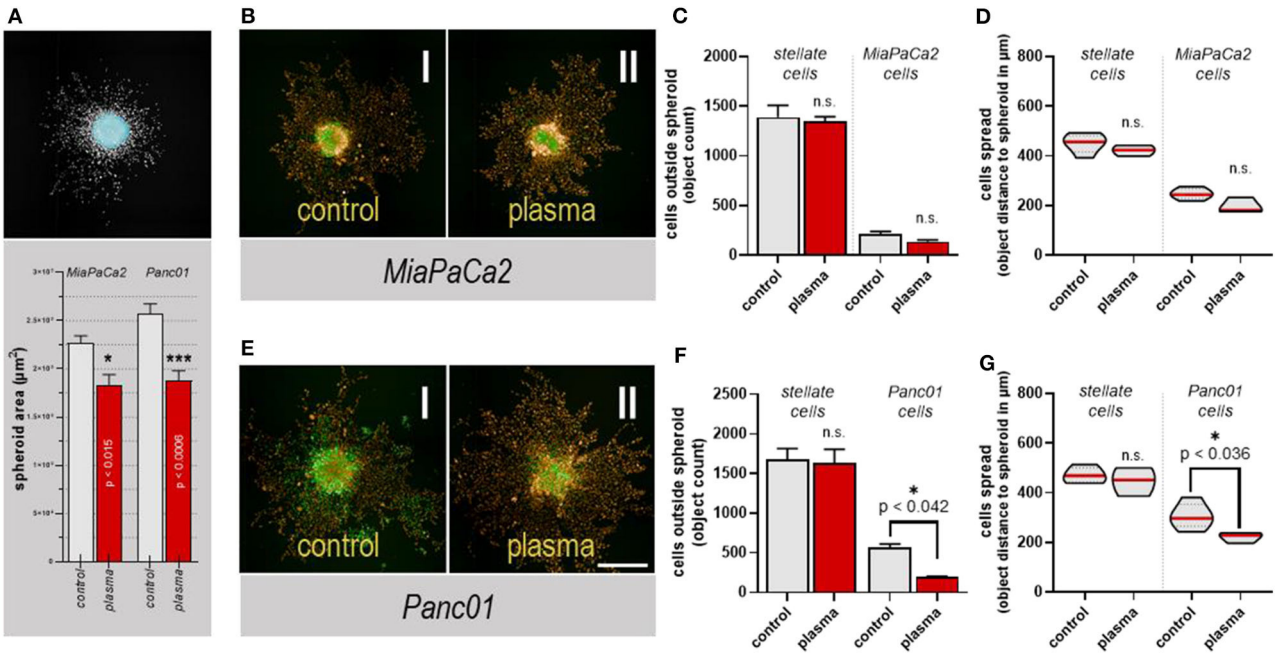

FIGURE 6 | Plasma treatment reduced cancer cell outgrowth in a matrix-3D-tumor model. **(A)** Representative images of a software-calculated, highly-contrasted image of the spheroid with the algorithm-based detection of the spheroid core area are as well as its quantification at the bottom; **(B)** representative images of (I) untreated and (II) 120 s plasma-treated spheroids of co-cultured MiaPaCa2 Green + RLT-PSC Red, in Matrigel 72 h after the treatment; **(C)** the quantification of the cell count outside the spheroid region; **(D)** the quantification of the cells' absolute distance to the spheroid core; **(E)** representative images of (I) untreated and (II) 120 s plasma-treated spheroids of co-cultured Panc01 Green + RLT-PSC Red, grown in Matrigel 72 h after the treatment; **(F)** the quantification of the cell count outside the spheroid region; **(G)** the quantification of the cells' absolute distance to the spheroid core. The data show **(A,C,F)** mean +SEM and **(D,G)** mean and 25% and 75% quartiles in violin plots, and are from 2 to 3 replicates of two independent experiments. Scale bar is 150 µm.

chicken eggs (TUM-CAM *in ovo* model) [28]. The TUM-CAM model provides a realistic setting for the growth of solid tumors. It supplies an extracellular matrix, as well as a supply of blood and nutrients through the chicken embryo's blood vessels [56]. Argon gas flow alone did not alter the metabolic activity of the tested cancer cell in the same setting, and more importantly, did also not significantly detach cells from the *in ovo* grown tumors. The role of mechanical stress that is applied through a similar plasma treatment can therefore be neglected, indicating the changes in EMT and adhesion marker profile to be more important for the initiation of metastasis. These investigations were now expanded to further downstream analysis of the tumor tissue. Despite a modest to substantial induction of apoptosis in plasma-treated tumor tissue, a change in some of the main cell adhesion molecules was not observed. Cells, including tumor cells, usually firmly adhere to the bulk mass via adhesion molecules, such as CD49b (integrin α-2), CD324 (E-cadherin), and CD326 (Ep-CAM) [15, 28, 57–59].

CD49b is an integrin involved in cellular contacts with laminin and collagen of extracellular matrices. Early work reported MiaPaCa2 cells to be void of CD49b [60], but similar to other studies [28] we found the molecule to be expressed in these and all other cell types. Ep-CAM plays a controversial role in the progression of epithelial tumors. This molecule is an adhesion molecule often found to be overexpressed in non-malignant epithelial. CD326 is also associated with tumor cell signaling (mandatory function in tumor cell invasion) and is–because of its higher expression in cancers—described as a tumor-antigen [61, 62]. Novel therapy approaches also use targeted-therapies against Ep-CAM to prevent tumor growth [63]. However, Ep-CAM was only found expressed in tissue from MiaPaCa2 and PaTuS tumors and was not modulated by their treatment with plasma. Cell-cell contacts are mediated via E-cadherin (CD324), which has a crucial function in preserving tissue stability [58]. Reduced expression or loss of CD324 is associated with a more motile, invasive cancer cell phenotype [64]. In our study, CD324 was only expressed in PaTuS and in PaTuT cells to a modest extent. This corresponds to our finding that both cell lines released the lowest number of viable floaters from *in ovo*-grown tumors to proliferate *in vitro*. MiaPaCa2 and Panc01 cells showed only background level of E-cadherin staining in tumor tissues. Subsequently, they showed more *in vitro* growth from cellular floaters initially detached from the *in ovo*-grown tumor. Importantly, plasma treatment reduced the amount of MiaPaCa2 and Panc01 cells grown *in vitro* after *in ovo* treatment of tumors. Similar findings were made for ZEB1 expression levels in the *in vitro* cultures. ZEB1 is a transcription factor highly associated with tumor progression and metastasis [65]. It is known that this factor is associated with EMT in pancreatic cancer and leads to signaling cascades changing the cellular polarity and reducing the expression of adhesion markers such as E-cadherin [18, 66, 67]. It is also associated with decreased prognosis in various types of tumors [68]. Besides ZEB1, another EMT marker is the TIMP2, which is involved in the suppression

of matrix metalloproteinase (MMP) activity and vascularization [39]. MiaPaCa2 and PaTuS cells had higher levels of *TIMP2* than PaTuT and Panc01 cells, suggesting these to be vulnerable to cellular outgrowth. Indeed, PaTuT showed more ZEB1 and vimentin expression than PaTuS cells. Also, other markers that are associated with the mesenchymal-like phenotype, such as αSMA, were not changed due to the treatment. These data suggest that plasma treatment was not promoting EMT and metastatic potential of human pancreatic cancer cells *in vitro* and *in ovo*. Even more, tumor cells with a more mesenchymal profile, such as Panc01, were particularly sensitive to plasma treatment in terms of reduced outgrowth, as seen in tumor spheroid experiments. In general, spheroids are utilized in several studies utilizing plasma treatments, while most of them are using plasma-oxidized media or lacked an additional extracellular matrix so that no outgrowth was monitored, but showed a strong reduction in the growth of these 3D-models [23, 28, 34, 69–76].

The inflammatory profile in the tumor microenvironment—especially regarding the crosstalk with stromal cells—is decisive in tumor metastasis ever since the discovery of the link between chronic inflammation and tumorigenesis by Rudolf Virchow in 1863 [77–79]. However, the specific traits of inflammation are as heterogeneous as are different tumor types and stages [80], but some universal findings include the pro-angiogenic property of TGFβ and VEGF [81]. While *in vitro* changes in both molecules were rather modest, we identified an increase in VEGF with plasma treatment *in ovo* with PaTuS and PaTuT, while VEGF was decreased in MiaPaCa2 and Panc01. It has to be stated, however, that the origin of targets measured in samples from *in ovo* experiments cannot be explicitly determined (due to, e.g., angiogenesis provided by the chicken embryo as well). Noteworthy, none of the 13 molecules investigated followed the same tendency after plasma treatment, neither *in vitro* nor *in ovo*. By contrast, for each cell line, there were clear and consistent patterns. For Panc01, the majority of targets were either similar or markedly decreased, especially *in vitro*. This supports other findings of this study, pointing to cellular senescence. This pathway has been recently unraveled in Panc01 cells, with miR-137 as a central switch [82] that may have also been activated with plasma treatment but warrants further studies. PaTuS and PaTuT, two sister cell lines with different metastatic potential, showed a similar regulation of chemokines and cytokines release (especially IL6, IL8, CXCL1, and VEGF) despite their different sensitivity to plasma treatment. VEGF production may be a consequence of hypoxia-inducible factor 1α (HIF1α) activation with IL8 serving as another molecule to support angiogenesis [83] and tumor growth [84]. By contrast, IL8 also is positively associated with oxidative immunogenic cancer cell death (ICD) in melanoma cells, together with the activation of dendritic cells [85]. This was similar to the increased levels of IL6 in that study. IL6 is a potent attractor of monocytes/macrophages [86], which can, in turn, be supportive or detrimental for tumor growth, depending on microenvironmental factors [87]. Being the ligand for CXCR2 [88] and a neutrophil chemoattractant [89], CXCL1 is associated with poor prognosis in cancer due to its growth-stimulating, pro-angiogenic properties [90], also in pancreatic cancer [91], by encouraging tumor-stromal interactions. Increased levels of this chemokine were found in PaTuS and PaTuT cells, which at least for PaTuS might explain the different tissue morphology observed for E-cadherin compared to that of PaTuS. Also, an increased release of IFNγ and TNFα was identified following plasma treatment. Both molecules were previously linked to antiproliferative effects in pancreatic cancer cells [92].

CONCLUSION

The results provide valuable insights into the effect of plasma treatment on metastasis-related properties of cancer cells *in vitro* and *in ovo* and did not suggest EMT-promoting effects of this novel cancer therapy. For future research, a detailed investigation of the EMT modulation through specific reactive species should be carried out. Although being technically challenging, future studies using *in vivo* models on cancer metastasis after plasma treatment are needed to validate our findings and the investigations should be extended to other tumor fields and clinical applications also. In addition, plasma treatment should be combined with existing therapies to identify its adjuvant potential.

DATA AVAILABILITY STATEMENT

The raw data supporting the conclusions of this article will be made available by the authors, without undue reservation.

ETHICS STATEMENT

Ethical review and approval was not required for the animal study because experiments with chicken embryos were terminated before day 15 from which on these experiments need to be declared to an ethics committee according to national regulations.

AUTHOR CONTRIBUTIONS

SB and AK designed the study. EF, CS, AS, and AP-M performed the experiments. EF and SB analyzed the data and prepared the figures and the manuscript draft. L-IP, AK, and SB supervised the study. AB, TvW, K-DW, C-DH, and SB provided funding and contributed to reagents and models. All authors have contributed the final manuscript.

FUNDING

This work was supported by the German Federal Ministry of Education and Research (grant numbers 03Z22DN11 and 03Z22Di1).

ACKNOWLEDGMENTS

We thankfully acknowledge the technical support by Felix Niessner and Antje Janetzko. We also thank Jonas Van Audenaerde and Evelien Smits for generating the transduced cell lines used in this study.

REFERENCES

1. Bray F, Ferlay J, Soerjomataram I, Siegel RL, Torre LA, Jemal A. Global cancer statistics 2018: globocan estimates of incidence and mortality worldwide for 36 cancers in 185 countries. *CA Cancer J. Clin.* (2018) **68**:394–424. doi: 10.3322/caac.21492
2. Ledford H, Else H, Warren M. Cancer immunologists scoop medicine nobel prize. *Nature.* (2018) **562**:20–1. doi: 10.1038/d41586-018-06751-0
3. Delyon J, Lebbe C, Dumaz N. Targeted therapies in melanoma beyond BRAF: targeting NRAS-mutated and KIT-mutated melanoma. *Curr Opin Oncol.* (2020) **32**:79–84. doi: 10.1097/CCO.0000000000000606
4. Domenichini A, Adamska A, Falasca M. Abc transporters as cancer drivers: potential functions in cancer development. *Biochim Biophys Acta Gen Subj.* (2019) **1863**:52–60. doi: 10.1016/j.bbagen.2018.09.019
5. Gondivkar SM, Gadbail AR, Choudhary MG, Vedpathak PR, Likhitkar MS. Photodynamic treatment outcomes of potentially-malignant lesions and malignancies of the head and neck region: a systematic review. *J. Investig. Clin. Dent.* (2018) **9**:e12270. doi: 10.1111/jicd.12270
6. Pinto A, Pocard M. Photodynamic therapy and photothermal therapy for the treatment of peritoneal metastasis: a systematic review. *Pleura Peritoneum.* (2018) **3**:20180124. doi: 10.1515/pp-2018-0124
7. Privat-Maldonado A, Schmidt A, Lin A, Weltmann KD, Wende K, Bogaerts A, et al. ROS from physical plasmas: redox chemistry for biomedical therapy. *Oxid. Med. Cell. Longev.* (2019) **2019**:9062098. doi: 10.1155/2019/9062098
8. von Woedtke T, Schmidt A, Bekeschus S, Wende K, Weltmann KD. Plasma medicine: a field of applied redox biology. *In Vivo.* (2019) **33**:1011–26. doi: 10.21873/invivo.11570
9. von Woedtke T, Schmidt A, Bekeschus S, Wende K. Introduction to plasma medicine. In: Metelmann H-R, von Woedtke T, Weltmann K-D, editors. *Comprehensive Clinical Plasma Medicine*. Cham: Springer International Publishing (2018). p. 3–21. doi: 10.1007/978-3-319-67627-2_1
10. Metelmann H-R, Seebauer C, Miller V, Fridman A, Bauer G, Graves DB, et al. Clinical experience with cold plasma in the treatment of locally advanced head and neck cancer. *Clin. Plas. Med.* (2018) **9**:6–13. doi: 10.1016/j.cpme.2017.09.001
11. Witzke K, Seebauer C, Jesse K, Kwiatek E, Berner J, Semmler M-L, et al. Plasma medical oncology: immunological interpretation of head and neck squamous cell carcinoma. *Plasma Process. Polym.* (2020). doi: 10.1002/ppap.201900258. [Epub ahead of print].
12. Hanahan D, Weinberg RA. Hallmarks of cancer: the next generation. *Cell.* (2011) **144**:646–74. doi: 10.1016/j.cell.2011.02.013
13. Mantovani A, Marchesi F, Malesci A, Laghi L, Allavena P. Tumour-associated macrophages as treatment targets in oncology. *Nat. Rev. Clin. Oncol.* (2017) **14**:399–416. doi: 10.1038/nrclinonc.2016.217
14. Tuting T, de Visser KE. Cancer. How neutrophils promote metastasis. *Science.* (2016) **352**:145–6. doi: 10.1126/science.aaf7300
15. Guan X. Cancer metastases: challenges and opportunities. *Acta Pharm Sin B.* (2015) **5**:402–18. doi: 10.1016/j.apsb.2015.07.005
16. Klaiber U, Schnaidt ES, Hinz U, Gaida MM, Heger U, Hank T, et al. Prognostic factors of survival after neoadjuvant treatment and resection for initially unresectable pancreatic cancer. *Ann. Surg.* (2019). doi: 10.1097/SLA.0000000000003270. [Epub ahead of print].
17. Mahajan UM, Langhoff E, Goni E, Costello E, Greenhalf W, Halloran C, et al. Immune cell and stromal signature associated with progression-free survival of patients with resected pancreatic ductal adenocarcinoma. *Gastroenterology.* (2018) **155**:1625–39.e1622. doi: 10.1053/j.gastro.2018.08.009
18. Krebs AM, Mitschke J, Lasierra Losada M, Schmalhofer O, Boerries M, Busch H, et al. The emt-activator zeb1 is a key factor for cell plasticity and promotes metastasis in pancreatic cancer. *Nat. Cell Biol.* (2017) **19**:518–29. doi: 10.1038/ncb3513
19. Granata V, Fusco R, Setola SV, Piccirillo M, Leongito M, Palaia R, et al. Early radiological assessment of locally advanced pancreatic cancer treated with electrochemotherapy. *World J. Gastroenterol.* (2017) **23**:4767–78. doi: 10.3748/wjg.v23.i26.4767
20. Jayson GC, Kerbel R, Ellis LM, Harris AL. Antiangiogenic therapy in oncology: current status and future directions. *Lancet.* (2016) **388**:518–29. doi: 10.1016/S0140-6736(15)01088-0
21. Tafuto S, von Arx C, De Divitiis C, Maura CT, Palaia R, Albino V, et al. Electrochemotherapy as a new approach on pancreatic cancer and on liver metastases. *Int. J. Surg.* (2015) **21**(Suppl. 1):S78–82. doi: 10.1016/j.ijsu.2015.04.095
22. Zheng X, Carstens JL, Kim J, Scheible M, Kaye J, Sugimoto H, et al. Epithelial-to-mesenchymal transition is dispensable for metastasis but induces chemoresistance in pancreatic cancer. *Nature.* (2015) **527**:525–30. doi: 10.1038/nature16064
23. Freund E, Liedtke KR, van der Linde J, Metelmann HR, Heidecke CD, Partecke LI, et al. Physical plasma-treated saline promotes an immunogenic phenotype in ct26 colon cancer cells *in vitro* and *in vivo*. *Sci. Rep.* (2019) **9**:634. doi: 10.1038/s41598-018-37169-3
24. Wende K, Schmidt A, Bekeschus S. Safety aspects of non-thermal plasmas. In: Metelmann H-R, von Woedtke T, Weltmann K-D, editors. *Comprehensive Clinical Plasma Medicine*. Cham: Springer International Publishing (2018). p. 83–109. doi: 10.1007/978-3-319-67627-2_5
25. Bekeschus S, Schmidt A, Kramer A, Metelmann HR, Adler F, von Woedtke T, et al. High throughput image cytometry micronucleus assay to investigate the presence or absence of mutagenic effects of cold physical plasma. *Environ. Mol. Mutagen.* (2018) **59**:268–77. doi: 10.1002/em.22172
26. Schmidt A, Woedtke TV, Stenzel J, Lindner T, Polei S, Vollmar B, et al. One year follow-up risk assessment in SKH-1 mice and wounds treated with an argon plasma jet. *Int. J. Mol. Sci.* (2017) **18**:868. doi: 10.3390/ijms18040868
27. Kluge S, Bekeschus S, Bender C, Benkhai H, Sckell A, Below H, et al. Investigating the mutagenicity of a cold argon-plasma jet in an het-mn model. *PLoS ONE.* (2016) **11**:e0160667. doi: 10.1371/journal.pone.0160667
28. Bekeschus S, Freund E, Spadola C, Privat-Maldonado A, Hackbarth C, Bogaerts A, et al. Risk assessment of kinpen plasma treatment of four human pancreatic cancer cell lines with respect to metastasis. *Cancers.* (2019) **11**:1237. doi: 10.3390/cancers11091237
29. Lademann J, Ulrich C, Patzelt A, Richter H, Kluschke F, Klebes M, et al. Risk assessment of the application of tissue-tolerable plasma on human skin. *Clin. Plas. Med.* (2013) **1**:5–10. doi: 10.1016/j.cpme.2013.01.001
30. Daeschlein G, Scholz S, Ahmed R, Majumdar A, von Woedtke T, Haase H. et al. Cold plasma is well-tolerated and does not disturb skin barrier or reduce skin moisture. *J Dtsch Dermatol Ges.* (2012) **10**:509–15. doi: 10.1111/j.1610-0387.2012.07857.x
31. Metelmann H-R, Vu TT, Do HT, Le TNB, Hoang THA, Phi TTT, et al. Scar formation of laser skin lesions after cold atmospheric pressure plasma (cap) treatment: a clinical long term observation. *Clin. Plas. Med.* (2013) **1**:30–5. doi: 10.1016/j.cpme.2012.12.001
32. Schuster M, Rutkowski R, Hauschild A, Shojaei RK, von Woedtke T, Rana A, et al. Side effects in cold plasma treatment of advanced oral cancer—clinical data and biological interpretation. *Clin. Plas. Med.* (2018) **10**:9–15. doi: 10.1016/j.cpme.2018.04.001
33. Cramer GM, Jones DP, El-Hamidi H, Celli JP. Ecm composition and rheology regulate growth, motility, and response to photodynamic therapy in 3D models of pancreatic ductal adenocarcinoma. *Mol. Cancer Res.* (2017) **15**:15–25. doi: 10.1158/1541-7786.MCR-16-0260
34. Privat-Maldonado A, Bengtson C, Razzokov J, Smits E, Bogaerts A. Modifying the tumour microenvironment: challenges and future perspectives for anticancer plasma treatments. *Cancers.* (2019) **11**:1920. doi: 10.3390/cancers11121920
35. Liao Z, Tan ZW, Zhu P, Tan NS. Cancer-associated fibroblasts in tumor microenvironment-accomplices in tumor malignancy. *Cell. Immunol.* (2018) **343**:103729. doi: 10.1016/j.cellimm.2017.12.003
36. Alonso-Nocelo M, Raimondo TM, Vining KH, Lopez-Lopez R, de la Fuente M, Mooney DJ. Matrix stiffness and tumor-associated macrophages modulate epithelial to mesenchymal transition of human adenocarcinoma cells. *Biofabrication.* (2018) **10**:035004. doi: 10.1088/1758-5090/aaafbc
37. Yilmaz M, Christofori G. EMT, the cytoskeleton, and cancer cell invasion. *Cancer Metastasis Rev.* (2009) **28**:15–33. doi: 10.1007/s10555-008-9169-0
38. Jesnowski R, Furst D, Ringel J, Chen Y, Schrodel A, Kleeff J, et al. Immortalization of pancreatic stellate cells as an *in vitro* model of pancreatic fibrosis: deactivation is induced by matrigel and n-acetylcysteine. *Lab. Invest.* (2005) **85**:1276–91. doi: 10.1038/labinvest.3700329

39. Seo D-W, Li H, Guedez L, Wingfield PT, Diaz T, Salloum R, et al. Timp-2 mediated inhibition of angiogenesis: an mmp-independent mechanism. *Cell.* (2003) **114**:171–80. doi: 10.1016/S0092-8674(03)00551-8
40. Collins A, Bloomston M. Diagnosis and management of pancreatic cancer. *Minerva Gastroenterol. Dietol.* (2009) **55**:445–54.
41. Ellenrieder V, Adler G, Gress TM. Invasion and metastasis in pancreatic cancer. *Ann. Oncol.* (1999) **10**:S46–50. doi: 10.1093/annonc/10.suppl_4.S46
42. Ghaneh P, Costello E, Neoptolemos JP. Biology and management of pancreatic cancer. *Postgrad. Med. J.* (2008) **84**:478–97. doi: 10.1136/gut.2006.103333
43. Flaum N, Hubner RA, Valle JW, Amir E, McNamara MG. Adjuvant chemotherapy and outcomes in patients with nodal and resection margin-negative pancreatic ductal adenocarcinoma: a systematic review and meta-analysis. *J. Surg. Oncol.* (2019) **119**:932–40. doi: 10.1002/jso.25440
44. Esposito I, Kleeff J, Bergmann F, Reiser C, Herpel E, Friess H, et al. Most pancreatic cancer resections are r1 resections. *Ann. Surg. Oncol.* (2008) **15**:1651–60. doi: 10.1245/s10434-008-9839-8
45. Bekeschus S, Kading A, Schroder T, Wende K, Hackbarth C, Liedtke KR, et al. Cold physical plasma-treated buffered saline solution as effective agent against pancreatic cancer cells. *Anticancer Agents Med. Chem.* (2018) **18**:824–31. doi: 10.2174/1871520618666180507130243
46. Liedtke KR, Diedrich S, Pati O, Freund E, Flieger R, Heidecke CD, et al. Cold physical plasma selectively elicits apoptosis in murine pancreatic cancer cells *in vitro* and *in ovo*. *Anticancer Res.* (2018) **38**:5655–63. doi: 10.21873/anticanres.12901
47. Masur K, von Behr M, Bekeschus S, Weltmann KD, Hackbarth C, Heidecke CD, et al. Synergistic inhibition of tumor cell proliferation by cold plasma and gemcitabine. *Plasma Process. Polym.* (2015) **12**:1377–82. doi: 10.1002/ppap.201500123
48. Yan D, Cui H, Zhu W, Nourmohammadi N, Milberg J, Zhang LG, et al. The specific vulnerabilities of cancer cells to the cold atmospheric plasma-stimulated solutions. *Sci. Rep.* (2017) **7**:4479. doi: 10.1038/s41598-017-04770-x
49. Hattori N, Yamada S, Torii K, Takeda S, Nakamura K, Tanaka H, et al. Effectiveness of plasma treatment on pancreatic cancer cells. *Int. J. Oncol.* (2015) **47**:1655–62. doi: 10.3892/ijo.2015.3149
50. Liedtke KR, Bekeschus S, Kaeding A, Hackbarth C, Kuehn JP, Heidecke CD, et al. Non-thermal plasma-treated solution demonstrates antitumor activity against pancreatic cancer cells *in vitro* and *in vivo*. *Sci. Rep.* (2017) **7**:8319. doi: 10.1038/s41598-017-08560-3
51. Sato Y, Yamada S, Takeda S, Hattori N, Nakamura K, Tanaka H, et al. Effect of plasma-activated lactated ringer's solution on pancreatic cancer cells *in vitro* and *in vivo*. *Ann. Surg. Oncol.* (2018) **25**:299–307. doi: 10.1245/s10434-017-6239-y
52. Partecke LI, Evert K, Haugk J, Doering F, Normann L, Diedrich S, et al. Tissue tolerable plasma (ttp) induces apoptosis in pancreatic cancer cells *in vitro* and *in vivo*. *BMC Cancer.* (2012) **12**:473. doi: 10.1186/1471-2407-12-473
53. Stoffels E, Kieft IE, Sladek REJ, van den Bedem LJM, van der Laan EP, Steinbuch M. Plasma needle for *in vivo* medical treatment: recent developments and perspectives. *Plasma Sources Sci. T.* (2006) **15**:S169–80. doi: 10.1088/0963-0252/15/4/S03
54. Stoffels E, Roks AJM, Deelmm LE. Delayed effects of cold atmospheric plasma on vascular cells. *Plasma Process. Polym.* (2008) **5**:599–605. doi: 10.1002/ppap.200800028
55. Stoffels E, Sakiyama Y, Graves DB. Cold atmospheric plasma: charged species and their interactions with cells and tissues. *IEEE Trans. Plasma Sci.* (2008) **36**:1441–57. doi: 10.1109/TPS.2008.2001084
56. Ribatti D. The chick embryo chorioallantoic membrane (cam). A multifaceted experimental model. *Mech. Dev.* (2016) **141**:70–7. doi: 10.1016/j.mod.2016.05.003
57. Izard T, Brown DT. Mechanisms and functions of vinculin interactions with phospholipids at cell adhesion sites. *J. Biol. Chem.* (2016) **291**:2548–55. doi: 10.1074/jbc.R115.686493
58. Shih HP, Panlasigui D, Cirulli V, Sander M. ECM signaling regulates collective cellular dynamics to control pancreas branching morphogenesis. *Cell Rep.* (2016) **14**:169–79. doi: 10.1016/j.celrep.2015.12.027
59. Beachley VZ, Wolf MT, Sadtler K, Manda SS, Jacobs H, Blatchley MR, et al. Tissue matrix arrays for high-throughput screening and systems analysis of cell function. *Nat. Methods.* (2015) **12**:1197–204. doi: 10.1038/nmeth.3619
60. Grzesiak JJ, Ho JC, Moossa AR, Bouvet M. The integrin-extracellular matrix axis in pancreatic cancer. *Pancreas.* (2007) **35**:293–301. doi: 10.1097/mpa.0b013e31811f4526
61. Ni J, Cozzi PJ, Duan W, Shigdar S, Graham PH, John KH, et al. Role of the EpCAM (CD326) in prostate cancer metastasis and progression. *Cancer Metastasis Rev.* (2012) **31**:779–91. doi: 10.1007/s10555-012-9389-1
62. Munz M, Baeuerle PA, Gires O. The emerging role of epcam in cancer and stem cell signaling. *Cancer Res.* (2009) **69**:5627. doi: 10.1158/0008-5472.CAN-09-0654
63. Baeuerle PA, Gires O. EpCAM (CD326) finding its role in cancer. *Br. J. Cancer.* (2007) **96**:417–23. doi: 10.1038/sj.bjc.6603494
64. Canel M, Serrels A, Frame MC, Brunton VG. E-cadherin-integrin crosstalk in cancer invasion and metastasis. *J. Cell Sci.* (2013) **126**:393–401. doi: 10.1242/jcs.100115
65. Spaderna S, Schmalhofer O, Wahlbuhl M, Dimmler A, Bauer K, Sultan A, et al. The transcriptional repressor ZEB1 promotes metastasis and loss of cell polarity in cancer. *Cancer Res.* (2008) **68**:537–44. doi: 10.1158/0008-5472.CAN-07-5682
66. Wellner U, Brabletz T, Keck T. Zeb1 in pancreatic cancer. *Cancers.* (2010) **2**:1617–28. doi: 10.3390/cancers2031617
67. Kurahara H, Takao S, Maemura K, Mataki Y, Kuwahata T, Maeda K, et al. Epithelial–mesenchymal transition and mesenchymal–epithelial transition via regulation of ZEB-1 and ZEB-2 expression in pancreatic cancer. *J. Surg. Oncol.* (2012) **105**:655–61. doi: 10.1002/jso.23020
68. Zhang GJ, Zhou T, Tian HP, Liu ZL, Xia SS. High expression of ZEB1 correlates with liver metastasis and poor prognosis in colorectal cancer. *Oncol. Lett.* (2013) **5**:564–68. doi: 10.3892/ol.2012.1026
69. Judee F, Fongia C, Ducommun B, Yousfi M, Lobjois V, Merbahi N. Short and long time effects of low temperature plasma activated media on 3D multicellular tumor spheroids. *Sci. Rep.* (2016) **6**:21421. doi: 10.1038/srep21421
70. Chauvin J, Gibot L, Griseti E, Golzio M, Rols MP, Merbahi N, et al. Elucidation of *in vitro* cellular steps induced by antitumor treatment with plasma-activated medium. *Sci. Rep.* (2019) **9**:4866. doi: 10.1038/s41598-019-41408-6
71. Gandhirajan RK, Rodder K, Bodnar Y, Pasqual-Melo G, Emmert S, Griguer CE, et al. Cytochrome C oxidase inhibition and cold plasma-derived oxidants synergize in melanoma cell death induction. *Sci. Rep.* (2018) **8**:12734. doi: 10.1038/s41598-018-31031-2
72. Sagwal SK, Pasqual-Melo G, Bodnar Y, Gandhirajan RK, Bekeschus S. Combination of chemotherapy and physical plasma elicits melanoma cell death via upregulation of SLC22A16. *Cell Death Dis.* (2018) **9**:1179. doi: 10.1038/s41419-018-1221-6
73. Privat-Maldonado A, Gorbanev Y, Dewilde S, Smits E, Bogaerts A. Reduction of human glioblastoma spheroids using cold atmospheric plasma: the combined effect of short- and long-lived reactive species. *Cancers.* (2018) **10**:394. doi: 10.3390/cancers10110394
74. Beaumont KA, Mohana-Kumaran N, Haass NK. Modeling melanoma *in vitro* and *in vivo*. *Healthcare.* (2013) **2**:27–46. doi: 10.3390/healthcare2010027
75. Griseti E, Kolosnjaj-Tabi J, Gibot L, Fourquaux I, Rols MP, Yousfi M, et al. Pulsed electric field treatment enhances the cytotoxicity of plasma-activated liquids in a three-dimensional human colorectal cancer cell model. *Sci. Rep.* (2019) **9**:7583. doi: 10.1038/s41598-019-44087-5
76. Freund E, Liedtke KR, Miebach L, Wende K, Heidecke A, Kaushik NK, et al. Identification of two kinase inhibitors with synergistic toxicity with low-dose hydrogen peroxide in colorectal cancer cells *in vitro*. *Cancers.* (2020) **12**:122. doi: 10.3390/cancers12010122
77. Balkwill F, Mantovani A. Inflammation and cancer: back to virchow? *Lancet.* (2001) **357**:539–45. doi: 10.1016/S0140-6736(00)04046-0
78. Coussens LM, Werb Z. Inflammation and cancer. *Nature.* (2002) **420**:860–7. doi: 10.1038/nature01322
79. Steele CW, Jamieson NB, Evans TR, McKay CJ, Sansom OJ, Morton JP, et al. Exploiting inflammation for therapeutic gain in pancreatic cancer. *Br. J. Cancer.* (2013) **108**:997–1003. doi: 10.1038/bjc.2013.24
80. Savant SS, Sriramkumar S, O'Hagan HM. The role of inflammation and inflammatory mediators in the development, progression, metastasis,

and chemoresistance of epithelial ovarian cancer. *Cancers.* (2018) **10**:251. doi: 10.3390/cancers10080251
81. Quail DF, Joyce JA. Microenvironmental regulation of tumor progression and metastasis. *Nat. Med.* (2013) **19**:1423–37. doi: 10.1038/nm.3394
82. Neault M, Mallette FA, Richard S. miR-137 modulates a tumor suppressor network-inducing senescence in pancreatic cancer cells. *Cell Rep.* (2016) **14**:1966–78. doi: 10.1016/j.celrep.2016.01.068
83. Mizukami Y, Jo WS, Duerr EM, Gala M, Li J, Zhang X, et al. Induction of interleukin-8 preserves the angiogenic response in hif-1alpha-deficient colon cancer cells. *Nat. Med.* (2005) **11**:992–7. doi: 10.1038/nm1294
84. Garofalo M, Iovine B, Kuryk L, Capasso C, Hirvinen M, Vitale A, et al. Oncolytic adenovirus loaded with l-carnosine as novel strategy to enhance the antitumor activity. *Mol. Cancer Ther.* (2016) **15**:651–60. doi: 10.1158/1535-7163.MCT-15-0559
85. Dudek-Peric AM, Ferreira GB, Muchowicz A, Wouters J, Prada N, Martin S, et al. Antitumor immunity triggered by melphalan is potentiated by melanoma cell surface-associated calreticulin. *Cancer Res.* (2015) **75**:1603–14. doi: 10.1158/0008-5472.CAN-14-2089
86. Clahsen T, Schaper F. Interleukin-6 acts in the fashion of a classical chemokine on monocytic cells by inducing integrin activation, cell adhesion, actin polymerization, chemotaxis, and transmigration. *J. Leukoc. Biol.* (2008) **84**:1521–9. doi: 10.1189/jlb.0308178
87. Najafi M, Hashemi Goradel N, Farhood B, Salehi E, Nashtaei MS, Khanlarkhani N, et al. Macrophage polarity in cancer: a review. *J. Cell. Biochem.* (2019) **120**:2756–65. doi: 10.1002/jcb.27646
88. Tsai H-H, Frost E, To V, Robinson S, ffrench-Constant C, Geertman R, et al. The chemokine receptor CXCR2 controls positioning of oligodendrocyte precursors in developing spinal cord by arresting their migration. *Cell.* (2002) **110**:373–83. doi: 10.1016/S0092-8674(02)00838-3
89. De Filippo K, Dudeck A, Hasenberg M, Nye E, van Rooijen N, Hartmann K, et al. Mast cell and macrophage chemokines CXCL1/CXCL2 control the early stage of neutrophil recruitment during tissue inflammation. *Blood.* (2013) **121**:4930–7. doi: 10.1182/blood-2013-02-486217
90. Acharyya S, Oskarsson T, Vanharanta S, Malladi S, Kim J, Morris PG, et al. A CXCL1 paracrine network links cancer chemoresistance and metastasis. *Cell.* (2012) **150**:165–78. doi: 10.1016/j.cell.2012.04.042
91. Ijichi H, Chytil A, Gorska AE, Aakre ME, Bierie B, Tada M, et al. Inhibiting CXCR2 disrupts tumor-stromal interactions and improves survival in a mouse model of pancreatic ductal adenocarcinoma. *J. Clin. Invest.* (2011) **121**:4106–17. doi: 10.1172/JCI42754
92. Schmiegel WH, Caesar J, Kalthoff H, Greten H, Schreiber HW, Thiele HG. Antiproliferative effects exerted by recombinant human tumor necrosis factor-alpha (tnf-alpha) and interferon-gamma (ifn-gamma) on human pancreatic tumor cell lines. *Pancreas.* (1988) **3**:180–8. doi: 10.1097/00006676-198804000-00012

Conflict of Interest: The authors declare that the research was conducted in the absence of any commercial or financial relationships that could be construed as a potential conflict of interest.

frontiers in Physics

ORIGINAL RESEARCH
published: 14 January 2021
doi: 10.3389/fphy.2020.613046

Biomolecules as Model Indicators of *In Vitro* and *In Vivo* Cold Plasma Safety

Caitlin Heslin[1], *Daniela Boehm*[1]*, *Brendan F. Gilmore*[2], *Julianne Megaw*[2], *Theresa A. Freeman*[3], *Noreen J. Hickok*[3], *P. J. Cullen*[1,4] and *Paula Bourke*[1,5,6]*

[1]School of Food Science and Environmental Health, Technological University Dublin, Dublin, Ireland, [2]School of Pharmacy, Queens University Belfast, Belfast, United Kingdom, [3]Department of Orthopaedic Surgery, Sidney Kimmel Medical College, Jefferson University, Philadelphia, PA, United States, [4]School of Chemical and Biomolecular Engineering, University of Sydney, Sydney, NSW, Australia, [5]School of Biological Sciences, Queens University Belfast, Belfast, United Kingdom, [6]Plasma Research Group, School of Biosystems and Food Engineering, University College Dublin, Dublin, Ireland

The potential applications for cold plasma in medicine are extensive, from microbial inactivation and induction of apoptosis in cancer cells to stimulating wound healing and enhancing the blood coagulation cascade. The safe bio-medical application of cold plasma and subsequent effect on complex biological pathways requires precision and a distinct understanding of how physiological redox chemistry is manipulated. Chemical modification of biomolecules such as carbohydrates, proteins, and lipids treated with cold plasma have been characterized, however, the context of how alterations of these molecules affect cell behavior or *in vivo* functionality has not been determined. Thus, this study examines the cytotoxic and mutagenic effects of plasma-treated molecules *in vitro* using CHO-K1 cells and *in vivo* in *Galleria mellonella* larvae. Specifically, albumin, glucose, cholesterol, and arachidonic acid were chosen as representative biomolecules, with established involvement in diverse bioprocesses including; cellular respiration, intracellular transport, cell signaling or membrane structure. Long- and short-term effects depended strongly on the molecule type and the treatment milieu indicating the impact of chemical and physical modifications on downstream biological pathways. Importantly, absence of short-term toxicity did not always correlate with absence of longer-term effects, indicating the need to comprehensively assess ongoing effects for diverse biological applications.

Keywords: cold atmospheric plasma, cytotoxicity, mutagenicity, safety, *In vivo* toxicity

OPEN ACCESS

Edited by:
Mounir Laroussi,
Old Dominion University,
United States

Reviewed by:
Vandana Miller,
Drexel University, United States
Katharina Stapelmann,
North Carolina State University,
United States

***Correspondence:**
Paula Bourke
paula.bourke@ucd.ie
Daniela Boehm
daniela.boehm@tudublin.ie

Specialty section:
This article was submitted to Plasma Physics, a section of the journal Frontiers in Physics

Received: *01 October 2020*
Accepted: *16 November 2020*
Published: *14 January 2021*

Citation:
Heslin C, Boehm D, Gilmore BF, Megaw J, Freeman TA, Hickok NJ, Cullen PJ and Bourke P (2021) Biomolecules as Model Indicators of In Vitro *and* In Vivo *Cold Plasma Safety. Front. Phys. 8:613046. doi: 10.3389/fphy.2020.613046*

INTRODUCTION

The biological effects of cold plasma are complex and occur at the biological interface between biophysics, biochemistry and cell biology. Cold plasma is produced by applying energy to a gaseous environment. As the gas is ionized a complex mixture of reactive components is generated. The application of cold plasma technology to biological targets has revealed effectiveness in a diverse range of activities from promoting cell proliferation [1], blood coagulation [2], cancer treatment [3, 4], and inducement of specific cell senescence [5]. Other noteworthy applications of cold plasma have included disinfection potentially with reduced risk of antimicrobial resistance [6–8], decontamination of fresh produce [9], bio-decontamination of heat sensitive products [10], seeds and grains with an aim for human consumption [11, 12] and areas key to the sustainability of food and agriculture [13, 14].

The biological effects of plasma and plasma generated chemistry are dependent on the surrounding liquid environment [15–18]. In fact, studies have indicated immense variability in the biological effects attributed to cold plasma, depending on both the composition of the sample substrate and that of the ionized gas. Thus, for successful application of cold plasma technology it is important to not only understand interactions at the bio-plasma interface during treatment, but also to understand the short-term and long-term consequences of plasma induced biomolecule alteration and the effect this may have on biochemical processes. In fact, plasma induced chemical modification of proteins and amino acids [19, 20] and lipids [21] have been studied in isolation. Additionally, both simulated, modeling studies and direct experimentation have shown how interactions of cold plasma chemical species modify amino acids [22, 23], change protein structure and function [19, 24–26] and oxidize lipids [27, 28] but these studies are limited in their ability to examine or understand the long-term biological effects of the plasma induced modifications in a complex biosystem.

Encouragingly, investigations of direct plasma jet [29] or surface micro-discharge treatment on mammalian cells showed negligible mutagenic effects [30] and no mutagenic potential using the *in vivo* HET-MN model [31]. In fact, a range of investigations on human or animal tissues *in vivo* and clinical application of several certified plasma devices suggest that cold plasma treatment under these conditions is well tolerated and safe [32] and no long-term adverse effects have been reported to-date [33, 34]. However, other studies have also demonstrated that cold plasma can be modulated to become a powerful mutagenesis tool under appropriate conditions [35, 36] and mutagenic effects of cold plasma treated complex bio-fluids on mammalian cells have been documented, but not directly elucidated [37], suggesting that genetic damage is possible where cells experience exposure to intense plasma or plasma reactive species over extensive periods of time.

In an effort to reconcile these differences, this study examines the cytotoxic and mutagenic potential of plasma-treated biomolecules using both *in vitro* and *in vivo* models chosen for relevance to a range of biological environments which incorporate protein, lipid and carbohydrate components. Bovine serum albumin was selected as a representative protein molecule and for its chemical similarity to human serum albumin which is an abundant antioxidant protein in the blood. Arachidonic acid was chosen as an essential omega-6 polyunsaturated fatty acid [38] with four cis double bonds that contributes to mammalian cell membrane fluidity at physiological temperatures and is a precursor of eicosanoids [39]. Cholesterol, a sterol synthesised by all animal cells, is required for membrane structural integrity and flexibility. Cholesterol is a monounsaturated fatty acid precursor for all steroid hormones and functions in intracellular transport and cell signaling with the formation of lipid rafts in the plasma membrane [40]. Glucose was selected as a model carbohydrate and ubiquitous fuel source in biology. The safe application of cold plasma and subsequent effect on complex biochemical pathways requires precision and a distinct understanding of how physiological redox chemistry is manipulated.

RESULTS

Cytotoxicity Dependent on Biomolecular Structure

To assess the short-term cytotoxic effect of plasma treated biomolecules, selected biomolecules were dissolved in deionised water and subjected to plasma treatment. CHO-K1 cells were seeded at 2.5×10^4 cells/ml with 20% v/v of these treated biomolecules and cell growth was assessed after 2–3 days (**Figure 1**).

Prolonged plasma treatment of the bio-molecular solutions induced cytotoxicity in the CHO-K1 cell line, which was dependent on plasma treatment time (**Figure 1**). Plasma treated cholesterol elicited the strongest cytotoxic reaction. The growth of CHO-K1 cells cultured with plasma treated cholesterol was reduced to 75% with 1 min of plasma treatment compared to 94% (BSA), 84% (arachidonic acid), and 96% (glucose) and was less than 1% when cultured with cholesterol treated for 5 and 10 min. This is in contrast to arachidonic acid and glucose, where cell growth was reduced to 62% and 74% with 5 min treatment and decreased to 35% and 43% with 10 min of treatment respectively. CHO-K1 cells cultured with BSA plasma treated for 5 min were reduced to 30% and failed to grow when cultured with BSA treated for 10 min.

Exposing aqueous solutions to cold plasma treatment leads to the generation of hydrogen peroxide among other molecules, which may be a useful indicator of plasma activity and potential predictor of the cytotoxicity of the solutions. The aqueous treatment environment provides the substrate to generate complex plasma-liquid chemistry without the same quenching effect that cell culture media provides. Measurements of pH and hydrogen peroxide were used as an indicator of plasma-liquid chemistry (**Figure 2**). The H_2O_2 quantification of the plasma treated biomolecular solutions indicated that the surrounding media influences the generated plasma chemistry and may have an effect on the biomolecules or generation of secondary products (**Figures 2B,C**). As hydrogen peroxide has been identified as a major contributor to cytotoxic effects of plasma treated liquids, cell growth was correlated to the hydrogen peroxide concentration of the respective biomolecule solution used at 20% v/v and the IC50 was determined. Cell growth data obtained from biomolecules dissolved in DMEM-F12 and used at 10% v/v for the mutagenicity assays below, are plotted in the same graphs for comparison purposes (**Figure 3**).

A comparison of the plasma-treated biomolecule solutions as a function of their hydrogen peroxide content, serves to indicate whether the differences in cytotoxicity are based on differences in their scavenging of hydrogen peroxide or on toxic modifications of the biomolecules themselves. The IC50 values of hydrogen peroxide for plasma treated biomolecules dissolved in deionised water ranged from 22 μM for BSA (**Figure 3A**), 34 μM for cholesterol (**Figure 3B**), to 60 μM for arachidonic acid (**Figure 3C**) and 71 μM for glucose solutions (**Figure 3D**). These data suggested that differences in hydrogen peroxide concentration were not the primary determinant of differences in toxicity. The dose-response curves obtained for biomolecules

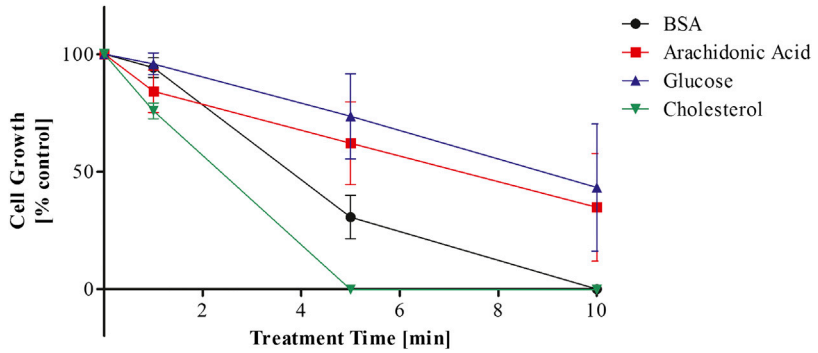

FIGURE 1 | Cytotoxicity of plasma treated biomolecules dissolved in deionised water over plasma treatment time.

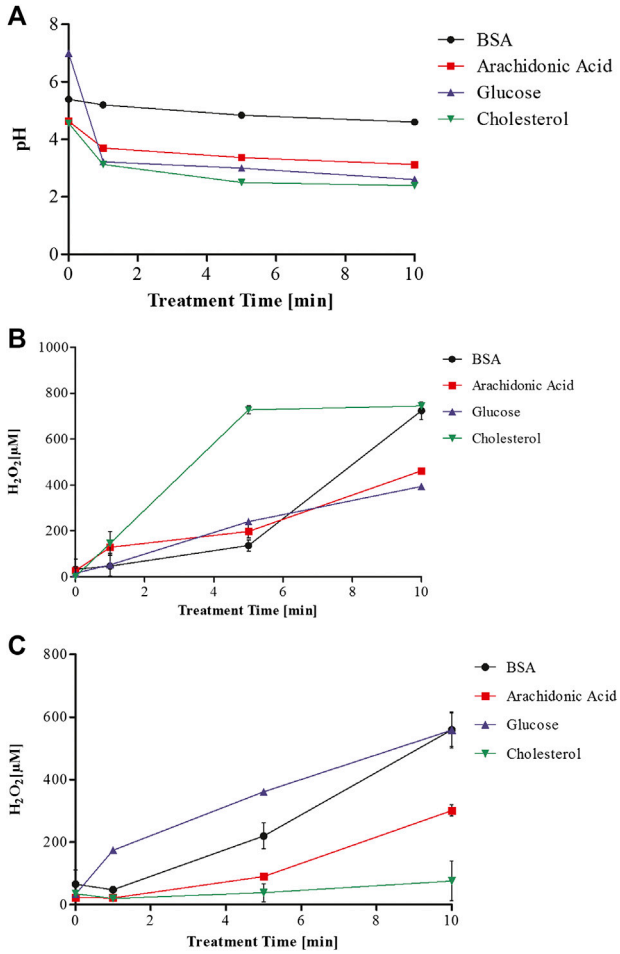

FIGURE 2 | pH of plasma treated biomolecules dissolved in deionised water **(A)** and hydrogen peroxide quantification of plasma treated biomolecules dissolved in deionised water **(B)** and dissolved in DMEM-F12 **(C)**.

dissolved in DMEM displayed similar trends to those for biomolecules treated in water with the notable exception of BSA. The increased cytotoxicity associated with plasma treated BSA-water solutions may be due to the lack of pH buffering capacity accompanied by the more oxidative environment of the water with less scavenging potential for plasma generated reactive species. These conditions could potentially lead to the generation of toxic bi-products in the plasma treated aqueous biomolecular solutions that may not occur in the DMEM-F12 solution.

Mutagenic Effect of Plasma Treated Biomolecules

CHO-K1 cells were cultured with 10% v/v of biomolecules dissolved in DMEM-F12 to assess the long term mutagenic effects of plasma treated biomolecules using the hypoxanthine phosphoribosyl transferase (HPRT) assay. The growth of CHO-K1 cells cultured in 10% v/v of plasma treated solutions was assessed to ensure cells were growing in selected conditions (**Figure 4**). Cell growth of CHO-K1 cells cultured in arachidonic acid solution treated with plasma for 10 min was reduced by 50%. Cells that were cultured with plasma treated BSA and glucose were reduced to 75% and 78% respectively for the 10 min treated biomolecule (**Figure 4**). Plasma treated cholesterol did not appear to exhibit the same degree of cytotoxicity following prolonged plasma treatment as cell growth remained stable even at the extended treatment time of 10 min. This is in contrast to effects found for cholesterol treated in water above (**Figure 3**). The cytotoxic effects observed were independent of pH as the value of the buffered solutions did not decrease below a pH of 6.8 for the prolonged treatment time of 10 min for glucose and cholesterol and a pH of 7.1 for BSA and arachidonic acid.

In order to assess the long-term mutagenic potential of plasma treated biomolecules, CHO-K1 cells were cultured with plasma treated biomolecule solutions over 34 days and monitored for HPRT-deficient mutants through colony formation in selective medium. Data is presented as cumulative data from experiments performed in triplicate, with all replicates plated in three independent plates at each time point and is displayed as percentage positive plates of the overall plates assessed at each time point (Original data available as **Supplementary Table S1**). Plasma treated biomolecules caused an increase in mutant colonies over time of culture and time of extended plasma treatment of the biomolecule solution (**Figure 5**).

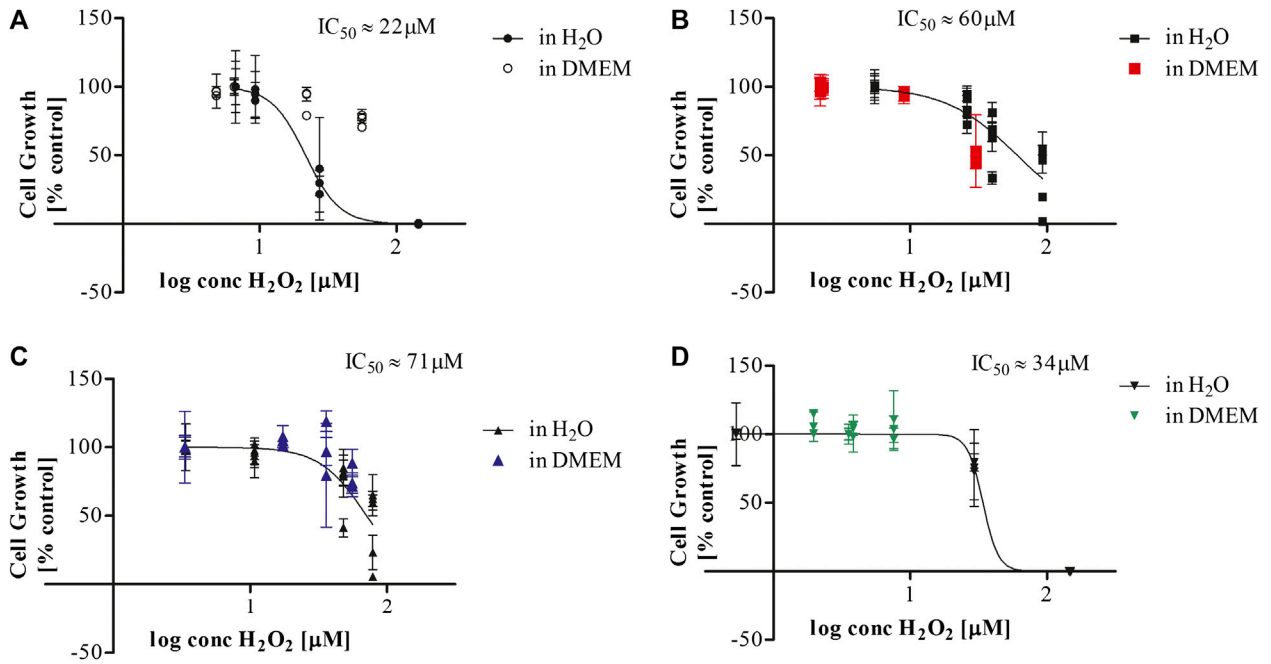

FIGURE 3 | IC50 determination for plasma treated biomolecules dissolved in deionised water and DMEM **(A)** BSA, **(B)** Arachidonic acid, **(C)** Glucose, **(D)** Cholesterol.

HPRT colony formation in CHO-K1 cells cultured with plasma-treated BSA increased over cell culture period and with the prolonged plasma treatment time of 10 min (**Figure 5A**) and reached a maximum HPRT+ of 56% of replicates for 10 min plasma treatment after 27 days of exposure. Plasma treated arachidonic acid was consistently HPRT+ after 13 days of culture for 5 and 10 min plasma treatment times, with a maximum of 50% HPRT+ replicates on day 34 of culture (**Figure 5B**). Glucose displayed the greatest mutagenic potential aligned with plasma treatment time and cell culture period (**Figure 5C**). There was a maximum of 78% HPRT+ replicates for the 10 min plasma treated glucose after 27 days in culture. Plasma treated cholesterol exhibited low mutagenic potential even with the extended treatment time of 10 min reaching a maximum of 22% HPRT+ after 27 days in culture (**Figure 5D**).

Plasma treated glucose exhibited the greatest mutagenic potential accounting for 36% of the total HPRT+ colonies (**Figure 6**).

In vivo Model System to Test Plasma Treated Biomolecule Toxicity

Larvae of the wax moth *Galleria mellonella* were used as a model system to assess the toxicity of plasma treated biomolecules *in vivo* through injection. The plasma treated biomolecules were found to be well tolerated by the *Galleria* larvae with ~100% survival (**Figure 7**). Haemocyte density was assessed as an indicator of overall larvae health. There was no significant increase in haemocyte density as would be observed if the larvae were under substantial stress (data not shown). For comparison, larvae were also injected with deionised water subjected to the same plasma treatment and hydrogen peroxide solutions at concentrations between 100 and 900 μM. The larvae tolerated the plasma treated deionised water well and haemocyte density was not affected (data not shown). The larvae did not tolerate the higher concentrations of hydrogen peroxide despite the concentrations being in the same range as measured in the plasma treated biomolecules (**Figure 9**). The surviving larvae were assessed for haemocyte density and levels were not significantly different from the control. This indicates that the immune system had not been challenged and that the solutions did not stimulate a non-selective immune response. Despite the equivalence in peroxide concentrations, this study indicated that there was no toxicity of the plasma treated biomolecules to the *in vivo* model *G. mellonella* under the conditions tested.

As a comparative indicator of their susceptibility, the IC50/LD50 for hydrogen peroxide was determined for both the *in vitro* and *in vivo* model systems used. In the CHO-K1 *in vitro* model, the IC50 of H_2O_2 was 140 μM (**Figure 8**) compared to the *G. mellonella in vivo* model that had an LD50 of 675 μM (**Figure 9**) for 20 μl of injected hydrogen peroxide. While the mode of exposure of the larvae/cells is not comparable, this nonetheless supports the much higher tolerance observed for *G. mellonella* larvae injected with biomolecules compared to the direct exposure of CHO-K1 cells to biomolecule-supplemented medium.

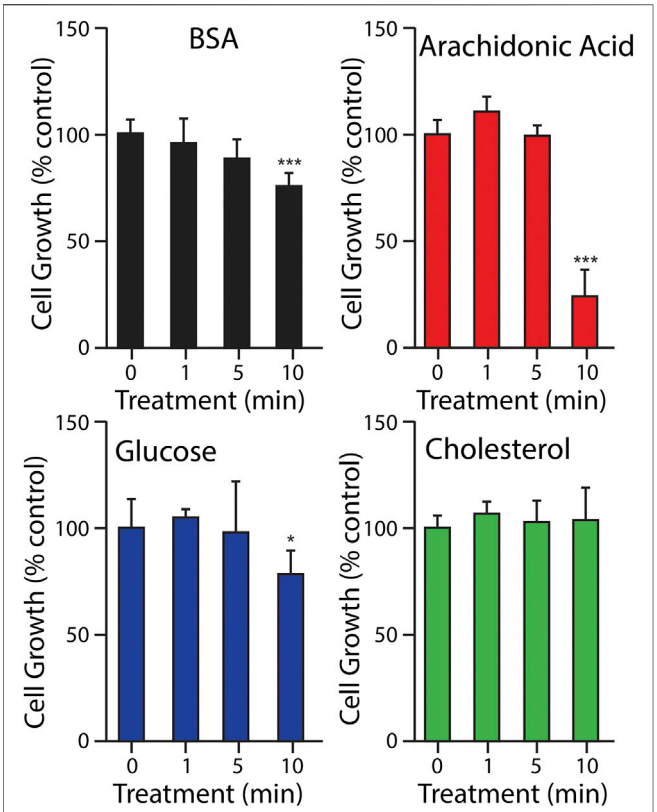

FIGURE 4 | Growth of CHO-K1 cells in 10% v/v of physiological levels of selected biomolecules after plasma treatment. Different letters indicate a significant difference between treatment times ($p < 0.05$).

DISCUSSION

Whilst eukaryotic cells have developed methods of dealing with oxidative stress induced biomolecule modification and have mechanisms to restore redox balance, detrimental effects due to excessive ROS do occur. The downstream biological effects of these structural changes remain to be investigated. To elucidate the mechanisms of actions and potential long-term effects of cold plasma, we chose four biomolecules involved in diverse biochemical pathways and a multitude of bioprocesses including; cellular respiration, intracellular transport, cell signaling or cell membrane structural components to analyse in this investigation. Plasma-induced chemical modifications of proteins, DNA, lipids and carbohydrates and associated structural modifications are dependent on gas composition, plasma discharge characteristics and liquid environment [22]. Results indicate that plasma induced chemical alterations to the biomolecular structure of these molecules has the potential to cause repercussions in cellular processes or to generate toxic/mutagenic metabolites.

The eukaryotic cell membrane is composed of two lipid monolayers embedded with proteins. The effects of cold plasma on cell membranes include transient pore formation through lipid peroxidation due to hydroxyl radicals [41]. H_2O_2 and O_3 are indirectly involved in lipid peroxidation through the generation of hydroxyl radicals through the iron-catalysed Haber–Weiss reaction [42] and the lipid radical is able to propagate a chain reaction of lipid peroxidation of nearby lipids. The direct exposure to oxidants such as hydrogen peroxide or lipid hydroperoxides has been shown to directly induce apoptosis in various cell types [43]. Cholesterol is a monounsaturated fatty acid found in cell membranes and is prone to oxidation by oxygen free-radicals generating products such as hydroperoxides and oxysterols [40]. When cholesterol dissolved in deionised water was treated with plasma, significant cytotoxic effects were observed on CHO-K1 cells after just 5 min of plasma treatment. The H_2O_2 measurement of plasma treated cholesterol in H_2O measured the highest of the biomolecules over 700 μM and can be correlated to the higher cytotoxic effects observed. However, as the IC50 indicates, H_2O_2 is not the only cytotoxic factor generated in the plasma treated solution. Despite the short-term cytotoxic effects observed for plasma treated cholesterol dissolved in H_2O *in vitro*, the treated biomolecule was well tolerated by the *in vivo* model of *G. mellonella*. Plasma treated cholesterol also exhibited the lowest mutagenic potential of the selected biomolecules despite oxidation products of cholesterol such as epoxide demonstrating mutagenic potential *in vitro* [44, 45]. The short-term cytotoxicity observed in this study may be attributed to differences in the biochemical structures of the biomolecules and the aqueous environment they were treated in.

Arachidonic acid is an essential polyunsaturated fatty acid released during epithelial disruption and wound healing and is a crucial mediator of inflammation. Either directly or after enzymatic conversion to eiconsanoids, arachidonic acid modulates the function of various organs and systems including the digestive, renal, reproductive and immune systems [38]. The ability of arachidonic acid to induce cytotoxic effects, which were apoptotic in nature, in liver cells was predominantly attributed to lipid peroxidation and oxidative stress, where lipid peroxidation endproducts were detected and the exposure of cells supplemented with arachidonic acid to exogenous antioxidants provided protective effects [46]. The four double bonds make this molecule more susceptible to lipid peroxidation compared to the single double bond found in cholesterol and allow the lipid to react readily with molecular oxygen promoting oxidative stress [47] and may make it susceptible to lipid peroxidation by plasma reactive species. However, even after 10 min of plasma treatment when dissolved in H_2O and used at 20% v/v in culture, cell growth showed very similar responses to those of cholesterol and remained just under 50%. Yet, arachidonic acid was the only biomolecule which showed pronounced cytotoxic effects at 10% v/v after plasma treatment in DMEM-F12. Arachidonic acid metabolism has been associated with the induction of genetic mutations by triggering hydroperoxide dependent oxidation products capable of inducing DNA damage and mutations [48]. Uncontrolled arachidonic acid lipid peroxidation and superoxide production may explain the cytotoxic and mutagenic potential of this bioactive molecule [39] and could play a role in the plasma-mediated effects observed here.

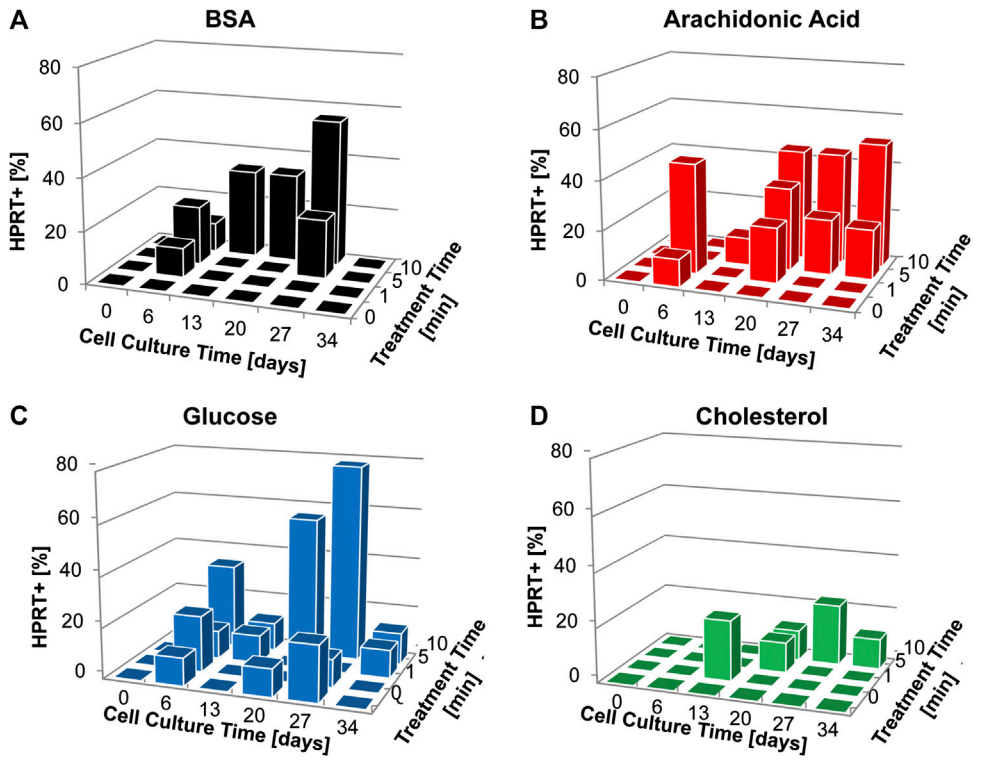

FIGURE 5 | Colony formation (% HPRT+) for cultures supplemented with plasma treated biomolecules over the course of cell culture and according to plasma treatment **(A)** BSA, **(B)** Archidonic acid, **(C)** Glucose, **(D)** Cholesterol. Data is presented as cumulative data from experiments performed in triplicate, with all replicates plated in three independent plates at each time point. Plates were scored as positive or negative based on the presence of colony formation and are displayed as percentage positive plates of the overall plates assessed at each time point.

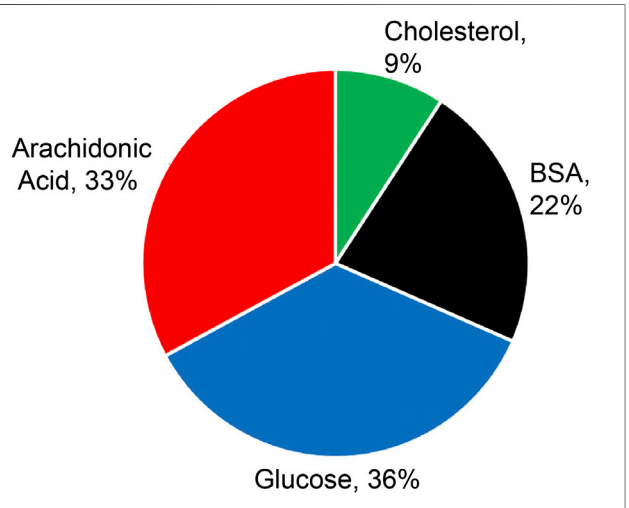

FIGURE 6 | Colony formation (% total HPRT+) according to selected biomolecules.

Serum albumin is the most abundant blood protein and acts as a circulating extracellular antioxidant. Its antioxidant properties arise from the flexible nature of the three domain design that enables the protein to adapt to a variety of ligands, including polyunsaturated fatty acids [38], long chain fatty acids (LCFA) and oxysterols. Albumin is important in the binding of the cationic ligands copper and iron preventing them from generating hydroxyl radials via the Fenton reaction with hydrogen peroxide. When BSA was dissolved in dH20, treated with plasma and cultured with CHO-K1 cells at 20% v/v, reduction of cell growth below 50% was observed after 5 min treatment time. BSA dissolved in DMEM-F12 and treated with plasma before being cultured with CHO-K1 cells at 10% v/v displayed no significant cytotoxic effects even at the prolonged treatment time of 10 min. The effects of plasma on protein structure are well documented. Unfolding and loss of activity in the model protein lysozyme was hypothesised to be due to chemical modifications of amino acids based on shifts in protein mass [49]. Oxidation of BSA and free methionine has been demonstrated using a capillary plasma jet [50] and investigations using a μAPPJ to treat BSA as a model protein indicated oxidation of sulfur-containing amino acids but no modification to cysteine involved in disulphide bonds [51]. Other studies using DBD plasma systems indicated that the thiol group of cysteine is modified by reactive oxygen and nitrogen species [52] and showed inactivation of proteins such as RNase by oxidation of sulfur-containing amino acids and over-oxidation of disulfide bonds [53].

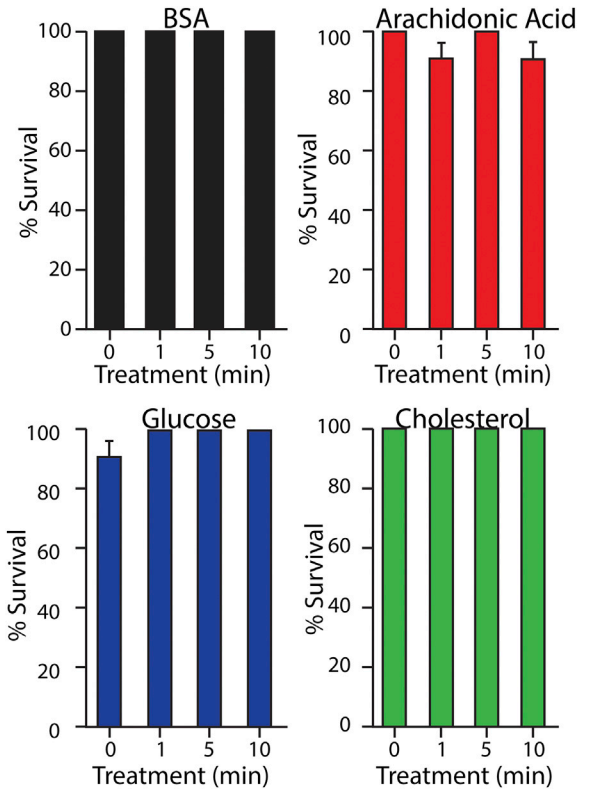

FIGURE 7 | *Galleria mellonella* larvae survival rates 24 h post injection with plasma treated biomolecules.

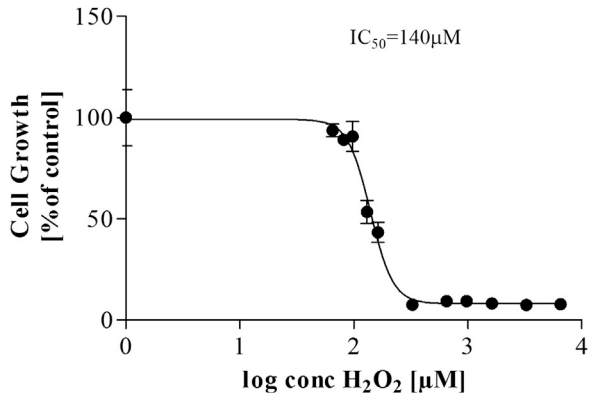

FIGURE 8 | Dose-response curve for CHO-K1 cells treated with H_2O_2.

Glucose was utilised in this study as a model carbohydrate and ubiquitous form of energy in cells. Plasma treated glucose exhibited the lowest cytotoxic potential under both treatment conditions but the highest mutagenic potential. H_2O_2 measurements were no different than the other treated biomolecules at 400 μM in H_2O and 600 μM in DMEM-F12. During carbohydrate oxidation, the hydroxyl groups are oxidised to carbonyl groups and then carboxyl groups. Li et al found that treating sugars including glucose in solutions of water and PBS with DBD plasma caused the decomposition of these sugars into formic acid, glycolic acid, glyceric acid, tartaric acid and oxalic acid in time dependent concentrations and these effects were attributed to reactive oxygen species, primarily the hydroxyl radical [54].

In summary, a general increase in mutagenesis was observed over time and with longer plasma treatment times in all biomolecules. This was not unexpected as plasma technology has proven to be a powerful mutagenesis tool in microbial breeding in bacteria, fungi and microalgae, causing greater DNA damage and higher mutation rate than conventional mutagenesis methods [35, 36]. A possible limitation in this study was the ability to detect mutations in mammalian cells which varies depending on the locus examined using a single-copy gene whose inactivation by the mutagen causes a detectable phenotype, allowing small-scale detection of deletions, transitions or transversions.

All of the tested biomolecules were well-tolerated in the short-term by the *in vivo Galleria* model after single exposure via injection and importantly this suggests that higher organisms may possess sufficient mechanisms for detoxifying toxic components in the plasma treated liquids to prevent noticeable impacts on morbidity or mortality. However, the injection of this larvae model with lettuce broth treated with the same plasma system showed severe toxicity of 5 min treated product in another study [55]. The disparity between the short- and long-term effects and the influence of the aqueous milieu in this study highlights the need for more extensive investigations into the conformational changes on biomolecules post-plasma treatment and the effect that such intended or unintended changes would have on biological pathways.

The large-scale biomedical application of cold plasma or wider applications in food preservation or disinfection require adequate scientific research and technical data evaluating the overall safety considerations of cold plasma treatment. Cytotoxic and mutagenic responses of plasma treated biomolecules observed *in vitro* may not carry over to the *in vivo* model. This could be due to numerous reasons, including metabolic transformation. Even if a possible mutagen is produced, it may not reach the target organ or cells in high enough concentrations to cause genetic damage. Cells and especially more complex cellular structures and organisms have developed a range of mechanisms to remove defective molecules such as the degradation of damaged proteins through the proteasome. The longevity of alterations to the biomolecules and their purpose or elimination in a biological system need to be considered, where their persistence may not be long enough to cause systemic toxicity or long-term effects such as genotoxicity. The *in vivo* model presented in this study represents a short-term toxicity study while the HPRT assay is a long-term model of continuous and therefore excessive exposure to the plasma-treated substances. Both approaches can add insight to the overall question of plasma technology and applications safety. Our short-term *in vivo* tolerance results agree with a number of studies showing tissue tolerance to plasma and low *in vitro* toxic and mutagenic risks, suggesting that plasma reactive species in limited doses are safe. Adverse cyto- and genotoxic effects of high cumulative doses over long-term nonetheless indicate the need for further extensive studies to define the limits beyond which treatments could pose risk. *In vivo* models on mammals to

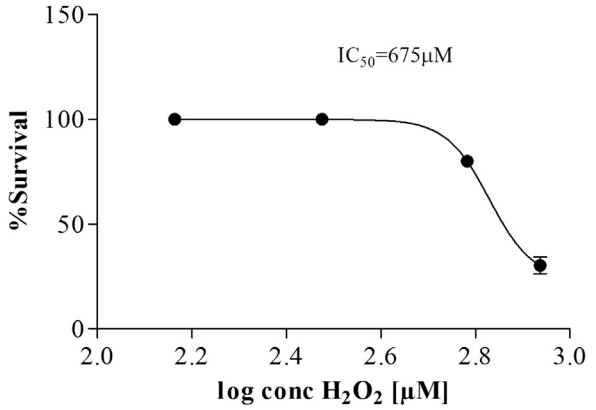

FIGURE 9 | Dose-response curve for *Galleria mellonella* larvae injected with H_2O_2.

examine possible mutagenic manifestations of direct plasma treatment or indirect plasma treatment including ingestion of plasma treated foods or liquids or application of plasma treated solutions should also be performed [56].

MATERIALS AND METHODS

All chemicals were obtained from Sigma-Aldrich (Arklow, Ireland) unless specified otherwise.

Plasma System

Cold plasma was generated using the previously described [57] high-voltage dielectric barrier discharge atmospheric cold plasma system, DIT-120, characterized in detail by Moiseev et al [58]. For the generation of plasma activated model solutions, samples were placed in Petri dishes inside a polypropylene container that operated as the dielectric barrier and the sample holder. The container was sealed in an air-tight film to ensure species retention. Plasma was generated by sine-wave excitation at 80 kV RMS and 50 Hz (ac frequency) in air and the distance between electrodes was kept constant at 3cm for all experiments. Model solutions were subjected to 24-h post treatment storage time within the sealed container before opening.

Preparation of Biomolecule Solutions

All biomolecules were dissolved within physiological ranges (BSA 530 mmol/l; glucose 4 mmol/l; cholesterol 5 mmol/l; arachidonic acid 10 μmol/l). For the short term *in vivo* and *in vitro* cytotoxicity study, biomolecules were dissolved in deionised water prior to plasma treatment. For the long term mutagenicity study, biomolecules were dissolved in DMEM-F12 prior to plasma treatment. All solutions were filter sterilised with a 0.2 μm syringe filter before and after plasma treatment.

Cell Culture

The Chinese hamster cell line CHO-K1 was used for the cytotoxicity and mutagenicity studies. CHO-K1 cells were cultivated in DMEM/F12 with 2 mM L-glutamine and 10% foetal bovine serum [24]. Cells were grown at 37°C and 5% CO_2 in a humidified incubator. Cells were detached using trypsin/EDTA and cell concentrations and viability were assessed using trypan blue exclusion assay. Cell viability was assessed by crystal violet staining: trypsinized cells seeded at 2.5×10^4 cells/ml were left to re-adhere and grow for 3 days. Culture supernatant was removed and cells were fixed with 70% methanol for 1 min followed by staining with 0.2% crystal violet solution for 10 min. Cells were washed with water and allowed to air-dry. Adherent crystal violet was dissolved with 10% acetic acid and the absorbance was measured at 600 nm on a spectrophotometric microplate reader (Biotek, Winooski, United States). Cell growth was expressed as a percentage of control cells.

HPRT Assay

The hypoxanthine phosphoribosyl transferase (HPRT) assay was employed to detect the potential of plasma treated biomolecules to induce mutations in the CHO-K1 cell line. Cells were cultured in T25 flasks or 6-well plates in DMEM/F12 medium supplemented with 10% FBS and 10% biomolecule solution, treated at 80 kV RMS for 0, 1, 5, and 10 min with 24 h post-treatment storage time. Cells were passaged every 3–4 days through trypsinisation and reseeded at 2.5×10^4 cells/ml into fresh 6-well plates. Once a week during reseeding, cells were also plated at 1×10^4 cells/ml in 60mm round dishes with DMEM/F12 10% FBS and 10 μg/ml 6-thioguanine (6-TG) as a selection agent. Colony formation was determined after 10–14 days of incubation at 37°C and 5% CO_2 by staining with crystal violet. Plates were recorded as HPRT+ or HPRT-based on the existence of colonies. CHO-K1 cells were cultured with plasma treated solutions in three independent models and 6-TG plates were set up in triplicate for each replicate. Data is presented as cumulative data in the form of percentage positive plates of total plates assessed at each time point. Control plates were negative for colony formation at the start of the 40 days exposure; ethyl methanesulfate (EMS) was used as a positive control to induce colony formation.

Insect Larvae

Sixth-star *G. mellonella* larvae were obtained commercially from livefoods.direct.co.uk and stored in wood shavings at 15°C prior to use. Dead larvae and those showing signs of melanisation were discarded. Three groups of ten randomly-selected larvae, each weighing 0.2–0.3 g were used for each treatment.

Galleria mellonella Intra-haemocoel Inoculation

The *G. mellonella* haemocoel was injected with 20 μl of selected biomolecular solution using a 0.3 ml Terumo® Myjector® U-100 insulin syringe through the base of the last proleg. Three control groups of ten larvae were injected with sterile deionised H_2O. Larvae were incubated at 30°C for 24 h. Larvae were assessed visually for viability 24 h after injection with plasma treated biomolecule solutions and percentage survival was noted. Larvae were considered dead if they were unmoving, failing to reorient themselves if placed on their backs or failed to respond to stimuli [59].

Harvesting of Insect Haemocytes

After 24 h incubation at 30°C, haemolymph was drained from five larvae in each group by piercing the anterior region and draining into chilled 1.5 ml microfuge tubes, which were kept on ice to prevent melanisation of the haemolymph. All samples were diluted by adding 100 µl haemolymph to 900 µl ice-cold PBS and for each extract concentration, haemocytes were enumerated microscopically using a haemocytometer, and compared to haemolymph samples of control larvae which were injected with 20 µl of sterile H_2O.

Colorimetric Determination of Peroxide Concentration

Concentrations of peroxide in plasma treated solutions were ascertained via spectrophotometrically measuring the oxidation of potassium iodide to iodine at 390 nm. 50 µl of phosphate buffer and 100 µl of 1 M KI solution were added to 50 µl of plasma treated biomolecule solution and incubated at room temperature for 30 min. Absorbance was read at 390 nm and a standard curve of known hydrogen peroxide concentrations was generated with each plate to correlate absorbances with peroxide concentrations.

Statistical Analysis

Experiments were performed in triplicate and results are presented as means with standard deviations and statistical analysis where applicable was performed by analysis of variance (ANOVA) using GraphPad Prism (GraphPad Software Inc., La Jolla, United States). Results obtained from the HPRT assay are presented as cumulative data of experiments performed in triplicate with three plates per replicate.

DATA AVAILABILITY STATEMENT

The raw data supporting the conclusions of this article will be made available by the authors, without undue reservation.

AUTHOR CONTRIBUTIONS

Conceptualization, CH, DB, and PB; methodology, CH, DB, BG, JM, and PB; formal analysis, CH and DB; resources, BG, PC, and PB; data curation, PB; writing—original draft preparation, CH; writing—review and editing, CH, DB, BG, JM, TF, NH, and PB; visualization, CH, DB, and NH; supervision, DB and PB; project administration, PB; funding acquisition, DB, BG, TF, NH, PC, and PB. All authors have read and agreed to the published version of the manuscript.

FUNDING

This work was conducted with the financial support of Science Foundation Ireland (SFI) under Grant Number 14/IA/2626 and 15/SIRG/3466 and by the Irish Research Council New Foundations Strand 3a–PLasmaAPPS grant. Research reported in this publication was also supported by a NIH/SFI/HRC tripartite consortium grant through NIAMS of the National Institutes of Health under award number RO1AR076941. The content is solely the responsibility of the authors and does not necessarily represent the official views of the National Institutes of Health.

ACKNOWLEDGMENTS

We thank Catherine Gurr for her assistance in data presentation and Prof. Mohamed Al-Rubeai (UCD) for provision of the CHO-K1 cell line used in this study.

SUPPLEMENTARY MATERIAL

The Supplementary Material for this article can be found online at: https://www.frontiersin.org/articles/10.3389/fphy.2020.613046/full#supplementary-material.

REFERENCES

1. Hasse S, Duong Tran T, Hahn O, Kindler S, Metelmann HR, von Woedtke T, et al. Induction of proliferation of basal epidermal keratinocytes by cold atmospheric-pressure plasma. *Clin Exp Dermatol* (2016) 41(2):202–9. doi:10.1111/ced.12735
2. Dobrynin D, Wasko KA, Friedman G, Fridman A, Fridman G. Fast blood coagulation of capillary vessels by cold plasma: a rat ear bleeding model. *Plasma Med* (2011) 1(3–4):241–7. doi:10.1615/PLASMAMED.2012005167
3. Conway GE, Casey A, Milosavljevic V, Liu Y, Howe O, Cullen PJ, et al. Non-thermal atmospheric plasma induces ROS-independent cell death in U373MG glioma cells and augments the cytotoxicity of temozolomide. *Br. J. Cancer* (2016) 114(4):435–43. doi:10.1038/bjc.2016.12
4. Volotskova O, Hawley TS, Stepp MA, Keidar M. Targeting the cancer cell cycle by cold atmospheric plasma. *Sci Rep* (2012) 2, 636. doi:10.1038/srep00636
5. Arndt S, Wacker E, Li YF, Shimizu T, Thomas HM, Morfill GE, et al. Cold atmospheric plasma, a new strategy to induce senescence in melanoma cells. *Exp Dermatol* (2013) 22(4):284–9. doi:10.1111/exd.12127
6. Nicol MJ, Brubaker TR, Honish BJ, Simmons AN, Kazemi A, Geissel MA, et al. Antibacterial effects of low-temperature plasma generated by atmospheric-pressure plasma jet are mediated by reactive oxygen species. *Sci Rep* (2020) 10(1):3066. doi:10.1038/s41598-020-59652-6
7. Matthes R, Assadian O, Kramer A. Repeated applications of cold atmospheric pressure plasma does not induce resistance in *Staphylococcus aureus* embedded in biofilms. *GMS Hyg Infect Control* (2014) 9(3):Doc17. doi:10.3205/dgkh000237
8. Zimmermann JL, Shimizu T, Schmidt H-U, Li Y-F, Morfill GE, and Isbary G Test for bacterial resistance build-up against plasma treatment. *New J Phys* (2012) 14(7):073037. doi:10.1088/1367-2630/14/7/073037/meta
9. Ziuzina D, Patil S, Cullen PJ, Keener KM, Bourke P. Atmospheric cold plasma inactivation of *Escherichia coli*, *Salmonella enterica* serovar Typhimurium and Listeria monocytogenes inoculated on fresh produce. *Food Microbiol* (2014) 42: 109–16. doi:10.1016/j.fm.2014.02.007
10. Weltmann KD, von Woedtke T, Ehlbeck J, Foest R, Stieber M, and Kindel E. Antimicrobial treatment of heat sensitive products by miniaturized atmospheric pressure plasma jets (APPJs). *J Phys D Appl Phys* (2008) 41(19):194008. doi:10.1088/0022-3727/41/19/194008
11. Ling L, Jiafeng J, Jiangang L, Minchong S, Xin H, Hanliang S, et al. Effects of cold plasma treatment on seed germination and seedling growth of soybean. *Sci Rep* (2014) 4:5859. doi:10.1038/srep05859
12. Mitra A. Inactivation of surface-borne microorganisms and increased germination of seed specimen by cold atmospheric plasma. *Food Bioprocess Technol* (2014) 7(3):645–53. doi:10.1007/s11947-013-1126-4
13. Sarangapani C, Patange A, Bourke P, Keener K, Cullen PJ. Recent advances in the application of cold plasma technology in foods. *Annu Rev Food Sci Technol* (2018) 9(1):609–29. doi:10.1146/annurev-food-030117-012517

14. Ranieri P. Plasma agriculture: review from the perspective of the plant and its ecosystem. *Plasma Process Polym* (2020):e2000162. 10.1002/ppap.202000162
15. Ranieri P. GSH modification as a marker for plasma source and biological response comparison to plasma treatment. *Appl Sci* (2020) 10:2025. doi:10.3390/app10062025
16. Khlyustova A, Labay C, Machala Z, Ginebra MP, Canal P. Important parameters in plasma jets for the production of RONS in liquids for plasma medicine: a brief review. *Front Chem Sci Eng* (2019) 13:238–52. doi:10.1007/s11705-019-1801-8
17. Labay C, Roldán M, Tampieri F, Stancampiano A, Bocanegra PE, Ginebra MP, et al. Enhanced generation of reactive species by cold plasma in gelatin solutions for selective cancer cell death. *ACS Appl Mater Interfaces* (2020) 12(42):47256–69. doi:10.1021/acsami.0c12930
18. Chauvin J, Judée F, Yousfi M, Vicendo P, Merbahi N. Analysis of reactive oxygen and nitrogen species generated in three liquid media by low temperature helium plasma jet. *Sci Rep* (2017) 7:4562. doi:10.1038/s41598-017-04650-4
19. Krewing M, Schubert B, Bandow JE. A dielectric barrier discharge plasma degrades proteins to peptides by cleaving the peptide bond. *Plasma Chem Plasma Process* (2020) 40(3):685–96. doi:10.1093/mnras/staa497
20. Lackmann JW, Schneider S, Edengeiser E, Jarzina F, Brinckmann S, Steinborn E, et al. Photons and particles emitted from cold atmospheric-pressure plasma inactivate bacteria and biomolecules independently and synergistically. *J R Soc Interface* (2013) 10(89):20130591. doi:10.1098/rsif.2013.0591
21. Hammer MU, Forbrig E, Weltmann KD. Influence of plasma treatment on the structure and function of lipids. *Plasma Med* (2013) 3(1-2):97–114. doi:10.1615/PlasmaMed.2014009708
22. Attri P, Kumar N, Park JH, Yadav DK, Choi S, Uhm HS, et al. Influence of reactive species on the modification of biomolecules generated from the soft plasma. *Sci Rep* (2015) 5, 8221. doi:10.1038/srep08221
23. Takai E. Chemical modification of amino acids by atmospheric-pressure cold plasma in aqueous solution. *J Phys Appl Phys* (2014) 47(28):285403. doi:10.1088/0022-3727/47/28/285403/meta
24. Sakudo A, Higa M, Maeda K, Shimizu N, Imanishi Y, Shintani H. Sterilization mechanism of nitrogen gas plasma: induction of secondary structural change in protein. *Microbiol Immunol* (2013) 57(7):536–42. doi:10.1111/1348-0421.12061
25. Yusupov M, Edengeiser E, Jarzina F. Impact of plasma oxidation on structural features of human epidermal growth factor. *Plasma Process Polym* (2018) 15(8):1800022. doi:10.1002/ppap.201800022
26. Krewing M. Dielectric barrier discharge plasma treatment affects stability, metal ion coordination, and enzyme activity of bacterial superoxide dismutases. *Plasma Process Polym* (2020) 17(10):2000019. doi:10.1002/ppap.202000019
27. Tero R, Yamashita R, Hashizume H, Suda Y, Takikawa H, Hori M, et al. Nanopore formation process in artificial cell membrane induced by plasma-generated reactive oxygen species. *Arch Biochem Biophys* (2016) 605:26–33. doi:10.1016/j.abb.2016.05.014
28. Yusupov M, Wende K, Kupsch S, Neyts EC, Reuter S, Bogaerts A. Effect of head group and lipid tail oxidation in the cell membrane revealed through integrated simulations and experiments. *Sci Rep* (2017) 7(1):5761. doi:10.1038/s41598-017-06412-8
29. Wende K, Bekeschus S, Schmidt A, Jatsch L, Hasse S, Weltmann KD, et al. Risk assessment of a cold argon plasma jet in respect to its mutagenicity. *Mutat Res Genet Toxicol Environ Mutagen* (2016) 798–799:48–54. doi:10.1016/j.mrgentox.2016.02.003
30. Boxhammer V, Li YF, Köritzer J, Shimizu T, Maisch T, Thomas HM, et al. Investigation of the mutagenic potential of cold atmospheric plasma at bactericidal dosages. *Mutat Res* (2013) 753(1):23–8. doi:10.1016/j.mrgentox.2012.12.015
31. Kluge S, Bekeschus S, Bender C, Benkhai H, Sckell A, Below H, et al. Investigating the mutagenicity of a cold argon-plasma jet in an HET-MN model. *PloS One* (2016) 11(9):e0160667. doi:10.1371/journal.pone.0160667
32. Boehm D, Bourke P. Safety implications of plasma-induced effects in living cells - a review of *in vitro* and *in vivo* findings. *Biol Chem* (2018) 400(1):3–17. doi:10.1515/hsz-2018-0222
33. Metelmann H-R. Scar formation of laser skin lesions after cold atmospheric pressure plasma (CAP) treatment: a clinical long term observation. *Clin Plasma Med* (2013) 1(1):30–5. doi:10.1016/j.cpme.2012.12.001
34. Schmidt A, Woedtke TV, Stenzel J, Lindner T, Polei S, Vollmar B, et al. One year follow-up risk assessment in SKH-1 mice and wounds treated with an argon plasma jet. *Int J Mol Sci* (2017) 18(4):868. doi:10.3390/ijms18040868
35. Zhang X, Zhang XF, Li HP, Wang LY, Zhang C, Xing XH, et al. Atmospheric and room temperature plasma (ARTP) as a new powerful mutagenesis tool. *Appl Microbiol Biotechnol* (2014) 98(12):5387–96. doi:10.1007/s00253-014-5755-y
36. Zhang X, Zhang C, Zhou Q-Q, Zhang X-F, Wang L-Y, Chang H-B, et al. Quantitative evaluation of DNA damage and mutation rate by atmospheric and room-temperature plasma (ARTP) and conventional mutagenesis. *Appl Microbiol Biotechnol* (2015) 99(13):5639–46. doi:10.1007/s00253-015-6678-y
37. Boehm D, Heslin C, Cullen PJ, Bourke P. Cytotoxic and mutagenic potential of solutions exposed to cold atmospheric plasma. *Sci Rep* (2016) 6, 21464. doi:10.1038/srep21464
38. Pompéia C, Lopes LR, Miyasaka CK, Procópio J, Sannomiya P, Curi R. Effect of fatty acids on leukocyte function. *Braz J Med Biol Res* (2000) 33(11):1255–68. doi:10.1590/s0100-879x2000001100001
39. Pompéia C, Cury-Boaventura MF, Curi R. Arachidonic acid triggers an oxidative burst in leukocytes. *Braz J Med Biol Res* (2003) 36(11):1549–60. doi:10.1590/s0100-879x2003001100013
40. Valenzuela A, Sanhueza J, Nieto S. Cholesterol oxidation: health hazard and the role of antioxidants in prevention. *Biol Res* (2003) 36(3-4):291–302. doi:10.4067/s0716-97602003000300002
41. Van der Paal J, Verheyen C, Neyts EC, Bogaerts A. Hampering effect of cholesterol on the permeation of reactive oxygen species through phospholipids bilayer: possible explanation for plasma cancer selectivity. *Sci Rep* (2017) 7:39526. doi:10.1038/srep39526
42. Xu D, Liu D, Wang B, Chen C, Chen Z, Li D, et al. *In Situ* OH generation from O2- and H2O2 plays a critical role in plasma-induced cell death. *PloS One* (2015) 10(6):e0128205. doi:10.1371/journal.pone.0128205
43. Slater AF, Nobel CS, Orrenius S. The role of intracellular oxidants in apoptosis. *Biochim Biophys Acta* (1995) 1271(1):59–62. doi:10.1016/0925-4439(95)00010-2
44. Sevanian A, Peterson AR. The cytotoxic and mutagenic properties of cholesterol oxidation products. *Food Chem Toxicol* (1986) 24(10–11):1103–10. doi:10.1016/0278-6915(86)90295-4
45. Sevanian A, Peterson AR. Cholesterol epoxide is a direct-acting mutagen. *Proc Natl Acad Sci USA* (1984) 81(13):4198–202. doi:10.1073/pnas.81.13.4198
46. Chen Q, Galleano M, Cederbaum AI. Cytotoxicity and apoptosis produced by arachidonic acid in hep G2 cells overexpressing human cytochrome P4502E1. *J Biol Chem* (1997) 272(23):14532–41. doi:10.1074/jbc.272.23.14532
47. Brash AR. Arachidonic acid as a bioactive molecule. *J Clin Invest* (2001) 107(11):1339–45. doi:10.1172/JCI13210
48. Biswas NK, Das S, Maitra A, Sarin R, Majumder PP. Somatic mutations in arachidonic acid metabolism pathway genes enhance oral cancer post-treatment disease-free survival. *Nat Commun* (2014) 5, 5835. doi:10.1038/ncomms6835
49. Takai E, Jarzina F, Brinckmann S, Steinborn E. Protein inactivation by low-temperature atmospheric pressure plasma in aqueous solution. *Plasma Process Polym* (2012) 9(1):77–82. doi:10.1002/ppap.201100063
50. Topala I, Nagatsu M. Capillary plasma jet: a low volume plasma source for life science applications. *Appl Phys Lett* (2015) 106(5).
51. Lackmann J-W. Effects of the effluent of a microscale Atmospheric pressure plasma-jet operated with He/O2 gas on bovine serum albumin. *Plasma Med* (2013) 3:115–24. doi:10.1038/s41598-018-25937-0
52. Kogelheide F, Kartaschew K, Strack M, Baldus S, Metzler-Nolte N, Havenith M, et al. FTIR spectroscopy of cysteine as a ready-to-use method for the investigation of plasma-induced chemical modifications of macromolecules. *J Phys Appl Phys* (2016) 49(8):084004. doi:10.1088/0022-3727/49/8/084004/meta
53. Lackmann JW, Baldus S, Steinborn E, Edengeiser E, Kogelheide F, Langklotz S, et al. A dielectric barrier discharge terminally inactivates RNase A by oxidizing sulfur-containing amino acids and breaking structural disulfide bonds. *J Phys Appl Phys* (2015) 48(49):494003. doi:10.1088/0022-3727/48/49/494003
54. Li Y. Decomposition of sugars under non-thermal dielectric barrier discharge plasma. *Clinical Plasma Medicine* (2014) 2(2):56–63. doi:10.3892/ijmm.2015.2405

55. Heslin C, Stenzel J, Lindner T, Polei S, Vollmar B. Safety evaluation of plasma-treated lettuce broth using *in vitro* and *in vivo* toxicity models. *J Phys Appl Phys* (2020) 53:274 doi:10.1088/1361-6463/ab7ac8/pdf
56. Schubert J. Mutagenicity and cytotoxicity of irradiated foods and food components. *Bull World Health Organ* (1969) 41(6):873–904. doi:10.1590/S1516-89132009000500026
57. Ziuzina D, Patil S, Cullen PJ, Keener KM, Bourke P. Atmospheric cold plasma inactivation of *Escherichia coli* in liquid media inside a sealed package. *J Appl Microbiol* (2013) 114(3):778–87. doi:10.1111/jam.12087
58. Moiseev T, Nobel CS, Orrenius S. Post-discharge gas composition of a large-gap DBD in humid air by UV–Vis absorption spectroscopy. *Plasma Sources Sci Technol* (2014) 23(6):065033. doi:10.1088/0963-0252/23/6/065033
59. Megaw J, Thompson TP, Lafferty RA, Gilmore BF. *Galleria mellonella* as a novel *in vivo* model for assessment of the toxicity of 1-alkyl-3-methylimidazolium chloride ionic liquids. *Chemosphere* (2015) 139: 197–201. doi:10.1016/j.chemosphere.2015.06.026

Conflict of Interest: The authors declare that the research was conducted in the absence of any commercial or financial relationships that could be construed as a potential conflict of interest.

frontiers in Physics

CORRECTION
published: 14 April 2021
doi: 10.3389/fphy.2021.664663

Corrigendum: Biomolecules as Model Indicators of *In Vitro* and *In Vivo* Cold Plasma Safety

Caitlin Heslin[1], Daniela Boehm[1], Brendan F. Gilmore[2], Julianne Megaw[2], Theresa A. Freeman[3], Noreen J. Hickok[3], P. J. Cullen[1,4] and Paula Bourke[1,5,6]**

[1]School of Food Science and Environmental Health, Technological University Dublin, Dublin, Ireland, [2]School of Pharmacy, Queens University Belfast, Belfast, United Kingdom, [3]Department of Orthopaedic Surgery, Sidney Kimmel Medical College, Jefferson University, Philadelphia, PA, United States, [4]School of Chemical and Biomolecular Engineering, University of Sydney, Sydney, NSW, Australia, [5]School of Biological Sciences, Queens University Belfast, Belfast, United Kingdom, [6]Plasma Research Group, School of Biosystems and Food Engineering, University College Dublin, Dublin, Ireland

Keywords: cold atmospheric plasma, cytotoxicity, mutagenicity, safety, *in vivo* toxicity

A Corrigendum on

Biomolecules as Model Indicators of In Vitro and In Vivo Cold Plasma Safety
by Heslin C, Boehm D, Gilmore BF, Megaw J, Freeman TA, Hickok NJ, et al. Front Phys (2021) 8: 613046. doi:10.3389/fphy.2020.613046

In the original article, the reference for [16] was incorrectly written as "Khlyustova A, Jarzina F, Brinckmann S. Important parameters in plasma jets for the production of RONS in liquids for plasma medicine: a brief review. *Front Chem Sci Eng* (2019) 13:238–52. doi: 10.1007/s11705-019-1801-8."

This should be "Khlyustova A, Labay C, Machala Z, Ginebra MP, Canal C. Important parameters in plasma jets for the production of RONS in liquids for plasma medicine: a brief review. *Front Chem Sci Eng* (2019) 13:238–52. doi: 10.1007/s11705-019-1801-8."

Further, the reference for [17] was incorrectly written as "Labay C, Shimizu T, Thomas HM, Morfill GE. Enhanced generation of reactive species by cold plasma in gelatin solutions for selective cancer cell death. *ACS Appl Mater Interfaces* (2020) 12(42):47256–69. doi: 10.1021/acsami.0c12930."

This should be "Labay, C, Roldán, M, Tampieri, F, Stancampiano, A, Escot Bocanegra, *P*, Ginebra, MP, Canal, C. Enhanced generation of reactive species by cold plasma in gelatin solutions for selective cancer cell death. *ACS Appl Mater Interfaces* (2020) 12(42):47256–69. doi: 10.1021/acsami.0c12930."

The authors apologize for these errors and state that this does not change the scientific conclusions of the article in any way. The original article has been updated.

REFERENCES

16. Khlyustova A, Labay C, Machala Z, Ginebra M-P, Canal C. Important parameters in plasma jets for the production of RONS in liquids for plasma medicine: a brief review. *Front Chem Sci Eng* (2019) 13:238–52. doi:10.1007/s11705-019-1801-8
17. Labay C, Roldán M, Tampieri F, Stancampiano A, Bocanegra PE, Ginebra MP, et al. Enhanced generation of reactive species by cold plasma in gelatin solutions for selective cancer cell death. *ACS Appl Mater Inter* (2020) 12(42):47256–69. doi:10.1021/acsami.0c12930

OPEN ACCESS

Approved by:
Frontiers Editorial Office, Frontiers Media SA, Switzerland

****Correspondence:***
Paula Bourke
paula.bourke@ucd.ie
Daniela Boehm
daniela.boehm@tudublin.ie

Specialty section:
This article was submitted to Plasma Physics, a section of the journal Frontiers in Physics

Received: *05 February 2021*
Accepted: *08 February 2021*
Published: *14 April 2021*

Citation:
Heslin C, Boehm D, Gilmore BF, Megaw J, Freeman TA, Hickok NJ, Cullen PJ and Bourke P (2021) Corrigendum: Biomolecules as Model Indicators of In Vitro and In Vivo Cold Plasma Safety. Front. Phys. 9:664663. doi: 10.3389/fphy.2021.664663

frontiers in Physics

REVIEW
published: 14 April 2021
doi: 10.3389/fphy.2021.617345

Mechanisms of Plasma-Seed Treatments as a Potential Seed Processing Technology

Alexandra Waskow, Alan Howling and Ivo Furno*

Swiss Plasma Center, École Polytechnique Fédérale de Lausanne, Lausanne, Switzerland

Plasma treatments are currently being assessed as a seed processing technology for agricultural purposes where seeds are typically subjected to pre-sowing treatments to improve the likelihood of timely and uniform germination. The aim of this review is to summarize the hypotheses and present the evidence to date of how plasma treatments affect seeds, considering that there is difficulty in standardizing the methodology in this interdisciplinary field given the plethora of variables in the experimental setup of the plasma device and handling of biological samples. The ever increasing interest for plasma agriculture drives the need for a review dedicated to seeds, which is understandable to an interdisciplinary audience of biologists and plasma physicists. Seeds are the first step of the agricultural cycle and at this stage, the plant can be given the highest probability of establishment, despite environmental conditions, to exploit the genetic potential of the seed. Furthermore, seedlings seem to be too sensitive to the oxidation of plasma and therefore, seeds seem to be the ideal target. This review intentionally does not include seed disinfection and sterilization due to already existing reviews. Instead, a summary of the mechanisms of how plasma may be affecting the seed and its germination and developmental properties will be provided and discussed.

Keywords: plasma, seeds, processing, mechanisms, germination, surface modification, stress or disease resistance

OPEN ACCESS

Edited by:
Mounir Laroussi,
Old Dominion University, United States

Reviewed by:
Eugen Stamate,
Technical University of Denmark, Denmark
Saikat Chakraborty Thakur,
Auburn University, United States

****Correspondence:***
Alexandra Waskow
alexandra.waskow@epfl.ch

Specialty section:
This article was submitted to Plasma Physics, a section of the journal Frontiers in Physics

Received: *14 October 2020*
Accepted: *17 March 2021*
Published: *14 April 2021*

Citation:
Waskow A, Howling A and Furno I (2021) Mechanisms of Plasma-Seed Treatments as a Potential Seed Processing Technology. Front. Phys. 9:617345. doi: 10.3389/fphy.2021.617345

INTRODUCTION

The motivation driving plasma-seed treatment research is the importance of food. The world population is projected to increase to 10 billion by 2050 and even without increasing the food supply, it is necessary to maintain the current food production and quality [1]. Most food begins with planting seeds.

The aim of this review is to centralize the hypotheses and present the evidence to date of how plasma treatments affect seeds, considering that there is difficulty in standardizing the methodology in this interdisciplinary field given the plethora of variables in the experimental setup of the plasma device and handling of biological samples. Considering that plasma agriculture has been gaining more attention recently, it is therefore useful to have a review dedicated to seeds, which is understandable to an interdisciplinary audience of biologists and plasma physicists.

The review is organized as follows. The Seed Structure and Development section will be presented first to establish a common ground, followed by a summary of current techniques used to improve seed survival in section Seed Performance. In section Non-thermal Plasma (NTP) as a Seed Processing Technology, plasma will be introduced and the motivation for its application on seeds followed by a corroboration of recent research to provide an overview of physical, chemical, and biological mechanisms that can be triggered by plasma components is in section Mechanisms of How Non-thermal Plasma Affects Seeds and Their Subsequent Development.

SEED STRUCTURE AND DEVELOPMENT

Although very diverse, all seeds have generally evolved to contain all their needs to develop into plantlets once the environmental conditions are perceived as appropriate. The living tissues of seeds are protected by the seed coat (testa), which can vary between species and cultivars, or depend on the plants being fertile or clones unable to produce the next generation. Inside the dry mature seed, the embryo is in a partially desiccated, quiescent state, poised to germinate upon the addition of water or in other words, imbibition. It is then provided with stored foods through the endosperm during germination, a process which is the transition from an inactive to active seed that grows, ruptures the seed coat and develops from a seedling first into a plantlet, which is generally still frail and particularly sensitive to external stresses, to then a more stress-resistant autotrophic plant.

The trigger for germination requires a number of external parameters to be met, which will vary from seed to seed, but are generally a combination of water, temperature and light. Additionally, each seed has different requirements due to structural differences, particularly in the seed coat. Imbibition is the first step where the seed undergoes three stages with initially rapid, then slow and finally rapid water uptake. Water reactivates the enzymes that can repair DNA and membrane damages by using pre-existing RNA transcripts produced during seed maturation, and activates enzymes involved in beta-oxidation and amylases to break down stored oil and starch into sugars for energy and cell wall production. Proteases break down storage proteins into amino acids for protein synthesis [2].

After the third water uptake stage, the seed is swollen since the tissues have expanded and the embryo grows. The first visible sign of germination is the protrusion of the radicle, which later becomes the root. From there, the hypocotyl, which connects the root and shoot, hooks out and brings out the shoot with the cotyledon/s, then the true leaves. Once photosynthesis starts, the plantlet can grow independently from prior storages of organic matter and will only take nutrients and water from the soil and the surrounding media.

Prior to germination, there are hormones and inhibitors that prevent the process, to ensure the right environment and maximize the probability of the germinated seed to survive and thrive. The hormone abscisic acid (ABA) is known for its role in maintaining dormancy and for inhibiting germination. When this is removed by a lengthy water imbibition, another hormone gibberellic acid (GA) is produced and germination begins. As the embryo grows, both auxin and cytokinin are involved in cell expansion and cell division, respectively, whereas later during the stressful life of the plant, hormones such as salicylic acid, jasmonic acid and ethylene will play a role in plant defense to protect it against abiotic stresses such as cold, heat, dehydration, and biotic stresses, such as herbivores, viral, fungal and bacterial pathogens. More information about plant defense can be found in Andersen et al. [3].

SEED PERFORMANCE

The best chance for survival is to provide the seed with an opportunity to germinate from the very beginning, assuming they are not dead, and for food production, there are additional criteria beyond successful germination which are germination uniformity and rate for a single harvest when done on an industrial scale. For this reason, many centuries ago, a method called priming was developed to ensure a more uniform and faster germination.

Seed priming is a method which can increase plant growth parameters, such as germination rate and uniformity and contribute to higher yields and greater plant resistance. As reviewed by Pawar and Laware [4] and Lutts et al. [5], the concept of priming is to provide water and activate the metabolism of the seed to repair damage before continuing the embryo development and the emergence of the root.

Priming is frequently applied using water (hydro-priming), which requires soaking the seeds for a given timeframe. This water treatment can be modified to ameliorate germination rate, efficiency and uniformity with the addition of salts (halo-priming), solutes to change the osmotic pressure (osmo-priming), micronutrients like boron and iron (nutri-priming), hormones like gibberellic acid (hormonal priming) or beneficial microorganisms, such as *Pseudomonas* species (bio-priming), and metallic nanoparticles like iron and silver (nano-priming). Priming can also be done without water by using a solid and non-soluble material such as sand or clay called matrix priming [4].

Depending on the seed and its structure, it can be primed with wet treatments by soaking in cold, warm, boiling water or dry treatments using dry heat or microwaves. Seeds can also be primed using acid scarification and physical scarification. Seeds, specifically their seed coats, can also be modified with compounds such as selenium or salicylic acid [6] or agents that are protectants, nutrients, symbionts, soil adjuvants (hydrogels) and colorants [7]. Protectants, such as pesticides, and colorants make up the bulk of coatings and are applied mostly to crops and vegetables to mainly deter insects (44%), weeds, and fungi [8].

Pesticides in the seed coatings can transfer into the soil through rain and enter the groundwater and wastewater treatment plants. Since these compounds are highly toxic, persist for a long time and become more toxic with time when held in storage, remediation methods, used to remove toxic chemical compounds, can be done with microorganisms, clay, polymeric

materials or UV-H_2O_2 and UV- ozone, and hydroxyl radicals and at times, even require additional water resources [9].

Although protective coatings are important and occupy a multi-billion-dollar market, the amount of investment in remediation techniques highlights that it would be beneficial to consider alternatives to minimize pesticide use. For this reason, alternatives have been considered such as biocontrol using fungi or bacteria, biopesticides derived from natural compounds such as grapefruit seed extract [10], physical methods such as ultrasound [11, 12] as well as genetic engineering [13]. It would also be ideal to find a method with minimal energy consumption in view of energy savings considering that energy input is five to ten times greater than the output in the form of food in North America [14].

NON-THERMAL PLASMA (NTP) AS A SEED PROCESSING TECHNOLOGY

Ideally, more effective solutions for seed treatment to ensure rapid and uniform germination should not include toxic residues, consume little energy, have low penetration depth to avoid injuring cells, and favor long storage time [15], while subsequently supporting optimal seed development. These criteria can possibly be met with non-thermal plasma (NTP) treatments.

Plasma is an ionized gas that can be ignited under low or atmosphere pressure conditions. The plasma composition depends on the operating parameters such as voltage, frequency, humidity, flow rate, and gas mixture. Gases such as argon, oxygen, nitrogen, helium, and/or air can be ionized by electric fields to form electrons, ions, UV, thermal radiation and reactive species. Specifically, air plasmas contain reactive oxygen species (ROS) such as superoxide ($O_2^{\cdot -}$), hydrogen peroxide (H_2O_2), hydroxyl radical ($OH^{\cdot}$), singlet oxygen ($^1O_2$), and ozone (O_3) and reactive nitrogen species (RNS) such as nitric oxide ($NO^{\cdot}$), peroxynitrite and nitrogen dioxide radical ($NO_2^{\cdot}$) [16]. Han et al. [17] and Laroussi [18] describe the types of plasma treatments in detail. Šimončicová et al. [19] describe the types of plasma treatments for biological applications. In short, they include dielectric barrier discharge (DBD) as the most common plasma source, followed by plasma jet, corona, microwave, radiofrequency, and gliding arc. The DBD generates plasma by alternating high voltage (kV) between two electrodes, one or both of which are insulated by a dielectric to prevent electric arcs. The DBD may generate the plasma in a volume of gas between the electrodes (VDBD) or on the surface of a dielectric adjacent to electrodes (SDBD). In a plasma jet, there is usually a DBD excitation of gas flowing in a thin tube. Corona ignites plasma at the tip of a sharp edge and forms diffuse plasma toward the ground electrode. Microwave plasma is produced using a magnetron at a very high frequency in the GHz range, whereas radiofrequency plasma is ignited in the MHz range; both are ignited in a vacuum chamber at low gas pressure. Gliding arc generates an arc at the shortest distance between two diverging electrodes, which then expands. The seeds and seedlings can be treated directly with the plasma or indirectly at a distance away from the plasma. They can also be soaked or watered using liquids exposed to plasma. These liquids are considered as plasma-activated media (PAM) and if water is used, it is called plasma-activated water (PAW). Comparing the gaseous and aqueous treatments, similar effects on macroscopic plant properties have been reported [20, 21].

Plasma treatment may enhance seed survival without toxic residues since all the constituents in plasmas may be found in nature and recombine shortly afterwards. Moreover, components in plasma have approximately 10 nm deep penetration, limiting it to surface functionalization [12]. Importantly, plasma treatments are considered to be low maintenance with low energy costs [22]. Therefore, many studies have been performed involving plasma treatments of agronomic interest, such as quinoa, basil, tomato, wheat, radish, soybean, mung bean, rice, Ajwain and Umbu and seeds deemed important for the landscape like Norway spruce [23].

Randeniya and de Groot [22] and Puac et al. [24] reviewed the observed effects on germination and subsequent plant growth. The extensive list of these effects in this review has been summarized in **Figure 1**. It can increase germination probability and biomass [25] or increase disease resistance or stress resistance [26, 27]. Additionally, it can accelerate or delay germination and subsequent development [28], decrease water consumption [29], decrease levels of microbial pathogens or insects [30, 31], without detectable toxic residues [20]. Molina et al. [32] proposed to make a hydro-absorbant polymer coating with short plasma treatments on specific seed types, and Kopacki et al. [33] suggested to use plasma for seed coatings against fungal pathogens.

Other than treating the seed or plant directly, plasma treatment can also be used on the plant's surroundings by degrading volatile organic compounds in the soil to improve soil health [34, 35]. It may also have potential as an alternative to fungicide [36] and be implemented in industry as field studies have shown [16, 37].

Table 1 shows the legend describing the categories of **Table 2**, which is a compilation of papers described in four categories: seed coat modification, growth parameters, metabolism, and disease or stress resistance and further divided by the scale of information i.e., macroscopic, microscopic or molecular properties. Seed disinfection and sterilization were intentionally left aside and can instead be found in more detail in the food processing field [108].

MECHANISMS OF HOW NON-THERMAL PLASMA AFFECTS SEEDS AND THEIR SUBSEQUENT DEVELOPMENT

Quite consistently, most reports refer to optimized plasma setups that can significantly change germination and plant growth parameters. For example, germination rate may be accelerated, shoot and root lengths may be longer [68] and more branching of the roots [25] or stronger root system [85] were reported although it is difficult to know the causative agent behind these effects due to varying plasma-seed treatment methodologies.

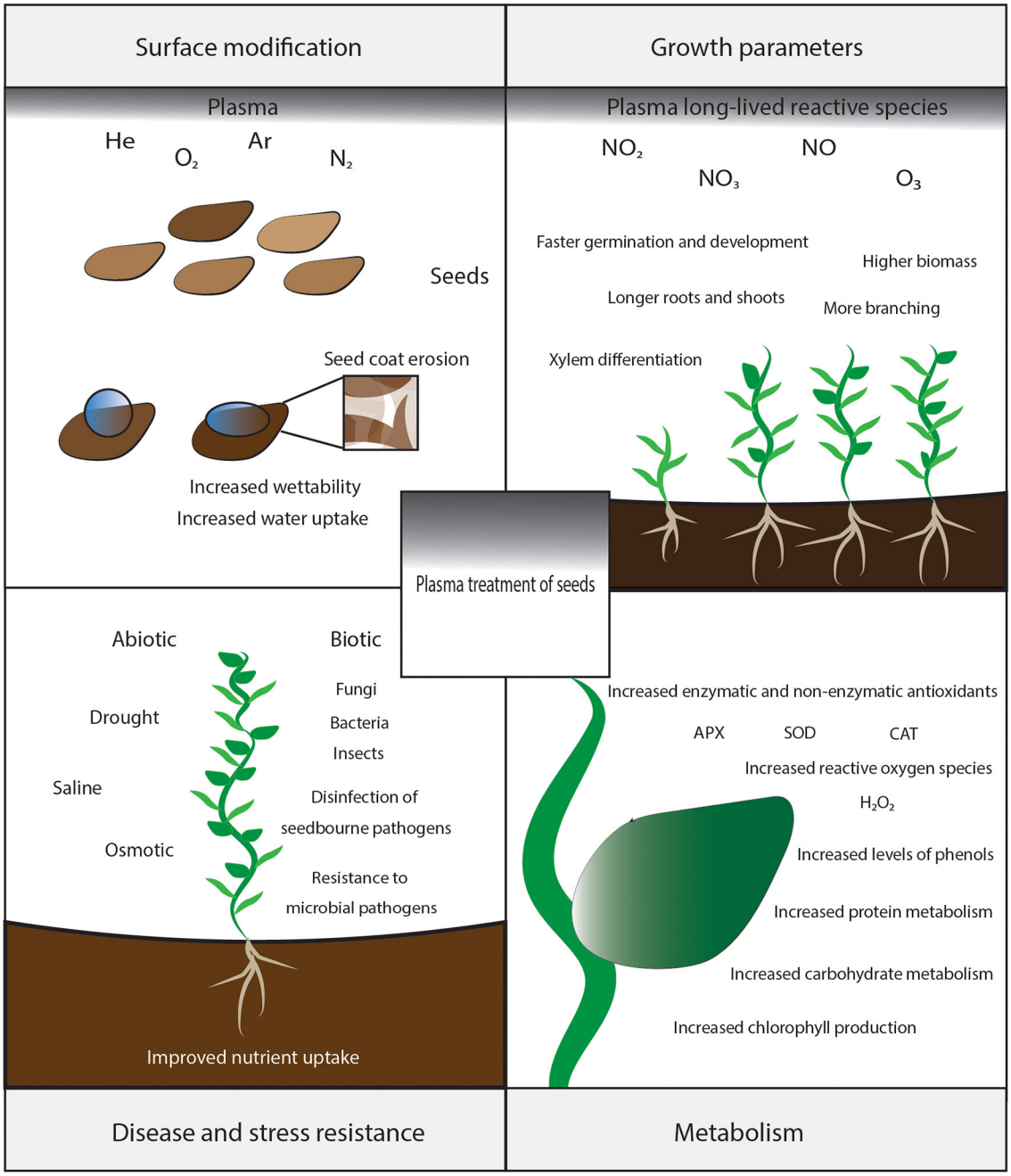

FIGURE 1 | Effects of plasma treatment on seeds which includes surface modifications, changing growth parameters, modulating disease, and stress resistance through metabolism.

Not all observe the same effects and instead, plant growth can be improved without changing germination rate [49] or scientists have strong variation in their experiments [53, 69]. This could mean that further optimization is required, which is time-consuming considering the number of variables in the experimental design. It is not yet clear by which mechanism(s) these effects arise but understanding this will simplify the experimental design and potential scale up for the future so that the results are reproducible. Here, we take a closer look at the physical, chemical, and biochemical factors derived from plasma treatments to have a more detailed understanding of what is happening to the seed. A summary of the plasma-seed interactions at the seed surface and at a molecular level are given in **Figures 2**, **3**, respectively.

TABLE 1 | Legend describing each category of **Table 2** for the type of plasma and seed used in the study as well as the main findings (see this table for a description of the categories).

Category	Description
Plasma	
Geometry	Volume or surface dielectric barrier discharge (VDBD/SDBD), radiofrequency (RF), jet
Pressure	Atmospheric or low
Gas type	Oxygen, nitrogen, argon as single or admixtures
Seed type	Radish, wheat, rice etc.
Micro(organism)	
Bacteria or fungi or insect	Native or artificial contamination of a microorganism or organism (pest)
Main findings	
Seed coat modification	Wettability, water uptake, morphology, surface chemistry
Growth parameters	Germination rate, root length, shoot length, seed vigor
Metabolism	Antioxidant enzymes, proline, soluble sugars
Disease or stress resistance	Plants grown in stressful conditions or include molecular component which contributes toward resistance
Scale	
Macroscopic	Seen by eye
Microscopic	Seen using a microscope (mostly light or scanning electron)
Molecular	Enzymes, proteins, DNA, RNA, DNA modification

Physical Factors

The physical factors such as heat, ultraviolet, and electromagnetic fields and mechanical scarification are the first contact point with the seed coat and may then trigger downstream consequences from this initial interaction. In the following section, each physical factor and its effect will be presented individually.

Heat

The temperature of plasma treatments can range from room temperature up to 90°C, so in principle it is possible to have an effect depending on the temperature and treatment time although not many authors think that increased temperature is responsible for the changes in plants. Temperature is monitored in a few studies by measuring the electrode temperature, calculating the gas temperature from spectra or measuring the temperature of the seed directly using an infrared camera or thermocouple [47, 109] but it has not yet been done on a molecular level by assessing the seed or plant response. Kitazaki et al. [110] compared plasma and heat treatments by heating the seeds on a hot plate but did not see the same effect on the plant development.

Others have tried to look into heat shock proteins (HSPs), which are induced with temperatures ranging from 31 to 37°C, but HSPs are often not exclusively induced by heat. They may also accumulate under oxidative stress, high intensity irradiation, and desiccation [111]. Iranbakhsh et al. [78] treated wheat seedlings with plasma and observed increased expression in heat shock factor A4A in both the root and shoot system in correlation with an increase of growth parameters and mitigating the negative effect of salinity stress. They only reached a maximum of 29°C in a 2 min plasma treatment, suggesting that heat alone is not responsible for the observed effects in this particular study but the role of HSPs during plasma treatment remains unclear since it was shown not to change in the study by Mildažiene et al. [53].

Ultraviolet Light (UV)

The role of high-energy photons in plasma-seed treatments has been controversial since UV has had a negligible effect so far but the effects of UV on seeds and plants could theoretically contribute to the wettability or growth enhancement effects indirectly; for example, by producing radicals or reactive oxygen species (ROS) such as ozone [60]. Gao et al. [52] checked the effects of UV separately from plasma and observed that UV had only a minor contribution toward the seed wettability. Sarinont et al. [102] also reported that there was no effect from UV when they saw the lack of growth enhancement effect after they blocked UV with a quartz plate.

It is known that just UV-B can accelerate germination of safflower seeds but then negatively affects growth [112]. Noble [113] made the same conclusions with kale, cabbage, radish and agave seeds. Likewise, Sadeghianfar et al. [114] showed accelerated germination of maize and sugar with UV-C treatment but instead, saw an increase in plant growth parameters and suspected this may be due to breaking down the seed coat and increase in temperature.

There may be differences in effects depending on the wavelength since it has been shown that UV-A had a more pronounced effect than UV-C but both were able to accelerate the germination rate and improve growth parameters [115]. On the one hand, UV is often associated with inducing DNA damage. Prakrajang et al. [46] compared gamma radiation with plasma and saw only with gamma irradiation that the plants did not grow well and thus suspected it was induced DNA damage. On the other hand, plants treated with UV were able to better cope with drought stress, possibly by activating DNA repair mechanisms [116]. This may be due to an increase in phenolic compounds, which often have a role in disease or stress resistance and this response can be triggered by intense UV light which is accompanied by high temperature and photo-oxidative damage in nature [117].

Babajani et al. [59] and Iranbakhsh et al. [118] both considered that plasma-derived UV may be detected by photoreceptors which then might affect secondary metabolism and trigger stress responses if the treatment is done briefly. UV is also linked with photomorphogenesis and cell elongation, division, and differentiation [119]. Iqbal et al. [63] compared laser and plasma treatment separately on seeds and saw similar types of effects: damage to the seed coat, an increase in water uptake and protein content.

Electromagnetic Fields (EMF)

Pauzaite et al. [23] and Mildažiene et al. [53] also attributed the changes in growth parameters to radiation since Mildažiene et al. [53] saw similar protein expression profiles when comparing seeds treated with plasma or electromagnetic fields (EMF). This is

TABLE 2 | Collection of plasma-seed treatment papers.

Citation	Plasma	Seed type	Micro (organism)	Main findings	Scale
Iranbakhsh et al. [38]	DBD; atm pressure; Ar	Hemp		Growth parameters, metabolism	Macroscopic and molecular
Kang et al. [39]	1) Arc discharge; low or atm pressure; underwater 2) DBD; low and atm pressure; (0.6–1 atm); not clear	Rice	*Fusarium fujikuroi*	Seed coat modification, growth parameters, disinfection/disease resistance	Macroscopic
Billah et al. [40]	DBD; low pressure (400 torr); air	Black gram		Seed coat modification, growth parameters, metabolism	Macroscopic and molecular
Rezaei et al. [41]	Not clear; atm pressure; air	Hyssop		Tissue modification (dried leaves)	Macroscopic
Koga et al. [42]	DBD; atm pressure; humid air	Radish		Seed coat modification (color)	Macroscopic
Ghasempour et al. [43]	DBD; atm pressure; Ar	Catharanthus roseus		Growth parameters, metabolism	Macroscopic and molecular
Mujahid et al. [44]	DBD; atm pressure; He and O_2	Grape cultivar Muscat of Alexandria		Growth parameters, metabolism	Macroscopic and molecular
Filatova et al. [45]	CCP RF; low pressure (200 Pa); air	Maize, wheat, lupine	Native fungi, *Fusarium culmorum*	Growth parameters, metabolism, disinfection/disease resistance	Macroscopic and molecular
Prakrajang et al. [46]	Not given; not given; Ar	Chili pepper		Growth parameters	Macroscopic
Kobayashi et al. [47]	DBD; atm pressure; air	Arabidopsis (seedlings)		Growth parameters	Macroscopic
Dawood [48]	RF; low pressure; Ar	Moringa		Seed coat modification, growth parameters	Macroscopic and microscopic
Sidik et al. [49]	Plasma jet/plume; atm pressure; He	Corn and eggplant		Growth parameters	Macroscopic
Ambrico et al. [50]	DBD; atm pressure; air	Basil		Seed coat modification, growth parameters,	Macroscopic and microscopic
Seddighinia et al. [51]	DBD; atm pressure; Ar	Bitter melon		Growth parameters	Macroscopic, microscopic
Gao et al. [52]	DBD; atm pressure; air	Pea		Seed coat modification, growth parameters	Macroscopic. microscopic
Mildažiene et al. [53]	CCP RF; low pressure (200 Pa); air	Sunflower		Growth parameters, metabolism	Macroscopic and molecular
Šerá et al. [54]	DBD; atm pressure; air	Pine		Growth parameters, disinfection	Macroscopic
Cui et al. [55]	DBD; atm pressure; air	Arabidopsis		Growth parameters, metabolism	Macroscopic and molecular
Liu et al. [56]	DBD jet; atm pressure; N_2, O_2, air	Radish, mung bean, wheat, tomato, lettuce, mustard, Dianthus and sticky bean		Growth parameters	Macroscopic
Los et al. [57]	DBD; atm pressure; air	Wheat		Seed coat modification, growth parameters, metabolism	Macroscopic and molecular
Moghanloo et al. [58]	DBD; atm pressure; Ar	Astragalus frida		Growth parameters, metabolism	Macroscopic and molecular
Pérez-Pizá et al. [36]	Needle to plane DBD; atm pressure; N_2, O_2	Soybean		Seed coat modification, growth parameters, metabolism	Macroscopic and molecular
Babajani et al. [59]	DBD; atm pressure; Ar	Melissa officinalis		Growth parameters, metabolism	Macroscopic and molecular
Lotfy et al. [60]	Plasma jet; atm pressure; N_2	Wheat		Seed coat modification (water uptake), growth parameters	Macroscopic
Bafoil et al. [61]	DBD; atm pressure; air	Arabidopsis		Seed coat modification, growth parameters	Macroscopic, microscopic?, and molecular
Singh et al. [62]	RF; low pressure; (0.40 mbar) O_2 and Ar	Basil		Growth parameters, metabolism	Macroscopic and molecular
Iqbal et al. [63]	Not clear; low pressure; Ar	Wheat		Seed coat modification, growth parameters, disease resistance	Macroscopic and molecular

(Continued)

TABLE 2 | Continued

Citation	Plasma	Seed type	Microbe	Main findings	Scale
Islam et al. [64]	DBD; low pressure (10 Torr); air, Ar, O_2	Rapeseed, mustard		Growth parameters, metabolism	Macroscopic and molecular
Kabir et al. [65]	DBD; low pressure (10 Torr); air, Ar, O_2	Wheat		Seed coat modification, growth parameters, metabolism	Macroscopic and molecular
Afsheen et al. [66]	RF capacitive; low pressure; Ar	Wheat	Beetle	Seed coat modification, pest resistance	Macroscopic
Lo Porto et al. [67]	RF; low pressure (800 mTorr); N_2, O_2	Asparagus		Seed coat modification, growth parameters	Macroscopic
Jiang et al. [68]	ICCP RF; low pressure (150 Pa); He	Tomato		Growth parameters	Macroscopic
Hosseini et al. [69]	CCP RF; low pressure; N_2	Artichoke		Seed coat modification, growth parameters, metabolism	Macroscopic, microscopic and molecular
Tounekti et al. [70]	DBD; atm pressure; He	Coffee and grape seeds		Growth parameters	Macroscopic
Zhang B. et al. [37]	CCP glow RF; low pressure (30-200 Pa); air, He	Maize, peppers, wheat, soybeans, tomatoes, eggplants, pumpkins		Growth parameters, metabolism	Macroscopic and molecular
Khatami and Ahmadinia [71]	Gliding arc; atm pressure; air	Pea, Zucchini	Native microflora	Growth parameters	Macroscopic
Pawłat et al. [72]	DBD plasma jet; atm pressure; He and N_2	Thuringian Mallow		Seed coat modification, growth parameters	Macroscopic and microscopic
Rahman et al. [73]	DBD; low pressure (10 Torr); air, Ar, O_2	Wheat		Seed coat modification, growth parameters, metabolism	Macroscopic, microscopic and molecular
Pawlat et al. [72]	Gliding arc; atm pressure; N_2	Thuringian Mallow		Seed coat modification, growth parameters	Macroscopic and microscopic
Hayashi et al. [74]	RF; low pressure (20-80 Pa); O_2, Ar	Arabidopsis, radish		Growth parameters, metabolism	Macroscopic and molecular
Matra [75]	Plasma flashlight; atm pressure Ar, O_2	Sunflower		Growth parameters	Macroscopic
Bafoil et al. [76]	1) DBD; atm pressure; air 2) plasma jet; atm pressure; He	Arabidopsis		Seed coat modification, growth parameters	Macroscopic, microscopic
Măgureanu et al. [25]	DBD (fluidized); atm pressure; air	Tomato		Growth parameters	Macroscopic
Štěpánová et al. [77]	DBD; atm pressure; air	Cucumber and pepper		Seed coat modification, growth parameters	Macroscopic and microscopic
Iranbakhsh et al. [78]	DBD; atm pressure; Ar	Wheat		Growth parameters, metabolism, stress resistance	Macroscopic and molecular
Iranbakhsh et al. [79]	DBD; atm pressure; Ar	Chili pepper		Growth parameters, metabolism	Macroscopic, microscopic and molecular
Pauzaite et al. [23]	CCP RF; low pressure (60 Pa); air	Norway spruce		Growth parameters	Macroscopic and molecular
Park et al. [80]	DBD; atm pressure; N_2 and air	Barley		Seed coat modification, growth parameters, metabolism	Macroscopic and molecular
Zhang J. et al. [81]	DBD; atm pressure; Ar	Soybean		Growth parameters	Macroscopic
Shapira et al. [82]	RF inductive; low pressure; air	Pepper and lentil		Seed coat modification	Microscopic
Lotfy (36b)	Plasma jet; atm pressure; N_2	Watermelon		Seed coat modification, growth parameters	Macroscopic
Wang et al. [83]	DBD; atm pressure; air, N_2	Cotton		Seed coat modification	Microscopic
Kim et al. [84]	Corona discharge plasma jet; atm pressure; air	Broccoli	Native Aerobic bacteria, molds and yeasts, *B. cereus*, *E. coli*, Salmonella spp.	Growth parameters, metabolism	Macroscopic and molecular

(Continued)

TABLE 2 | Continued

Citation	Plasma	Seed type	Microbe	Main findings	Scale
Mildažiene et al. [85]	CCP RF; low pressure (60 Pa); air	Purple coneflower		Growth parameters	Macroscopic and molecular
Li et al. [86]	DBD; atm pressure; air	Wheat		Seed coat modification, growth parameters, metabolism	Macroscopic, microscopic, molecular
Sera et al. [87]	1) gliding arc; atm pressure; humid air 2) microwave plasma discharge; low pressure (140 Pa); Ar, O_2	3 cultivars of hemp		Growth parameters	Macroscopic
Puligundla et al. [88]	Corona discharge plasma jet; atm pressure; air	Rapeseed	Native	Growth parameters, metabolism	Macroscopic and molecular
Puligundla et al. [89]	Corona discharge plasma jet; atm pressure air	Radish	Native	Growth parameters, metabolism	Macroscopic and molecular
Gómez-Ramírez et al. [90]	1) DBD; low pressure (500 mbar); dry air 2) RF; low pressure (0.1 mbar); dry air	Quinoa		Seed coat modification, growth parameters	Macroscopic, microscopic
Guo et al. [91]	DBD; atm pressure; air	Wheat		Seed coat modification, growth parameters, metabolism, stress resistance	Macroscopic, microscopic, molecular
Zhang et al. [92]	Needle to plane DBD; atm pressure; Ar	Soybean		Growth parameters, metabolism	Macroscopic, molecular
da Silva et al. [93]	DBD; atm pressure; air	Mimosa		Seed coat modification, growth parameters	Macroscopic and microscopic
Meng et al. [94]	DBD; atm pressure; air, Ar, O_2, N_2	Wheat		Seed coat modification, growth parameters, metabolism	Macroscopic, microscopic, molecular
Nalwa et al. [95]	Glow discharge; low pressure (0.2 mbar); O_2	Bell pepper		Seed coat modification, growth parameters,	Macroscopic, microscopic
Junior et al. [96]	Plasma jet DBD; atm pressure; He	Mulungu		Seed coat modification, growth parameters	Macroscopic, microscopic
Zahoranová et al. [97]	DBD; atm pressure; air	Wheat	Native	Seed coat modification, growth parameters	Macroscopic
Zhou et al. [98]	Plasma jet array; atm pressure; He, N_2, air, O_2	Mung bean		Seed coat modification, growth parameters, metabolism	Macroscopic, microscopic, molecular
Khamsen et al. [99]	Hybrid microcorona discharge; atm pressure; air, Ar;	Rice	Native fungi	Seed coat modification, growth parameters	Macroscopic and microscopic
Li et al. [16]	CCP RF; low pressure (150 Pa); He	Peanut		Seed coat modification, growth parameters	Macroscopic
Gholami et al. [100]	CCP RF; low pressure; air	Ajwain		Seed coat modification, growth parameters	Macroscopic
Matra [101]	Plasma flashlight; atm pressure; Ar	Radish		Growth parameters	Macroscopic
Sarinont et al. [102]	DBD; atm pressure; air, O_2, NO, He, Ar, N_2	Radish		Growth parameters	Macroscopic
Dobrin et al. [103]	DBD; atm pressure; air	Wheat		Seed coat modification, growth parameters	Macroscopic
Stolárik et al. [104]	DBD; atm pressure; air	Pea		Seed coat modification, growth parameters, metabolism	Macroscopic, microscopic, molecular
Munkhuu et al. [105]	Not clear; not clear; not clear	Clover		Growth parameters	Macroscopic
Ji et al. [106]	1) DBD; atm pressure; Ar, N_2, air 2) microwave plasma torch for NO; N_2, O_2	Coriander		Seed coat modification, growth parameters	Macroscopic
Kadowaki and Kurisaka [107]	DBD; atm pressure; air	Arabidopsis		Growth parameters	Macroscopic

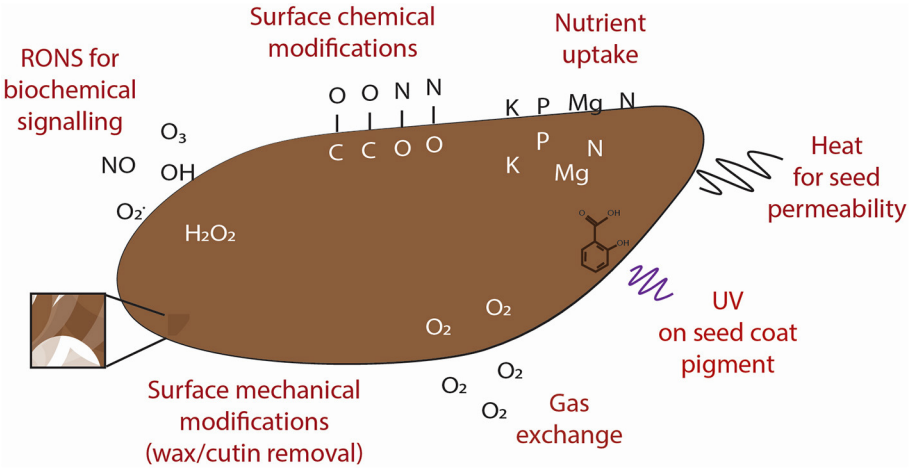

FIGURE 2 | Summary of the possible mechanical, chemical, and biochemical interactions of plasma components with the seed surface.

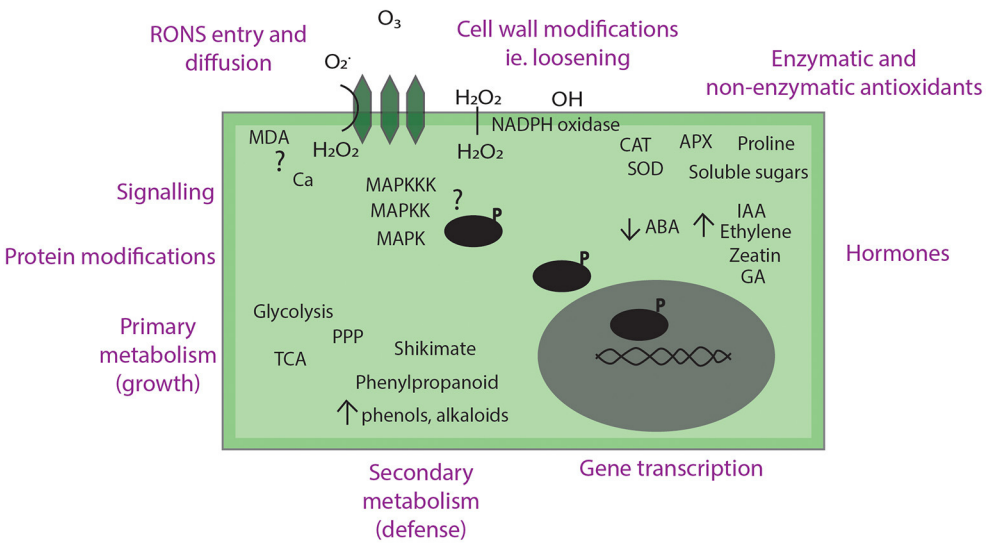

FIGURE 3 | Summary of hypotheses and current evidence of plasma-seed treatments on a molecular scale.

not entirely surprising since pulsed electric fields also affect seed germination [120, 121]. It needs to be kept in mind though that electric field treatment is also accompanied by oxidative stress and ozone [122] where ozone has been suggested by Patwardhan and Gandhare [123] to be the main effective parameter in the treatment.

Static or alternating magnetic fields can also change germination probability, growth rates, increase root, and shoot length, change redox status of plants possibly by increasing hydrogen peroxide (H_2O_2), altering photosynthesis, alleviating drought stress or increasing mineral content [124, 125]. Arguably, UV may have a role but a minor contribution in terms of direct effect considering that the above studies used several hours long UV treatments to have an effect whereas most plasma treatment are in the seconds or minutes range. Nevertheless, photons and electromagnetic fields can still possibly contribute indirectly through the production of RONS.

Mechanical Scarification and Erosion

In terms of mechanical effects, it has been suggested that altering the seed coat may play a role in modifying germination rate. Typically, a seed has four layers: the cuticle, epidermis, hypodermis, and parenchyma. The differences in the microstructures and chemistry of these layers determine differences between species and even cultivars. The seed coat role is like a water modulator; it controls the entry of water so it can be absorbed slowly by the cotelydons to minimize or avoid imbibition damage [126].

It has been suggested that the removal of the lipid layer allows for better access to water, a requirement for triggering germination [127]. Bafoil et al. [61] showed the importance

of the seed coat by using mutants of *Arabidopsis* plant model L*er* and Col-0 ecotypes and showed the rearrangement of lipid components, changes in lignin and seed coat erosion. Many, although not all authors have observed with scanning electron microscopy (SEM) that seed surfaces treated with plasma have an eroded appearance [52, 83, 86, 93, 96, 104], where Mildažiene et al. [128] only saw etching on the seed surface facing plasma treatment and others did not see any changes [29, 110, 129].

A majority of these authors have been able to correlate these changes with increased water uptake. For example, Pawlat et al. [72] observed that plasma treatment changed the seed structure by removing the upper cuticle layers covered with wax, a polymer present to prevent water loss under heat stress, and may form micro-pores to aid water absorption. Bafoil et al. [61] also worked with an *Arabidopsis* mutant *gtap5,* which is not able to make suberin or cutin and saw that plasma was not able to improve the germination without these polymers in the seed coat, suggesting their importance. This waxy layer was even considered as a parameter in the experimental design of a study done by Park et al. [80]. They used two seed types, one with and the other without a waxy layer, and their results indirectly implied that this waxy layer plays a role in the effect that plasma treatment will have on the seeds, suggesting plasma indeed may be improving the seed coat permeability, considering wax limits water loss and controls gas exchange.

Billah et al. [40] pointed out that there may be exothermic reactions from the plasma that release heat and may melt the wax due to its low evaporation temperature of 37°C or eroded by reactive species. This was also pointed out by Holc et al. [130]. Wang et al. [83] also suggested that through surface modification via etching, the seed is able to absorb water through increased hydrophilicity. This enhanced water absorption by modifying the seed structure is further supported by others who observed the degradation of cellulose on seed surfaces [131]. Currently, the analysis of components with FTIR-ATR is limited to cellulose since it is difficult to differentiate between different organic plant components like cellulose, hemicellulose, pectins, etc. Wang et al. [83] used both FTIR-ATR to measure seed surface changes as well as FTIR to analyze the gas exhaust from the plasma treatment. They needed to omit wavenumbers i.e., peaks below 1,500 cm^{-1} that were difficult to assign to specific functional groups during analysis but also suggested that the spectral bands are mainly attributed to cellulose rather than wax.

Junior et al. [96] showed that water may be guided differently after plasma treatment due to surface modifications. They observed that the hilum increased the amount of water absorption, the micropyle had a more open configuration and in particular, the water absorption was improved mainly through the hilum rather than micropyle. In any case, by thinning the seed coat, it is logical to assume that water will be more readily absorbed.

Interestingly, the water absorption can be controlled by the plasma treatment using different gases and coating thickness as mentioned by Volin et al. [28]. Depending on the working gas, 0.5–2 μm thick coatings were applied and their thickness modified imbibition. This suggests that the seed coat thickness can be mechanically modified by etching or by changing the chemical properties.

Despite adding to the thickness with an additional layer of coating, germination was improved in a few instances, which highlights the importance of chemistry, but it is difficult to separate the etching effect from the chemistry in this study. As it still remains, it is not known yet whether this increased permeability is principally due to mechanical mechanisms such as etching as Pawlat et al. [132] suggested, a combination of both mechanical and chemical as mentioned by Gómez-Ramírez et al. [90], Tounekti et al. [70], and Park et al. [80] or solely due to chemistry.

SEM is an insightful tool, which can provide quick qualitative results of the plasma-seed treatment. Nevertheless, caution should be exercised when interpreting SEM images because plant genetics influence the seed coat pattern. Otherwise, observed changes might already be pre-existing and should instead be attributed to biological variation rather than plasma treatment and therefore, using the same seed before and after treatment is recommended.

Pawlat et al. [132] noticed that the seed shape influences the type of change affecting the seed and showed in their SEM images that the seed edge was torn off whereas the middle grew in sharpness. This brings attention to the fact that this process needs to be delicately handled. For example, Cui et al. [55] used tape to prevent the movement of seeds during the plasma treatment but this may affect the seed coat especially if it is done in the presence of moisture. As a result, it seems that there is a limit to how much information can be extracted from surface analysis using microscopy. Instead, it would be useful to further explore the chemical modifications since this is currently limited at the moment in the literature.

It may very well be that the chemistry is sufficient to affect downstream processes considering that an effect in growth parameters without visible seed coat modifications has been observed [57]. Mildažiene et al. [85] also observed positive growth effects using vacuum and EMF without visibly changing the seed coat structure using SEM. It may also be the case that the results will depend partly on whether there is physical or physiological dormancy meaning whether dormancy is due to the seed coat or embryo.

Chemical Factors

On the one hand, etching may play more of a role in certain seed types with impermeable seed coats but, on the other hand, it may be that a specific concentration and/or mixture of reactive species from a higher power plasma is required to observe an effect. In the latter, mechanical damage might merely be a side effect, which too can contribute to enhanced water absorption but is not the primary factor. For this reason, chemical factors will now be discussed in the next section.

Nutrient Absorption

In addition to analyzing mechanical damage, SEM can be coupled with energy dispersive X-rays (EDX) to look at the composition of seed surface. Other methods such as X-ray Photoelectron

Spectroscopy (XPS) and micro X-ray fluorescence spectroscopy (μ-XRF) can also be used to acquire information about the elemental distribution. It has been observed by several authors like Pérez-Pizá et al. [36] and da Silva et al. [93] that lipid layers undergo chemical oxidation, which can therefore improve interaction with water.

Shapira et al. [82] found that irreversible wettability is not due to electric charging, which could indirectly imply that it may be done chemically. Pérez-Pizá et al. [36] also correlated the increased hydrophilicity with oxidized seed using nitrogen and oxygen plasmas. This perhaps suggests that hydrophilicity again is done through chemical rather than mechanical changes. This may not be entirely dependent on the gas type but rather about producing an appropriate profile of reactive species at sufficient concentrations that will oxidize the outermost lipids. It has been shown by Gómez-Ramírez et al. [90] using XPS and EDX that plasma treatment can oxygenate carbon and deposit nitrogen groups on the seed surface. They hypothesized that these elements, as well potassium, are later absorbed by the seed in the presence of water [133].

Ambrico et al. [50] instead used μ-XRF and showed the concentration and redistribution of macro- and micronutrients such as potassium after plasma treatment. As an example, on the one hand, the diffusion of potassium into the seed interior may improve the germination through enzyme activation, help with water retention, or detoxify ROS [134]. On the other hand, potassium at the surface can be interpreted as seed damage since it may be used as an indicator of cell membrane integrity [135]. Interestingly, Zhou et al. [98] exposed seeds to plasma-treated water and they had the lowest leakage rate by measuring electrical conductivities, which is used to measure the cell membrane integrity. This mobilization of nutrients perhaps is not lost to the environment but is loosened and absorbed immediately by the seed [136].

Gas Exchange

When considering gases, it could be that oxygen on the surface is responsible for not only increased wettability but may also assist in seed respiration. Considering that oxygen is another requirement for germination, Sarinont et al. [102] observed oxygen, NO and nitrogen gas to be the most effective for plant growth but fumigation with oxygen gas already had an effect on growth parameters, albeit mild compared to plasma. This fumigation might be sufficient to improve plant growth like in the case of nanobubbles [137]. Although fumigation had a positive effect on plant growth, plasma application had a stronger effect which may be due to the transport process being more efficient i.e., speed up the process by not relying on diffusion or provide more directionality. This highlights the presumably overlooked importance of oxygen especially considering that Rahman et al. [73] saw also more obvious changes in growth parameters when using an oxygen admixture instead of air.

This principle could likewise work for nitrogen gas but instead of modifying respiration, it may be directed toward other cellular processes such as photosynthesis since it is a major component of chlorophyll or protein synthesis [138]. As mentioned in the paper of Gao et al. [52], the presence of CO and O_2^+ signals confirmed that chemical etching of the seed surface by plasma played an important role in stimulation of seed germination [139]. These chemical changes may then be responsible for changing the biochemistry and molecular events in the plant and therefore, these will be discussed in the next section.

Biochemical and Molecular Factors

Chemical Species

RONS and Seed Coat Interactions

Regardless of whether the changes to the seed coat surface might loosen an elicitor such as oligosaccharins, as mentioned by Iranbakhsh et al. [78], many authors are in agreement and speculate that it is principally reactive oxygen and nitrogen species (RONS) that trigger biological processes.

Oxidation of the seed coat is very often observed but this can be propagated internally since there can be an increase in maldonaldehyde (MDA), a product of lipid peroxidation, after plasma treatment as seen by both Los et al. [57] and Cui et al. [55]. This may be among the first steps in the signal transduction considering that lipid peroxidation does not rely on enzymatic activity, which is very limited in dry seeds [140].

Mujahid et al. [44] mentioned that it may be instead the hydroxyl radicals which are responsible for the cell wall loosening. Bafoil et al. [61] calculated an increased expression of 23 genes for class III peroxidases after plasma treatment, which are proteins localized in the seed coat which regulate concentrations of hydrogen peroxide and precede the rupture for germination. Pauzaite et al. [23] also suggested that ROS may alter the seed coat pigmentation, which is known to be linked to germination. The flavonoid biosynthetic pathways and abscisic acid, a hormone for dormancy, are regulated by the same gene locus. Although they had changes in the seed coat flavonoids, they could not find any clear connection in their study between flavonoids and seed germination parameters.

Others have seen that the seed coat pigmentation does in fact influence seed permeability and the rate of imbibition where brown seeds had faster water uptake, reached a germination optimum sooner but were more susceptible to imbibition damage than black seeds [141]. Liu et al. [56] also attempted to decipher between seed types using PAW and brought up in their discussion that seed storage proteins are typically oxidized during germination, which may facilitate the mobilization of the storage reserve. Therefore, it may be possible that plasma-derived ROS may be affecting the seed pigmentation first and then downstream the germination rate. Additionally, considering that Mueller et al. [142] suggested that ROS play a role in the cleavage of cell wall polymers, it may be that changes inside the seed in turn modify the outer layers. The mechanical pressure on the endosperm needs to be relieved for the radical protrusion but this is based on cell wall loosening, which is linked to the action of ROS [140] and this, again, may be another argument that external seed coat erosion might not be necessary for modifying germination.

Alternatively, it could also be that chemical modifications to the seed coat, for example through lipid oxidation, may lead to

the carbonylation of proteins, rendering them more susceptible to cleavage and leading to the breakdown of aleurone layer [140, 143]. Therefore, post-translational modifications, such as carbonylation and sulfhydryl group's oxidation, are also another mechanism by which ROS, specifically H_2O_2, can shift a seed from a dormant to non-dormant state as shown by Oracz et al. [144] and Valderrama et al. [145].

ROS Entry and Involvement in Seed Development

Generally, it is not fully understood how external ROS are detected and how these signals are transduced in seed cells but this process may partly depend on the presence of water. Water is needed to trigger germination and increase respiration, a reaction which oxidizes sugars to release energy in the form of ATP. During respiration, ROS are produced as by-products and thus, ROS generation is the hallmark from dormant to metabolically active seeds [140]. Where the moisture content is low, there is very little, if any, enzymatic activity but there may be hydrated pockets within the seed, permitting limited metabolic activity. It could be that this pocket of water may assist the diffusion and retention of ROS in the seed and, therefore it may be that plasma-derived ROS accumulate in these pockets and trigger signaling for intracellular programs. This process may be done more efficiently with hydrated instead of desiccated seeds due to the higher water content. Nevertheless, in dry conditions, ROS may have an effect that is simply paused until imbibition [140] and this may be why there are long-term effects [23] or why long-term storage of plasma-treated seeds can still have a positive effect on growth parameters relative to the untreated seeds [102]. On the other hand, the effects of the plasma treatment may be continuously ongoing but are not morphologically obvious until imbibition and subsequent growth. Mildažiene et al. [128] pointed out that biochemical changes continue to occur in seeds at various levels, including hormonal balance, gene expression, oxidative processes, mRNA content, and protein translation during storage and these changes may occur across all of these levels after plasma treatment.

Although it is not known which ROS is/are responsible for the effect and how it/they enter, it is known that seeds have pores whose size is genetically regulated and this also may assist the diffusion of ROS into the seed [126]. H_2O_2 can interact with the surface and diffuse through the membrane but charged species such as superoxide are not able to bypass the membrane and are dependent on voltage-dependent anion channels called porins, which are only found in the mitochondria [146]. Despite its charge, superoxide can break down into hydroxyl and singlet oxygen and these may be able to bypass more easily [147]. In some cases, RONS bypass the membrane using aquaporins, protein channels used for water transport [148]. Transport also depends on the life stage of the plant since ozone can be taken up through the stomata in the leaves. Seol et al. [149] observed an accumulation of ROS in chloroplasts, and suggested that through the micropores, ROS can travel down further into the plant tissue, from the epidermis into the mesophyll but if too potent, chloroplast degradation occurs.

Considering the lifetime and complexity of the reactive species reactions, there is a bias for researchers to measure longer-lived species like H_2O_2, O_3, and NO and therefore, most of the focus for this section will be dedicated to these species herein [150].

Ozone

Surprisingly, little has been done to monitor and measure ozone during plasma treatments and it seems that many overlook the effect of ozone on seed germination despite it being possible to enhance germination with optimized treatment parameters. On the one hand, ozone can impair plant growth by replacing CO_2 and reducing photosynthesis. This is done by inhibiting the opening of the stomata due to the reduced flow of potassium ions [151]. In some cases, plants like mung beans are not able to overcome ozone stress with their antioxidant defenses [152]. On the other hand, ozone has been used to enhance seed germination [153] or improve fruit quality [154]. Ozone seemingly has an ambivalent role that is dependent on the concentration and length of treatment [155] as it is the case for many other treatments i.e., hormone, nanoparticles, heat. The authors mentioned that there is a variable response to the same ozone treatment based on the species and it is weak and transient. By using electron paramagnetic resonance (EPR), they showed that O_3 increased the concentration of radicals (carbon and oxygen species) in all tested species except one.

Pawlat et al. [72] measured 0.01 ppm of ozone produced during plasma treatment and had an effect on the growth parameters but it is not clear whether this is due to ozone or other treatment parameters, such as the short heat treatment at 40°C. Perhaps this ozone treatment might not have been sufficient, in terms of concentration and exposure time but is a good example to point out that it would be helpful to include as a control in studies to clarify whether the effect is due to ozone, other reactive species or other parameters.

It is especially interesting to differentiate this because ozone can trigger the production of ethylene, which then breaks down abscisic acid, the seed dormancy hormone [156]. Alternatively, it could be that ozone generates short-lived species inside the seed, which may be recognized as a signal for germination since the accumulation of ROS and peroxidation products is linked with seed dormancy alleviation [144]. As Sudhakar et al. [157] pointed out, the production of hydrogen peroxide is observed in the early imbibition period of tomato seeds and nitric oxide, hydroxyl radicals and superoxide radicals accumulate during seed germination in different species. For this reason, many scientists speculate that H_2O_2 and NO are the reason for the observed effects using plasma treatments, whether or not it is the short-lived species such as superoxide, hydroxyl and NO that are eventually converted into H_2O_2 [55].

Wang et al. [83] used a nitrogen plasma in open air and suggested that nitrogen oxides, which are known to have a role in dormancy and germination signaling, are present after plasma treatment and may initiate these biological processes [158]. Instead, Puac et al. [159] looked at meristematic cells of carrots treated with a RF plasma for <2 min and suggested that at least H_2O_2 and superoxide can pass through the cell membrane and reactive species may be one mechanism

since they observed fluctuations in levels of redox quenching antioxidant enzymes such superoxide dismutase (SOD), catalase (CAT), ascorbate peroxidase (APX), which control and limit damage from excessive levels of ROS. This was also observed by Henselova et al. [160] in maize using a DSCBD for <2 min. Simultaneously, these antioxidative enzymes may behave like sensors to detect ROS availability and redox perturbations so that an organism can respond appropriately [145, 161]. There is also an overlapping relationship between these enzymes, NO and H_2O_2 where NO positively regulates APX1 through a post-translation modification, S-nitrosylation, which then enhances resistance to oxidative stress and improves immune responses [162] and NO regulates itself as well as ROS [145, 163].

NO and H_2O_2

Rahman et al. [73] suggested that plasma induces H_2O_2 formation, which is found in hydrated seeds and is involved in imbibition and early germination. They compared Ar/O_2 to Ar/air admixtures and observed higher concentrations of H_2O_2 with Ar/O_2 without inducing scavengers that counter H_2O_2 production. They concluded that plants treated with this admixture had better growth parameters due to the increased H_2O_2 concentration and did not see any changes in NO. Likewise, after plasma treatment, an increase in H_2O_2 concentration was correlated with positive effects on germination, whereas a decrease was correlated with negative effects on germination [23]. The same authors also showed for the first time the oscillatory dynamics of H_2O_2, which occurs in *Arabidopsis* and conifers but it is not characteristic for other seed types such as radishes and sunflowers. This already suggests that there can be differences between species including on a molecular level.

Kang et al. [39] interestingly did not see an effect and observed high variation in rice germination. Los et al. [57] also saw no changes in H_2O_2 levels in wheat but still had growth enhancement. This suggests that there are either differences in the plasma that do not necessarily lead to changes in H_2O_2 and requires optimization, or that seeds respond differently, and it is not exclusively due to H_2O_2 but instead to nitrites and nitrates.

This latter point was heavily emphasized by Billah et al. [40] who observed an increase in H_2O_2 but think that nitrogen is the main contributor for enhanced growth in gram seeds. In contrast, Liu et al. [56] compared different gases using direct and indirect plasma treatments to produce PAW and soaked a variety of seeds. They were tempted to believe that effects are more likely due to oxygen-derived species. Interestingly, NO can downregulate the signal for H_2O_2 and will activate genes for antioxidant enzymes as pointed out by Iranbakhsh et al. [118] so once again, it is difficult to separate the effects of both H_2O_2 and NO.

In the case of H_2O_2, it is considered a long-distance signaling molecule, which is highly interconnected with hormones, metabolism and gene transcription. The signaling likely includes MAPK cascades as pointed out also by Babajani et al. [59]. ROS mediated signaling includes calcium signaling, protein phosphorylation and gene transcription which are redox sensitive. The relationship between ROS and MAPK is not fully elucidated and both are able to regulate each other. These complexes phosphorylate transcription factors, kinases, phosphatases or other proteins, which can then change enzyme activity or gene expression [164].

Additionally, ROS may produce changes in calcium signaling and use different signatures in terms of duration and amplitude depending on the species and this will dictate what happens downstream, for example root elongation [165]. It was shown by Cui et al. [55] that there was increased calcium in the roots of 4-day-old *Arabidopsis* seedlings which were previously plasma-treated as seeds and they mentioned this may eventually lead to plant growth if maintained at a low level. Since there is little evidence about signaling due to plasma treatments, the focus now will shift from signal transduction to how hormones, metabolism and gene expression are modified with plasma, starting first with hormones.

Hormones

It is difficult to differentiate between the action of ROS and hormones because ROS are highly interconnected with hormones like salicylic acid (SA) and jasmonic acid (JA), which are widely reported. Information remains scarce with auxin and cytokinins, which are hormones that affect germination properties [150]. Nevertheless, "hormones modulate the effects of ABA/GA balance: auxin IAA (indole-3-acetic acid) is a negative regulator of germination; ethylene, cytokinins, brasinosteroids, and strigolactones can stimulate germination; SA and jasmonate (stress hormones) may affect germination positively or negatively depending on the situation" [53].

There are authors like Kitazaki et al. [110], who agree on the importance of reactive species. Specifically, they think it is the relationship between ROS and the hormones, which stimulates plant growth. It is true that the importance of hormones cannot be overlooked considering that the seed coat is a source of hormones for the developing seed [166, 167]. Mildažiene et al. [85] also demonstrated how a dry seed undergoes subtle metabolic modulation by using proteomics. They showed that vacuum affected the auxin/cytokine balance, cold plasma increased GA, and EMF decreased the amount of ABA and increased IAA and SA without changing GA despite not being able to make a clear connection between phytohormones and germination kinetics. Ji et al. [168, 169] also observed an increase in GA in spinach seeds but did not measure any other hormones. The increase in GA may be the result of plasma-derived ozone [157] although it is often speculated that it is specifically auxin and cytokinins that are affected, which are hormones that increase and stimulate cell division, proliferation and elongation. Perez Pizá et al. [170] showed that with plasma treatment, there was a decrease in ABA and increase in IAA, a hormone which increases growth by regulating enzyme activity. They also detected H_2O_2, which coincided with an increase in ethylene after 24 h of imbibition.

It may be that plasma-derived ROS regulate hormone production while for example increased auxin levels may be the reason for increased lateral root growth as pointed out by Wang et al. [171] where the authors correlated increased levels of auxin in tomato with lateral root growth under drought stress. Stolárik

et al. [104] found changes in auxin and cytokinins with a 2-min plasma treatment in peas. They found an increase in IAA and oxIAA as well as zeatin, the most common cytokinin, and correlated this with increased growth parameters. This is logical since these two hormones work together; auxin is responsible for DNA replication and initiating the cell cycle whereas cytokinins trigger cell division and mitosis [172].

It seems that plasmas may somehow modulate concentrations of hormones and there may be a link with auxin especially considering that this hormone also affects xylem differentiation [173]. It has been observed that plasma treatment modified the diameters of root and stems as well as the differentiation of tissues such as xylem and phloem [51, 52, 58, 174]. These changes in root morphology may then enhance nutrient exchange [68] which was also proposed by Zahoranová et al. [97]. Moreover, Babajani et al. [59] pointed out that auxin transport may also be affected by NO, which is often produced in plasmas. Additionally, it could very well be the case that auxin biosynthesis is upregulated because it is known that abiotic or biotic stresses increase the shikimate pathway which produces the precursor for IAA.

Metabolism

As stated previously, there is a link between hormones and metabolism and both primary and secondary metabolism, which are involved in growth and defense, respectively, are altered after plasma treatment [175].

Regarding primary metabolism, increased ATP levels along with ethanol were observed, suggesting increased anaerobic respiration [92]. Moreover, higher concentrations of protein and sugar were observed by Islam et al. [64] and Billah et al. [40] due to an increase in reserve utilization enzymes. Billah et al. [40] explained that this could be because H_2O_2 transduces the signal for soluble sugar synthesis and therefore, more soluble sugar and protein are seen after plasma treatment [62]. Moreover, exogenous treatment with H_2O_2 can stimulate germination by breaking dormancy through the oxidative pentose phosphate pathway, which provides reducing power and carbon for the new growth [176]. This pathway also links primary and secondary metabolism because it provides the precursor for the shikimate pathway, which is important for plant defense.

Regarding secondary metabolism, an increase in enzymatic antioxidants like catalase [58], superoxide dismutase [78], phenylalanine ammonia lyase (PAL) and peroxidases [59] as well as non-enzymatic antioxidants like total soluble sugar and proline to better tolerate stress have been observed, likely due to the increased concentration of ROS. Furthermore, Ghasempour et al. [43] showed an increase in phenols, chlorophyll, flavonoids and alkaloids with plasma treatment. Pauzaite et al. [23] has seen changes in flavonoids after plasma treatment while others have observed increased phenolic compounds [45, 168, 177].

Defense

ROS may also trigger defense compounds which can originate from the shikimate pathway and phenylpropanoid pathway to induce the production of precursors. For example, H_2O_2 can activate the shikimate pathway [178, 179]. ROS can also make the plant readily available in a redox state to respond quickly to stress as stated by Filatova et al. [45]. Iranbakhsh et al. [118] suggests that the defense response, triggered by ROS and/or UV, modulates the hormone balance since they saw an increase in PAL, a key enzyme in the phenylpropanoid pathway. This pathway also produces protective proteins called pathogenesis-related proteins and depending on whether they are acidic or basic, they can be upregulated by salicylic acid and ROS or methyl jasmonate and ethylene, respectively [180].

Although Perez et al. [181] used PAW, they looked at several genes involved in plant defense in an infected tomato plant and saw an increase in the gene expression of *pal* (phenylalanine ammonia lyase) but not *pr1a, pr4, pr5* (pathogenesis related protein) or *erf1* (ethylene response factor). The gene *pal* is involved in the phenylpropanoid pathway and makes defense compounds like phytoalexins and phenolic compounds and therefore, this information complements the increase in phenolic compounds seen experimentally by others previously mentioned in the section Metabolism.

Gene Expression

ROS can also affect gene transcription either directly or indirectly through hormone conjugates as mentioned by Stolárik et al. [104]. Redox sensitive transcription factors are widespread among animal, bacteria and plants [147] and these factors can be modified through the formation of disulfides upon sensing ROS [140].

Unsurprisingly, there are others who think plasma also modifies gene expression although molecular information concerning plasma-seed treatments is very limited. Hayashi et al. [182] suggested that ROS generated in plasma with water vapor may be a method to control the redox state of the plant by changing the thiol quantity (oxidizing cysteine to cysteine with OH radicals). This has an important role in gene transcription and therefore can change the plant response.

Iranbakhsh et al. [38] observed an increase in the transcription factor WRKY1 and other enzymes involved in secondary metabolism in plasma-treated hemp seeds. WRKY is of particular interest since it is a family of transcription factors involved in many biotic and abiotic stress responses such as fungus, cold stress, salt stress, and drought tolerance. Furthermore, they are known for regulating phenolic compounds and there are specific factors such as AtWRKY23 that regulate auxin. Moreover, there are also interactions between MAPK cascades and this WRKY family and they can also activate PR proteins [183].

The other genes that have been studied were by Guo et al. [91] who observed an increase in LEA chaperone during stress, Ji et al. [168] who saw increased expression of a hydrolytic enzyme called pullulanase in spinach seeds, Ghasempour et al. [43] who saw an increase in gene expression for DAT, an enzyme in the biosynthesis of vinblastine and vincristine, alkaloids with anti-cancerous properties and Islam et al. [64] who showed changes in gene expression of ascorbate peroxidase and catalase but not superoxide dismutase with an air plasma in rapeseed.

These few preliminary studies demonstrate that plasma treatment can change gene expression for both primary and secondary metabolism, for growth and defense, respectively.

Epigenetics and Genetics

These changes by the plasma treatment in the short-term may be due to epigenetics such as regulating DNA cytosine methylation, which inactivates gene expression [74, 184].

Zhang et al. [92] checked the methylation of genes involved in ATP synthase, an enzyme needed to produce energy for the cell, and TOR kinase, an enzyme which may increase metabolism and biosynthesis for energy and biomass production, and saw decreased methylation, meaning that the expression of these genes increased. Nevertheless, it cannot be ruled out yet that there may be changes to the DNA considering that genotoxic effects from plasma treatment have been observed [185].

Although it was not verified, Mildažiene et al. [85] found many similarities between cold plasma and electromagnetic treatment in protein expression but this may also be done epigenetically or through post-translational modifications. Despite the authors attributing the changes to radiation, it may be the action of hydroxyl radicals or other ROS since they too are produced from high energy radiation [186]. Additionally, there also remains the possibility that instead the DNA repair process is triggered by for example ozone and this may be responsible for the improvement in germination kinetics [187, 188].

Lastly, the plant genome itself may play a role in sensitivity to plasma treatment. Kobayashi et al. [47] treated *Arabidopsis* seedlings and saw that the ecotypes Col and L*er* responded differently to the same plasma treatment although the results were not statistically significant. Lo Porto et al. [67] also pointed out that asparagus germination is strongly influenced by ecotype although they did not include this in their study. Therefore, the genetic component should not be overlooked when considering plasma-seed treatments and studies should be done on multiple generations since plasma treatment can have long-lasting effects in the same generation as observed by Sarinont et al. [102] where the growth enhancing effects remained even after 17 months of storage of plasma-treated radish seeds.

In summary, it remains difficult to infer whether these effects are primarily attributed to the action of a single mechanism like mechanical scarification, chemical modifications, or changes in biochemistry through ROS; even within ROS, each species behaves and functions differently. Additionally, variables such as the state of dehydration or hydration of the seed may influence the interaction and retention of ROS.

Ozone specifically in the presence of UV radiation may undergo reactions to eventually generate superoxide and hydroxyl radicals in the seed coat or these short-lived species may directly interact with the seed coat and this could be the critical point that determines how the external physical and chemical stimuli are transformed into internal biological stimuli.

The seed coat pigments can be altered and seed coat embedded enzymes like superoxide dismutase, NADPH oxidases or peroxidases can transform these species into signaling molecules like H_2O_2, which can more easily diffuse through the membrane or the apoplastic space, and then transduce this signal either through secondary messengers like calcium and MAPK cascade or be transmitted without the assistance of enzymes. Once the signal is sent, the hormonal balance may be modulated between GA and ABA to break dormancy, to increase auxin and cytokinin to accelerate the germination process, and increase ethylene, SA and JA for stress or disease resistance.

In parallel, metabolism may be modulated through the addition of water and enhanced gas exchange to modify enzyme activity to break down food reserves but at the same time, increase enzymatic and non-enzymatic antioxidants to shield against this sudden burst of ROS either externally derived or from metabolism. As a result of this stressful stimulus, metabolism in other defense pathways like shikimate and phenylpropanoid may be then activated to produce precursors in anticipation of future stressful events such as hormones or protective proteins.

CONCLUSION AND FUTURE OUTLOOK

What has been shown to date is a combination of plasma device geometries, treatment methods and seeds that are able to alter the plant parameters. On the one hand, this diversity emerges from individual researchers considering what is relevant for their society and local economy, but on the other hand, this also makes it difficult to standardize the current research. We seem to have reached a point where there is potential in this technology as a proof-of-concept although there may be an inherent bias by publishing solely positive results, giving the impression that finding these setups is simple and it only takes trial-and-error to optimize the treatment conditions. Therefore, it would be helpful for the readers to also publish negative results to know what is not working when designing these treatments to move toward standardization and improve our fundamental understanding.

Most scientists are using DBD plasma enclosed in a chamber with air as the process gas although there is flexibility in choosing the type of plasma device. Air plasma is practical and produces a rich chemistry. However, the role of humidity in these plasma-seed treatments is still debated. Is it best to work with dry or wet seeds? Should one control and add or remove humidity, for example, by a gas flow?

Many authors reported evidence, more often than not, that plasma treatment modifies the seed surface in such a way that water uptake increases; this is either done by poration, removal of the topmost layers or through oxidizing the surface to improve the water interaction. It is not yet clear whether it is through mechanical, chemical means or both and whether this is dependent on the plasma treatment, seed type or both. How much energy needs to be injected into the plasma to obtain these effects? To address this, future studies should continue correlating surface modifications with changes in germination in a systematic manner and clearly record the electrical characteristics. This would clarify if mechanical erosion is necessary to induce a change, under which circumstances mechanical erosion or chemical alterations are needed, and specifically which gas types and electrical properties are needed.

It also seems that most authors agree that RONS are predominantly responsible for the observed plant growth effects. However, it is not yet clear whether it is ROS, RNS or the synergistic action of both. It is also not clear if it is purely a RONS effect because plasma is a synergy of individual mechanisms.

Although most authors agree that the effects are not due to heat, it remains difficult to define temperature in these studies, especially in the presence of a gas flow. Is the seed temperature after treatment, the plasma temperature or the temperature of the device measured? Is it certain that an increase of a few degrees is not enough to trigger a heat shock response? Is the relative humidity altered by the plasma heating? For this reason, it would be useful for scientists to include controls in their studies for heat, ozone, electric fields, and humidity, mimicking what they are using in the plasma treatment where possible.

Most authors observe changes at the molecular level although these studies are still extremely limited. More studies focusing on gene and protein expression would at least provide insight about whether the same genes are activated across different plasma treatments and across different seed types. It is also not clear whether these effects are long-term and at which point they would be considered genotoxic or adverse for plant growth. The bottleneck here will be that gene expression studies are limited to already sequenced plant genomes. However, these results may be applicable to closely related species.

As a next step, it would be useful to understand how each parameter in the plasma treatment affects the outcome so it is more predictable to be able to control the output. To accomplish this, it will require the continued collaborative efforts of biologists, chemists and physicists and these standardized protocols will likely need to be tailored to the seed type due to the diversity in the seed coat and build on the information from industry or associations such as AOSA (Association of Official Seed Analysts) where plasma is an added parameter.

Much of the outcome of the plasma-seed treatment seems to depend on both the plasma setup and seed features. If the seed has many layers that need to be scarified, plasma may help with mechanical erosion through etching or by melting the wax with the heat produced as a by-product of plasma generation. If the seed is rather permeable, it may functionalize the surface through the addition of chemical groups on the surface to become more hydrophilic and enhance gas exchange to then affect the seed biochemistry. Therefore, it may be that there are several modes of plasma treatment that can be selected i.e., if you need mechanical scarification and erosion, then use high power AC and argon for ion bombardment, if you need a gentle dose with ROS for chemical modification of seed coat, use nanopulse power for better ROS generation and lower temperature, or if you want to generate NO or H_2O_2 or if you want to delay or accelerate germination for storage or sowing, respectively, choose the appropriate gas type.

Very little has been done in terms of economic analysis other than by Niemira [189] but it would be useful to mention explicitly the power density of the device, the maximum number of seeds that can be treated to have an effect and potentially disclose the cost of manufacturing the plasma device to then see which designs would be easiest to implement and scale-up. This does not mean one plasma device is used universally as one of the advantages is the flexibility in design so people can adapt their treatment to their surroundings (seeds may vary in their value or importance depending on the country). By understanding the plasma-seed interactions and mechanisms, this will also help with setting up regulations around this technology since it is still ill-defined.

Generally, future studies should ideally correlate results using methods from different fields as far as possible, such as combining material science techniques with biological analysis and recording plasma parameters to find trends across experiments. The most urgent questions are: which treatment parameters are necessary to see a reproducible beneficial effect on seeds, can these parameters be applied to a plethora of seeds or is it necessary to tailor them to each seed type, how is the plasma treatment affecting the seed on a molecular level, is it possible to have these plasma treatments and biological effects consistently reproduced, can the plasma treatment be reliably scaled up for industrial applications, and how does plasma treatment compare to already existing methods such as acid or mechanical scarification? Provided that scientists now focus on the molecular effects of plasmas, with time, we might understand in detail how plasma-seed treatments work to develop this into a viable seed processing technology. Our hope is that plasma treatments will be another technology useful to the agriculture community.

AUTHOR CONTRIBUTIONS

AW conceptualized the review and figures, performed literature search, designed the figures, and wrote the manuscript. IF and AH read and approved the manuscript. All authors contributed to the article and approved the submitted version.

FUNDING

This work was supported by an *ad-hoc* grant of the Swiss Federal budgetary framework 2017–2020 for the ETH Domain.

ACKNOWLEDGMENTS

The authors thank Prof. Pierre Goloubinoff for the useful comments.

REFERENCES

1. FAO. *The Future of Food and Agriculture – Trends and Challenges*. Rome (2017).
2. Dekkers BJ, Pearce S, van Bolderen-Veldkamp RP, Marshall A, Widera P, Gilbert J, et al. Transcriptional dynamics of two seed compartments with opposing roles in Arabidopsis seed germination. *Plant Physiol*. (2013) 163:205–15. doi: 10.1104/pp.113.223511
3. Andersen EJ, Ali S, Byamukama E, Yen Y, Nepal MP. Disease resistance mechanisms in plants. *Genes*. (2018) 9:339. doi: 10.3390/genes9070339
4. Pawar VA, Laware SL. Seed priming A critical review. *Int J Sci Res Biol Sci*. (2018) 31:94–101. doi: 10.26438/ijsrbs/v5i5.94101
5. Lutts S, Benincasa P, Wojtyla L, Kubala S, Pace R, Lechowska K, et al. *Seed Priming: New Comprehensive Approaches for an Old Empirical Technique. New Challenges in Seed Biology-Basic and Translational Research Driving Seed Technology*. Rijeka: InTechOpen (2016). p. 1–46.

6. Wang W, Chen Q, Hussain S, Mei J, Dong H, Peng S, et al. Pre-sowing seed treatments in direct-seeded early rice: consequences for emergence, seedling growth and associated metabolic events under chilling stress. *Sci Rep*. (2016) 6:19637. doi: 10.1038/srep19637
7. Pedrini S, Merritt DJ, Stevens J, Dixon K. Seed coating: science or marketing spin? *Trends Plant Sci*. (2017) 22:106–16. doi: 10.1016/j.tplants.2016.11.002
8. Aktar W, Sengupta D, Chowdhury A. Impact of pesticides use in agriculture: their benefits and hazards. *Interdiscip Toxicol*. (2009) 2:1–12. doi: 10.2478/v10102-009-0001-7
9. Marican A, Durán-Lara EF. A review on pesticide removal through different processes. *Environ Sci Pollut Res*. (2018) 25:2051–64. doi: 10.1007/s11356-017-0796-2
10. Choi JS. Seed-surface disinfection and germination effects of grapefruit seed extract (GSE) on *Lactuca sativa* seeds. *Toxicol Environ Health Sci*. (2017) 9:169–75. doi: 10.1007/s13530-017-0318-0
11. Tito SI. Utilization of ultrasonic waves (*Acheta domesticus*) as a biocontrol of mosquito in Malang Agricultural Institute. In: *AIP Conference Proceedings,* Vol. 1908. East Java: AIP Publishing (2017). p. 050006.
12. Guo Q, Meng Y, Qu G, Wang T, Yang F, Liang D, et al. Improvement of wheat seed vitality by dielectric barrier discharge plasma treatment. *Bioelectromagnetics*. (2018) 39:120–31. doi: 10.1002/bem.22088
13. Paoletti MG, Pimentel D. Environmental risks of pesticides versus genetic engineering for agricultural pest control. *J Agric Environ Ethics*. (2000) 12:279–303. doi: 10.1023/A:1009571131089
14. Lockeretz W, editor. *Agriculture and Energy*. St.Louis, MO: Elsevier (2012). p. 715.
15. Hussain S, Zheng M, Khan F, Khaliq A, Fahad S, Peng S, et al. Benefits of rice seed priming are offset permanently by prolonged storage and the storage conditions. *Sci Rep*. (2015) 5:8101. doi: 10.1038/srep08101
16. Li L, Li J, Shen M, Hou J, Shao H, Dong Y, et al. Improving seed germination and peanut yields by cold plasma treatment. *Plasma Sci Technol*. (2016) 18:1027–33. doi: 10.1088/1009-0630/18/10/10
17. Han Y, Cheng JH, Sun DW. Activities and conformation changes of food enzymes induced by cold plasma: a review. In: *Critical Reviews in Food Science and Nutrition*, Vol. 59. Oxford: Taylor and Francis Inc. (2019). pp. 794–811.
18. Laroussi M. Cold plasma in medicine and healthcare: the new frontier in low temperature plasma applications. *Front Phys*. (2020) 8:74. doi: 10.3389/fphy.2020.00074
19. Šimončicová J, Kryštofová S, Medvecká V, Durišová K, Kalináková B. Technical applications of plasma treatments: current state and perspectives. *Appl Microbiol Biotechnol*. (2019) 103:5117–29. doi: 10.1007/s00253-019-09877-x
20. Sivachandiran L, Khacef A. Enhanced seed germination and plant growth by atmospheric pressure cold air plasma: combined effect of seed and water treatment. *RSC Adv*. (2017) 7:1822–32. doi: 10.1039/C6RA24762H
21. Sajib SA, Billah M, Mahmud S, Miah M, Hossain F, Omar FB, et al. Plasma activated water: the next generation eco-friendly stimulant for enhancing plant seed germination, vigor and increased enzyme activity, a study on black gram (*Vigna mungo* L.). *Plasma Chem Plasma Proc*. (2019) 40:119–43. doi: 10.1007/s11090-019-10028-3
22. Randeniya LK, de Groot GJJB. Non-Thermal plasma treatment of agricultural seeds for stimulation of germination, removal of surface contamination and other benefits: a review. *Plasma Proc Polym*. (2015) 12:608–23. doi: 10.1002/ppap.201500042
23. Pauzaite G, Malakauskiene A, Nauciene Z, Zukiene R, Filatova I, Lyushkevich V, et al. Changes in Norway spruce germination and growth induced by pre-sowing seed treatment with cold plasma and electromagnetic field: short-term versus long-term effects. *Plasma Proc Polym*. (2018) 15:1700068. doi: 10.1002/ppap.201700068
24. Puač N, Gherardi M, Shiratani M. Plasma agriculture: a rapidly emerging field. *Plasma Proc Polym*. (2018) 15:1700174. doi: 10.1002/ppap.201700174
25. Măgureanu M, Sîrbu R, Dobrin D, Gîdea M. Stimulation of the germination and early growth of tomato seeds by non-thermal plasma. *Plasma Chem Plasma Proc*. (2018) 38:989–1001. doi: 10.1007/s11090-018-9916-0
26. Jinkui F, Decheng W, Changyong S, Zhang L, Xin T. Effects of cold plasma treatment on alfalfa seed growth under simulated drought stress. *Plasma Sci Technol*. (2018) 20:035505. doi: 10.1088/2058-6272/aa9b27
27. Wu ZH, Chi LH, Bian SF, Xu KZ. Effects of plasma treatment on maize seeding resistance. *J Maize Sci*. (2007) 15:111–3.
28. Volin JC, Denes FS, Young RA, Park SM. Modification of seed germination performance through cold plasma chemistry technology. *Crop Sci*. (2000) 40:1706–18. doi: 10.2135/cropsci2000.4061706x
29. Bormashenko E, Grynyov R, Bormashenko Y, Drori E. Cold radiofrequency plasma treatment modifies wettability and germination speed of plant seeds. *Sci Rep*. (2012) 2:1–8. doi: 10.1038/srep00741
30. Shintani H, Shimizu N, Imanishi Y, Sekiya T, Tamazawa K, Taniguchi A, et al. Inactivation of microorganisms and endotoxins by low temperature nitrogen gas plasma exposure. *Biocontrol Sci*. (2007) 12:131–43. doi: 10.4265/bio.12.131
31. Shintani H, Sakudo A, Burke P, McDonnell G. Gas plasma sterilization of microorganisms and mechanisms of action. *Exp Ther Med*. (2010) 1:731–8. doi: 10.3892/etm.2010.136
32. Molina R, López-Santos C, Gómez-Ramírez A, Vílchez A, Espinós JP, González-Elipe AR. Influence of irrigation conditions in the germination of plasma treated Nasturtium seeds. *Sci Rep*. (2018) 8:16442. doi: 10.1038/s41598-018-34801-0
33. Kopacki M, Pawlat J, Terebun P, Kwiatkowski M, Starek A, Kiczorowski P. Efficacy of non-thermal plasma fumigation to control fungi occurring on onion seeds. In: *Electromagnetic Devices and Processes in Environment Protection With Seminar Applications of Superconductors (ELMECO and AoS), 2017 International Conference* on IEEE, Naleczow (2017). pp. 1–4.
34. Chen HL, Lee HM, Chen SH, Chang MB, Yu SJ, Li SN. Removal of volatile organic compounds by single-stage and two-stage plasma catalysis systems: a review of the performance 25 enhancement mechanisms, current status, and suitable applications. *Environ Sci Technol*. (2009) 43:2216–27. doi: 10.1021/es802679b
35. Stryczewska HD, Ebihara K, Takayama M, Gyoutoku Y, Tachibana M. Non-thermal plasma- based technology for soil treatment. *Plasma Proc Polym*. (2005) 2:238–45. doi: 10.1002/ppap.200400061
36. Pérez-Pizá MC, Prevosto L, Grijalba PE, Zilli CG, Cejas E, Mancinelli B, et al. Improvement of growth and yield of soybean plants through the application of non-thermal plasmas to seeds with different health status. *Heliyon*. (2019) 5:e01495. doi: 10.1016/j.heliyon.2019.e01495
37. Zhang B, Li R, Yan J. Study on activation and improvement of crop seeds by the application of plasma treating seeds equipment. *Arch Biochem Biophys*. (2018) 655:37–42. doi: 10.1016/j.abb.2018.08.004
38. Iranbakhsh A, Oraghi Ardebili Z, Molaei H, Oraghi Ardebili N, Amini M. Cold plasma up-regulated expressions of WRKY1 transcription factor and genes involved in biosynthesis of cannabinoids in hemp (*Cannabis sativa* L.). *Plasma Chem Plasma Proc*. (2020) 40:527–37. doi: 10.1007/s11090-020-10058-2
39. Kang MH, Veerana M, Eom S, Uhm H, Ryu S, Park G. Plasma mediated disinfection of rice seeds in water and air. *J Phys D Appl Phys*. (2020) 53:14. doi: 10.1088/1361-6463/ab79de
40. Billah M, Sajib SA, Roy NC, Rashid MM, Reza MA, Hasan MM, et al. Effects of DBD air plasma treatment on the enhancement of black gram (*Vigna mungo* l.) seed germination and growth. *Arch Biochem Biophys*. (2020) 681:108253. doi: 10.1016/j.abb.2020.108253
41. Rezaei S, Ghobadian B, Ebadi MT, Jangi F, Ghomi H. Effects of cold plasma on the color parameters of Hyssop (*Hyssopus officinalis* L.) using color imaging instrumentation and spectrophotometer. *Color Res Appl*. (2020) 45:29–39. doi: 10.1002/col.22433
42. Koga K, Attri P, Kamataki K, Itagaki N, Shiratani M, Mildažiene V. Impact of radish sprouts seeds coat color on the electron paramagnetic resonance signals after plasma treatment. *Jap J Appl Phys*. (2020) 59:SHHF01. doi: 10.35848/1347-4065/ab7698
43. Ghasempour M, Iranbakhsh A, Ebadi M, Oraghi Ardebili Z. Seed priming with cold plasma improved seedling performance, secondary metabolism, and expression of deacetylvindoline O-acetyltransferase gene in *Catharanthus roseus*. *Contrib Plasma Phys*. (2020) 60:e201900159. doi: 10.1002/ctpp.201900159

44. Mujahid Z, Tounekti T, Khemira H. Cold plasma treatment to release dormancy and improve growth in grape buds: a promising alternative to natural chilling and rest breaking chemicals. *Sci Rep*. (2020) 10:1–10. doi: 10.1038/s41598-020-59097-x
45. Filatova I, Lyushkevich V, Goncharik S, Zhukovsky A, Krupenko N, Kalatskaja J. The effect of low-pressure plasma treatment of seeds on the plant resistance to pathogens and crop yields. *J Phys D Appl Phys*. (2020) 53:244001. doi: 10.1088/1361-6463/ab7960
46. Prakrajang K, Sarapirom S, Mai Sci CJ, Thisawech M, Saritnum O, Phakham W. *Effects of Plasma Technique and Gamma Irradiation on Seed Germination and Seedling Growth of Chili Pepper*, Vol. 47 (2020). Available online at: http://epg.science.cmu.ac.th/ejournal/.
47. Kobayashi M, Wang Y, Kumagai S, Uraoka Y, Ito T. Effects of cold atmospheric plasma irradiation on Arabidopsis seedlings. *Jap J Appl Phys*. (2020) 59:SAAB09. doi: 10.7567/1347-4065/ab4e7b
48. Dawood N. Effect of RF plasma on Moringa seeds germination and growth. *J Taibah Univ Sci*. (2020) 14:279–84. doi: 10.1080/16583655.2020.1713570
49. Sidik MAB, Buntat Z, Nawawi Z, Jambak MI, Buntat Y, Musa FN. Effects of cold plasma treatment on the growth rate of corn and eggplant plants. In: *Proceedings of 2018 International Conference on Electrical Engineering and Computer Science, ICECOS* 2018 (2019). p. 441–6.
50. Ambrico PF, Šimek M, Ambrico M, Morano M, Prukner V, Minafra A. et al. On the air atmospheric pressure plasma treatment effect on the physiology, germination and seedlings of basil seeds. *J Phys D Appl Phys*. (2019) 53:104001. doi: 10.1088/1361-6463/ab5b1b
51. Seddighinia FS, Iranbakhsh A, Oraghi Ardebili Z, Nejad Satari T, Soleimanpour S. Seed Priming with cold plasma and multi-walled carbon nanotubes modified growth, tissue differentiation, anatomy, and yield in bitter melon (*Momordica charantia*). *J Plant Growth Regul.* (2019) 39:87–98. doi: 10.1007/s00344-019-09965-2
52. Gao X, Zhang A, Héroux P, Sand W, Sun Z, Zhan J, et al. Effect of dielectric barrier discharge cold plasma on pea seed growth. *J Agric Food Chem*. (2019) 67:10813–22. doi: 10.1021/acs.jafc.9b03099
53. Mildažiene V, Aleknavičiute V, Žukiene R, PauŽaite G, Naučiene Z, Filatova I, et al. Treatment of common sunflower (*Helianthus annus* L.) seeds with radio-frequency electromagnetic field and cold plasma induces changes in seed phytohormone balance, seedling development and leaf protein expression. *Sci Rep*. (2019) 9:1–12. doi: 10.1038/s41598-019-42893-5
54. Šerá B, Zahoranová A, Bujdáková H, Šerý M. Disinfection from pine seeds contaminated with *Fusarium circinatum* Nirenberg and O'Donnell using non-thermal plasma treatment. *Romanian Rep Phys.* (2019) 71.
55. Cui D, Yin Y, Wang J, Wang Z, Ding H, Ma R, et al. Research on the physio-biochemical mechanism of non-thermal plasma-regulated seed germination and early seedling development in arabidopsis. *Front Plant Sci*. (2019) 10:1322. doi: 10.3389/fpls.2019.01322
56. Liu B, Honnorat B, Yang H, Arancibia J, Rajjou L, Rousseau A. Non-thermal DBD plasma array on seed germination of different plant species. *J Phys D Appl Phys*. (2019) 52:025401. doi: 10.1088/1361-6463/aae771
57. Los A, Ziuzina D, Boehm D, Cullen PJ, Bourke P. Investigation of mechanisms involved in germination enhancement of wheat (*Triticum aestivum*) by cold plasma: effects on seed surface chemistry and characteristics. *Plasma Proc Polymers*. (2019) 16:1800148. doi: 10.1002/ppap.201800148
58. Moghanloo M, Iranbakhsh A, Ebadi M, Nejad Satari T, Oraghi Ardebili Z. Seed priming with cold plasma and supplementation of culture medium with silicon nanoparticle modified growth, physiology, and anatomy in *Astragalus fridae* as an endangered species. *Acta Physiol Plant*. (2019) 41:1–13. doi: 10.1007/s11738-019-2846-5
59. Babajani A, Iranbakhsh A, Oraghi Ardebili Z, Eslami B. Seed priming with non-thermal plasma modified plant reactions to selenium or zinc oxide nanoparticles: cold plasma as a novel emerging tool for plant science. *Plasma Chem Plasma Proc*. (2019) 39:21–34. doi: 10.1007/s11090-018-9934-y
60. Lotfy K, Al-Harbi NA, Abd El-Raheem H. Cold atmospheric pressure nitrogen plasma jet for enhancement germination of wheat seeds. *Plasma Chem Plasma Proc*. (2019) 39:897–912. doi: 10.1007/s11090-019-09969-6
61. Bafoil M, Le Ru A, Merbahi N, Eichwald O, Dunand C, Yousfi M. New insights of low-temperature plasma effects on germination of three genotypes of Arabidopsis thaliana seeds under osmotic and saline stresses. *Sci Rep*. (2019) 9:8649. doi: 10.1038/s41598-019-44927-4
62. Singh R, Prasad P, Mohan R, Verma MK, Kumar BRadiofrequency cold plasma treatment enhances seed germination and seedling growth in variety CIM-Saumya of sweet basil (*Ocimum basilicum* L.). *J Appl Res Med Aromatic Plants*. (2019) 12:78–81. doi: 10.1016/j.jarmap.2018.11.005
63. Iqbal T, Farooq M, Afsheen S, Abrar M, Yousaf M, Ijaz M. Cold plasma treatment and laser irradiation of *Triticum* spp. seeds for sterilization and germination. *J Laser Appl*. (2019) 31:042013. doi: 10.2351/1.5109764
64. Islam S, Omar FB, Sajib SA, Roy NC, Reza A, Hasan M, et al. Effects of LPDBD plasma and plasma activated water on germination and growth in rapeseed (*Brassica napus*). *Gesunde Pflanzen*. (2019) 71:175–85. doi: 10.1007/s10343-019-00463-9
65. Kabir AH, Rahman MM, Das U, Sarkar U, Roy NC, Reza MA, et al. Reduction of cadmium toxicity in wheat through plasma technology. *PLoS ONE*. (2019) 14:e0214509. doi: 10.1371/journal.pone.0214509
66. Afsheen S, Fatima U, Iqbal T, Abrar M, Muhammad S, Saeed A, et al. Influence of cold plasma treatment on insecticidal properties of wheat seeds against red flour beetles. *PlST*. (2019) 21:085506. doi: 10.1088/2058-6272/ab19ee
67. Lo Porto C, Sergio L, Boari F, Logrieco AF, Cantore V. Cold plasma pretreatment improves the germination of wild asparagus (*Asparagus acutifolius* L.) seeds. *Sci Hortic*. (2019) 256:108554. doi: 10.1016/j.scienta.2019.108554
68. Jiang J, Li J, Dong Y. Effect of cold plasma treatment on seedling growth and nutrient absorption of tomato. *Plasma Sci Technol*. (2018) 20:044007. doi: 10.1088/2058-6272/aaa0bf
69. Hosseini SI, Mohsenimehr S, Hadian J, Ghorbanpour M, Shokri B. Physico-chemical induced modification of seed germination and early development in artichoke (*Cynara scolymus* L.) using low energy plasma technology. *Phys Plasmas*. (2018) 25:013525. doi: 10.1063/1.5016037
70. Tounekti T, Mujahid ZUI, Khemira H. Non-thermal dielectric barrier discharge (DBD) plasma affects germination of coffee and grape seeds. *AIP Conf Proc*. (2018) 1976:020029. doi: 10.1063/1.5042396
71. Khatami S, Ahmadinia A. Increased germination and growth rates of pea and Zucchini seed by FSG plasma. *J Theoret Appl Phys*. (2018) 12:33–8. doi: 10.1007/s40094-018-0280-5
72. Pawłat J, Starek A, Sujak A, Terebun P, Kwiatkowski M, Budzeń M, et al. Effects of atmospheric pressure plasma jet operating with DBD on *Lavatera thuringiaca* L. seeds' germination. *PLoS ONE*. (2018) 13:e0194349. doi: 10.1371/journal.pone.0194349
73. Rahman MM, Sajib SA, Rahi MS, Tahura S, Roy NC, Parvez S, et al. Mechanisms and signaling associated with LPDBD plasma mediated growth improvement in wheat. *Sci Rep*. (2018) 8:1–11. doi: 10.1038/s41598-018-28960-3
74. Hayashi N, Ono R, Nakano R, Shiratani M, Tashiro K, Kuhara S, et al. DNA microarray analysis of plant seeds irradiated by active oxygen species in oxygen plasma. *Plasma Med*. (2016) 6:459–71. doi: 10.1615/PlasmaMed.2016018933
75. Matra K. Atmospheric non-thermal argon-oxygen plasma for sunflower seedling growth improvement. *Jpn J Appl Phys*. (2018) 57:01AG03. doi: 10.7567/JJAP.57.01AG03
76. Bafoil M, Jemmat A, Martinez Y, Merbahi N, Eichwald O, Dunand C, et al. Effects of low temperature plasmas and plasma activated waters on Arabidopsis thaliana germination and growth. *PLoS ONE*. (2018) 13:e0195512. doi: 10.1371/journal.pone.0195512
77. Štěpánová V, Slavíček P, Kelar J, Prášil J, Smékal M, Stupavská M. et al. Atmospheric pressure plasma treatment of agricultural seeds of cucumber (*Cucumis sativus* L.) and pepper (*Capsicum annuum* L.) with effect on reduction of diseases and germination improvement. *Plasma Processes Polym*. (2018) 15:1700076. doi: 10.1002/ppap.201700076
78. Iranbakhsh A, Ardebili NO, Ardebili ZO, Shafaati M, Ghoranneviss M. Non-thermal plasma induced expression of heat shock factor A4A and improved wheat (*Triticum aestivum* L.) growth and resistance against salt stress. *Plasma Chem Plasma Proc*. (2018) 38:29–44. doi: 10.1007/s11090-017-9861-3
79. Iranbakhsh A, Oraghi Ardebili Z, Oraghi Ardebili N, Ghoranneviss M, Safari N. Cold plasma relieved toxicity signs of nano zinc oxide in *Capsicum*

annuum cayenne via modifying growth, differentiation, and physiology. *Acta Physiol Plantarum*. (2018) 40:154. doi: 10.1007/s11738-018-2730-8
80. Park Y, Oh KS, Oh J, Seok DC, Kim SB, Yoo SJ, et al. The biological effects of surface dielectric barrier discharge on seed germination and plant growth with barley. *Plasma Proc Polym*. (2018) 15:1600056. doi: 10.1002/ppap.201600056
81. Zhang J, Kwon T, Kim S, Jeong D. Plasma farming: non-thermal dielectric barrier discharge plasma technology for improving the growth of soybean sprouts and chickens. *Plasma*. (2018) 1:285–96. doi: 10.3390/plasma1020025
82. Shapira Y, Chaniel G, Bormashenko E. Surface charging by the cold plasma discharge of lentil and pepper seeds in comparison with polymers. *Colloids Surf B Biointerfaces*. (2018) 172:541–4. doi: 10.1016/j.colsurfb.2018.09.004
83. Wang XQ, Zhou RW, De Groot G, B.azaka K, Murphy AB, Ostrikov KK. Spectral characteristics of cotton seeds treated by a dielectric barrier discharge plasma. *Sci Rep*. (2017) 7:1–9. doi: 10.1038/s41598-017-04963-4
84. Kim J-W, Puligundla P, Mok C. Effect of corona discharge plasma jet on surface-borne microorganisms and sprouting of broccoli seeds. *J Sci Food Agric*. (2017) 97:128–34. doi: 10.1002/jsfa.7698
85. Mildažiene V, Pauzaite G, Naucienė Z, Malakauskiene A, Zukiene R, Januskaitiene I, et al. Pre-sowing seed treatment with cold plasma and electromagnetic field increases secondary metabolite content in purple coneflower (*Echinacea purpurea*) leaves. *Plasma Processes and Polymers*. (2018) 15:1700059. doi: 10.1002/ppap.201700059
86. Li Y, Wang T, Meng Y, Qu G, Sun Q, Liang D, et al. Air atmospheric dielectric barrier discharge plasma induced germination and growth enhancement of wheat seed. *Plasma Chem Plasma Proc*. (2017) 37:1621–34. doi: 10.1007/s11090-017-9835-5
87. Sera B, Sery M, Gavril B, Gajdova I. Seed germination and early growth responses to seed pre-treatment by non-thermal plasma in hemp cultivars (*Cannabis sativa* L.). *Plasma Chem Plasma Proc*. (2017) 37:207–21. doi: 10.1007/s11090-016-9763-9
88. Puligundla P, Kim JW, Mok C. Effect of corona discharge plasma jet treatment on decontamination and sprouting of rapeseed (*Brassica napus* L.) seeds. *Food Control*. (2017) 71:376–82. doi: 10.1016/j.foodcont.2016.07.021
89. Puligundla P, Kim JW, Mok C. Effects of non-thermal plasma treatment on decontamination and sprouting of radish (*Raphanus sativus* L.) seeds. *Food Bioproc Technol*. (2017) 10:1093–102. doi: 10.1007/s11947-017-1886-3
90. Gómez-Ramírez A, López-Santos C, Cantos M, García JL, Molina R, Cotrino J, et al. Surface chemistry and germination improvement of Quinoa seeds subjected to plasma activation. *Sci Rep*. (2017) 7:1–12. doi: 10.1038/s41598-017-06164-5
91. Guo Q, Wang Y, Zhang H, Qu G, Wang T, Sun Q, et al. Alleviation of adverse effects of drought stress on wheat seed germination using atmospheric dielectric barrier discharge plasma treatment. *Sci Rep*. (2017) 7:1–14. doi: 10.1038/s41598-017-16944-8
92. Zhang JJ, Jo JO, Huynh DL, Mongre RK, Ghosh M, Singh AK, et al. Growth-inducing effects of argon plasma on soybean sprouts via the regulation of demethylation levels of energy metabolism-related genes. *Sci Rep*. (2017) 7:1–12. doi: 10.1038/srep41917
93. da Silva ARM, Farias ML, da Silva DLS, Vitoriano JO, de Sousa RC, Alves-Junior C. Using atmospheric plasma to increase wettability, imbibition and germination of physically dormant seeds of Mimosa Caesalpiniafolia. *Colloids Surf B Biointerfaces*. (2017) 157:280–5. doi: 10.1016/j.colsurfb.2017.05.063
94. Meng Y, Qu G, Wang T, Sun Q, Liang D, Hu S. Enhancement of germination and seedling growth of wheat seed using dielectric barrier discharge plasma with various gas sources. *Plasma Chem Plasma Proc*. (2017) 37:1105–19. doi: 10.1007/s11090-017-9799-5
95. Nalwa C, Thakur AK, Vikram A, Rane R, Vaid A. Studies on plasma treatment and priming of seeds of bell pepper (*Capsicum annuum* L.). *J Appl Nat Sci*. (2017) 9:1505–9. doi: 10.31018/jans.v9i3.1392
96. Junior CA, De Oliveira Vitoriano J, Da Silva DLS, De Lima Farias M, De Lima Dantas NB. Water uptake mechanism and germination of Erythrina velutina seeds treated with atmospheric plasma. *Sci Rep*. (2016) 6:33722. doi: 10.1038/srep33722
97. Zahoranová A, Henselová M, Hudecová D, Kalináková B, Kováčik D, Medvecká V, et al. Effect of cold atmospheric pressure plasma on the wheat seedlings vigor and on the inactivation of microorganisms on the seeds surface. *Plasma Chem Plasma Proc*. (2016) 36:397–414. doi: 10.1007/s11090-015-9684-z
98. Zhou R, Zhou R, Zhang X, Zhuang J, Yang S, Bazaka K, et al. Effects of atmospheric-pressure N2, He, Air, and O2 microplasmas on mung bean seed germination and seedling growth. *Sci Rep*. (2016) 6:32603. doi: 10.1038/srep32603
99. Khamsen N, Onwimol D, Teerakawanich N, Dechanupaprittha S, Kanokbannakorn W, Hongesombut K, et al. Rice (*Oryza sativa L.*) seed sterilization and germination enhancement via atmospheric hybrid nonthermal discharge plasma. *ACS Appl Mater Interfaces*. (2016) 8:19268–75. doi: 10.1021/acsami.6b04555
100. Gholami A, Navab Safa N, Khoram M, Hadian J, Ghomia H. Effect of low-pressure radio frequency plasma on ajwain seed germination. *Plasma Med*. (2016) 6:389–96. doi: 10.1615/PlasmaMed.2017019157
101. Matra K. Non-thermal plasma for germination enhancement of radish seeds. *Proc Comput Sci*. (2016) 86:132–5. doi: 10.1016/j.procs.2016.05.033
102. Sarinont T, Amano T, Attri P, Koga K, Hayashi N, Shiratani M. Effects of plasma irradiation using various feeding gases on growth of *Raphanus sativus* L. *Arch Biochem Biophys*. (2016) 605:129–40. doi: 10.1016/j.abb.2016.03.024
103. Dobrin D, Magureanu M, Mandache NB, Ionita MD. The effect of non-thermal plasma treatment on wheat germination and early growth. *Innov Food Sci Emerg Technol*. (2015) 29:255–60. doi: 10.1016/j.ifset.2015.02.006
104. Stolárik T, Henselová M, Martinka M, Novák O, Zahoranová A, Cernák M. Effect of low-temperature plasma on the structure of seeds, growth and metabolism of endogenous phytohormones in pea (*Pisum sativum* L.). *Plasma Chem Plasma Proc*. (2015) 35:659–76. doi: 10.1007/s11090-015-9627-8
105. Munkhuu N, Shao C, Wang D, Liu L, Muhammad I, He C, et al. Stimulating effect of low-temperature plasma on seed germination characteristics of *Trifolium repens*. In: Li D., Chen Y. (eds) *Computer and Computing Technologies in Agriculture VIII. CCTA 2014. IFIP Advances in Information and Communication Technology,* Cham: Springer (2015) 452. doi: 10.1007/978-3-319-19620-6_21
106. Ji SH, Kim T, Panngom K, Hong YJ, Pengkit A, Park DH, et al. Assessment of the effects of nitrogen plasma and plasma-generated nitric oxide on early development of *Coriandum sativum*. *Plasma Proc Polymers*. (2015) 12:1164–73. doi: 10.1002/ppap.201500021
107. Kadowaki K, Kurisaka N. Stimulation and inhibition of Arabidopsis seed germination with repetitive barrier discharges produced by polarity-reversed voltage pulses. *Electr Commun Japan*. (2014) 97:38–43. doi: 10.1002/ecj.11603
108. Butscher D, Waskow A, von Rohr PR. Disinfection of granular food products using cold plasma. In: Bermudez-Arguirre D, editor *Advances in Cold Plasma Applications for Food Safety and Preservation*. Richland, WA: Academic Press (2020). pp. 185–228.
109. Lotfy K. Effects of cold atmospheric plasma jet treatment on the seed germination and enhancement growth of watermelon. *Open J Appl Sci*. (2017) 7:705–19. doi: 10.4236/ojapps.2017.712050
110. Kitazaki S, Sarinont T, Koga K, Hayashi N, Shiratani M. Plasma induced long-term growth enhancement of Raphanus sativus L. using combinatorial atmospheric air dielectric barrier discharge plasmas. *Curr Appl Phys*. (2014) 14:S149–53. doi: 10.1016/j.cap.2013.11.056
111. Al-Whaibi MH. Plant heat-shock proteins: a mini review. *J King Saud Univ Sci*. (2011) 23:139–50. doi: 10.1016/j.jksus.2010.06.022
112. Farokh P, Mahmoodzadeh H, Satari TN. Response of seed germination of safflower to UV-B radiation. *Res J Environ Sci*. (2010) 4:70–4. doi: 10.3923/rjes.2010.70.74
113. Noble RE. Effects of UV-irradiation on seed germination. *Sci Total Environ*. (2002) 299:173–6. doi: 10.1016/S0048-9697(02)00232-2
114. Sadeghianfar P, Nazari M, Backes G. Exposure to Ultraviolet (UV-C) radiation increases germination rate of maize (*Zea maize* L.) and sugar beet (*Beta vulgaris*) seeds. *Plants*. (2019) 8:49. doi: 10.3390/plants8020049

115. Ibrahim M, Imram M, Hussain A, Aslam M, Rehmani FS, Ali B, et al. Phytochemical studies on *Amberboa ramose*. *Pak J Chem*. (2012) 2:24–8. doi: 10.15228/2012.v02.i01.p04
116. Caldwell MM, Björn LO, Bornman JF, Flint SD, Kulandaivelu G, Teramura AH, et al. Effects of increased solar ultraviolet radiation on terrestrial ecosystems. *J Photochem Photobiol B Biol*. (1998) 46:40–52. doi: 10.1016/S1011-1344(98)00184-5
117. Veberic R. The impact of production technology on plant phenolics. *Horticulturae*. (2016) 2:8. doi: 10.3390/horticulturae2030008
118. Iranbakhsh A, Ghoranneviss M, Oraghi Ardebili Z, Ardebili NO, Hesami Tackallou S, Nikmaram H. Non-thermal plasma modified growth and physiology in *Triticum aestivum* via generated signaling molecules and UV radiation. *Biol Plant*. (2017) 61:702–8. doi: 10.1007/s10535-016-0699-y
119. Huché-Thélier L, Crespel L, Le Gourrierec J, Morel P, Sakr S, Leduc N. Light signaling and plant responses to blue and UV radiations—perspectives for applications in horticulture. *Environ Exp Bot*. (2016) 121:22–38. doi: 10.1016/j.envexpbot.2015.06.009
120. Su B, Guo J, Nian W, Feng H, Wang K, Zhang J, et al. Early growth effects of nanosecond pulsed electric field (nsPEFs) exposure on Haloxylon ammodendron. *Plasma Proc Polym*. (2015) 12:372–9. doi: 10.1002/ppap.201400131
121. Dymek K, Dejmek P, Panarese V, Vicente AA, Wadsö L, Finnie C, et al. Effect of pulsed electric field on the germination of barley seeds. *Lwt-Food Sci Technol*. (2012) 47:161–6. doi: 10.1016/j.lwt.2011.12.019
122. Teissie J, Golzio M, Rols MP. Mechanisms of cell membrane electropermeabilization: a minireview of our present (lack of?) knowledge. *Biochim Biophys Acta Gen Subj*. (2005) 1724:270–80. doi: 10.1016/j.bbagen.2005.05.006
123. Patwardhan MS, Gandhare WZ. High voltage electric field effects on the germination rate of tomato seeds. *Acta Agrophys*. (2013) 20, 403–13.
124. Maffei ME. Magnetic field effects on plant growth, development, and evolution. *Front Plant Sci*. (2014) 5:445. doi: 10.3389/fpls.2014.00445
125. Bilalis DJ, Katsenios N, Efthimiadou A, Karkanis A, Efthimiadis P. Investigation of pulsed electromagnetic field as a novel organic pre-sowing method on germination and initial growth stages of cotton. *Electromagn Biol Med*. (2012) 31:143–50. doi: 10.3109/15368378.2011.624660
126. Souza FH, Marcos-Filho J. The seed coat as a modulator of seed-environment relationships in Fabaceae. *Braz J Bot*. (2001) 24:365–75. doi: 10.1590/S0100-84042001000400002
127. Sehrawat R, Thakur AK, Vikram A, Vaid A, Rane R. Effect of cold plasma treatment on physiological quality of okra seed. *J Hill Agric*. (2017) 8:66–71. doi: 10.5958/2230-7338.2017.00010.6
128. Mildažiene V, Pauzaite G, Malakauskiene A, Zukiene R, Nauciene Z, Filatova I, et al. Response of perennial woody plants to seed treatment by electromagnetic field and low-temperature plasma. *Bioelectromagnetics*. (2016) 37:536–48. doi: 10.1002/bem.22003
129. Sera B, Spatenka P, Sery M, Vrchotova N, Hruskova I. Influence of plasma treatment on wheat and oat germination and early growth. *IEEE Transac Plasma Sci*. (2010) 38:2963–8. doi: 10.1109/TPS.2010.2060728
130. Holc M, Primc G, Iskra J, Titan P, Kovač J, Mozetič M, et al. Effect of oxygen plasma on sprout and root growth, surface morphology and yield of garlic. *Plants*. (2019) 8:462. doi: 10.3390/plants8110462
131. Yamauchi Y, Kuzuya M, Sasai Y, Kondo S, Surface treatment of natural polymer by plasma technique - promotion of seed germination. *J Photopol Sci Technol*. (2012) 25:535–8. doi: 10.2494/photopolymer.25.535
132. Pawlat J, Starek A, Sujak A, Kwiatkowski M, Terebun P, Budzeń M. Effects of atmospheric pressure plasma generated in GlidArc reactor on *Lavatera thuringiaca* L. seeds' germination. *Plasma Proc Polym*. (2018) 15:1700064. doi: 10.1002/ppap.201700064
133. Cakmak I. The role of potassium in alleviating detrimental effects of abiotic stresses in plants. *J Plant Nutr Soil Sci*. (2005) 168:521–30. doi: 10.1002/jpln.200420485
134. Wang M, Zheng Q, Shen Q, Guo S. The critical role of potassium in plant stress response. *Int J Mol Sci*. (2013) 14:7370–90. doi: 10.3390/ijms14047370
135. Miguel MVDC, Marcos Filho J. Potassium leakage and maize seed physiological potential. *Sci Agric*. (2002) 59:315–19. doi: 10.1590/S0103-90162002000200017
136. Carvalho LFD, Sediyama CS, Reis MS, Dias DC, Moreira MA. Influência da temperatura de embebição da semente de soja no teste de condutividade elétrica para avaliação da qualidade fisiológica. *Rev Brasil Sementes*. (2009) 31:9–17. doi: 10.1590/S0101-31222009000100001
137. Ahmed AKA, Shi X, Hua L, Manzueta L, Qing W, Marhaba T, et al. Influences of air, oxygen, nitrogen, and carbon dioxide nanobubbles on seed germination and plant growth. *J Agric Food Chem*. (2018) 66:5117–24. doi: 10.1021/acs.jafc.8b00333
138. Leghari SJ, Wahocho NA, Laghari GM, HafeezLaghari A, MustafaBhabhan G, HussainTalpur K, et al. Role of nitrogen for plant growth and development: a review. *Adv Environ Biol*. (2016) 10:209–19.
139. Filatova I, Azharonok V, Kadyrov M, Beljavsky V, Gvozdov A, Shik A, et al. The effect of plasma treatment of seeds of some grain and legumes on their sowing quality and productivity. *Rom J Phys*. (2011) 56:139–43.
140. El-Maarouf-Bouteau H, Bailly C. Oxidative signaling in seed germination and dormancy. *Plant Signal Behav*. (2008) 3:175–82. doi: 10.4161/psb.3.3.5539
141. Siddiqui ZS, Khan MA. The role of seed coat phenolics on water uptake and early protein synthesis during germination of dimorphic seeds of *Halopyrum mucronatum* (L.) Staph. *Pak J Bot*. (2010) 42:227–38.
142. Müller K, Hess B, Leubner-Metzger G. Chapter V: a role for Reactive Oxygen Species in Endosperm Weakening. In: Adkins SW, Navie SC, Ashmore S, editors. *Germination and Dormancy of Seeds: Biology, Development and Ecology*. Wallingford: CAB International (2007). p. 287.
143. Weber D, Davies MJ, Grune T. Determination of protein carbonyls in plasma, cell extracts, tissue homogenates, isolated proteins: focus on sample preparation and derivatization conditions. *Redox Biol*. (2015) 5:367–80. doi: 10.1016/j.redox.2015.06.005
144. Oracz K, Bouteau HEM, Farrant JM, Cooper K, Belghazi M, Job C, et al. ROS production and protein oxidation as a novel mechanism for seed dormancy alleviation. *Plant J*. (2007) 50:452–65. doi: 10.1111/j.1365-313X.2007.03063.x
145. Valderrama R, Begara-Morales JC, Chaki M, Mata-Pérez C, Padilla MN, Barroso JB. Hydrogen Peroxide (H2O2)- and Nitric Oxide (NO)-derived posttranslational modifications. In: Gupta D, Palma J, Corpas F, editors. *Nitric Oxide and Hydrogen Peroxide Signaling in Higher Plants*. Cham: Springer (2019) 37–67.
146. Ahmad P. *Oxidative Damage to Plants: Antioxidant Networks and Signaling*. Chapter 2. Srinagar: Elsevier Academic Press (2004).
147. Grene R. Oxidative stress and acclimation mechanisms in plants. *Arabidopsis Book*. (2002) 1:e0036. doi: 10.1199/tab.0036.1
148. Yusupov M, Razzokov J, Cordeiro RM, Bogaerts A. Transport of reactive oxygen and nitrogen species across aquaporin: a molecular level picture. *Oxid Med Cell Longev*. (2019) 2019:2930504. doi: 10.1155/2019/2930504
149. Seol YB, Kim J, Park SH, Chang HY. Atmospheric pressure pulsed plasma induces cell death in photosynthetic organs via intracellularly generated ROS. *Sci Rep*. (2017) 7:1–11. doi: 10.1038/s41598-017-00480-6
150. Mhamdi A, Van Breusegem F. Reactive oxygen species in plant development. *Development*. (2018) 145:dev164376. doi: 10.1242/dev.164376
151. Torsethaugen G, Pell EJ, Assmann SM. Ozone inhibits guard cell K+ channels implicated in stomatal opening. *Proc Nat Acad Sci USA*. (1999) 96:13577–82. doi: 10.1073/pnas.96.23.13577
152. Chaudhary N, Agrawal SB. The role of elevated ozone on growth, yield and seed quality amongst six cultivars of mung bean. *Ecotoxicol Environ Saf*. (2015) 111:286–94. doi: 10.1016/j.ecoenv.2014.09.018
153. Avdeeva V, Zorina E, Bezgina J, Kolosova O. Influence of ozone on germination and germinating energy of winter wheat seeds. In: *Proceedings of the International Scientific Conference*. Jelgava: Latvijas Lauksaimniecibas universitāte (2018).
154. Rodoni L, Casadei N, Concellón A, Chaves Alicia AR, Vicente AR. Effect of short-term ozone treatments on tomato (Solanum *lycopersicum* L.) fruit quality and cell wall degradation. *J Agric Food Chem*. (2009) 58:594–9. doi: 10.1021/jf9029145
155. Abeli T, Guasconi DB, Mondoni A, Dondi D, Bentivoglio A, Buttafava A, et al. Acute and chronic ozone exposure temporarily affects seed germination in alpine plants. *Plant Biosyst*. (2017) 151:304–15. doi: 10.1080/11263504.2016.1174169

156. Emberson LD, Pleijel H, Ainsworth EA, Van den Berg M, Ren W, Osborne S, et al. Ozone effects on crops and consideration in crop models. *Eur J Agron*. (2018) 100:19–34. doi: 10.1016/j.eja.2018.06.002
157. Sudhakar N, Nagendra-Prasad D, Mohan N, Hill B, Gunasekaran M, Murugesan K. Assessing influence of ozone in tomato seed dormancy alleviation. *Am J Plant Sci*. (2011) 2:443. doi: 10.4236/ajps.2011.23051
158. Giba Z, Grubisic D, Konjevic R. Nitrogen oxides as environmental sensors for seeds. *Seed Sci Res*. (2003) 13:187. doi: 10.1079/SSR2003136
159. Puač N, Živković S, Selaković N, Milutinović M, Boljević J, Malović G. et al. Long and short term effects of plasma treatment on meristematic plant cells. *Appl Phys Lett*. (2014) 104:214106. doi: 10.1063/1.4880360
160. Henselová M, Slováková L, Martinka M, Zahoranová A. Growth, anatomy and enzyme activity changes in maize roots induced by treatment of seeds with low-temperature plasma. *Biologia*. (2012) 67:490–7. doi: 10.2478/s11756-012-0046-5
161. Noctor G, Reichheld JP, Foyer CH. ROS-related redox regulation and signaling in plants. *Semin Cell Dev Biol*. (2017) 80:3–12. doi: 10.1016/j.semcdb.2017.07.013
162. Yang H, Mu J, Chen L, Feng J, Hu J, Li L, et al. S-nitrosylation positively regulates ascorbate peroxidase activity during plant stress responses. *Plant Physiol*. (2015) 167:1604–15. doi: 10.1104/pp.114.255216
163. Romero-Puertas MC, Sandalio LM. Nitric oxide level is self-regulating and also regulates its ROS partners. *Front Plant Sci*. (2016) 7:316. doi: 10.3389/fpls.2016.00316
164. Jalmi SK, Sinha AK. ROS mediated MAPK signaling in abiotic and biotic stress-striking similarities and differences. *Front Plant Sci*. (2015) 6:769. doi: 10.3389/fpls.2015.00769
165. Wilkins KA, Matthus E, Swarbreck SM, Davies JM. Calcium-mediated abiotic stress signaling in roots. *Front Plant Sci*. (2016) 7:1296. doi: 10.3389/fpls.2016.01296
166. Smýkal P, Vernoud V, Blair MW, Soukup A, Thompson RD. The role of the testa during development and in establishment of dormancy of the legume seed. *Front Plant Sci*. (2014) 5:351. doi: 10.3389/fpls.2014.00351
167. Sabelli PA, Larkins BA, editors. *Advances in Seed Biology*. Lausanne: Frontiers Media SA (2015). p. 238–41.
168. Ji SH, Choi KH, Pengkit A, Im JS, Kim JS, Kim YH, et al. Effects of high voltage nanosecond pulsed plasma and micro DBD plasma on seed germination, growth development and physiological activities in spinach. *Arch Biochem Biophys*. (2016) 605:117–28. doi: 10.1016/j.abb.2016.02.028
169. Ji SH, Ki SH, Kang MH, Choi JS, Park Y, Oh J, et al. Characterization of physical and biochemical changes in plasma treated spinach seed during germination. *J Phys D Appl Phys*. (2018) 51:145205. doi: 10.1088/1361-6463/aab2a2
170. Perez Pizá MC, Prevosto L, Zilli C, Cejas E, Kelly H, Balestrasse K. Effects of non–thermal plasmas on seed-borne Diaporthe/Phomopsis complex and germination parameters of soybean seeds. *Innov Food Sci Emerg Technol*. (2018) 49:82–91. doi: 10.1016/j.ifset.2018.07.009
171. Wang C, Zhao Y, Gu P, Zou F, Meng L, Song W, et al. Auxin is involved in lateral root formation induced by drought stress in tobacco seedlings. *J Plant Growth Regul*. (2018) 37:539–49. doi: 10.1007/s00344-017-9752-0
172. Heldt HW, Piechulla B. *Plant Biochemistry*, 4th edn. London, UK: Academic Press (2010).
173. Fabregas N, Formosa-Jordan P, Confraria A, Siligato R, Alonso JM, Swarup R, et al. Auxin influx carriers control vascular patterning and xylem differentiation in *Arabidopsis thaliana*. *PLoS Genet*. (2015) 11:e1005183. doi: 10.1371/journal.pgen.1005183
174. Safari N, Iranbakhsh A, Ardebili ZO. Non-thermal plasma modified growth and differentiation process of *Capsicum annuum* PP805 Godiva in *in vitro* conditions. *Plasma Sci Technol*. (2017) 19:055501. doi: 10.1088/2058-6272/aa57ef
175. Ljung KAuxin metabolism and homeostasis during plant development. *Development*. (2013) 140:943–50. doi: 10.1242/dev.086363
176. Tian WN, Braunstein LD, Pang J, Stuhlmeier KM, Xi QC, Tian X, et al. Importance of glucose-6-phosphate dehydrogenase activity for cell growth. *J Biol Chem*. (1998) 273:10609–17. doi: 10.1074/jbc.273.17.10609
177. Scholtz V, Pazlarova J, Souskova H, Khun J, Julak J. Nonthermal plasma — a tool for decontamination and disinfection. *Biotechnol Adv*. (2015) 33:1108–19. doi: 10.1016/j.biotechadv.2015.01.002
178. Moon UR, Mitra A. A mechanistic insight into hydrogen peroxide-mediated elicitation of bioactive xanthones in Hoppea fastigiata shoot cultures. *Planta*. (2016) 244:259–74. doi: 10.1007/s00425-016-2506-6
179. Noctor G, Lelarge-Trouverie C, Mhamdi A. The metabolomics of oxidative stress. *Phytochemistry*. (2015) 112:33–53. doi: 10.1016/j.phytochem.2014.09.002
180. Jain D, Khurana JP. Role of pathogenesis-related (PR) proteins in plant defense mechanism. In: Singh A, Singh I, editors *Molecular Aspects of plant-Pathogen Interaction*. Singapore: Springer (2018). pp. 265–81.
181. Perez SM, Biondi E, Laurita R, Proto M, Sarti F, Gherardi M, et al. Plasma activated water as resistance inducer against bacterial leaf spot of tomato. *PLoS ONE*. (2019) 14:e0217788. doi: 10.1371/journal.pone.0217788
182. Hayashi N, Nakahigashi A, Goto M, Kitazaki S, Koga K, Shiratani M. Redox characteristics of thiol compounds using radicals produced by water vapor radio frequency discharge. *Jap J Appl Phys*. (2011) 50:08JF04. doi: 10.1143/JJAP.50.08JF04
183. Phukan UJ, Jeena GS, Shukla RK. WRKY transcription factors: molecular regulation and stress responses in plants. *Front Plant Sci*. (2016) 7:760. doi: 10.3389/fpls.2016.00760
184. Mira S, Pirredda M, Martín-Sánchez M, Marchessi JE, Martín C. DNA methylation and integrity in aged seeds and regenerated plants. *Seed Sci Res*. (2020) 30:1–9. doi: 10.1017/S0960258520000021
185. Kyzek S, Holubová L, Medvecká V, Zahoranová A, Ševčovičová A, Gálová E. Genotoxic effect of low temperature plasma treatment on plant seeds. *Toxicol Lett*. (2017) 280:S119. doi: 10.1016/j.toxlet.2017.07.333
186. Tuteja N, Singh MB, Misra MK, Bhalla PL, Tuteja R. Molecular mechanisms of DNA damage and repair: progress in plants. *Crit Rev Biochem Mol Biol*. (2001) 36:337–97. doi: 10.1080/20014091074219
187. Kurek K, Plitta-Michalak B, Ratajczak E. Reactive oxygen species as potential drivers of the seed aging process. *Plants*. (2019) 8:174. doi: 10.3390/plants8060174
188. Pandiselvam R, Mayookha VP, Kothakota A, Sharmila L, Ramesh SV, Bharathi CP, et al. Impact of ozone treatment on seed germination-a systematic review. *Ozone Sci Eng*. (2019) 42:1–16. doi: 10.1080/01919512.2019.1673697
189. Niemira BA. Cold plasma decontamination of foods. *Annu Rev Food Sci Technol*. (2012) 3:125–42. doi: 10.1146/annurev-food-022811-101132

Conflict of Interest: The authors declare that the research was conducted in the absence of any commercial or financial relationships that could be construed as a potential conflict of interest.

GLOSSARY

Glossary of abbreviations (in alphabetical order).

Abbreviation	Full name	Short description
ABA	Abscisic acid	Hormone known for its role in maintaining dormancy and for inhibiting germination
AC	Alternating current	Usually in the kHz range in these applications
APX	Ascorbate peroxidase	A H_2O_2 scavenging enzyme found in plants to protect the cell from damage by H_2O_2 or OH radicals
AtWRKY23	Auxin regulation factor	Auxin-inducible gene and member of WRKY transcription factor family involved in growth and development, biotic and abiotic stress, and signal transduction
auxin IAA	Indole-3-acetic acid	IAA is the most abundant form of the hormone auxin; auxin is involved in cell elongation, cell division and differentiation, phototropism, geotropism
CAT	Catalase	Enzyme which catalyzes the decomposition of H_2O_2 to water and oxygen; protects from oxidative stress
CCP	Capacitively-coupled plasma	A continuous discharge maintained in a gas by AC voltage between electrodes
DAT	Acetylvindoline O-acetyltransferase enzyme	An enzyme involved in the biosynthesis of vindoline, a precursor of vinblastine and vincristine
DBD	Dielectric barrier discharge	Electric gaseous plasma between electrodes, of which at least one has a dielectric (insulating) surface layer
DSCBD	Diffuse coplanar surface barrier discharge	A type of dielectric barrier discharge
EDX	Energy dispersive X-rays	Analysis of X-rays after sample irradiation by high energy electrons
EMF	Electromagnetic fields	Electric and magnetic fields; pulsed, or low frequency (kHz) or high frequency (GHz)
EPR	Electron paramagnetic resonance	Analysis of electron spin by excitation and detection
erf1	Ethylene response factor	Gene encoding a protein belonging to the ERF transcription factors, one of the largest groups involved in biotic and abiotic stresses using a hormone ethylene
FTIR	Fourier-transform infrared absorption spectroscopy	Absorption spectroscopy suitable for identifying polar molecules
FTIR-ATR	Attenuated total reflectance FTIR	Absorption spectroscopy suitable for the surface of opaque samples
GA	Gibberellic acid	Hormone produced to trigger germination
HSPs	Heat shock proteins	Proteins produced when cells are exposed to temperatures above their normal growth temperature; can also be triggered by oxidative stress, toxins, heavy metals
JA	Jasmonic acid	Hormone involved in wound response, which can be inflicted by herbivores, and systemic acquired resistance
LEA	Late embryogenesis abundant protein	Proteins associated with seed development and involved in responding to abiotic stresses such as desiccation and cold stress
MAPK(KK)	Mitogen-activated protein kinase cascade	Major signal transduction pathway in eukaryotes composed of several proteins called kinases which take extracellular stimuli and convert into cellular responses; activity altered with the addition of a phosphate group (phosphorylation); can regulate plant development, growth, ripening, hormone signaling and in response to biotic and abiotic stresses
MDA	Maldonaldehyde	A product of lipid peroxidation
NADPH (oxidase)	Nicotinamide adenine dinucleotide phosphate (oxidase)	Co-factor involved in oxidation-reduction reactions, protects against ROS, regenerates glutathione (GSH) (membrane-bound enzyme which generates superoxide or H_2O_2)
NTP	Non-thermal plasma	Plasma in which the electron temperature far exceeds the gas temperature
PAL	Phenylalanine ammonia lyase	Catalyzes first reaction of phenylpropanoid pathway which is involved in polyphenol biosynthesis (flavonoids, lignin, phenylpropanoids); belongs to secondary metabolism used for plant defense
PAM	Plasma-activated media	Any liquid, or other medium, exposed to plasma activation
PAW	Plasma-activated water	Water exposed to plasma treatment
PR proteins	Pathogenesis-related proteins	Proteins induced upon pathogen attack; part of systemic acquired resistance
pr	Pathogenesis-related protein	Gene encoding for pathogenesis related protein
RF	Radio frequency	Alternating voltage, generally from 1 MHz to 300 MHz
RNS	Reactive nitrogen species	Reactive radicals containing nitrogen, such as nitric oxide, for example
RONS	Reactive nitrogen and oxygen species	Any combination of ROS and RONS
ROS	Reactive oxygen species	Reactive radicals containing oxygen, such as ozone, superoxide, hydroxyl radicals
SA	Salicylic acid	Hormone synthesized in response to pathogens; part of local and systemic acquired resistance; induces PR proteins
SDBD	Surface dielectric barrier discharge	Dielectric barrier discharge between electrodes disposed on a surface
SEM	Scanning electron microscopy	Electron microscopy suited to surface analysis
SOD	Superoxide dismutase	An enzyme which catalyzes superoxide into H_2O_2 and oxygen

(Continued)

GLOSSARY | Continued

Abbreviation	Full name	Short description
TOR kinase	Target of rapamycin kinase	An enzyme which may increase metabolism and biosynthesis for energy and biomass production according to nutritional, hormonal or other cues
UV	Ultra violet radiation	100–400 nanometer wavelength, including UV-A, UV-B and UV-C regions
VDBD	Volume dielectric barrier discharge	Dielectric barrier discharge in a gas between electrodes
WRKY1	Transcription factor	Family of transcription factors involved in many biotic and abiotic stress responses
XPS	X-ray photoelectron spectroscopy	Analysis of high-energy electrons after sample irradiation by X-rays
μ-XRF	Micro X-ray fluorescence	Fluorescence of X-rays from a sample bombarded by high energy radiation

frontiers in Physics

REVIEW
published: 26 May 2021
doi: 10.3389/fphy.2021.677971

Decontamination Of Endospores By Plasma Sources On Dried Surfaces: A Review Of Key Parameters And Inactivation Results

A Salmon, G. D Stancu and C. O Laux*

Laboratoire EM2C, CNRS, UPR 288, CentraleSupélec, Université Paris Saclay, 8-10 rue Joliot Curie, F-91190 Gif-sur-Yvette, France

The efficiency of plasmas sources for the decontamination of heat-sensitive devices has been proven for more than 20 years, but commercial plasma-based sterilizers still have a narrow range of applications. This can be partially explained by difficulties to determine reliable bio-indicators and standardized microbiological test procedures required by industrial uses. In this paper, we examine the influence of environmental factors on the inactivation rate of microorganisms deposited on surfaces and treated by plasma sources. In addition, we present a literature review showing that several in-discharge and afterglow plasma sterilizers offer shorter treatment times than conventional low-temperature sterilizers to reduce the concentration of endospores on contaminated surfaces by 6-log. Finally we make a few recommendations for future plasma decontamination standards.

Keywords: plasma, endospores, decontamination, sterilization, non-thermal

OPEN ACCESS

Edited by:
Mounir Laroussi,
Old Dominion University,
United States

Reviewed by:
James L Walsh,
University of Liverpool,
United Kingdom
Luc Stafford,
Université de Montréal, Canada
Zdenko Machala,
Comenius University, Slovakia

****Correspondence:***
A Salmon
arthur.salmon@centraliens.net

Specialty section:
This article was submitted to Plasma Physics, a section of the journal Frontiers in Physics

Received: *08 March 2021*
Accepted: *10 May 2021*
Published: *26 May 2021*

Citation:
Salmon A, Stancu GD and Laux CO (2021) Decontamination Of Endospores By Plasma Sources On Dried Surfaces: A Review Of Key Parameters And Inactivation Results. Front. Phys. 9:677971. doi: 10.3389/fphy.2021.677971

1 INTRODUCTION

Low-temperature decontamination methods are increasingly used for the treatment of heat-sensitive materials in devices exposed to biohazards, such as endoscopes in hospitals [1], containers in the food industry [2], spacecraft components [3] or contaminated equipment in areas exposed to war acts [4]. Standard non-thermal sterilization methods suffer from limitations related to their toxicity, high cost, low material compatibility, and/or long sterilization cycles (several hours). An alternative approach consists in using atmospheric pressure nonequilibrium plasmas produced by electric discharges. The use of plasma sources for low-temperature decontamination has been widely studied for more than 20 years [5–7]. Various biocidal mechanisms of plasmas have been demonstrated, including cell lysis induced by charged species [8, 9], DNA inactivation by radiation from excited molecules and atoms [8, 10], and alteration of cell components by chemical products such as reactive oxygen and nitrogen species (RONS). This combination of inactivation mechanisms is attractive because a broad range of microorganisms can be treated, namely bacteria, viruses [11] including Sars-CoV2 [12], fungi [13, 14] and prions [15]. However, the intensities of the mentioned biocidal mechanisms strongly depend on the type of plasma source (discharge kind, gas flow, power,...), working distance between the plasma and the contaminated surface, and operating conditions (surface nature, humidity,...). Therefore, it is difficult to compare decontamination results using plasma sources because the inactivation results are highly dependent on the operating conditions. Comparing the results requires to define standard microbiological test conditions, and thus the major parameters that need to be controlled.

TABLE 1 | Standard sterilization methods and microorganisms commonly used as bio-indicators for these methods, modified from [6].

Method	Microorganism	Form	Standard
Wet heat	*G. Stearothermophilus*	Spore	ISO 11138-3
Dry heat	*B. Atrophaeus*	Spore	ISO 11138-4
Radiation (γ,X,e-beam)	*B. Pumilus*	Spore	ISO 11137
O_3	*G. Stearothermophilus*	Spore	
C_2H_4O	*B. Atrophaeus*	Spore	ISO 11138-2
CH_2O	*G. Stearothermophilus*	Spore	ISO 11138-5
H_2O_2	*B. Atrophaeus*	Spore	ISO 11138-6

O_3: ozone, C_2H_4O: ethylene oxide; CH_2O: formaldehyde; H_2O_2: hydrogen peroxide

The present paper first aims to identify the influence of several environmental parameters that are not systematically mentioned in publications. Second, the decontamination efficiency of various plasma sources is assessed on the basis of the treatment time required to obtain a 6-log reduction of endospores, which are commonly used as bio-indicators (BI) to validate the efficiency of sterilizers. These results are classified according to the gas pressure and to the working distance between the plasma and the treated sample because the biocidal effects of plasmas are reduced as the working distance increases. In addition, the working distance is an important parameter for certain applications, particularly the decontamination of long tubes, where sensitive surfaces cannot be treated directly by the plasma. The observed trends are discussed and compared with inactivation results obtained against the same microorganisms using standard low-temperature sterilizers.

The paper is organized as follows. The first part introduces the definitions of the microbiological quantities used in the article, namely log-reduction, D-value, and bio-indicators. The second part shows the influence of various environmental factors on the inactivation of microorganisms treated by plasma sources or by chemicals. The third part compares and discusses literature results on the basis of the key environmental factors introduced in part 2.

2 DEFINITIONS OF THE PARAMETERS USED TO ASSESS DECONTAMINATION METHODS

The efficiency of decontamination methods is usually assessed by direct cell-counting methods that are based on the following procedure. First, a suspension of microorganisms is prepared, generally in sterile water. The concentration of the suspension is adjusted by subsequent dilution. Second, a fraction of the suspension is deposited onto two carriers and dried. In general, about ~10^6 microorganisms are deposited on the carriers so as to follow ISO 11138 series and ISO 14161 standards. Third, one of the carriers is treated while the other is used as a control. Fourth, the microorganisms are extracted from the carriers and counted using a plate count method. To this end, the suspension of recovered microorganisms is diluted, spread on plates, and incubated. The number of Colony Forming Units (CFU) on the plate is finally counted. If N is the number of CFU after the decontamination treatment, and N_0 the number of CFU on the control sample, the log-reduction factor (RF) is defined as follows:

$$RF = \log \frac{N_0}{N}$$

For an initial load of 10^6 microorganisms on a surface, the maximum reduction factor measurable by direct cell counting is 6-log. On the basis of a statistical analysis, a reduction factor as low as 8-log can be determined by a fraction negative method [16].

The ISO 11138 series and ISO 14161 standards define sterility as a Sterility Assurance Level (SAL) of 10^{-6}. The SAL denotes the probability that only one viable microorganism survives the treatment. Sterility cannot be verified in practice but can be extrapolated from the kinetics of inactivation of the most resistant microorganism, named the bio-indicator (BI). **Table 1** lists some of the commonly used bio-indicators. It should also be noted that other standards, e.g. EN 13697, are used in industrial applications for disinfection purposes.

Figure 1 shows the inactivation kinetics on a semi-logarithmic scale, and the methods used to analyze it. Direct cell counting methods are based on measurings the number of surviving microorganisms. Fraction negative methods, e.g. Stumbo-Murphy-Cochran method and Spearman-Karber method, are statistical techniques applied in the region of the inactivation curve where only a fraction of the treated items have no viable microorganisms after the treatment, i.e. the so-called quantal zone. The technique allows to demonstrate SAL up to 10^{-2} and to determine the D-value from a reduced range of the inactivation curve. Demonstrating lower SAL (SAL < 10^{-2}) is difficult because of the large number of tests required, so extrapolation of the inactivation curve is necessary.

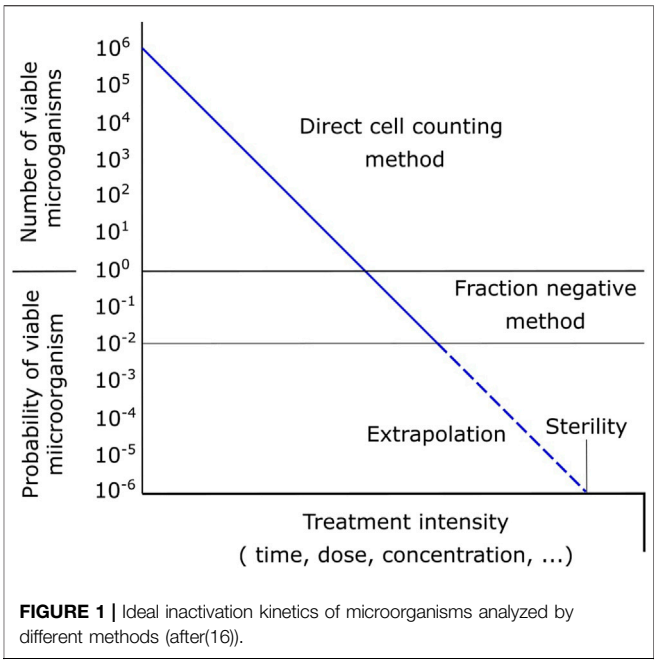

FIGURE 1 | Ideal inactivation kinetics of microorganisms analyzed by different methods (after(16)).

For sterilization methods such as steam heat, the inactivation kinetics follow an ideal exponential decay, and the inactivation curve can be easily extrapolated to determine the conditions for which sterility can be guaranteed. The slope of the semi-logarithmic line is termed the *D-value* and is widely used to assess the efficiency of a sterilization process. It corresponds to the time required to reduce the population of one type of microorganism by one order of magnitude.

In the case of non-thermal decontamination, a multi-step decay of microorganisms is regularly reported, e.g. [17–20]. The multi-step decay is generally attributed to a clumping of microorganisms that reduces the number of microorganisms attainable by the antimicrobial agents [5, 21] or to space-varying mechanisms of inactivation [16, 22] possibly related to an inhomogeneous distribution of the plasma agents across the test sample. Such multiphase decay prevents the determination of accurate D-values and thus does not allow plasma decontamination methods to reach the SAL of 10^{-6} required for sterilization. However, appropriate preparation and deposition of bioindicators may allow to observe a monophasic inactivation curve.

3 ENVIRONMENTAL FACTORS

In this section, we review preparation methods and operating conditions that can significantly modify the inactivation results of plasma decontamination processes.

Effect of the preparation method

The initial suspension of microorganisms is generally prepared in sterile water. However, in realistic conditions, the bioburden is surrounded by organic and inorganic matter (soil). The soil can be well-removed by a preliminary cleaning using water (lowest bio-decontamination level) according to the guidelines of Rutala et al. [23]. However inorganic residues may still persist after cleaning. These residues can be simulated in microbiological treatments by adding salt or serum to the initial suspension of microorganisms. Such additives are known to strongly reduce the efficiency of most decontamination methods [24]. In particular, it has been shown that a high concentration of crystalline-type materials provides a greater protection to spores than serum with high protein content [23]. Using a surface microdischarge (SMD), Klämpfl et al. [25] observed by scanning electron microscopy (SEM) that *Clostridium Difficile* (NCTC 13366) endospores prepared with 0.03% BSA (bovine serum albumine), deposited and dried on stainless steel substrates, form clusters with surrounding saline structures. This barrier decreases the number of spores attainable by plasma species. As a result, the inactivation rate was lowered by 3-log when BSA was added to the suspension. Thus the inactivation results are highly sensitive to the method of preparation, which must be specified to make useful comparisons between decontamination systems.

Effect of the deposition method

Two main techniques are commonly used to deposit microorganisms on substrates : the spot and spray methods. The spot technique is more common and consists in placing a droplet of the prepared suspension of microbes on the inoculation surface. This method does not allow an accurate control of the local concentration of microorganisms, which readily form clusters and multilayered structures. In contrast, the spray method allows to deposit a monolayer of microorganisms onto the surface, thus ensuring a homogeneous and controlable surface concentration of microorganisms [26–28]. For this reason, the spray deposition method is interesting for standardized inoculation on substrates(29). Raguse et al. [29] compared the reduction factor for 5×10^{7} *B. Subtilis* spores deposited by spray and liquid spot methods on a glass substrate exposed to a low-pressure argon plasma. After 90 s of exposure, a 0.8-log reduction was measured on the substrate inoculated using the spot method while a 4.8-log-reduction was achieved using the spray method. The slower inactivation observed using the spot method can be attributed to the slower diffusion of germicidal agents inside the multi-layered cell structures. According to Shintani et al. [21], [30], the characteristic penetration depth of plasma species is about ~10 nm, and ~1 μm for hydrogen peroxide. Since, the dimension of a microbe is typically ~1 μm, chemical sterilants readily diffuse deeply through multiple layers of cells while plasma species only access the first layer.

As a result, the method of microorganism deposition strongly influences the decontamination efficiency of non-penetrating surface agents such as plasma species, but also UV radiation [31]. However, Raguse et al. [29] showed that highly-penetrating agents such as X-rays were not influenced by the deposition technique.

Effect of surface concentration

The surface concentration of microorganisms is defined as the ratio of the initial microorganisms load to the inoculation area. Increasing the surface concentration of microorganisms enhances the formation of multi-layered structures preventing the diffusion of plasma species in the case of microorganisms deposited by a spot method [32]. Thus, decreasing the initial load of microorganisms or increasing the inoculation area may lead to higher inactivation rates. In Ref. [33], different dilutions of *E. Coli* on Agar were treated by surface microdischarges (SMD). A difference of 4-log in the initial load caused a difference of about 1 log in the inactivation rate after 10 s of treatment. A similar behaviour was observed in Ref. [34] with a corona discharge.

Effect of the type strain

Variations in the strains of a single microorganism species are referenced in collections –e.g. American Type Culture Collection (ATCC), National Collection of Type Culture (NCTC). The susceptibility of different strains of *E. Coli* (ATCC 25922 and NCTC 12900) to air DBD exposure was studied in Ref. [35]. After 30 sec of air plasma treatment, it was shown that the strain ATCC 25922 was reduced by 3.4 log whereas the strain NCTC 12900 (corresponding to collection n° ATCC 700728) was only reduced by 1.8 log. The different efficiencies are due to intrinsinc DNA variations within the same type of microorganism. It is important

TABLE 2 | Different names of some bacillus strains of bacteria (after [63])

Microorganism	DSM collection References number	Previous names	References number in other collections
B. Atrophaeus	DSM 675	*Bacillus Globigii* 'red strain'	ATCC 9372, NCIB 8058,
		→ *Bacillus Subtilis var. Niger*	CIP 77.17, NRS 121A
		→ *Bacillus Subtilis*	IFO 13721, NCDO 738
B. Atrophaeus	DSM 2277	*Bacillus Globigii*	ATCC 51189, NCTC 10073, NCIB 8649,
		→ *Bacillus Subtilis*	CIP 103406
B. Atrophaeus	DSM 7264^T	*Bacillus Subtilis var. Niger*	ATCC 49337 ^{T} NRRL-NRS 213^T,
B. Subtilis	DSM 10^T		ATCC 6051^T, CCM 2216^T, NCIB 3610^T, NCTC 3610^T, IFO 12210^T, NBRC 13719^T
B. Subtilis	DSM 402		NCIB 10106, NBRC 111470
B. Pumilus	DSM 492		ATCC 27142, CIP 77.25, NCTC 10327, NCIB 10692
G. Stearothermophilus	DSM 22		ATCC 12980, NBRC 12950, CCM 2062
G. Stearothermophilus	DSM 5934		ATCC 7953

CCM: Czech Collection of Microorganisms; CIP: Collection de l'Institut Pasteur; DSM, DSMZ: Deutsche Sammlung von Mikroorganismen und Zellkulturen; IFO: Institute for Fermentation, Osaka; NCDO: National Collection of Dairy Organisms; NCIB: National Collection of Industrial Bacteria; NCTC: National Collection of Type Cultures; NRRL: Northern Regional Research Laboratory; NRS: Nathan R. Smith, NBRC: Biological Resource Center NITE. T superscript refers to the type strain.

to note also that the name of microorganisms is subject to adjustments. **Table 2** gives the correspondance of DSM (German Collection of Microorganisms and Cell Cultures) collection numbers with other collection numbers of some bacillus strains of bacteria, as well as previous designations that may also be encountered. It should also be noted that microorganisms available from culture collections are typically less resistant than their real-world counterparts, because the latter have been subjected to environmental stresses and have evolved to adapt over countless generations.

Effect of the relative humidity

High relative humidity (RH) is known to cause the swelling of endospores [36], which enhances the efficiency of many decontamination methods –e.g. EtO and formaldehyde [37] – because of the higher water content in the spore core allowing the formation of aggressive chemicals, such as OH, inside the spore. In Ref. [37], the moisture content (hydration) of *B. Subtilis* was measured for different RH. It was shown that the moisture content slightly increases from 0 to 20% when the RH is varied from 0 to 75%, and strongly increases at higher RH (from 20 to 70% between 75 and 95% RH). At RH > 75 %, the strong increase of the water content causes spore swelling.

The relative humidity (RH) also affects the gas-phase plasma chemistry [36]. **Figure 2** shows the influence of the RH on the spore moisture content and the log-reduction of spores treated by atmospheric cold plasma (ACP) [38] and dielectric barrier discharge (DBD) [39]. The results indicate that a higher RH is always correlated with higher sporicidal activity, probably because of the formation of water-related biocides, such as OH, H_2O_2, HNO_2, HNO_3. Similar conclusions were obtained in Ref. [26]

Effect of the surface material

The effect of the material and the structure of the treated surface on the antimicrobial agent efficacy is complex. Sigwarth et al. [40] studied the reduction of *G. Stearothermophilus* (ATCC 7953) endospores deposited on various surface materials after exposure to hydrogen peroxide. Up to a 3-log difference in the reduction was measured on different materials, but the authors saw no clear correlation between the material properties and the shift in the resistance of endospores.

Figure 3 shows the inactivation of endospores *B. Anthracis*, *B. Subtilis* and *G. Stearothermophilus* on different substrates exposed to formaldehyde and hydrogen peroxide [41, 42]. With formaldehyde, the inactivation results are fairly similar for all materials. In contrast, for hydrogen peroxide exposure, the inactivation results strongly depend on the substrate material as shown in Ref. [40]. These results suggest that endospores are less likely inactivated by H_2O_2 when they are deposited on porous

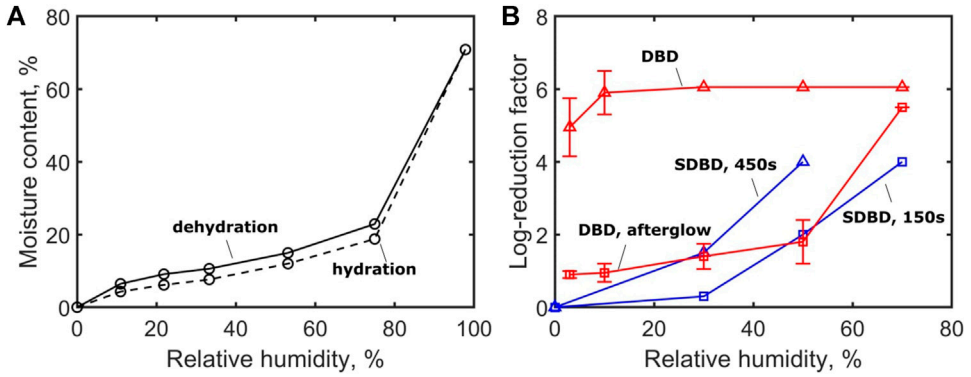

FIGURE 2 | Effect of air relative humidity on **(A)** the moisture content of *B. Subtilis* in contact with air at 25°C estimated from water desorption of wet cells and water adsorption of dessicated cells [37], and **(B)** the inactivation of *B. Atrophaeus* endospore by direct (Δ) and post-discharge (□) DBD treatment [38], and surface DBD (SDBD) after exposures of 150 s (□) and 450 s (Δ), [39].

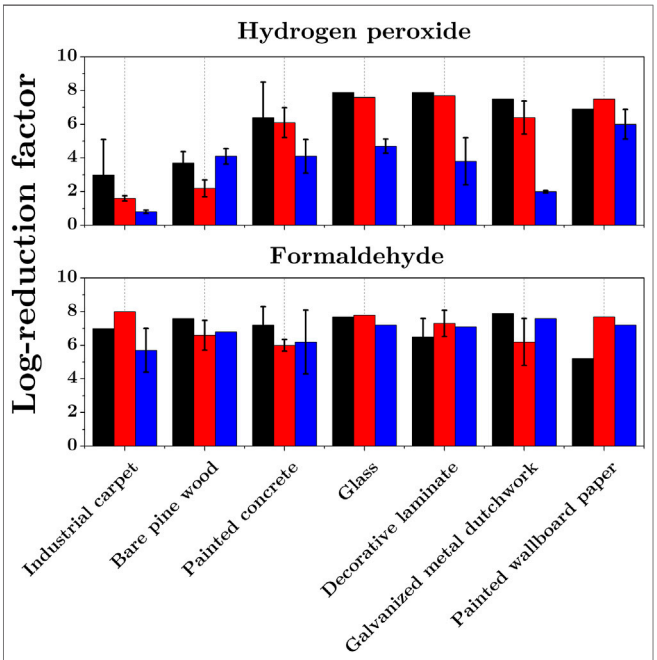

FIGURE 3 | Inactivation of *B. Anthracis* (black), *B. Subtilis* (red) and *G. Stearothermophilus* (blue) endospores dried on various surface materials and exposed to hydrogen peroxide H_2O_2 **(top graph)** and gaseous formaldehyde CH_2O **(bottom)**, adapted from [41, 42].

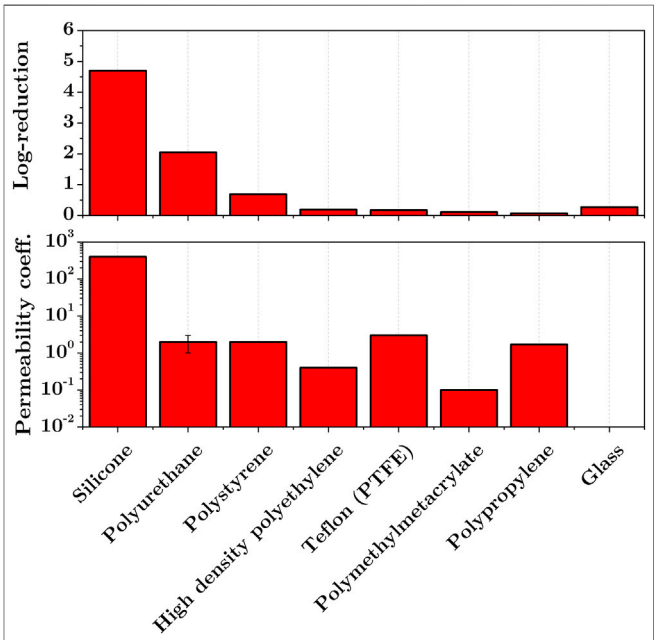

FIGURE 4 | Effect of exposure to dry gaseous ozone (4000 ppm, 60 min, RH < 2 %) on the inactivation of *B. Atrophaeus* endospores dried on pyrex glass and polymeric surfaces (**top**, modified from [36]), and permeability coefficients (units: 10^{-13} $cm^3.cm.cm^{-2}.s^{-1}.Pa^{-1}$) of treated materials (**bottom**, data taken from GoodFellow).

materials. According to the authors, a possible penetration of spores inside porous substrates precludes interaction of H_2O_2 with a significant fraction of spores because of the comparatively small penetration depth of H_2O_2 [23].

The effect of material permeability can be further understood from the work of Mahfoudh et al. [36] who studied the effect of dry gaseous ozone on the inactivation of endospores deposited on different polymeric surfaces. **Figure 4** shows the results obtained by exposing the samples contaminated by *B. Atrophaeus* to 4000 ppm of dry ozone for 1 hour. The log-reductions are shown together with the permeability coefficients of the materials studied (values taken from GoodFellow). The results show a correlation between the permeability of the surface material and the achieved inactivation rate with a maximum 4.6-log reduction obtained on a highly permeable silicone surface. Similar results were obtained in decontamination using ethylene oxide (EtO) in Ref. [37].

In direct plasma decontamination, additional interactions between the plasma and the surfaces increase the influence of the surface material. Interactions between the surface material

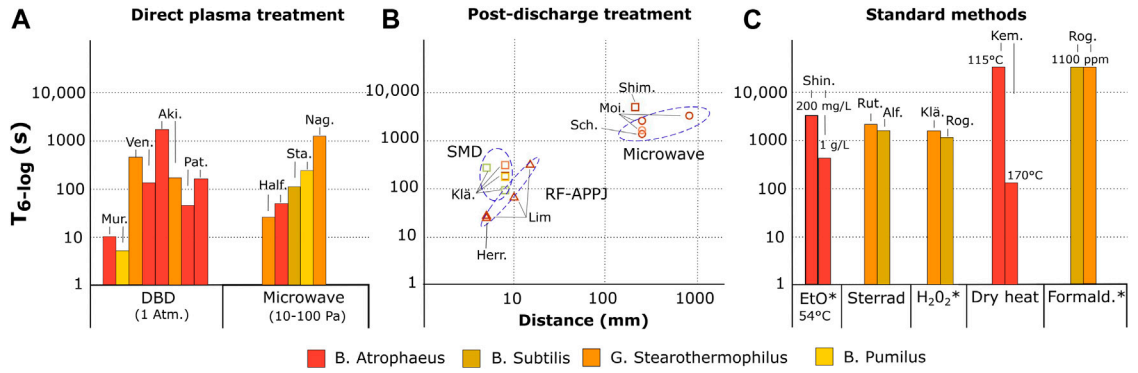

FIGURE 5 | Exposure time T_{6log} required to achieve at least a 6-log reduction of various types of spores on dried surface using different methods. **(A)** direct plasma exposure with DBD (Mur. [26, 49], Ven. [44], Aki. [45], Pat [38]) microwave plasma (Half. [27], Sta. [50], Nag [51]) **(B)** post-discharge exposure as a function of the distance between the plasma and the treated sample using SMD (□, Klä. [25, 52], Shim [53]), RF-APPJ (Δ, Lim [54], Herr [55]) and microwave plasma (○, Sch. [56], Moi [57]). **(C)** standard decontamination methods including ethylene oxide (EtO, Shin [58]), Sterrad systems (Rut. [59], Alf [24]), hydrogen peroxide (H_2O_2, Klä. [25], Rog [41]), dry heat (Kem [60]) and formaldehyde (Rog [42]). The colors of the bars and symbols refer to the type of spores treated. Experimental conditions are detailed in Supplementary material and in the mentioned references. The asterisk indicates that the technique requires an additional aeration time (typically 15 h) in order to remove toxic residuals.

and the gas phase species were observed by Levif et al. [43]. Operating at reduced pressure, the authors demonstrated that *B. Atrophaeus* spores deposited on polystyrene petri dishes were more resistant than on a glass surface, because of the interaction between the plasma and the surface material. As a result, treating microorganisms on porous surfaces significantly increases the inactivation rate. A possible reason for this is the penetration of spores inside the material, thus preventing clumping and shielding of microorganisms at the surface. In the case of direct plasma treatment, interaction of the plasma with the surface material influences the gas phase chemistry and thus the inactivation mechanisms.

4 OVERVIEW OF ENDOSPORE DECONTAMINATION RESULTS ON DRIED SURFACES

In several demonstrations of plasma treatments of spores, the D-values could not be determined. In these cases, the inactivation curve cannot be extrapolated and the sterility cannot be guaranteed according to the sterility assurance level criteria (SAL of 10^{-6}). Rather than speaking of "sterilization", von Woedtke et al. [16] proposed the microbiological safety qualification "proof of antimicrobial efficiency on the highest experimentally accessible level" as the highest possible qualification for plasma decontamination. Here we report the experimental results for which a 6-log reduction of bacterial spores (most common BIs) dried on surfaces was demonstrated according to the von Woedtke definition. The time required to ensure a 6-log reduction of BIs is noted T_{6log}.

Figure 5 shows an overview of spore inactivation results on dried surfaces by atmospheric and reduced pressure plasmas, as a function of the distance between the plasma source and the sample. **Figure 5** also shows typical T_{6log} values for standard decontamination methods. We only plot the experimental results for which a 6-log reduction of spores was measured or extrapolated from a single D-value. The experimental conditions of the reported results are detailed in Supplementary material (**Supplementary table S1, S2**) and in the cited references. An additional table (**Supplementary table S3**) provides a review of the experimental results that could not be included in **Figure 5**.

Figure 5A. shows that two types of plasma sources demonstrated a 6-log reduction of endospores on dried surfaces in the plasma phase: microwave (MW) sources operating at reduced pressure, and dielectric barrier discharges (DBD) operating at atmospheric pressure. The lowest $T_{6\text{-log}}$ value was reported by Muranyi et al. on *B. Pumilis*, *B. Atrophaeus* and *A. Niger* spores using a cascaded-DBD (CDBD) in atmospheric pressure air. The reported $T_{6\text{-log}}$ is about 10 seconds whereas other DBDs required about 100 seconds [38, 44, 45]. This difference can be partially explained by the fact that Muranyi et al. sprayed the initial microbial load of 10^6 CFU on a dried polyethylene terephthalate (PET) sample of 16 cm^2, so that a homogeneous concentration of spores of about 6×10^4 spores/cm^2 was obtained. In the other reports, the concentration was typically 10^6 spores/cm^2, thus increasing the risk of formation of multiple layers of spores, and preventing the contact of plasma agents with the spores. This example shows that standardized microbiological test procedures are needed to better compare the efficiencies of different plasma sources.

In the post-discharge (see **Figure 5B**), surface micro-discharges (SMD), radiofrequency atmospheric pressure plasma jets (RF-APPJ) and reduced pressure MW plasma sources were also able to reach 6-log reduction. The $T_{6\text{-log}}$ values range from about 20 seconds at a few millimeters from the discharge using RF-APPJ to several thousands of seconds at 1 meter using MW plasmas. As expected, increasing the distance from the plasma source lowers the dose of biocidal agents, but provides lower material

degradation and higher treatment area. This configuration is promising for the decontamination of long, small diameter tubes such as the lumens of endoscopes [19, 46], for which the diffusion of the sterilant along the whole length of the lumen is still a major concern [24], particularly in the presence of residual inorganic and organic soil [47, 48].

All reported results showed that a 6-log reduction can be achieved in less than a few thousands of seconds, which is comparable with the typical performances of standard low temperature sterilizers (see **Figure 5C**).

5 CONCLUSIONS

Plasma decontamination has various advantages compared to other methods including:

i/ compatibility with heat-sensitive devices,
ii/ ability to penetrate into narrow devices (e.g. endoscopes),
iii/ absence of toxic waste,
iv/ no shelf life of the sterilization products
v/ onsite operational characteristic.

To date, however, the role of plasma is minor in commercial sterilizing processes. For instance, the efficiency of hydrogen peroxide plasma(e.g. Sterrad sterilization system from Johnson & Johnson) is mainly due to hydrogen peroxide exposure, while the plasma phase is employed to eliminate toxic residues[61]. Nonetheless one application of low-pressure plasma has been clearly identified recently for packaging sterilization in the pharmaceutical industry [62]. Its efficiency against endospores typically used as bio-indicators shows that plasma is a promising candidate as a sterilization method. Yet, multiphase inactivation curves indicate that the biocidal agents are not distributed uniformly (low penetration depth and inhomogeneous plasma) thus preventing efficient contact with the microorganisms and making it difficult to compare with literature results. In order to avoid this, standardized microbiological test procedures are needed, and the following recommendation can be made. First a **monolayer of spores** should be used to obtain reproducible results. To this end, the concentration of spores should be low and the **spray deposition** method should be employed in order to prevent the formation of clusters. Second, a **small inoculation area** should be used to ensure that the distribution of plasma agents is homogeneous across the test sample. Third, **non-porous and inert substrate material** (e.g. glass holder) should be used, except if a specific application is considered (e.g. decontamination of polymer surfaces). In particular, we expect that a high permeability of the substrate allows diffusion of spores inside the material, thus preventing homogeneous exposure of the spores to the plasma, and increasing the risk of incomplete collection of the spores before counting.

The literature review indicates that the relative humidity (RH) increases the sporicidal activity of the plasma phase through the swelling of spores. We suggest that RH should be considered as a parameter to optimize the process, keeping in mind that high RH may be detrimental for the treatment of moisture-sensitive devices such as electronics.

We gave a summary of plasma inactivation results for which a 6-log reduction of endospores dried on surfaces was achieved. We found that several types of plasma sources operating in various gases and pressures can achieve a 6-log reduction in less than one minute, which is comparable with the processing time of standard low-temperature sterilization methods. From the literature review, we could not identify a single relevant bioindicator for plasma sterilization, because this depends on the dominant biocidal mechanism, which is specific to each plasma source.

In conclusion, plasma sources have demonstrated to be competitive sterilizing techniques. A number of biocidal plasma mechanisms are now well-known, but inadequate preparation and control of the environmental conditions does not allow a fair comparison of the biocidal efficiencies of different plasma sources. We recommend that future studies carefully consider the preparation and deposition of bioindicators in order to accurately determine the processing time required for sterility, and thus provide a means to rigorously compare the efficiency of different plasma devices. In summary, we recommend using:

- monolayer of spores for reproducibility
- spray deposition method to prevent the formation of clusters
- inoculation area smaller than size of the plasma to ensure homogeneous treatment
- inert standard deposition material with low permeability to prevent the diffusion of spores inside the material (good candidate substrates could be glass holder)

AUTHOR CONTRIBUTIONS

AS, GDS, COL, have contributed equally to this manuscript.

FUNDING

This research was supported by DGA grant DESDEMONA (RAPID contract EJ nr. 2101 241 872).

SUPPLEMENTARY MATERIAL

The Supplementary Material for this article can be found online at: https://www.frontiersin.org/articles/10.3389/fphy.2021.677971/full#supplementary-material

REFERENCES

1. Mikhail M, and Young T. *Sterilization of Flexible Endoscopes. Decontamination in Hospitals and Healthcare*. Elsevier (2019). p. 519–29.
2. Kumar P, and Han JH. Packaging Materials for Non-thermal Processing of Food and Beverages. *Emerging Food Packaging Technologies*. Elsevier (2012). p. 323–34. doi:10.1533/9780857095664.3.323
3. Cortesão M, de Haas A, Unterbusch R, Fujimori A, Schütze T, Meyer V, et al. Aspergillus niger Spores Are Highly Resistant to Space Radiation. *Front Microbiol* (2020) 11:1–12. doi:10.3389/fmicb.2020.00560
4. Rastogi VK, and Wallace L. *Handbook on Biological Warfare Preparedness*. Elsevier (2019). p. 195–208.Environmental Sampling and Bio-Decontamination-Recent Progress, Challenges, and Future Direction.
5. Moisan M, Barbeau J, Moreau S, Pelletier J, Tabrizian M, and Yahia LH. Low-temperature Sterilization Using Gas Plasmas: a Review of the Experiments and an Analysis of the Inactivation Mechanisms. *Int J Pharmaceutics* (2001) 226: 1–21. doi:10.1016/s0378-5173(01)00752-9
6. Ehlbeck J, Schnabel U, Polak M, Winter J, Von Woedtke T, Brandenburg R, et al. Low Temperature Atmospheric Pressure Plasma Sources for Microbial Decontamination. *J Phys D Appl Phys* (2011) 44(1):013002. doi:10.1088/0022-3727/44/1/013002
7. Moreau M, Orange N, and Feuilloley MGJ. Non-thermal Plasma Technologies: New Tools for Bio-Decontamination. *Biotechnol Adv* (2008) 26:610–7. doi:10.1016/j.biotechadv.2008.08.001
8. Laroussi M. Low Temperature Plasma-Based Sterilization: Overview and State-Of-The-Art. *Plasma Process Polym* (2005) 2:391–400. doi:10.1002/ppap.200400078
9. Lunov O, Zablotskii V, Churpita O, Jäger A, Polívka L, Syková E, et al. The Interplay between Biological and Physical Scenarios of Bacterial Death Induced by Non-thermal Plasma. *Biomaterials* (2016) 82:71–83. doi:10.1016/j.biomaterials.2015.12.027
10. Rossi F, De Mitri R, Bobin S, and Eloy R. *Plasma Sterilisation: Mechanisms Overview and Influence of Discharge Parameters. Plasma Processes and Polymers*. Wiley VCH (2005). p. 319–31. doi:10.1002/3527605584.ch24Plasma Sterilisation: Mechanisms Overview and Influence of Discharge Parameters
11. Filipić A, Gutierrez-Aguirre I, Primc G, Mozetič M, and Dobnik D. Cold Plasma, a New Hope in the Field of Virus Inactivation. *Trends Biotechnol* (2020) 38(11):1278–91. doi:10.1016/j.tibtech.2020.04.003
12. Chen Z, Garcia G, Arumugaswami V, and Wirz RE. Cold Atmospheric Plasma for SARS-CoV-2 Inactivation. *Phys Fluids* (2020) 32:111702. doi:10.1063/5.0031332
13. Misra NN, Yadav B, Roopesh MS, and Jo C. Cold Plasma for Effective Fungal and Mycotoxin Control in Foods: Mechanisms, Inactivation Effects, and Applications. *Compr Rev Food Sci Food Saf* (2019) 18:106–20. doi:10.1111/1541-4337.12398
14. Hojnik N, Modic M, Ni Y, Filipič G, Cvelbar U, and Walsh JL. Effective Fungal Spore Inactivation with an Environmentally Friendly Approach Based on Atmospheric Pressure Air Plasma. *Environ Sci Technol* (2019) 53:1893–904. doi:10.1021/acs.est.8b05386
15. Elmoualij B, Thellin O, Gofflot S, Heinen E, Levif P, Séguin J, et al. Decontamination of Prions by the Flowing Afterglow of a Reduced-Pressure N2–O2 Cold-Plasma. *Plasma Process. Polym* (2012) 9:612–8. doi:10.1002/ppap.201100194
16. von Woedtke T, Kramer A, and Weltmann K-D. Plasma Sterilization: What Are the Conditions to Meet This Claim?. *Plasma Process Polym* (2008) 5(6): 534–9. doi:10.1002/ppap.200800013
17. Moisan M, Levif P, Séguin J, and Barbeau J. Sterilization/disinfection Using Reduced-Pressure Plasmas: Some Differences between Direct Exposure of Bacterial Spores to a Discharge and Their Exposure to a Flowing Afterglow. *J Phys D Appl Phys* (2014) 47(28). doi:10.1088/0022-3727/47/28/285404
18. Boudam MK, Moisan M, Saoudi B, Popovici C, Gherardi N, and Massines F. Bacterial Spore Inactivation by Atmospheric-Pressure Plasmas in the Presence or Absence of UV Photons as Obtained with the Same Gas Mixture. *J Phys D: Appl Phys* (2006) 39(16):3494–507. doi:10.1088/0022-3727/39/16/s07
19. Pointu A-M, Ricard A, Odic E, and Ganciu M. Nitrogen Atmospheric Pressure post Discharges for Surface Biological Decontamination inside Small Diameter Tubes. *Plasma Process Polym* (2008) 5(6):559–68. doi:10.1002/ppap.200800016
20. Becker K, Koutsospyros A, Yin SM, Christodoulatos C, Abramzon N, Joaquin JC, et al. *Plasma Physics and Controlled Fusion* (2005). Environmental and Biological Applications of Microplasmas.
21. Shintani H. Current Mistaken Interpretation of Microbiological Data on Gas Plasma Sterilization. *Pharm Regul Aff Open Access* (2015) 04(02). doi:10.4172/2167-7689.1000138
22. Kogelheide F, Voigt F, Hillebrand B, Moeller R, Fuchs F, Gibson AR, et al. The Role of Humidity and UV-C Emission in the Inactivation of B. Subtilis Spores during Atmospheric-Pressure Dielectric Barrier Discharge Treatment. *J Phys D Appl Phys* (2020) 53:295201. doi:10.1088/1361-6463/ab77cc
23. Rutala WA, and Weber DJ. *Guideline for Disinfection and Sterilization in Guideline for Disinfection and Sterilization in Healthcare Facilities* (2008).
24. Alfa MJ, Degagne P, Olson N, Puchalski T, Degagne P, Olson N, et al. Comparison of Ion Plasma, Vaporized Hydrogen Peroxide, and 100% Ethylene Oxide Sterilizers to the 12/88 Ethylene Oxide Gas Sterilizer. *Infect Control Hosp Epidemiol* (1996) 17(2):92–100. doi:10.1086/647252
25. Klämpfl TG, Shimizu T, Koch S, Balden M, Gemein S, Li Y-F, et al. Decontamination of Nosocomial Bacteria IncludingClostridium difficileSpores on Dry Inanimate Surface by Cold Atmospheric Plasma. *Plasma Process Polym* (2014) 11(10):974–84. doi:10.1002/ppap.201400080
26. Muranyi P, Wunderlich J, and Heise M. Sterilization Efficiency of a Cascaded Dielectric Barrier Discharge. *J Appl Microbiol* (2007) 103(5):1535–44. doi:10.1111/j.1365-2672.2007.03385.x
27. Halfmann H, Bibinov N, Wunderlich J, and Awakowicz P. A Double Inductively Coupled Plasma for Sterilization of Medical Devices. *J Phys D: Appl Phys* (2007) 40(14):4145–54. doi:10.1088/0022-3727/40/14/008
28. Heise M, Neff W, Franken O, Muranyi P, and Wunderlich J. Sterilization of Polymer Foils with Dielectric Barrier Discharges at Atmospheric Pressure. *Plasmas Polym* (2004) 9(1):23–33. doi:10.1023/b:papo.0000039814.70172.c0
29. Raguse M, Fiebrandt M, Stapelmann K, Madela K, Laue M, Lackmann J-W, et al. Improvement of Biological Indicators by Uniformly Distributing Bacillus Subtilis Spores in Monolayers to Evaluate Enhanced Spore Decontamination Technologies. *Appl Environ Microbiol* (2016) 82(7):2031–8. doi:10.1128/aem.03934-15
30. Shintani H, Shimizu N, Y I, Imanishi T, Tamazawa K, Taniguchi A, et al. Inactivation of Microorganisms and Endotoxins by Low Temperature Nitrogen Gas Plasma Exposure. *Biocontrol Sci* (2007) 12(4):131–43. doi:10.4265/bio.12.131
31. Coohill TP, and Sagripanti J-L. Overview of the Inactivation by 254 Nm Ultraviolet Radiation of Bacteria with Particular Relevance to Biodefense. *Photochem Photobiol* (2008) 84:1084–90. doi:10.1111/j.1751-1097.2008.00387.x
32. Fernández A, Shearer N, Wilson DR, and Thompson A. Effect of Microbial Loading on the Efficiency of Cold Atmospheric Gas Plasma Inactivation of *Salmonella enterica* Serovar Typhimurium. *Int J Food Microbiol* (2012) 152(3): 175–80. doi:10.1016/j.ijfoodmicro.2011.02.038
33. Li Y-F, Shimizu T, Zimmermann JL, and Morfill GE. Cold Atmospheric Plasma for Surface Disinfection. *Plasma Process. Polym* (2012) 9(6):585–9. doi:10.1002/ppap.201100090
34. Dobrynin D, Friedman G, Fridman A, and Starikovskiy A. Inactivation of Bacteria Using Dc corona Discharge: Role of Ions and Humidity. *New J Phys* (2011) 13:103033. doi:10.1088/1367-2630/13/10/103033
35. Lu H, Patil S, Keener KM, Cullen PJ, and Bourke P. Bacterial Inactivation by High-Voltage Atmospheric Cold Plasma: Influence of Process Parameters and Effects on Cell Leakage and DNA. *J Appl Microbiol* (2014) 116(4):784–94. doi:10.1111/jam.12426
36. Mahfoudh A, Moisan M, Séguin J, Barbeau J, Kabouzi Y, and Kéroack D. Inactivation of Vegetative and Sporulated Bacteria by Dry Gaseous Ozone. *Ozone: Sci Eng* (2010) 32(3):180–98. doi:10.1080/01919511003791971
37. Gilbert GL, Gambill VM, Spiner DR, Hoffman RK, Phillips CR, and Gambill M. *Effect of Moisture on Ethylene Oxide Sterilization*. Vol. 12, Applied Microbiology (1964).
38. Patil S, Moiseev T, Misra NN, Cullen PJ, Mosnier JP, Keener KM, et al. Influence of High Voltage Atmospheric Cold Plasma Process Parameters and

Role of Relative Humidity on Inactivation of Bacillus Atrophaeus Spores inside a Sealed Package. *J Hosp Infect* (2014) 88(3):162–9. doi:10.1016/j.jhin.2014.08.009

39. Hähnel M, Von Woedtke T, and Weltmann K-D. Influence of the Air Humidity on the Reduction ofBacillusSpores in a Defined Environment at Atmospheric Pressure Using a Dielectric Barrier Surface Discharge. *Plasma Process Polym* (2010) 7:244–9. doi:10.1002/ppap.200900076
40. Sigwarth V, and Stärk A. Effect of Carrier Materials on the Resistance of Spores of Bacillus Stearothermophilus to Gaseous Hydrogen Peroxide. *PDA J Pharm Sci Technol* (2003) 57(1):3–11.
41. Rogers JV, Sabourin CLK, Choi YW, Richter WR, Rudnicki DC, Riggs KB, et al. Decontamination Assessment of Bacillus Anthracis, Bacillus Subtilis, and Geobacillus Stearothermophilus Spores on Indoor Surfaces Using a Hydrogen Peroxide Gas Generator. *J Appl Microbiol* (2005) 99(4):739–48. doi:10.1111/j.1365-2672.2005.02686.x
42. Rogers JV, Choi YW, Richter WR, Rudnicki DC, Joseph DW, Sabourin CLK, et al. Formaldehyde Gas Inactivation ofBacillus Anthracis,Bacillus Subtilis, andGeobacillus Stearothermophilusspores on Indoor Surface Materials. *J Appl Microbiol* (2007) 103(4):1104–12. doi:10.1111/j.1365-2672.2007.03332.x
43. Levif P, Séguin J, Moisan M, Soum-Glaude A, and Barbeau J. Packaging Materials for Plasma Sterilization with the Flowing Afterglow of an N_2-O_2 Discharge: Damage Assessment and Inactivation Efficiency of Enclosed Bacterial Spores. *J Phys D Appl Phys* (2011) 44(40). doi:10.1088/0022-3727/44/40/405201
44. Venezia RA, Orrico M, Houston E, Yin S-M, and Naumova YY. Lethal Activity of Nonthermal Plasma Sterilization against Microorganisms. *Infect Control Hosp Epidemiol* (2008) 29(5):430–6. doi:10.1086/588003
45. Akitsu T, Ohkawa H, Tsuji M, Kimura H, and Kogoma M. Plasma Sterilization Using Glow Discharge at Atmospheric Pressure. *Surf Coat Tech* (2005) 193:29–34. doi:10.1016/j.surfcoat.2004.07.042
46. Bhatt S, Mehta P, Chen C, Schneider CL, White LN, Chen HL, et al. Efficacy of Low-Temperature Plasma-Activated Gas Disinfection against Biofilm on Contaminated GI Endoscope Channels. *Gastrointest Endosc* (2018) 89(1):105–14. doi:10.1016/j.gie.2018.08.009
47. Alfa MJ, DeGagne P, Olson N, and Hizon R. Comparison of Liquid Chemical Sterilization with Peracetic Acid and Ethylene Oxide Sterilization for Long Narrow Lumens. *Am J Infect Control* (1998) 26:469–77. doi:10.1016/s0196-6553(98)70018-5
48. Humphries RM, and McDonnell G. Superbugs on Duodenoscopes: the Challenge of Cleaning and Disinfection of Reusable Devices. *J Clin Microbiol* (2015) 53:3118–25. doi:10.1128/jcm.01394-15
49. Muranyi P, Wunderlich J, and Heise M. Influence of Relative Gas Humidity on the Inactivation Efficiency of a Low Temperature Gas Plasma. *J Appl Microbiol* (2008) 104(6):1659–66. doi:10.1111/j.1365-2672.2007.03691.x
50. Stapelmann K, Fiebrandt M, Raguse M, Awakowicz P, Reitz G, and Moeller R. Utilization of Low-Pressure Plasma to Inactivate Bacterial Spores on Stainless Steel Screws. *Astrobiology* (2013) 13(7):597–606. doi:10.1089/ast.2012.0949
51. Nagatsu M, Zhao Y, Motrescu I, Mizutani R, Fujioka Y, and Ogino A. Sterilization Method for Medical Container Using Microwave-Excited Volume-Wave Plasma. *Plasma Process. Polym* (2012) 9(6):590–6. doi:10.1002/ppap.201100111
52. Klämpfl TG, Isbary G, Shimizu T, Li Y-F, Zimmermann JL, Stolz W, et al. Cold Atmospheric Air Plasma Sterilization against Spores and Other Microorganisms of Clinical Interest. *Appl Environ Microbiol* (2012) 78(15):5077–82. doi:10.1128/aem.00583-12
53. Shimizu S, Barczyk S, Rettberg P, Shimizu T, Klaempfl T, Zimmermann JL, et al. Cold Atmospheric Plasma - A New Technology for Spacecraft Component Decontamination. *Planet Space Sci* (2014) 90:60–71. doi:10.1016/j.pss.2013.10.008
54. Lim JP, Uhm HS, and Li SZ. Influence of Oxygen in Atmospheric-Pressure Argon Plasma Jet on Sterilization of Bacillus Atrophaeous Spores. *Phys Plasmas* (2007) 14(9). doi:10.1063/1.2773705
55. Herrmann HW, Henins I, Park J, and Selwyn GS. Decontamination of Chemical and Biological Warfare (CBW) Agents Using an Atmospheric Pressure Plasma Jet (APPJ). *Phys Plasmas* (1999) 6(5):2284–9. doi:10.1063/1.873480
56. Schnabel U, Andrasch M, Weltmann K-D, and Ehlbeck J. Inactivation of Vegetative Microorganisms andBacillus atrophaeusEndospores by Reactive Nitrogen Species (RNS). *Plasma Process Polym* (2014) 11(2):110–6. doi:10.1002/ppap.201300072
57. Moisan M, Boudam K, Carignan D, Kéroack D, Levif P, Barbeau J, et al. Sterilization/disinfection of Medical Devices Using Plasma: the Flowing Afterglow of the Reduced-Pressure N2-O2discharge as the Inactivating Medium. *Eur Phys J Appl Phys* (2013) 63:10001. doi:10.1051/epjap/2013120510
58. Shintani H. Ethylene Oxide Gas Sterilization of Medical Devices. *Biocontrol Sci* (2017) 22(1):1–16. doi:10.4265/bio.22.1
59. Rutala WA, Gergen MF, and Weber DJ. Comparative Evaluation of the Sporicidal Activity of New Low-Temperature Sterilization Technologies: Ethylene Oxide, 2 Plasma Sterilization Systems, and Liquid Peracetic Acid. *Am J Infect Control* (1998) 26(4):393–8. doi:10.1016/s0196-6553(98)70034-3
60. Kempf MJ, Schubert WW, and Beaudet RA. Determination of Lethality Rate Constants and D-Values forBacillus Atrophaeus(ATCC 9372) Spores Exposed to Dry Heat from 115°C to 170°C. *Astrobiology* (2008) 8(6):1169–82. doi:10.1089/ast.2007.0208
61. Krebs MC, Bécasse P, Verjat D, and Darbord JC. Gas-plasma Sterilization: Relative Efficacy of the Hydrogen Peroxide Phase Compared with that of the Plasma Phase. *Int J Pharmaceutics* (1998) 160(1):75–81. doi:10.1016/s0378-5173(97)00296-2
62. Denis B, Steves S, Semmler E, Bibinov N, Novak W, and Awakowicz P. Plasma Sterilization of Pharmaceutical Products: From Basics to Production. *Plasma Process. Polym* (2012) 9(6):619–29. doi:10.1002/ppap.201100211
63. Fritze D, and Pukall R. Reclassification of Bioindicator Strains Bacillus Subtilis DSM 675 and Bacillus Subtilis DSM 2277 as Bacillus Atrophaeus. *Int J Syst Evol Microbiol* (2001) 51:35–7. doi:10.1099/00207713-51-1-35

Conflict of Interest: The authors declare that the research was conducted in the absence of any commercial or financial relationships that could be construed as a potential conflict of interest.

frontiers in Physics

REVIEW
published: 01 June 2021
doi: 10.3389/fphy.2021.683118

Non-Thermal Plasma as a Novel Strategy for Treating or Preventing Viral Infection and Associated Disease

Hager Mohamed[1†], *Gaurav Nayak*[2†], *Nicole Rendine*[3], *Brian Wigdahl*[1], *Fred C. Krebs*[1‡], *Peter J. Bruggeman*[2‡] *and Vandana Miller*[1*‡]

[1]*Department of Microbiology and Immunology, and Institute for Molecular Medicine and Infectious Disease, Drexel University College of Medicine, Philadelphia, PA, United States,* [2]*Department of Mechanical Engineering, College of Science and Engineering, University of Minnesota, Minneapolis, MN, United States,* [3]*Department of Chemistry, College of Arts and Sciences, Drexel University, Philadelphia, PA, United States*

OPEN ACCESS

Edited by:
Mounir Laroussi, Old Dominion University, United States

Reviewed by:
Toshiro Kaneko, Tohoku University, Japan
Zhitong Chen, Shenzhen Institutes of Advanced Technology, Chinese Academy of Sciences (CAS), China

***Correspondence:**
Vandana Miller
vam54@drexel.edu

†These authors have contributed equally to this work and share first authorship.
‡These authors have contributed equally to this work and share senior authorship.

Specialty section:
This article was submitted to Plasma Physics, a section of the journal Frontiers in Physics

Received: *19 March 2021*
Accepted: *06 May 2021*
Published: *01 June 2021*

Citation:
Mohamed H, Nayak G, Rendine N, Wigdahl B, Krebs FC, Bruggeman PJ and Miller V (2021) Non-Thermal Plasma as a Novel Strategy for Treating or Preventing Viral Infection and Associated Disease. Front. Phys. 9:683118. doi: 10.3389/fphy.2021.683118

Pathogenic viruses cause many human, animal, and plant diseases that are associated with substantial morbidity, mortality and socio-economic impact. Although effective strategies for combatting virus transmission and associated disease are available, global outbreaks of viral pathogens such as the virus responsible for the COVID-19 pandemic demonstrate that there is still a critical need for new approaches that can be used to interrupt the chain of viral infection and mitigate virus-associated pathogenesis. Recent studies point to non-thermal plasma (NTP), a partly ionized gas comprised of a complex mixture of reactive oxygen and nitrogen species along with physical effectors, as the potential foundation for new antiviral approaches. A more thorough understanding of the antiviral properties and safety of NTP has stimulated explorations of NTP as the basis for treatments of viral diseases. The recently described immunomodulatory properties of NTP are also being evaluated for potential use in immunotherapies of viral diseases as well as in antiviral vaccination strategies. In this review, we present the current state-of-the-art in addition to compelling arguments that NTP merits further exploration for use in the prevention and management of viral infections and associated diseases.

Keywords: reactive oxygen and nitrogen species, virus inactivation, disinfection, antiviral, immunotherapy, adjuvant, vaccine, SARS-CoV-2

INTRODUCTION

Viruses are a major group of ubiquitously present microbes responsible for many acute and chronic infectious diseases. Viral infections spread easily, either from person to person or through contact with contaminated objects or ingestion of contaminated foods. Some of these infections are self-limiting, while others require aggressive therapeutic interventions or lead to loss of life [1]. Viruses also challenge food safety and cause tremendous economic loss in agriculture due to infection of plants or livestock [2, 3]. As an example of the global impact of viruses, the current coronavirus disease-2019 (COVID-19) pandemic has brought to the forefront unresolved challenges in prevention and treatment of viral diseases. Severe Acute Respiratory Syndrome Coronavirus 2 (SARS-CoV-2), the viral cause of this pandemic, has become the source of widespread morbidity, mortality, and economic burden [4, 5].

Despite extensive efforts directed toward new drug development, there are few effective, broad-spectrum antiviral drugs available. Prevention of infection is currently the most effective method of

combating virus infection and associated disease. There is a dire need for novel approaches that can be used to prevent and control viral infections. Recently, there has been increased interest in defining roles for non-thermal plasma (NTP), an ionized gas containing a complex mixture of reactive oxygen and nitrogen species, in strategies effective against viral infection and disease. This review discusses the potential for NTP in mitigating viral infections and the points of intervention where state-of-the-art plasma medicine approaches can be applied. We also highlight collaboration opportunities for engineers and virologists to develop novel methods for both prevention and treatment of viral infections.

GLOBAL HEALTH CHALLENGES AND ECONOMIC BURDENS

Viral infections have been the cause of considerable disease and many deaths around the globe for centuries. The Antonine plague in the second century A.D., now believed to be attributed to either the smallpox or measles virus, is the earliest documented instance of a large-scale viral outbreak (although cases of smallpox are suspected to have occurred in China and Egypt in 3 BCE) [6, 7]. In modern history, smallpox outbreaks were documented starting in the early 16th century. Eradicated in 1980, smallpox virus was the cause of disfigurement and loss of sight in many who were infected with this pathogen and, by conservative estimates, the cause of over 500 million deaths during the 20th century [6]. The Spanish flu, attributed to the spread of the H1N1 influenza virus in 1918–1920, had the second highest lethality rate, but took only two years to kill 40–50 million people, representing 2.1% of the world population [8]. Because this pandemic strain of influenza virus disproportionately affected young adults, its socio-economic impact was tremendous.

The acquired immunodeficiency syndrome (AIDS) epidemic, caused by the human immunodeficiency virus type 1 (HIV-1), is another infection associated with widespread loss of life. Current estimates of the HIV-1 global impact have reached 33 million lives lost since the mid-1970s and over 38 million people now living with pharmaceutically-controlled HIV-1 infection [9]. The societal and demographic impact of AIDS at the level of families, communities, and nations has been considerable and has driven major policy decisions [10]. The worldwide spread of HIV-1 fostered the development of new public health measures, new surveillance programs, and expanded international cooperation in the management of emerging diseases.

In the 21st century, coronaviruses have been the cause of the most frequently emerging epidemics and pandemics. These include the 2002 Severe Acute Respiratory Syndrome-1 (SARS-1) outbreak, the 2012 spread of the Middle Eastern Respiratory Syndrome (MERS), and the current COVID-19 pandemic [11]. Just over one year after the initial outbreaks, SARS-CoV-2 continues to spread through populations on all seven continents, resulting in a total of 119,220,681 cases and 2,646,826 deaths (as of March 10th, 2021) [12]. The emergence of new viral variants, such as the B.1.1.7 variant, further complicates efforts to contain the virus and raises important questions about the efficacies of approved vaccines that were developed against the original viral isolate [13]. The COVID-19 pandemic continues to be the cause of considerable morbidity, mortality, socio-economic burden and brings acute attention to the disruptive potential of emerging pathogenic viruses and the urgent need to find new methods for stopping them [4, 5].

While not the cause of massive global outbreaks, other viruses nevertheless present significant public health challenges. For example, the measles virus continues to reemerge in the form of local outbreaks every 2–3 years resulting in loss of life, mainly in children under 5 years of age [14]. Because the measles virus is highly contagious, exposure almost always results in infection in the unimmunized. Since the introduction of the measles vaccine in 1963, global deaths attributable to measles virus infection have gone down by 73% [14]. Other viruses, particularly those associated with foodborne illnesses, continue to cause outbreaks around the world due to inefficient decontamination of consumable products. Such is the case for norovirus, which annually causes close to 700 million cases of gastrointestinal illness worldwide, many of which require hospitalizations [15]. Inefficient decontamination also contributes to ongoing outbreaks caused by respiratory viruses that cause the common cold and influenza. The potentially lethal influenza virus A, the cause of the seasonal flu, causes hundreds of thousands of deaths annually [16]. Analogous to virus outbreaks among humans, loss of livestock due to disease caused by viruses like avian influenza and porcine reproductive respiratory syndrome virus (PRRSV) or loss of economic crops from uncontrolled infections by plant viral pathogens like tobacco mosaic virus result in the loss of billions of dollars annually in the U.S. alone [2].

VIRUS STRUCTURE AND THE REPLICATION CYCLE

Viruses are submicroscopic particles that are dependent on a host cell for replication. They are not considered "living" but have unique structural elements that allow them to enter (infect) and hijack living cells for the purpose of replication. In general, most viruses consist of a capsid (protein) that encloses the genetic material (nucleic acid) carrying the codes for their structural and functional components [17] (**Figure 1**). The capsid is made of small subunits arranged in specific patterns that give each virus its unique shape and host cell specificity. Some viruses are naked, consisting of the protein capsid as the outermost layer of the virus. Other viruses are enveloped, which means that they are surrounded by a membrane derived from the host cell. The envelope is composed of phospholipids acquired from the host cell as well as glycoproteins that are encoded by the virus and are key to virus entry into the host cell. Because of the fragility of the envelope, enveloped viruses are generally more sensitive to environmental factors (e.g., low humidity and increased temperature) that adversely affect the structure of the virus and reduce its infectivity [17]. Both types of viruses—including enveloped (SARS-CoV-2, influenza virus A, and HIV-1) and non-enveloped (norovirus and rhinoviruses)—have caused considerable economic disruption and loss of life [4, 5, 18–22].

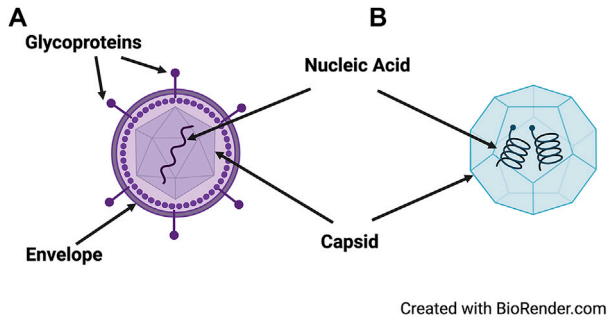

FIGURE 1 | Structure of a generic enveloped and non-enveloped virus. Viruses may be enveloped, containing an outermost layer of glycoproteins surrounding the capsid **(A)**, or non-enveloped **(B)**. They carry necessary genetic information on their nucleic acid (DNA or RNA) that is enclosed in a capsid.

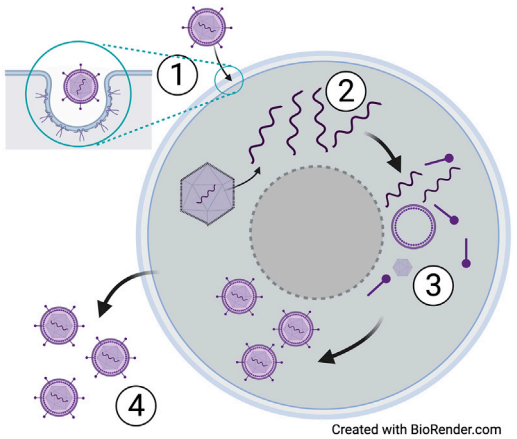

FIGURE 2 | Life cycle of a generic virus. Infection of a host cell begins with attachment of glycoproteins (enveloped virus) or capsid proteins (non-enveloped) to receptors on the host cell (1). Replication of the viral DNA or RNA then occurs using the host cell machinery (2), followed by assembly of new virions (3) and release of newly assembled virions (4) that are released to subsequently infect other host cells.

The information necessary for a virus to replicate and cause disease is stored in the viral genome, which can take the form of DNA or RNA. As a consequence, DNA and RNA viruses use viral enzymes called DNA- or RNA-dependent polymerases, respectively, to facilitate replication in the host cell. During replication, the nucleic acids of RNA viruses are more prone to accumulate mutations relative to DNA viruses. Mutations that confer a survival advantage for the virus include resistance to antiviral drugs [23, 24] or the ability to replicate in new species [25]. Several of the emerging or re-emerging viruses that are contemporary threats to global public health are RNA viruses, including the coronavirus SARS-CoV-2, Zika virus, influenza virus A, Ebola virus, and HIV-1 [23–25].

Despite the simple structure of viruses and their genomes, interactions between viruses and their host cells during viral replication are quite complex, largely because viruses are obligatory intracellular parasites. A single virus particle or virion is sufficient to initiate infection, which is accomplished by the attachment of proteins on the virus capsid or envelope to corresponding receptors on the cell surface. This interaction defines the host range and cellular tropism of a virus and also facilitates the entry of the virus into the cell so that it can access the cellular machinery to replicate its genome and assemble new copies of itself. It is during the stage of egress from the cell that enveloped viruses acquire their host-derived envelope through the process of budding. In contrast, most non-enveloped viruses lyse their host cells as the endpoint of replication cycle. Newly produced progeny virions (infectious virus particles) that exit their host cells by either mechanism can attach to and infect new cells, further facilitating their spread (**Figure 2**). The time required for a single replication cycle (the process that starts with virus entry and concludes with the release of new viruses from the infected cell) varies considerably between viruses. For example, the replication cycle of the influenza virus can be as short as 6 h while the replication cycle for HIV-1 is completed in approximately 24 h [26, 27]. The consequence of a faster replication cycle can be the production of higher numbers of progeny viruses and faster spread of the infection.

Some viruses, such as herpes simplex virus type 1 (HSV-1) and HIV-1, infect the host cell and then establish a state of dormancy (latency) in which the viral genome persists in the host cell but is not used to synthesize viral proteins or new viruses for some time. Latently infected cells pose a particular challenge to the host, because they may be undetected by host immune defenses and may be unaffected by antiviral drug therapies [28, 29].

VIRUS SPREAD AND METHODS OF CONTROLLING INFECTION

A productive virus replication cycle produces more copies of the virus that spread to other cells in the infected person and can also be transmitted to other individuals. Control of transmission can be accomplished through efficient disinfection strategies to prevent exposure of new hosts to the virus. Additionally, strategies that provide prophylactic protection from infection or a therapeutic host immune response to an established infection also reduce the risk of virus transmission.

Virus Transmission Is Necessary to Sustain Virus Propagation in a Population

Viruses spread among populations by a process called transmission, in which uninfected individuals become infected subsequent to virus exposure. Most infectious viruses are spread by direct contact with a contaminated item (fomite) in the environment or an infected individual. Therefore, spread of infection in a community may be controlled by creating spatio-temporal distance between an individual and the source of the virus. This may be achieved by the following measures, implemented separately or in combination: disinfection/sanitation of the environment to reduce the quantity of viruses, physical barriers to reduce contact with viruses, prophylactic drugs and vaccines to prevent disease, isolation of infected individual(s) (quarantine), and therapeutics for infected individuals.

The ease with which a virus becomes transmitted from person to person depends on the production of transmissible virus during an infection and the size of the inoculum. After the initial infection, there is a lag period, called the incubation period, during which time the virus replicates productively. The infected individual may or may not have clinical symptoms during the incubation period but may still be capable of transmitting the virus to others. For example, a person infected with varicella-zoster virus (VZV) is contagious up to 1–2 days before the appearance of lesions characteristic of varicella (chickenpox). Asymptomatic transmission has also been a major challenge in containing the COVID-19 pandemic and the spread of SARS-CoV-2, as infected individuals who are asymptomatic can spread the virus to the vulnerable in close proximity [30]. This is also true of infections by other viruses (e.g., HIV-1), for which clinically apparent symptoms may not develop until several days or months after infection [31, 32] but the asymptomatic individual can serve as a carrier and spread the pathogen.

The route of transmission also has an important role in sustained virus transmission within a population. Viruses like HIV-1 and HSV-1 are spread primarily through direct, physical contact with infected individuals. In contrast, airborne transmission of viruses like influenza virus A and measles virus may involve the spread of the virus over distances exceeding 2 m, resulting in the infection of multiple people simultaneously despite control measures [22, 33]. VZV can be spread not only by direct contact, but also by inhalation of aerosolized fluids from skin lesions and potentially by inhalation of respiratory secretions exhaled by someone infected by VZV. SARS-CoV-2 is transmitted between people through contact with or inhalation of virus-laden respiratory droplets [34, 35]. These droplets also settle on objects and contaminate surfaces with viruses that may remain infectious for several hours to a few days [36, 37].

Infectious large and small droplets have typical travel lengths of less than 6 feet. However, mucus or water evaporation from the droplets create sub-micrometer- to micrometer-sized droplet nuclei that can remain airborne nearly indefinitely and travel due to indoor air currents created by heating, ventilation, and air-conditioning (HVAC) systems and by the movement of building occupants. As an example of long-distance infection, livestock and poultry farms are subject to airborne transmission of disease-causing viruses. Investigations of the distances to which viruses could be carried in the air demonstrated detection of RNA of an animal coronavirus in the air at 16.1 km from an infected farm in the US [38]. Although many viruses are transmitted via aerosols, the potential of airborne transmission has been an overlooked problem [39], at least until the COVID-19 pandemic.

Resolution of Viral Infection in the Mammalian Host Relies on the Innate and Adaptive Immune Responses

In humans, viruses can be cleared by host defense mechanisms once an infection has been detected. Defense against a viral infection begins with the non-specific innate immune response followed by activation of the virus-specific adaptive immune response, which may be cell-mediated (T cell), or antibody-mediated (B cell). Many common viral infections can be cleared by these host defense mechanisms before clinically apparent symptoms develop [40–43] (**Figure 3**).

The first line of defense against viral infection is the innate immune system, which can detect free virus as well as infected host cells that display distinct markers on their surface that reflect ongoing virus replication and virus-associated cell death [44]. Recognition of either free virus or virus-infected cells is accomplished by dendritic cells or macrophages, often called sentinel cells or antigen presenting cells (APCs), because they constantly survey the body for invading pathogens and infected cells. These cells engulf and break down the virus or virus-infected cell through the process of phagocytosis. Activation and recruitment of APCs is a critical step for engagement of innate cells key for inhibition of viral infection. APCs display the digested viral peptides on their cell surface and migrate to local lymph nodes to present them to the adaptive immune cells (T and B cells) in order to produce a cell or antibody-mediated response, respectively. Both responses target the specific virus against which they are generated and usually have no effect against other types of viruses [40–43].

The second host defense mechanism is the adaptive immune response, which is a long-term response to infection. It takes the form of a cell-mediated response and a process that results in the production of pathogen-specific antibodies. The cell-mediated immune response depends on activation of $CD8^+$ T cells that can recognize the viral peptide displayed on APCs by virtue of an appropriate receptor on their cell membrane. This response can be broadened by engagement of $CD4^+$ T helper cells that also recognize that specific virus and provide additional signals to enhance the antiviral function of $CD8^+$ T cells. Once $CD8^+$ T cells are activated, they proliferate to expand and then migrate to different sites in the body to kill the virus-infected cells displaying the viral antigen, achieving clearance of infection. A small subset of these virus-specific $CD8^+$ T cells become long-lived memory cells and may be called back into service at a later time to prevent disease caused by the same virus. Vaccines rely on the use of pathogen-derived antigens to generate memory responses that provide specific recognition of infected cells and their elimination by $CD8^+$ T cells [40–43].

An antibody-mediated immune response is mounted by B cells, which can be activated by interactions with APCs and/or signals from the $CD4^+$ T helper cells. Activated B cells mature to produce antibodies that specifically bind to free virus, preventing it from binding to uninfected host cells by a process called neutralization. The generation of neutralizing antibodies is thus critical for reducing viral burden in the body, which enables the cell-mediated immune response to be more effective at controlling the disease. Like the $CD8^+$ T cells, memory B cells are formed, providing protection against a later re-exposure to the virus [40–43].

Despite innate and adaptive immune responses, many viruses often succeed in causing clinical disease. A virus may gain a foothold in the host due to deficiencies in immune responses (such as an inability of immune cells to recognize infected cells), a lack of engagement between innate and adaptive immune cells, or

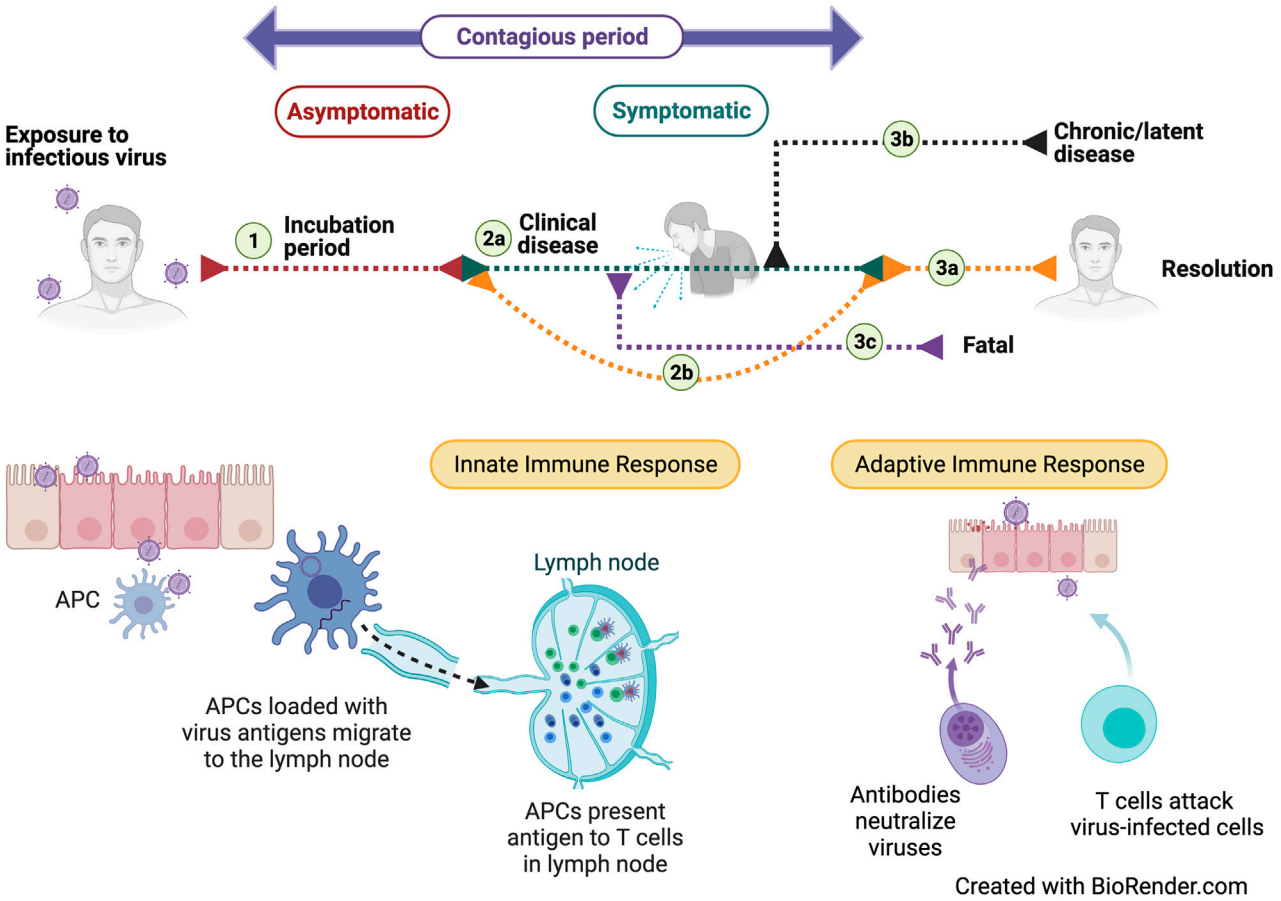

FIGURE 3 | Course of disease and the associated immune responses after exposure to an infectious virus. Exposure to an infectious virus is followed by an asymptomatic incubation period (1) during which the virus replicates. During this phase, the tissue-resident innate immune responses are initiated but may still allow disease symptoms to develop (2A). Stimulation of protective, adaptive immune responses results in resolution (3A) of the disease. In some cases, the patient may remain asymptomatic (2B) because of a strong adaptive immune response. Certain viruses can transition to a chronic disease (3B) while others may have a fatal outcome (3C). Successful immune responses may also lead to viral clearance.

inefficient killing of infected cells by either innate or adaptive immune cells [45]. Additionally, mutations in the capsid or envelope of the virus that prevent it from being neutralized by antibodies or provide other survival and transmission benefits contribute to its continued propagation. A poor clinical outcome from viral diseases can also be caused by an intensified immune response. In some diseases (including COVID-19), the clinical outcome may be worsened by severe, dysregulated inflammation that occurs in response to the virus infection [45, 46]. Each of these factors could potentially counter strategies intended to prevent viral infections or treat virus-associated diseases.

Current Strategies for Controlling Viral Infections

Current antiviral strategies are aimed at mitigating host exposure to the virus (prevention of transmission), prevention of infection or disease development following exposure (prophylaxis), or treatment of disease. All three approaches, if effective, can collectively decrease the prevalence of viruses in the population over time, thus minimizing the impact of virus infections in the population and potentially leading to its eradication.

Disinfection of Viruses in the Environment

Antiviral strategies that focus on preventing transmission target early events in the spread of the virus. One important preventative strategy that serves to limit individuals' exposure to a virus in the environment is disinfection, intended to reduce the virus load on surfaces. This can be accomplished by using chemical agents (e.g., bleach), alcohol, and oxidizing agents (e.g., hydrogen peroxide or chlorine) that disrupt the viral envelope or capsid [47]. However, these approaches are not feasible against viruses that are airborne (such as influenza and coronaviruses). For airborne viruses, high-efficiency particulate air (HEPA) filters are the most efficacious approach available for removing virus-containing droplets and aerosols from the air. It is estimated that 99.97% of aerosolized particles of 3 μm in size can be captured with HEPA filters, making them suitable for capturing droplets or aerosols that potentially contain infectious viruses [48, 49].

However, efficacy in viral decontamination and the ability to capture viruses depends critically on airflow [50, 51]. While HEPA filters are highly effective in HVAC systems, most HVAC systems in office buildings have less than one air exchange per hour. As a consequence, removal of virus-containing aerosols and droplets by HEPA filtration of recirculated room air may be less effective. Decontamination of more contained indoor spaces can be accomplished with exposure of room surfaces to ultraviolet light (UV), which causes damage to viral proteins and the genome [52]. Despite the frequent use of these control measures, there remains a risk of exposure to respiratory viruses in especially densely populated environments.

Prophylaxis to Prevent Disease Development or Progression

Prophylaxis is a strategy used to prevent initial infection with a virus, prevent the transition to virus-associated disease, or reduce the severity of disease caused by the infection. It may be achieved through the use of vaccines that stimulate immunity and are intended to provide long-term protection against subsequent exposure(s) with the same virus. Antiviral drugs, on the other hand, limit viral replication early in infection, usually prior to emergence of symptoms, and are typically administered after a suspected virus exposure. These drugs may not be effective if the infection has progressed too far or once disease symptoms have developed. For example, oseltamivir (Tamiflu) prevents emergence of influenza symptoms, but only when administered within the first 48 h after exposure to the virus [53, 54]. Prophylaxis for disease prevention or mitigation subsequent to infection is not to be confused with prophylactic approaches intended to prevent the initial infection. For example, pre-exposure prophylaxis (PreP) is a drug-based regimen designed to protect people from becoming infected with HIV-1 rather than a therapy for preventing HIV-1-associated disease in those who are already infected.

The most effective prophylactic measure against viral diseases is a vaccine, which evokes a pathogen-specific immune response. Vaccines function by educating the host immune system to create immunological memory against a specific virus in response to administration of a subset component of the virus or an inactivated virus. This protects the host against disease upon a subsequent encounter with the virus [55] because the reactivated immune cells clear the virus and infected cells soon after re-exposure. Several vaccines specific to viral diseases like smallpox (now eradicated), measles, and poliovirus are part of the regular childhood vaccination schedule. These and other vaccines are advantageous relative to prophylactic drugs because they build lifelong immunity that potentially protects immunized individuals long after the vaccine was administered.

Treatment of Viral Diseases

When an infected person develops disease symptoms, one recourse is treatment with antiviral drugs to control the severity of symptoms and also prevent the spread of virus in the community. Since viruses replicate inside the cells of the host, such drugs need to have high selectivity, i.e., a high degree of antiviral efficacy with little or no effect on host cell viability, metabolism, or functions. Antiviral drugs target virus-specific proteins or enzymes to inhibit viral replication and reduce the virus burden. In some cases, this allows the immune system to engage, resulting in the resolution of infection by complete elimination of the virus from the body and establishment of long-term immunity. In other diseases caused by viral pathogens like HIV-1 or hepatitis C, the antiviral drugs control or prevent severe disease but cannot affect the virus that has established a latent infection [28, 56]. The symptoms and severity of a viral infection may also be moderated by drugs that are administered to either boost the host's antiviral immune response, as in AIDS, or dampen it, as in COVID-19 [57, 58]. The therapeutic options available for viral infections are limited to a few diseases; there is an urgent need for broad-spectrum antiviral approaches, as is highlighted by the emergence of many recent viral outbreaks and global epidemics.

Non-Thermal Plasma as a Potential New Broad-Spectrum Antiviral Strategy

Non-thermal plasma has emerged as a technology with the potential to be used to prevent viral infection and disease. NTP is an ionized gas containing free energetic electrons that enable a highly reactive environment at near ambient temperatures. The plasma-produced free energetic electrons have energies that are large enough to electronically excite, dissociate, and ionize molecules, and produce more than 80 different species in humid air [59, 60]. The resulting highly reactive oxygen and nitrogen species (RONS) are extremely effective in inactivation of pathogens. We provide evidence in this section that NTP technology has potential as a new broad-spectrum antiviral strategy and has several advantages over existing decontamination technologies. Investigation of the antiviral effects of this technology has increased around the world in the last ten years (**Figure 4**). A summary of the studies investigating antiviral strategies utilizing NTP application is provided in **Table 1**. We briefly review conventional decontamination technologies with some of their limitations and contrast them with NTP technology.

UV-C germicidal irradiation, in which UV is produced in lamps by plasma (although recently can also be produced by LEDs), is a well-established decontamination technology for pathogen inactivation both in water as well as on surfaces [61–64]. However, UV-C radiation is limited by the requirement for its proximity to the target and the shadowing effect, as UV-C cannot penetrate opaque surfaces [65, 66]. Because plasma can flow around complex 3D surfaces, decontamination by plasma technology is not limited by shadowing. A recent study compared UV-C with plasma-based inactivation of feline calicivirus (FCV) on surfaces and showed that the energy cost of plasma-based inactivation can be similar to UV-C [67]. However, UV-C was effective both on dry and humid surfaces, while plasma was shown to be less effective on dry substrates [67].

Other emerging non-thermal decontamination technologies include pulsed electric fields (PEF) and high hydrostatic pressure (HHP) [68]. Although PEF has been commonly used for destruction of several non-sporing bacterial pathogens [69–72],

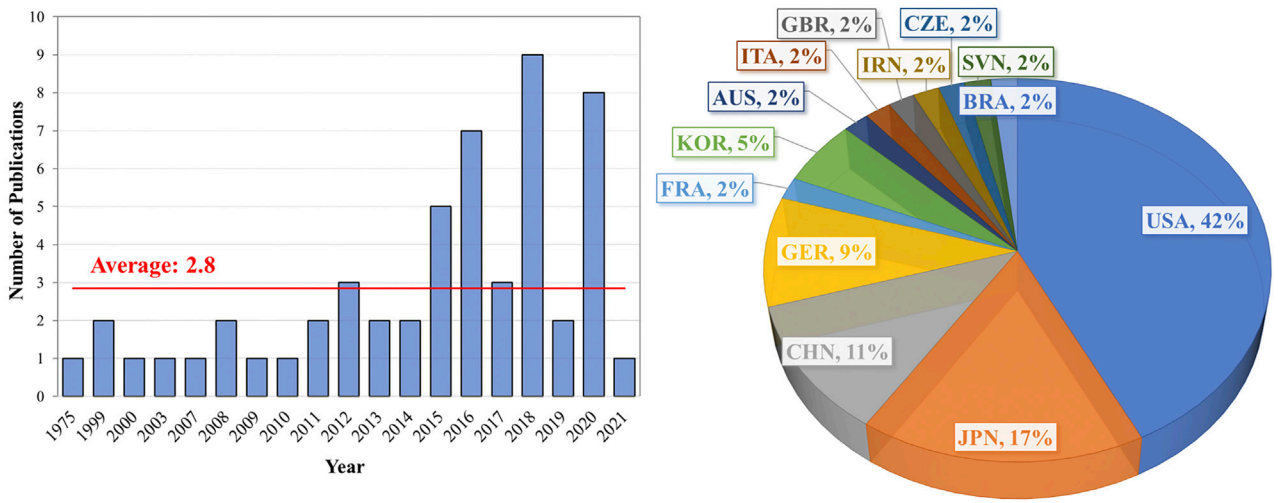

FIGURE 4 | Timeline and distribution of studies by geography investigating the antiviral effects of NTP (data for 2021 includes publications as of March 10, 2021). The number of studies utilizing NTP for antiviral applications increased over the last ten years **(A)** and were predominantly performed in the United States **(B)**. Abbreviations: AUS: Australia; BRA: Brazil; CZE: Czech Republic; CHN: China; FRA: France; GER: Germany; GBR: Great Britain; IRN: Iran; ITA: Italy; KOR: South Korea; SVN: Slovenia; USA: United States of America.

its effect on viruses has not been well investigated [73–75]. While PEF might have advantages over NTP for specific foods in liquid form such as juices or milk (where oxidation of the food should be minimized), NTP seems more effective against viruses. HHP, on the other hand, has been extensively investigated for both inactivation of bacteria and virus [65, 76, 77] and is an accepted technology in the food industry around the world [78]. While HHP offers homogeneous treatment, its use is limited due to the requirement for sophisticated equipment and its impact on food structure [78]. Furthermore, HHP is limited in its throughput as a batch process, while NTP could be implemented in a continuous treatment process.

Ionizing radiation has the capability to inactivate microorganisms and is being used for food decontamination. However, its development and commercialization have suffered because of unfavorable public opinion [79]. Ionizing radiations, such as x-rays, gamma rays, or electron beams, can deliver energy as they pass through a food product. Absorption of the energy leads to the generation of free radicals, which upon reaction with pathogens, assist decontamination. While NTP technology also intrinsically produces radicals and ions, the associated energies of the energetic species are much smaller. This reduces the penetration depth of plasma-produced species significantly, and the majority of reactions of plasma-produced species are limited to the (near) surface of objects.

In addition to physical decontamination processes, many chemical intervention methods are used [80]. Due to their similarity, fresh produce washing and water treatment share many technologies. Examples of chemicals used for the purpose of decontamination include chlorine, chlorine dioxide, ozone, and hydrogen peroxide [81, 82]. Ozonation, a plasma-based technology, can be a highly effective decontamination approach for water, surfaces, and food, particular in the gas phase. However, its use leads to off-target effects in food decontamination [25, 82, 83].

While NTP-induced decontamination has similarities to chemical decontamination approaches, it can be considered a physical decontamination technology since it only requires air and electricity. Its key advantage is that the RONS are produced *in situ* and no external supply of chemicals is needed. Nonetheless, similarities between NTP and ozonation are obvious. The more intense interaction of NTP with the substrate being treated relative to ozonation leads to a broader range of species that have been shown to enhance virucidal efficacy.

NTP VIRUCIDAL ACTION

Although virucidal activity of NTP has been thoroughly established, the underlying pathway leading to virus inactivation is not clear because of the inherent complexity of NTP. While NTP is also an effective source of UV radiation and electric fields, there is growing consensus that RONS are the key enablers of atmospheric pressure NTP virucidal activity, as in the case of plasma-based bacterial inactivation [84–87]. Plasma-produced RONS, including O_3, O_2 (a), O, OH, HO_2/O_2^-, NO, NO_2^-, ONOOH/$ONOO^-$, H_2O_2, HNO_2, and N_2O_5, are proposed as key agents for pathogen inactivation [60, 85–93]. A schematic of these key species with reaction pathways in a gas phase plasma impinging on a liquid surface is shown in **Figure 5**. Different plasma sources are used by different researchers to investigate the inactivation of different viruses. Since not all plasma sources have

TABLE 1 | Compilation of studies investigating antiviral effects of NTP. These studies used either infectious human viruses or surrogate viruses to evaluate the antiviral effect of NTP.

Author	Year	Country	Virus/Bacteriophage (Phage)	References
Burleson et al.	1975	United States	VSV, EMC, GDVII Virus	[240]
Vickery et al.	1999	AUS	DHBV	[241]
Kelly-Wintenberg et al.	1999	United States	Bacteriophage Phi X174	[242]
Kelly-Wintenberg et al.	2000	United States	Bacteriophage Phi X174	[243]
Shin et al.	2003	United States	NV, PV1, Coliphage MS2	[244]
Roth et al.	2007	United States	Bacteriophage Phi X174	[245]
Venezia et al.	2008	United States	Λ and Lytic Bacteriophage, HSV-2, AdV, PV, PIV	[246]
Yasuda et al.	2008	JPN	λ Bacteriophage	[247]
Terrier et al.	2009	FRA	hPIV-3, RSV, H5N2	[198]
Yasuda et al.	2010	JPN	λ Bacteriophage	[173]
Kalghatgi et al.	2011	United States	Lentivirus	[248]
Zimmerman et al.	2011	GER	AdV	[96]
Brun et al.	2012	ITA	HSV-1	[249]
Mizuno et al.	2012	JPN	λ Bacteriophage, M13 Bacteriophage	[74]
Shi et al.	2012	CHN	HBV	[250]
Alshraiedeh et al.	2013	GBR	MS2 Bacteriophage	[122]
Sakudo et al.	2013	JPN	Influenza A Virus, Influenza B Virus	[179]
Alekseev et al.	2014	United States	HSV-1	[197]
Isbary et al.	2014	GER	Varicella-zoster virus	[102]
Wu et al.	2015	CHN	MS2 Bacteriophage	[127]
Bae et al.	2015	KOR	MNV-1, HAV	[103]
Aboubakr et al.	2015	United States	FCV	[121]
Ahlfeld et al.	2015	GER	NoV	[200]
Takamatsu et al.	2015	JPN	CV, FCV	[125]
Wang et al.	2016	CHN	NDV, AIV	[126]
Min et al.	2016	United States	TV	[251]
Sakudo et al.	2016	JPN	AdV	[179]
Aboubakr et al.	2016	United States	FCV	[94]
Ryan et al.	2016	United States	HPV-16	[124]
Volotskova et al.	2016	United States	HIV-1	[221]
Amiran et al.	2016	IRN	HIV	[220]
Sakudo et al.	2017	JPN	RSV	[252]
Lacombe et al.	2017	United States	TV, MNV-1	[104]
Braga et al.	2017	BRA	HPV	[253]
Park et al.	2018	KOR	MNV-1, HAV	[254]
Nayak et al.	2018	United States	FCV	[101]
Štěpánová et al.	2018	CZE	CMV, ZYMV, WMV	[255]
Hanbal et al.	2018	JPN	TMV	[256]
Aboubakr et al.	2018	United States	FCV	[174]
Guo et al.	2018	CHN	MS2, Phi 174 and T4 Bacteriophages	[99]
Bunz et al.	2018	GER	HAdV	[257]
Su et al.	2018	CHN	NDV	[163]
Yamashiro et al.	2018	JPN	FCV	[162]
Filipić et al.	2019	SVN	PVY	[123]
Xia et al.	2019	United States	MS2 Bacteriophage	[206]
Aboubakr et al.	2020	United States	HuNoV, FCV	[180]
Chen et al.	2020	United States	SARS-CoV-2	[199]
Guo et al.	2020	CHN	SARS-CoV-2	[92]
Hongzhuan et al.	2020	CHN	NDV	[213]
Moldgy et al.	2020	United States	FCV	[95]
Moldgy et al.	2020	United States	FCV	[67]
Nayak et al.	2020	United States	PRRSv	[115]
Bunz et al.	2020	GER	HSV-1	[258]
Roh et al.	2020	KOR	TV	[259]
Xia et al.	2020	United States	PRRSv	[208]
Attri et al.	2021	JPN	SARS-CoV-2	[172]
Mohamed et al.	2021	United States	HIV-1	[232]

been characterized in detail and different viruses might respond differently to NTP treatment, the reported data are difficult to compare quantitatively. We provide a summary of these results that have been obtained mainly in the last decade, draw general conclusions when possible, and outline some remaining important research questions.

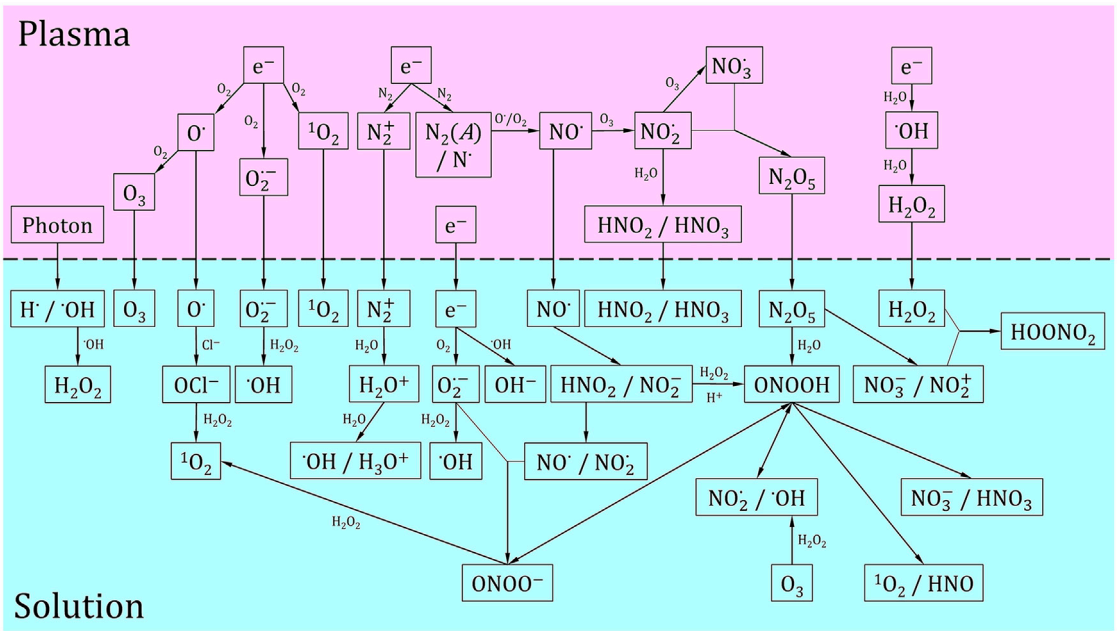

FIGURE 5 | Schematic of key plasma-produced species relevant to virus inactivation. Reaction pathways are also provided both in the gas phase and liquid phase. In the liquid phase, we also show the production of radicals from long-lived plasma produced chemistry. The horizontal dashed line represents the plasma-liquid interface. This set of reactions is a compilation of the reactions that are believed to be dominant for virus inactivation and is adapted from [59, 94, 184, 238, 239].

Plasma Sources

Plasmas can be generated with different electrode geometries, plasma power, excitation voltages, dominant reactive species, gas temperatures, feed gases, and gas residence times, all of which alter the plasma impact on virus. In addition to the changes in plasma properties, the target virus, and target substrate (surfaces, solutions, or tissues) could be of key importance for virus inactivation. A schematic of the most common plasma sources used for virus inactivation, including different treatment modalities, is shown in **Figure 6**. The majority of the reported studies have been performed by three types of plasma sources: plasma jets, dielectric barrier discharges (DBDs), and gliding arcs [94–96]. Plasma jets, one of the most commonly used plasma sources in decontamination studies, are typically generated in a capillary and the plasma and/or reactive species are convectively transported to the substrate being treated [97]. Plasma jets are often operated in a noble gas (Ar or He) with different molecular admixtures (e.g., O_2, H_2O and N_2) and are point sources that facilitate topical treatment. Nonetheless, plasma jets have high virucidal activity, most likely due to the efficient production of short-lived reactive species such as $O_2(a)$ and their longer lifetime in a noble gas compared to a humid air environment. However, comparison of results from different research groups becomes rather complex because they often use in-house built plasma jets of different designs. While the majority of plasma jets have the same operating principles, differences in RONS production are to be expected.

Different types of DBDs—a plasma discharge generated between two metal electrodes covered by a dielectric material [98]—have been investigated for decontamination applications. The key advantage of DBDs is that they enable the production of near room temperature plasma in air through the generation of self-limiting micro-discharges. DBDs are generated by time varying voltage excitation approaches with varying geometries. Examples include nanosecond-pulsed direct DBDs (**Figure 6A**) [67, 95], surface DBDs (**Figure 6H**) [67, 96, 99], and a 2D array of integrated coaxial microhollow DBD (**Figure 6G**) [95, 100, 101].

Plasma sources less commonly used for virus inactivation include microwave (MW) plasma [102] and gliding arc discharge (**Figure 6F**) [95, 103, 104]. A key disadvantage of MW and gliding arc discharges is their elevated gas temperature, typically in excess of 1000 K [105–108], although near room temperature MW discharges similar to plasma jets have been developed for biomedical applications [109–111]. The high gas temperatures in MW and gliding arc discharges operating in air favor the production of NO, while for low gas temperatures, the production of O_3 and a broader range of RONS is reported [95]. At similar plasma power, the gliding arc discharge was found to be less effective against FCV as compared to DBDs, suggesting that very high concentrations of NO, the dominant species produced in gliding arcs operating in air are needed to inactivate virus [95]. As an example, the inactivation curves of these different plasma sources and configuration against FCV treated on surfaces and in solution are shown in (**Figure 7A**). Although different plasma sources offer uniquely different inactivation pathways, direct comparisons of different sources for identical treatment conditions suggest that DBD-based devices show significant promise for decontamination applications because of their

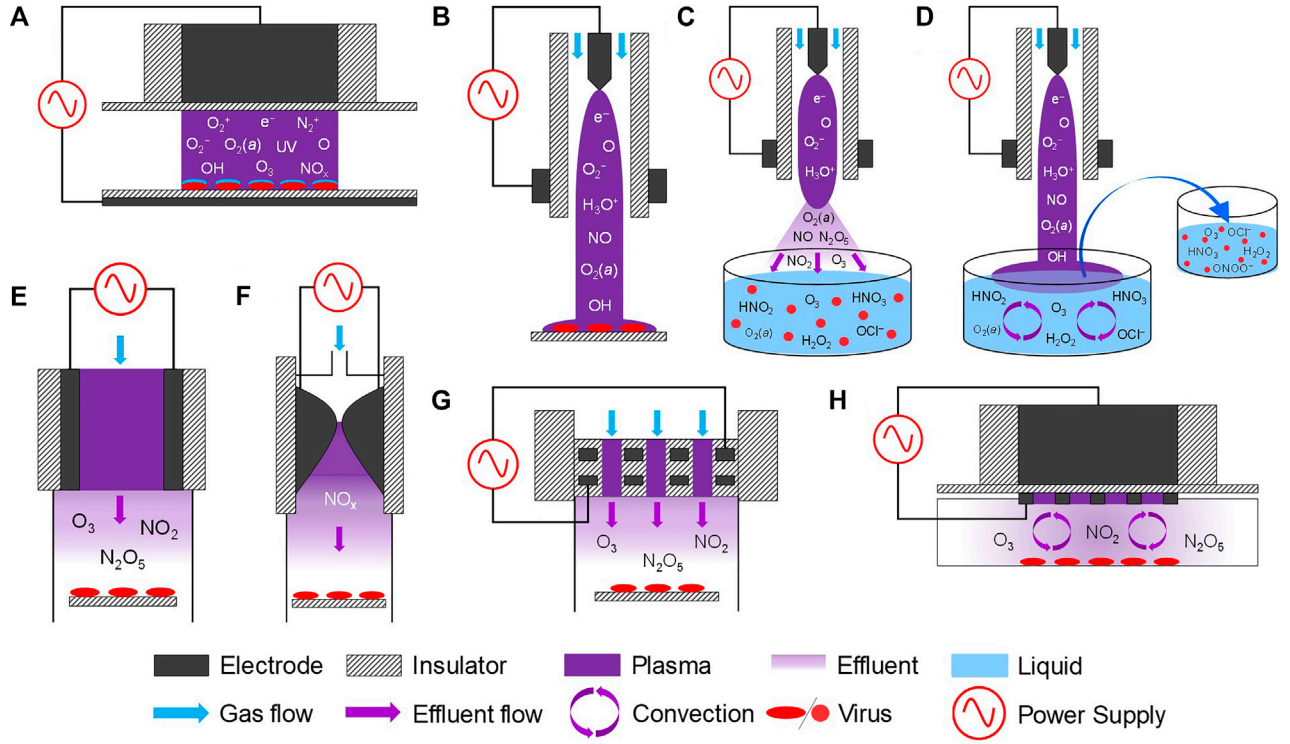

FIGURE 6 | Schematic of different plasma sources used for virus inactivation including different treatment modalities: **(A)** DBD for direct treatment, **(B)** plasma jet in contact with a substrate, **(C)** plasma jet (remote treatment), **(D)** indirect treatment (PAL/PAM), **(E)** volumetric DBD (remote treatment), **(F)** gliding arc (remote treatment), **(G)** two-dimensional array of integrated coaxial microhollow DBD (remote treatment), and **(H)** surface DBD (remote treatment). Substrate treated by each of these plasma sources could either be a surface or a liquid volume. The reactive species provided are the dominant species produced in dry air or O_2-containing plasmas. Additional species like HNO_2 and H_2O_2 can be formed for dry substrates when humidity is added to the feed gas.

high virucidal effects at ambient operational temperatures and their ability to be scaled up for large volume or area treatments (**Figure 7A**).

Direct Versus Indirect Treatment

Depending on the plasma source configuration and the proximity of the virus samples from the discharge, three distinct NTP treatment modalities can be distinguished: direct, remote, and indirect treatments (**Figures 6A,D,E**). During direct treatment, the electrical current through the discharge flows through the virus samples, which acts as one of the electrodes. Since the virus is in direct contact with plasma, the exposure of virus to short-lived plasma-produced species, including electrons, ions, radicals, and UV, is significantly higher as compared to the other treatment modalities. During direct treatments, the virus will also be subjected to high electric fields at the plasma-substrate interface [112]. For remote treatments, the plasma is generated at a remote location relative to the sample and the plasma effluent is convectively transported to the virus samples (**Figures 6C,E–H**). The plasma effluent contains reactive species with a lifetime longer than the characteristic convective transport time scales determined by the gas velocity, typically leading to gas residence times on the order of milliseconds to seconds. This gas residence time is larger than the lifetime of many radical and ionic species, which are significantly depleted in the remote treatment modality. While the dominant species in the plasma effluent will often be significantly less reactive than in the plasma, remote treatment modalities have been shown to be highly effective for virus inactivation [95, 101]. Finally, the indirect treatment modality refers to the treatment of virus samples with liquid pre-treated with plasma, more commonly referred to as plasma-activated medium or liquid (PAM or PAL) (**Figure 6D**). While PAM/PAL has been extensively studied in the context of bacterial inactivation and for cancer treatment [113, 114] and less so for virus decontamination, similarities between virus and bacteria inactivation have been found, as expected [94].

In general, the direct treatment modality is more effective against viruses compared to remote treatment. In particular, it was found that remote DBD treatments were not effective for dry virus, while direct treatment could inactivate virus on both dry and humid substrates [67, 101]. Although complete inactivation (>4 $\log_{10}$ reductions) was achieved for both treatment modalities, the inactivation could be reduced from a minute to a second time scale with direct treatment [95] (**Figure 7A**). When aerosolized virus was sent through the plasma, the virus inactivation timescale was further reduced to 10 ms [115]. While the direct treatment modality is more effective, it does not always entail larger energy efficiency for surface decontamination expressed as energy per unit area [67]. In first order approximation, this unanticipated result is due to the potential of a remote plasma

source to treat surfaces that are much larger than its cross-sectional area.

Humidity and Transport Limitations

Plasma-induced inactivation of virus in solution is dependent on the effective transfer of RONS produced in the gas-phase plasma to the liquid. Short-lived species usually have a limited penetration depth (determined by their lifetimes) and will react near the plasma-liquid interface, making the reactivity transfer extremely transport limited. For example, OH radicals have penetration depths up to a few μm in water [116–118]. The solvation of neutral species into liquid water depends on its Henry's law solubility constant. H_2O_2 with a large solubility constant can easily be transferred from the gas to the liquid phase while O_3 and NO_2 only solvate minimally into the liquid due to almost 7 orders of magnitude lower solubility constants [119]. However, enhanced mass transfer of O_3 into bulk liquid by vortexing the sample has been shown to induce efficient inactivation of pathogens [101, 120]. Highly convective transport of species can be achieved by using plasma jets, which have been used extensively for virus inactivation in solution [121–127]. Kondeti *et al.* reported on the decomposition of crystal violet by a plasma jet and found a correlation between decomposition efficacy and liquid phase convection induced by impinging gas jets onto the liquid [128]. Virus inactivation in solution is similarly transport-limited and can be impacted by altering the transport processes, either by diffusion or convection. Note that liquid agitated by a jet airflow will lead to convection of the virus particles in the solution, which might lead to significantly different efficacies compared to treatment of bacterial biofilms or cells attached to the bottom of a well, where plasma-produced species have to be transported through a liquid layer before reaching the cells. The above transport limitations can considerably impact which species are dominant for the inactivation of virus and might explain why often longer-lived species or secondary species derived from these species might dominate virus inactivation compared to plasma-produced radicals (**Figure 5**).

Virus inactivation by NTP on substrates is augmented by humidity relative to dry substrates [101]. This effect has also been previously reported for virus inactivation by O_3 where short duration exposure at >90% relative humidity significantly enhanced virus inactivation [64]. A water layer on the substrate acts as a solvent to facilitate biochemical reactions such as lipid peroxidation at larger water activities [129]. Hence, even for surface decontamination in the gas phase, in the presence of a liquid layer on the substrate, multiphase transport limitations might be important.

RONS Enabling Virus Inactivation

As described above, plasma-produced RONS, including O_3, $O_2(a)$, O, OH, HO_2/O_2^-, NO, NO_2^-, $ONOOH/ONOO^-$, H_2O_2, and N_2O_5, are proposed as key agents for pathogen inactivation [85–87, 92, 93]. A subset of these species (O_3, $O_2(a)$ and H_2O_2) has been studied in the context of virus inactivation for other disinfection technologies; we will review the key findings of these species before summarizing the studies of plasma produced RONS and our key conclusions.

Ozone, an ROS produced by commercial ozonizers, has been extensively studied for its potential for virus inactivation both in water and gas phase [80, 130]. At appropriate concentrations, a physiological solution with a dissolved O_3/O_2 mixture (ozonized saline solution) has proven to be effective against viral pathogens and has been formalized for use in hospitals in Russia and Ukraine [131–133]. Aqueous solutions of O_3 were shown to inactivate poliovirus 1 (PV1), Venezuelan Equine Encephalomyelitis virus, and Hepatitis A virus (HAV) in liquid phase [134, 135]. In the gas phase, O_3 is shown to have maximal virucidal efficacy against different viruses for a short period in high humidity (>90% RH) at peak concentrations of 20–25 ppm [136]. It was also effective against Norovirus and its animal surrogates, FCV, enterovirus 71 (EV71), and bacteriophages [137–140]. A large range of Ct-values (a value defined as the product of O_3 concentration and contact time with virus) for different viruses have been reported, indicating that the sensitivity of different viruses to O_3 can vary significantly [138, 141].

Similarly, H_2O_2 is a well-known disinfectant and has been extensively tested for virus inactivation. Many commercial H_2O_2-based decontamination systems, registered with the Environmental Protection Agency (EPA) have been tested against different viruses including FCV, adenovirus, TGEV, AIV, African swine fever virus, Hog cholera virus, Newcastle disease virus (NDV), pseudorabies virus, swine vesicular disease virus, and MS2 bacteriophage [142–145]. In all cases, complete inactivation compared to the control was achieved with exposure times ranging from 10 min to 3 h. The effectiveness of H_2O_2 decontamination was reduced significantly in the presence of blood for some of the viruses [144, 145]. H_2O_2 has been demonstrated to inactivate FCV on different surfaces such as stainless steel, plastic, glass, vinyl flooring, and ceramic tile [142], and H1N1 influenza viruses on stainless steel coupons [146]. It has also been used to decontaminate laboratory equipment with no adverse effects [144]. Aqueous solutions of H_2O_2 have been utilized to inactivate both RNA and DNA viruses without significant damage to virus immunogenicity, which might suggest possibilities for the development of an H_2O_2-based vaccine preparation platform [146, 147].

$O_2(a)$ is the key species in photodynamic therapy (PDT), which has been much used against viral infection. The scientific community has known for at least 12 years that HIV-1 can be completely destroyed with PDT. For instance, the lipid envelope of HIV-1 is cholesterol rich with an oxidizable carbonic bond (C=C), which can be oxidized using $O_2(a)$ [148]. Several studies have reported the use of PDT for inactivation of HIV-1 using different photosensitizers such as methylene blue, rose Bengal, hypocrellin, and hypericin [149, 150] as well as for HPV and HSV [151, 152]. A list of virus-mediated infectious diseases that have been treated with PDT in clinical settings is previously summarized [153]. Due to its advancement in decontamination of blood components, PDT has also been investigated for blood banking applications [154–156]. $O_2(a)$ has been used to inactivate HSV-1 and Suid herpesvirus type 1 (SHV-1) and was shown to inactivate these viruses in the presence of human plasma [157]. Numerous studies also report inactivation of MS2 bacteriophage in aqueous

suspension by $O_2(a)$ [158–160], which was also confirmed by using histidine as a quencher of $O_2(a)$ [161].

Since all of these oxidants along with other reactive species are readily generated by plasmas, it is not surprising that NTP can be highly virucidal. Nonetheless, the required treatment times in plasma can be much smaller than typically used in H_2O_2 and O_3 decontamination approaches, implying that other species contribute to the inactivation. When the role of O_3 produced by NTPs was assessed, it was observed that the virus inactivation was enhanced by the presence of RNS [101]. Further studies showed that the combination of O_3 and NO_2 in the gas phase leads to the production of N_2O_5, which most likely leads to the formation of peroxynitrite ($ONOO^-$/ONOOH) in the humid water layer on the substrate being treated [92, 95]. RNS were confirmed to be the only active agent in the case of virus inactivation in bulk liquids for the same plasma source [101]. At low pH, the importance of ONOOH produced from H_2O_2 and NO_2^- in PAW has already been shown for bacterial inactivation by air plasma [86]. A detailed study to assess the key species responsible for virus inactivation by NTPs through a scavenger study was performed by Aboubakr *et al.* [94]. These studies suggest that, in addition to O_3, peroxynitrous acid (or so-called acidified nitrides at reduced pH [86]) and $O_2(a)$ are the dominant species responsible for FCV inactivation in solution in an oxygen plasma [94]. Similar scavenger studies and comparison with positive controls by Yamashiro et al. confirm the role of $ONOO^-$ and $O_2(a)$ in FCV inactivation with a different plasma source [162]. Guo et al. confirmed that the inactivation of bacteriophages (T4, Φ174, MS2) is similarly strongly mediated by $O_2(a)$ [99]. They further showed, through scavenger studies, that OH radicals, superoxide (O_2^-), and $ONOO^-$ make no significant contributions to virus inactivation, although some of these radicals might have been less abundant for the plasma conditions used. The effect of H_2O_2 is mostly deemed as secondary in the inactivation of FCV, potato virus Y (PVY), and adenovirus, while it is suggested that it might play a dominant role in the inactivation of RSV and influenza A virus [84].

While the aforementioned reactive species are important for virus inactivation in solution, the effect of short-lived reactive species such as O and OH radicals is more likely in airborne virus when the radicals can directly inactivate the virus or have to diffuse into a micrometer sized droplet that is similar to the reactive diffusion length of the radical [115]. While the effect of OH against NDV in plasma-activated solution [163] is suggested, other studies imply that OH had no role in virus inactivation [99, 121]. The demonstration that OH radicals can decompose 50% of the hydrocarbons in a droplet of 60 μm [117] suggests that a similar effect could be anticipated for virus in small droplets or virus particles present in the plasma. Although the role of plasma generated O radicals on virus inactivation has not been reported to date, several studies report plasma conditions that enable the inactivation of *Penicillium digitatum* spores [164], cancer (THP-1 leukemia) cells [165], bacteria (*E. coli*) [166], and yeast cells (*Saccharomyces cerevisiae*) [167] by O radicals. In addition, O atoms react with Cl^- in saline solution forming hypochlorite ion (OCl^-) at concentrations sufficient to inactive bacteria (*Pseudomonas aeruginosa* and *Staphylococcus aureus*) [168]. Similarly, the possible role of HO_2/O_2^-, although well established as bioactive molecules [169, 170], needs to be further established for virus inactivation.

Depending on the treatment mode, conditions and plasma source, the virus inactivation pathways could be through ROS, RNS, or a combination of both. The species that are ultimately responsible for the inactivation of the virus might not only depend on the dominant species produced by the plasmas but also on the environmental and treatment conditions, since transport limitations are exceedingly important for plasma-based decontamination. This might unfortunately add some system- and treatment-specific aspects to the inactivation mechanisms of virus by NTP.

Mechanisms Associated With Antiviral Effect of Plasma

The biological effects of plasma produced RONS on the ability of the virus to bind with host receptors, enter into host cells, and replicate its genome have only partly been quantified to date. Plasma has many different species and hence a variety of mechanisms are to be expected. One of the earlier studies showed that plasma significantly reduced the infectivity as well as the replication ability of human adenovirus [96]. Recent work has also shown that plasma can degrade purified SARS-CoV-2 RNA, as well as modify outer components of the virus necessary for attachment such as the spike protein [92, 171, 172]. In addition, several other investigators reported that plasma leads to significant protein oxidation of the virus coat or capsid. Yasuda et al. [173], reported that the inactivation of bacteriophage lambda by NTP was mainly due to oxidation of the coat protein; the plasma impact on the DNA did not significantly contribute to bacteriophage inactivation.

Similarly, Aboubakr et al. showed that, for short treatment times, seemingly intact viruses were still present, as observed by TEM [94, 174]. A proteomics study of the virus showed significant oxidation of the virus capsid and specific amino acids responsible for attachment and entry of the virus into the host cell. Singlet oxygen, a dominant species in the NTP used, was independently reported to inactivate viruses by damaging nucleic acid and the viral envelope [175]. The inactivation of bacteriophage f2 by ozone treatment was similarly attributed to the breakdown of viral coat proteins, which hindered the adsorption of the phage to the host cells [176]. However, other studies have shown that the impact of ozone is mainly on virus genome [177]. Even when the ROS are known, the mechanism can depend significantly on the type of virus investigated or the treatment condition used, as was the case for UV described above.

Not all studies suggest that plasma impacts the capsid or viral coat. Plasma has been shown to impact both the virus surface proteins and RNA genes of bacteriophage MS2 [178]. Sakudo et al. [179] report that a nitrogen plasma inactivated adenovirus by damaging its genomic DNA with limited impact on the capsid

protein. The results show that the mechanisms might be both virus- and plasma source-specific. A detailed comparison of the plasma impact on different viruses for the same plasma conditions might shed further light on the mechanisms.

Plasma Efficacy on Different Virus and Virus Surrogate Models

The evaluation of the efficacy of plasma-induced inactivation of pathogenic human viruses can entail significant health hazards, mandating the use of specialized laboratories such as a biosafety level 3 (BSL-3) facility. Such resources are expensive, require specialized training, and do not always justify extensive testing with these viruses. As such, surrogate animal viruses compatible with BSL-1 and BSL-2 laboratories have been favored for initial testing and plasma technology optimization [92, 101, 104, 172, 180, 181].

Animal viruses are also considered good models for airborne human viruses [182, 183]. However, due to the increased risk for testing airborne virus compared to substrates or solutions spiked with virus, bacteriophages are often used as surrogates for airborne pathogenic viruses. They are not only easier to handle but can also be produced in large quantities and quantified by plaque-based infectivity assays [184–186].

While care should be taken in translating established surrogates from one disinfection technology to the other or from one plasma source to another, the reported results on a variety of viruses, further supported by our yet unpublished results, suggest that plasma can be effective against a large range of investigated pathogens and its decontamination efficacy is, in first approximation, largely independent of the virus being treated [180]. While further research in this area is needed to assess whether the effectiveness of NTP against different virus can be impacted by plasma conditions, the complex mixture of reactive species produced by NTP might indeed overcome some of the virus-specific differences observed with other non-thermal technologies, such as O_3 or UV, which might be favored because of specific chemical compositions of the RNA, DNA, or proteins in the virus capsid and coating.

APPLICATION OF NTP FOR VIRUS INACTIVATION

Pathogenic viruses can be spread in liquids, by contact with contaminated surfaces, and through airborne routes of dissemination. Each avenue of transmission poses unique challenges with respect to disinfection by NTP.

Decontamination of Liquids and Solutions

The interaction of NTP with liquids produces reactive species in the liquid phase which are critical for many chemical and biological applications. Liquids in contact with NTP are rich sources of OH radicals and are in fact considered a form of advanced oxidation technology enabling the breakdown of organic and inorganic compounds in water [187]. More recently, NTP containing air interacting with water have been studied for its exceptional bactericidal effects that can last for several minutes to several days after water is treated by plasma (PAW) [188, 189]. Many studies have shown that the bactericidal effect of plasma treated solutions requires an acidic environment (typically, pH values of 3–4) [189, 190]. These conditions are attributed to reactive nitrogen species (RNS), particularly acidified nitrites, and peroxynitrite chemistry as highlighted above. In some cases, the bactericidal effect of PAW is ascribed to ROS such as O_3 and specifically O_2^- related chemistry [120, 191]. Plasma treatment of solutions is also dependent on the composition of the solution. Treatment of virus suspensions in solutions with different compositions is shown to impact virus inactivation, particularly in the presence of pH buffers (impacting peroxynitrite chemistry), hydrocarbons (scavenging of oxidizing plasma-produced species) and saline (Cl^- is a scavenger of OH and can react with plasma-produced O forming OCl^-) [168]. PAM for use of cancer treatments is a nice example of how plasma generates long-lived hydrocarbon radicals that have biological impact.

The decontamination of liquids can be highly effective against bacteria [192]; there is no doubt this can be extended to its use for virus decontamination [94, 99]. Nonetheless, the efficacy of the decontamination will diminish with increasing concentrations of organic compounds. Plasma might be most effective in conditions where O_3 and UV are also effective.

Decontamination of Surfaces

Both low pressure and atmospheric pressure NTP have been well established over the past 3 decades as excellent tools for decontamination of heat sensitive surfaces [109, 193]. This work was preceded by plasma-assisted decontamination devices, which used disinfectants such as H_2O_2 injected in the plasma [194]. Nonetheless, all these developments focused on bacteria and were, more recently, extended to wound healing and inactivation of biofilms [195, 196]. Most of these studies were performed in the context of decontamination of medical devices and other heat sensitive substrates.

Until 2015, only a handful of studies reported on the effect of NTP against viruses, including influenza viruses, adenovirus, corneal HSV-1, and MS2 bacteriophage [96, 121, 127, 197, 198]. These studies have been extended significantly; the state-of-the art shows that plasma-based decontamination of surfaces is possible using direct treatment on timescales of ~1 s [95] and remote treatments on timescales of ~1 min [101]. A more recent study demonstrated NTP can inactivate SARS-CoV-2 on various surfaces including plastic, cardboard, and metal in less than 180 s [199]. With regard to foodborne viruses, Bae et al. inactivated murine norovirus (MNV) and HAV on meat samples [103]. Ahlfeld et al. observed a significant reduction in human NoV GII-4 on plastic dry surfaces by exposure to air-based plasma generated by a DBD setup [200]. Lacombe et al. reported a significant decrease in the titer of TV and MNV on blueberries after exposure to air-based gliding arc-plasma [104]. The antibacterial efficacy of NTP against foodborne bacterial pathogens *in vitro* and on food and food packaging materials has been previously reviewed [201–203]. Nonetheless, virucidal effects of plasmas are much less studied and research on NTP treatment of foodborne viruses has only recently begun. Studies report NTP inactivation of murine NoV, hepatitis A virus, HuNoV, TV, and FCV [101, 103, 104, 121, 200]. The effect of NTP-produced

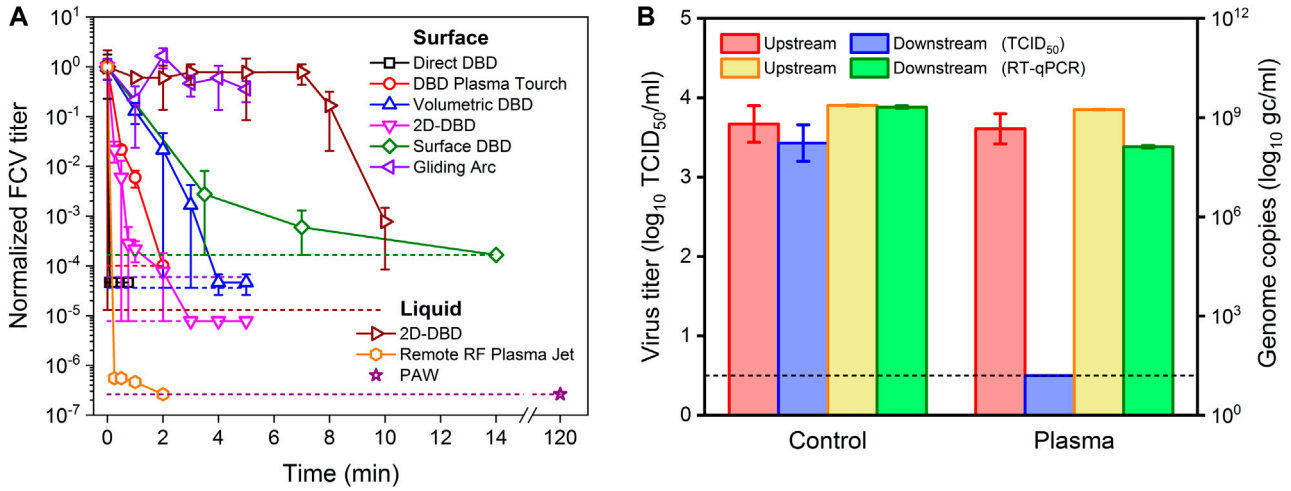

FIGURE 7 | (A) Inactivation curves for FCV treated on surfaces and in liquid solution by different plasma sources and configuration shown in **Figure 6**. The data are taken from [67, 94, 95, 101, 162] and are normalized to the reference virus titer. The short dashed colored lines represent the detection limit for each of the corresponding plasma treatment. Note that the plasma power was 14.5 W for volumetric DBD, 2D-DBD and gliding arc, while a lower power was used for direct DBD (12 W), surface DBD (0.7 W) and RF plasma jet (2.5 W). The treatment of liquids is solution and volume dependent. In this case, the solution was distilled water and the volume was kept constant at 100 μL. **(B)** Schematic representation of the inactivation of aerosolized PRRS virus by a volumetric DBD treatment in wind tunnel test conditions at sampling time of 5 min and discharge power of 39.6 W. The graph compares the amount of infectious virus before (control) and after (plasma) treatment as obtained by the $TCID_{50}$ approach with a measure of the remaining genome obtained with the RT-qPCR method. The results show a reduction of 3.5 $\log_{10}$ (remaining infectivity is below detection limit), while the genome remains, confirming that the majority of the inactivated virus is still collected downstream of the plasma treatment [115].

oxidative species on the nutritive value, sensory quality attributes, and chemical safety of treated food has not been comprehensively investigated to date [204, 205].

Direct contact between plasma and substrate can lead to more effective inactivation of viruses compared to remote plasma treatments for which long-lived reactive oxygen and nitrogen species (RONS) in the plasma effluent enable inactivation. Nonetheless, direct plasma-substrate interactions are highly substrate dependent and are limited by substrate morphologies and composition. Hence, several researchers have focused on decontamination by remote plasmas. A recent report shows similar inactivation of norovirus and FCV on stainless steel or lettuce [180]. Inactivation of *Salmonella* heidelberg with the same plasma source on Romaine lettuce, chicken breast, and stainless steel showed significant differences in inactivation efficacies [180]. While the non-smooth structure of lettuce and chicken meat can contribute to the reduced inactivation efficiency, the authors suggested that the inactivation was impacted by the protein concentration present on the substrate, as evidenced by their experiments with different concentrations of bovine serum albumin deposited on the stainless surface. Hence, the reduction in inactivation efficacies on substrates could be enhanced by a competitive process of substrate and virus inactivation.

Mitigation of Airborne Virus Transmission

Until early 2020, only a handful of studies reported the inactivation efficacy of plasmas against airborne pathogens [115, 178, 198, 206]. With the advent of the COVID-19 pandemic, many research groups started investigating the effectiveness of NTP as a decontamination tool against virus transmission [171, 207, 208]. The use of cold oxygen plasma in a single-pass flow tunnel with a particle residence time of 0.44 s in the plasma resulted in 3.1, 2, and 2.1 $\log_{10}$ $TCID_{50}$/ml reductions in hPIV-3, RSV and influenza virus A (H5N2) titers, respectively [198]. Wu et al. achieved more than 95% inactivation of aerosolized MS2 bacteriophage in ambient air [127]. Xia et al. reported a reduction in the infectivity of MS2 bacteriophage greater than 2.3 $\log_{10}$ using a packed-bed non-thermal plasma reactor at a high air flow rate of 170 slm or a particle residence time of 0.25 s [206]. Using the same packed-bed DBD reactor embedded in a test tunnel, a maximum of 1.3 $\log_{10}$ reduction in the titer of the aerosolized PRRS virus was achieved at a high flow rate of 400 slm [208]. Nayak et al. reported complete inactivation with a 3.5 $\log_{10}$ reduction in the aerosolized PRRS virus using a DBD reactor under all investigated operating conditions [115]. **Figure 7B** shows a summary of the results in this work. The virus aerosol residence time in most of these studies was in the order of milliseconds, which is a timescale relevant for typical HVAC conditions. This reinforces the importance of direct contact of virus aerosols with the plasma and the presence of abundant short-lived reactive species.

The studies summarized above highlight plasma as a promising technology with similar advantages as electrostatic precipitation [209], but possibly superior to filters. Plasma will directly inactivate the airborne virus with efficacies in excess of 99.9%, comparable to HEPA efficacies. The small pressure-drop across the plasma systems when mounted in air handling systems compared to HEPA filters will potentially require smaller

investment of energy for air handling. In some HVAC systems, significant vibrations associated with their operation cause loss of fibers from the HEPA filters, resulting in diminished filtration efficacy. In contrast, NTP technology and virus inactivation by NTP are not affected by physical disturbances. Another advantage of NTP over HEPA filtration is that plasma inactivates infectious virus. In contrast, virus captured on HEPA filters can remain infectious for extended periods of time unless HEPA filtration is combined with UV-C or other decontamination technologies. Air treatment devices based on plasma technology are being currently used, although often in the context of odor control [210, 211]. The potential for broader implementation of NTP technology, already used in selected air handling systems, to enable reductions in virus transmission has considerable potential but requires further collaborative research and development.

UNIQUE OPPORTUNITIES FOR USING NTP AGAINST VIRAL INFECTIONS

Because application of NTP involves the delivery of reactive chemical species that can adversely affect the integrity and structures of nucleic acids, proteins, and lipids that are the building blocks for infectious viruses, early uses of NTP as an antiviral agent involved direct inactivation of viruses on inanimate surfaces. However, the same NTP-associated mechanisms that directly affect virus integrity and infectivity can also be used indirectly to reduce the risk of transmission and affect the course of virus-associated disease. Recent studies have paved the way for developing roles for NTP in vaccine preparation and delivery, treatment of virus-infected cells and tissues, and therapies that leverage the capacity of NTP to induce immunomodulation.

Roles for NTP in Vaccination

Vaccination remains the most effective antiviral strategy against many pathogenic viruses including poliovirus, HAV, and the measles virus [212]. In any vaccination strategy, vaccine preparation and delivery are both important elements in the developmental process to ensure that a vaccine is highly effective in preventing viral infection or virus-associated disease. Roles for NTP in both of these important aspects of vaccine development are under active exploration.

Use of NTP in Preparation of Vaccines

The essential component of any antiviral vaccine is the antigen, which is derived specifically from the virus. The antigen can take one of several forms, including peptides and whole proteins, inactivated virus preparations, and attenuated live viruses. Antigens to be delivered in vaccine preparations may also be encoded in nucleic acids (RNA or DNA). To date, few studies have explored the use of NTP to enhance the ability of antigens to generate an adaptive immune response.

NTP was demonstrated to inactivate whole viruses which were tested as antigens in vaccine formulations against two poultry viral infections in livestock, Newcastle disease virus and the avian influenza virus. The NTP-created vaccine formulation resulted in better B and T cell responses in chickens as compared to those vaccinated with the traditional formaldehyde inactivated virus [126, 213]. These enhanced immune responses may have been due to better preservation of viral antigen structures by NTP relative to formaldehyde-mediated inactivation. Hypothetically, greater preservation of the antigen structure would translate into a higher fidelity immune response through better recognition of viral antigens in their native conformations. Extrapolating on these studies, it may be possible to use NTP to prepare viral antigens with greater capacities to elicit virus-specific immune responses for pathogens and diseases that do not yet have a vaccine.

Use of NTP to Augment Vaccine Delivery

Vaccines are typically administered by intradermal, subcutaneous, subdermal, or intramuscular injection, as well as mucosal application and electroporation-assisted injection. The last method shares a common element—application of an electric field to alter cell membrane integrity and enable antigen delivery into cells—with generation and delivery of NTP [214]. This suggests that NTP may also be used for facilitated vaccine delivery. This was investigated in a murine model of vaccination, where NTP was used to aid in the intradermal delivery of an HIV-1 envelope-expressing DNA plasmid vaccine via direct application to the skin at the site of injection. Dermal application of NTP resulted in an increase in stimulated cytotoxic $CD8^+$ T cells as compared to DNA plasmid injected without NTP application. This strongly suggested that NTP enhanced vaccine delivery and promoted an optimal immune response against the vaccine antigen that may not have been achieved due to inefficient delivery by other methods. NTP was proposed to be a better alternative to electroporation because NTP application is non-invasive. Additionally, NTP delivers active effectors (e.g., RONS) in addition to or instead of an electric field, dependent on the device used to generate NTP. These effectors, as shown in other studies, likely stimulate beneficial changes in mechanisms that underlie immune responses (immunomodulation) to vaccine antigens, thereby increasing vaccine efficacy [126, 213–215].

Inhibition of Viral Replication in Infected Cells Using NTP

In considering the use of NTP as a therapy for viral infections, the spread of the virus and ensuing infection must be reconciled with the ability to deliver NTP to infected cells. Some virus infections result in localized clinical manifestations e.g., HSV-1 infection of the lip produces a herpetic lesion (i.e., cold sore), while a human papillomavirus (HPV) infection can take the form of a wart. The application of NTP to such localized lesions can be of therapeutic value. In addition, NTP treatment is projected to have a considerable margin of safety, as suggested by animal and human studies where no significant acute or long-term adverse effects of therapeutic NTP application to skin were noted [215, 216]. For infections by viruses that spread to multiple tissues, organs, and compartments (e.g., HIV-1 and SARS-CoV-2), it will be impractical to deliver NTP to all cells that harbor the virus because of the focal nature of NTP application.

The antiviral effect of focal NTP application to an HSV-1 infection was demonstrated in a model of HSV-1 herpes keratitis, a cause of blindness from HSV-1 replication in the cornea [217]. Alekseev et al., modeled this condition using both corneal epithelial cells and corneal explants from human donors in a study that PAL. Application of NTP-conditioned media caused a reduction in HSV-1 infection, as demonstrated by reduced HSV-1-mediated cytotoxicity in corneal epithelial cells, inhibition of viral replication, and a reduction in the number of infectious virus particles produced in corneal explants [197]. Importantly, this study demonstrated that NTP-mediated antiviral effects were accomplished in the absence of any cytotoxicity in the human corneas [197]. These results may be especially useful in guiding the development of topical NTP-based treatments to alleviate local viral infections and the associated pathogenesis.

The antiviral effects of NTP may also be useful in treating warts, which are lesions on the mucosa and skin caused by several strains of the human papillomavirus (HPV). Although warts are typically benign, infection by high-risk subtypes of HPV can result in malignant transformation. Warts can be painful, difficult to treat, and a continued source of infectious virus that can be spread by direct or indirect contact. The resolution of warts in patients after application of NTP suggests the potential of NTP to eliminate local human papillomavirus infections [218, 219]. Since NTP application was followed by lesion resolution over a period of 3–4 months, it is fair to speculate that wart clearance observed in these case studies could be attributed to the immediate antiviral effects of NTP. These patients suffered no immediate or long term side effects, reinforcing the safety of NTP demonstrated in many animal models of cancer [218, 219]. Furthermore, demonstrations of NTP-stimulated immunomodulation in animal models of cancer suggest roles for anti-HPV immune responses stimulated by NTP in establishing long-term clinical outcomes.

NTP was also shown to have antiviral effects against HIV-1-infected cells. To investigate the potential for NTP to affect the course of replication in HIV-1-infected cells, Amiran et al. applied NTP to either cell-free suspensions of HIV-1 prior to infection or to the HeLa cell-based HIV-1 reporter cell line after infecting them with HIV-1 [220]. While inhibition of viral replication was observed under both conditions, the doses of NTP that yielded antiviral effects were also cytotoxic, resulting in considerable losses in cell viability [220]. Potential mechanisms whereby NTP exhibits anti-HIV-1 effects were also explored by Volotskova et al., where monocyte-derived macrophages were exposed to NTP prior to infection. Pre-infection exposure to NTP caused a reduction in the macrophage cell surface markers, CD4 and CCR5, which are critical cell attachment receptors for HIV-1. Reductions in HIV-1 replication subsequent to NTP application were attributed to down regulation of cell surface HIV-1 receptors, which would prevent viral entry into the macrophages by decreasing virus fusion with the cell [221]. Additional assessments of pre-infection NTP application suggested that NTP also inhibited HIV-1 replication by affecting post-entry events in the virus replication cycle. While the results of these investigations do not provide a path toward a practical use for NTP to treat systemic HIV-1 infection, the antiviral effects observed for both HIV-1 (and HSV-1) demonstrate the potential of NTP to inhibit infection in cells infected with disparate viruses.

Application of NTP-Mediated Immunomodulation to Antiviral Strategies

The focal nature of NTP would seem to preclude the use of NTP to treat viral infections that are widely disseminated in the body. However, recent investigations in plasma medicine suggest an intriguing strategy for addressing systemic viral infections with NTP that overcomes this limitation. This approach relies on the intersection of two growing areas of interest: immunotherapies effective against infectious diseases [222] and NTP-induced immunomodulation in eukaryotic cells [223, 224].

In the absence of effective antiviral drugs available to control or clear a viral infection, immunotherapies are emerging as promising alternatives. They are being investigated for their usefulness as treatments for viral infections and virus-associated diseases, particularly those characterized by dysfunction of the immune system. They typically involve the isolation of cells from infected patients, exposure of the cells *ex vivo* to appropriate stimulants to achieve a specific immunological outcome, and then administration of the altered cells to the patient as an immunotherapy (similar to vaccination) [225]. Successful treatment promotes development of immune responses against the virus to control infection, diminishes the symptoms associated with infection, and (perhaps) accelerates the clearance of the virus from the body. Such treatments allow control of the infection by the patient's immune system without the need for antiviral drugs, even if virus is not fully cleared from the body.

NTP is shown to boost immune response against cancer while being well tolerated [215, 226, 227]. In these studies, the induction of immunogenic cell death (ICD), characterized by the release or display of various danger signals from tumor cells that alert innate immune cells, was a common measure of the immunomodulation attributed to NTP [215, 226, 227]. A similar immunotherapy approach for systemic viral disease involving NTP would rely on the delivery of NTP effectors to virus-infected cells *ex vivo* for the purpose of inducing specific immunological changes (immunomodulation) in those cells for subsequent administration to the patient. Furthermore, the successful use of NTP in combination in with other immunostimulatory agents *ex vivo* for enhanced therapeutic efficacy in murine cancer models suggests that similar lines of attack may be feasible in viral diseases [215, 226, 227]. The apparent role of NTP in these studies is to enhance the immunostimulatory capacity of cancer cells following NTP exposure in order to facilitate a stronger immune response *in vivo* when patients are immunized with their own NTP-exposed tumor cells.

This approach may be particularly beneficial for people living with HIV-1 (PLWH) where the infection can be suppressed by a lifelong regimen of antiretroviral drugs but is not cleared from the body [228]. The virus is instead maintained as a latent infection in reservoirs throughout the body. Latent viruses in these reservoirs remain

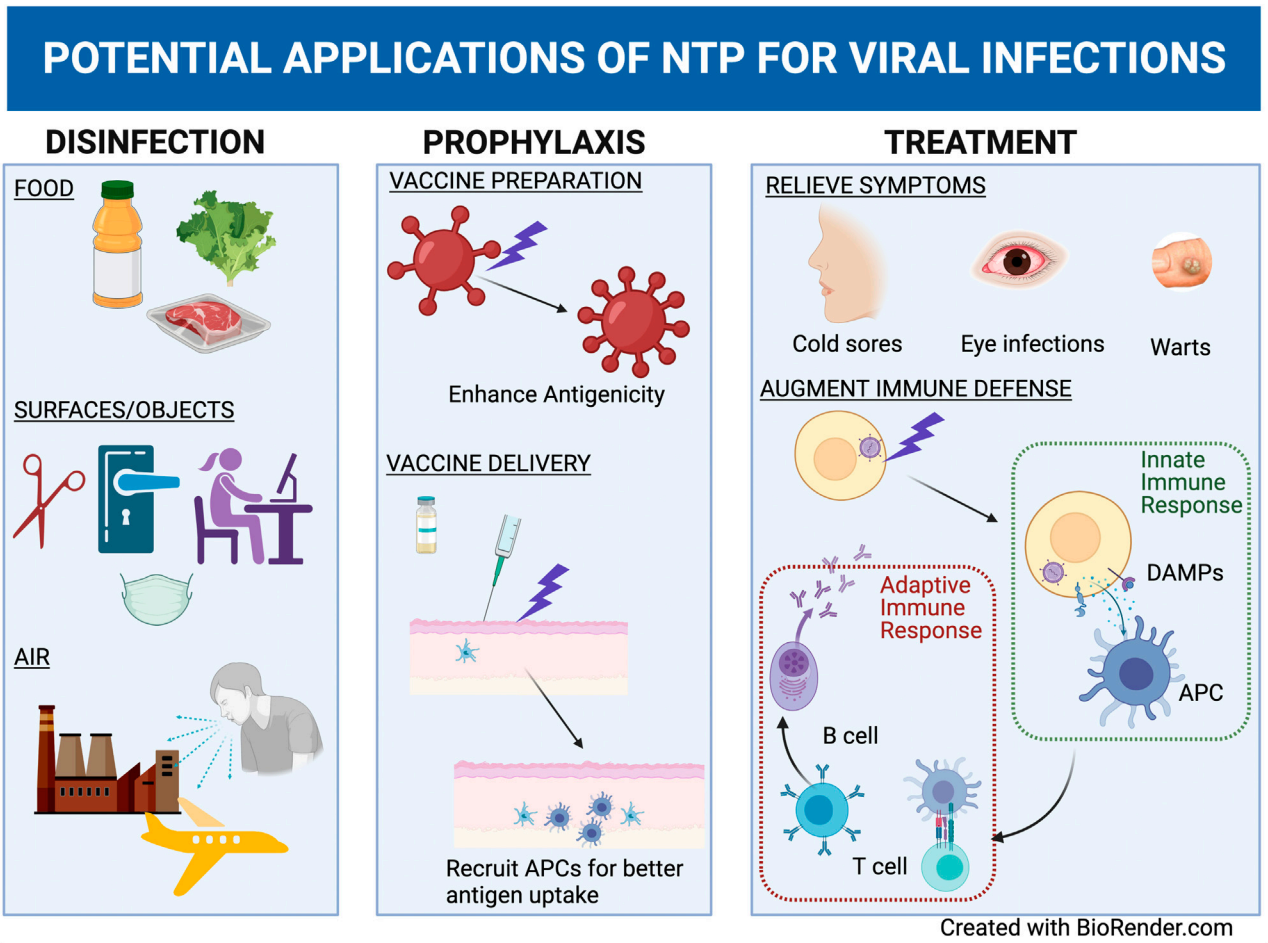

FIGURE 8 | NTP application has potential roles in mitigating virus transmission, in prophylaxis of viral diseases and in treatments of certain focal and systemic viral infections. NTP may be used to prevent virus transmission through disinfection of viruses from food, surfaces/objects, and air. To prevent disease following exposure to viruses, NTP may be used to enhance antigenicity of viruses in vaccine preparations following inactivation or can be applied to skin to promote antigen presenting cell (APC) functions that are beneficial for vaccination. Treatments for various symptoms of viral diseases such as cold sores or warts can also incorporate NTP to exert antiviral effects and to modulate symptoms. Augmentation of the immune response may be accomplished through stimulation of damage associated molecular pattern (DAMP) emission from NTP-exposed cells, which promotes APC function and a subsequent adaptive immune response.

unaffected by concentrations of antiretroviral drugs that effectively inhibit actively replicating virus. Specific deficiencies in HIV-1-specific immune responses further sustain the chronic HIV-1 infection in PLWH [229–231].

Given the capacity of NTP to stimulate immunomodulation in cells and tissues, we are investigating NTP as the basis of an immunotherapy for patients with well suppressed HIV-1 infections. Such a therapy would have parallels to other immune-based therapies, such as CAR T cell therapy and dendritic cell vaccination, in that an NTP-based immunotherapy for HIV-1 infection will elicit an effective immune response against the virus using the patient's own cells. In this envisioned therapeutic strategy, latently infected T cells will be removed from the patient and exposed *ex vivo* to NTP which will induce beneficial immunological changes in these HIV-1-infected cells. NTP-exposed cells will then be injected back into the patient as a personalized vaccination. The personalized aspect of this approach is particularly important, since each HIV-1-infected patient harbors a unique population of viral variants (quasispecies) characterized by distinct viral genomic sequences and phenotypes. This personalized approach overcomes a major limitation of traditional vaccines, which are targeted typically to a single viral genotype and would be less effective against viral quasispecies in patients that deviate from that specific genetic sequence.

An NTP-based immunotherapy will rely on effects of NTP exposure in three different phases of the therapy. During the first phase in which patient cells are exposed *ex vivo* to NTP, one effect of NTP will be to increase antigenicity in latently infected cells. Along these lines, our investigations demonstrated that NTP exposure stimulated viral gene expression in a cell line model of latent HIV-1 infection [232]. The expression of viral proteins is a necessary first step in presenting viral antigens to host immune cells and generating an adaptive immune response to HIV-1.

NTP exposure of latently infected cells will also increase cellular immunogenicity, which will be an important part of the second phase of the therapy: administration of NTP-exposed cells to the patient. A vaccine product injected for the purpose of inducing an antigen-specific immune response must stimulate local responses at the injection site, including recruitment (chemotaxis) of immune cells involved in mounting adaptive immune responses and a level of inflammation that facilitates those immune responses. We have shown that *in vitro* application of NTP to T lymphocytes stimulates the release of pro-inflammatory cytokines and chemokines [232] that will have roles in creating an immunogenic environment at the site of injection [233].

In the final phase of the therapy, the presentation of viral antigens to cells of the immune system will result in an HIV-1-specific adaptive immune response. Our investigations into the effect of NTP exposure on epitope presentation revealed that NTP application to a human T lymphocyte cell lines altered the arrays of peptides presented on cell surface MHC class I molecules [232]. Comparisons of peptides detected on Jurkat T lymphocyte cells and the latently infected J-Lat cell line showed differences in host cell peptide display attributed to cell type and NTP exposure. Furthermore, NTP exposure of J-Lat cells appeared to alter the HIV-1-specific peptides displayed on these cells [232]. The strongly suggests that NTP exposure will alter the breadth of viral peptides presented in the surfaces of HIV-1-infected cells. A more diverse peptide pool is often desirable for maximizing the $CD8^+$ T cell response, for diseases like HIV-1 infection that are highly dependent on $CD8^+$ T cells for clearance [234, 235]. Hypothetically, altering and/or broadening the range of HIV-1-specific peptides through the effects of NTP exposure of cells during the *ex vivo* phase will result in a more effective HIV-1-targeted immune response capable of controlling reemergence of infection without the use of antiretroviral drugs.

The development of an NTP-based immunotherapy against HIV-1 still poses many challenges. For example, viral escape mutations and an inability to maintain robust B and T cell responses may reduce the long-term efficacy of the approach. This would be true for any viral infection in which escape variants can emerge. Additionally, NTP-induced immunotherapy will possibly be insufficient on its own to effect control over the infection. While NTP-based immunotherapy is hypothesized to offset deficiencies in the HIV-1-specific immune response, it may have limited capacity to reverse latent infection, which will be necessary to make infected cells "visible" to immune surveillance (as these cells, which do not express HIV-1 proteins, will appear to immune surveillance as uninfected cells). As one solution, NTP immunotherapy may be combined with a latency reversal agent (LRA), which will reactivate viral replication in latently infected cells. Cells harboring latent HIV-1 infections would then become productively infected, producing viral proteins and displaying virus-derived peptides that will be recognized and targeted by immune cells [29].

The hypothesized use of NTP-based immunotherapy against viral infections combined with animal studies that have explored the application of NTP as an immunomodulatory treatment for cancer indicate an additional use for NTP: treating infections by oncogenic viruses, or viruses capable of causing cancer [236]. In treating disease caused by oncogenic viruses, the dual challenge is to effectively mitigate the spread of the virus while simultaneously clearing the body of proliferating cancerous cells (which can also contribute to the spread of the virus). Treatments for proliferative diseases that are systemic, such as Hodgkin lymphoma caused by Epstein-Barr virus infection, will need to rely solely on immunomodulation induced in neoplastic cells that are exposed to NTP *ex vivo* and then injected into the patient as a form of immunotherapy. For more localized virus-associated cancers, such as pre-cancerous and cancerous cervical lesions caused by HPV-16/18 infection, NTP may have a direct effect on the replicating virus as well as an indirect effect in the form of a more effective adaptive immune response mounted against proliferating cells that form the lesions [237]. These and various other potential applications of NTP to prevent or treat viral diseases are summarized in **Figure 8**.

CONCLUSION

Efforts focused on the development of novel NTP-based interventions for viruses and viral infections have revealed that non-thermal plasma is an effective virucidal agent. NTP reduces virus burdens on contaminated surfaces and airborne viruses for the purposes of virus inactivation. In the course of investigations in this field, different devices have been used to generate NTP and achieve effective disinfection of viral pathogens. These highlight the promise for NTP as a broad-spectrum disinfectant.

Demonstrations of NTP-mediated virus inactivation have more recently been complemented by investigations of NTP as an antiviral agent that can be applied to prevent infection, interfere with virus replication, or indirectly impact viral infection and virus-associated disease by modifying host virus-specific immune responses. While the direct effects of NTP on virus infection and replication can be viewed as a derivation of the use of NTP for surface decontamination, the use of NTP as a basis for immunotherapies against viral infections is a novel and intriguing advancement of biomedical applications for NTP.

In developing NTP for use as an antiviral agent, numerous challenges remain to be addressed. First, NTP and the active effectors delivered during its generation can vary between devices and plasma forms, necessitating studies to determine the optimal form of plasma and device for a particular application. Second, the effectiveness of virus disinfection by NTP can be diminished by a number of external factors, including environmental conditions, the amount of virus on the contaminated surface, and the materials to be disinfected. Third, in applications involving disinfection of airborne viruses, there are challenges imposed by the need to scale up NTP application to meet the needs of large structures and the need for sufficient contact time between NTP effectors and airborne viruses in high flow air handling systems. Fourth, the focal nature of NTP contrasts with the disseminated nature of some viral infections. The application of NTP to localized manifestations of viral infections relies more on the direct effects of NTP on viral replication and infection. However, the use of NTP to treat viral pathogens that are disseminated throughout the body will rely less on the direct effect of NTP application and more on indirect NTP-mediated immunomodulation to enhance systemic antiviral immune responses. The use of NTP as the basis for immunotherapy or

prophylactic vaccination against virus infections represents a challenging but high reward direction for the field of plasma medicine.

As a tool demonstrated to be effective for diverse applications, NTP provides many opportunities for developing effective strategies for preventing virus transmission, mitigating virus-associated disease, and protecting against infection through vaccination. Efforts to expand on these opportunities will require considerable collaboration between plasma scientists, virologists, and immunologists to develop NTP-based antiviral approaches for pathogens that are current global challenges as well as viral pathogens that have yet to emerge.

AUTHOR CONTRIBUTIONS

HM and GN contributed equally to this original article and share first authorship. VM, FK, and PB contributed equally and share senior authorship. NR contributed to research and figures. BW contributed to review and editing of the article. All authors approved the submitted version of the article.

ACKNOWLEDGMENTS

HM, FK, and VM acknowledge the support of the Coulter Foundation and the Department of Microbiology and Immunology and the Institute for Molecular Medicine and Infectious Disease at the Drexel University College of Medicine. PB and GN acknowledge the support by the Department of Energy, Office of Fusion Energy Science by Award DE-SC0016053 and by the National Science Foundation by Award PHY 2020695.

REFERENCES

1. Rouse BT, and Sehrawat S. Immunity and Immunopathology to Viruses: what Decides the Outcome? *Nat Rev Immunol* (2010) 10(7):514–26. doi:10.1038/nri2802
2. Nicaise V. Crop Immunity against Viruses: Outcomes and Future Challenges. *Front Plant Sci* (2014) 5:660. doi:10.3389/fpls.2014.00660
3. Bosch A, Gkogka E, Le Guyader FS, Loisy-Hamon F, Lee A, van Lieshout L, et al. Foodborne Viruses: Detection, Risk Assessment, and Control Options in Food Processing. *Int J Food Microbiol* (2018) 285:110–28. doi:10.1016/j.ijfoodmicro.2018.06.001
4. Hamilton JJ, Turner K, and Lichtenstein Cone M. COVID-19 and Public Health: Looking Back, Moving Forward, 27 (2021). p. S80–S86. doi:10.1097/phh.0000000000001299 Responding to the Pandemic: Challenges with Public Health Surveillance Systems and Development of a COVID-19 National Surveillance Case Definition to Support Case-Based Morbidity Surveillance during the Early Response *J Public Health Manag Pract* Suppl 1.
5. Mishra V, Seyedzenouzi G, Almohtadi A, Chowdhury T, Khashkhusha A, Axiaq A, et al. Health Inequalities during COVID-19 and Their Effects on Morbidity and Mortality. *Jhl* (2021) Vol. 13:19–26. doi:10.2147/jhl.s270175
6. Henderson DA. The Eradication of Smallpox - an Overview of the Past, Present, and Future. *Vaccine* (2011) 29(Suppl 4):D7–D9. doi:10.1016/j.vaccine.2011.06.080
7. Mayr A. [Historical Review of Smallpox, the Eradication of Smallpox and the Attenuated Smallpox MVA Vaccine]. *Berl Munch Tierarztl Wochenschr* (1999) 112(9):322–8.
8. Reid A. The Effects of the 1918-1919 Influenza Pandemic on Infant and Child Health in Derbyshire. *Med Hist* (2005) 49(1):29–54. doi:10.1017/s0025727300008279
9. World Health Organization (W.H.O). HIV/AIDS (2020). November 30, 2020. [cited 2021.; Available from: https://www.who.int/news-room/fact-sheets/detail/hiv-aids.
10. Zaba B, Whiteside A, and Boerma JT. Demographic and Socioeconomic Impact of AIDS. *AIDS* (2004) 18(Suppl 2):S1–S7. doi:10.1097/00002030-200406002-00001
11. Čivljak R, Markotić A, and Kuzman I. The Third Coronavirus Epidemic in the Third Millennium: What's Next? *Croat Med J* (2020) 61(1):1–4.
12. World Health Organization (W.H.O). *Coronavirus (COVID-19) Dashboard* (2021). March 14th, 2021. [cited 2021.; Available from: https://covid19.who.int/.
13. Firestone MJ, Lorentz AJ, Wang X, Como-Sabetti K, Vetter S, Smith K, et al. First Identified Cases of SARS-CoV-2 Variant B.1.1.7 in Minnesota — December 2020–January 2021. Morbidity and Mortality Weekly. *Febrary* (2021) 17:2021, 2021 ([cited 2021].
14. World Health Organization (W.H.O). Measles (2019) 2019, 2019 . [cited 2021.; Available from: https://www.who.int/news-room/fact-sheets/detail/measles.
15. Bartsch SM, Lopman BA, Ozawa S, Hall AJ, and Lee BY. Global Economic burden of Norovirus Gastroenteritis. *PLoS One* (2016) 11(4):e0151219. doi:10.1371/journal.pone.0151219
16. Luliano AD, Roguski KM, Chang HH, Muscatello DJ, Palekar R, Tempia S, et al. Estimates of Global Seasonal Influenza-Associated Respiratory Mortality: a Modelling Study. *Lancet* (2018) 391(10127):1285–300.
17. Johnson J, and Chiu W. Structures of Virus and Virus-like Particles. *Curr Opin Struct Biol* (2000) 10(2):229–35. doi:10.1016/s0959-440x(00)00073-7
18. Blanco A, Abid I, Al-Otaibi N, Pérez-Rodríguez FJ, Fuentes C, Guix S, et al. Glass Wool Concentration Optimization for the Detection of Enveloped and Non-enveloped Waterborne Viruses. *Food Environ Virol* (2019) 11(2):184–92. doi:10.1007/s12560-019-09378-0
19. Cho JG, and Dee SA. Porcine Reproductive and Respiratory Syndrome Virus. *Theriogenology* (2006) 66(3):655–62. doi:10.1016/j.theriogenology.2006.04.024
20. Jacobs SE, Lamson DM, St. George K, and Walsh TJ. Human Rhinoviruses. *Clin Microbiol Rev* (2013) 26(1):135–62. doi:10.1128/cmr.00077-12
21. Macias AE, McElhaney JE, Chaves SS, Nealon J, Nunes MC, Samson SI, et al. The Disease burden of Influenza beyond Respiratory Illness. *Vaccine* (2020) 39:A6–A14. doi:10.1016/j.vaccine.2020.09.048
22. Setti L, Passarini F, De Gennaro G, Barbieri P, Perrone MG, Borelli M, et al. Airborne Transmission Route of COVID-19: Why 2 Meters/6 Feet of Inter-personal Distance Could Not Be Enough. *Ijerph* (2020) 17(8):2932. doi:10.3390/ijerph17082932
23. Irwin KK, Renzette N, Kowalik TF, and Jensen JD. Antiviral Drug Resistance as an Adaptive Process. *Virus Evol* (2016) 2(1):vew014. doi:10.1093/ve/vew014
24. Domingo E, and Holland JJ. RNA Virus Mutations and Fitness for Survival. *Annu Rev Microbiol* (1997) 51:151–78. doi:10.1146/annurev.micro.51.1.151
25. Parrish CR, Holmes EC, Morens DM, Park E-C, Burke DS, Calisher CH, et al. Cross-species Virus Transmission and the Emergence of New Epidemic Diseases. *Mmbr* (2008) 72(3):457–70. doi:10.1128/mmbr.00004-08
26. Abdoli A, Soleimanjahi H, Tavassoti Kheiri M, Jamali A, and Jamaati A. Determining Influenza Virus Shedding at Different Time Points in Madin-darby Canine Kidney Cell Line. *Cell J* (2013) 15(2):130–5.
27. Mohammadi P, Desfarges S, Bartha I, Joos B, Zangger N, Munoz M, et al. 24 Hours in the Life of HIV-1 in a T Cell Line. *Plos Pathog* (2013) 9(1):e1003161. doi:10.1371/journal.ppat.1003161
28. Roizman B, and Sears AE. An Inquiry into the Mechanisms of Herpes Simplex Virus Latency. *Annu Rev Microbiol* (1987) 41:543–71. doi:10.1146/annurev.mi.41.100187.002551
29. Ait-Ammar A, Kula A, Darcis G, Verdikt R, De Wit S, Gautier V, et al. Current Status of Latency Reversing Agents Facing the Heterogeneity of HIV-1 Cellular and Tissue Reservoirs. *Front Microbiol* (2019) 10:3060. doi:10.3389/fmicb.2019.03060
30. Saurabh S, and Vohra C. What Should Be the Criteria for Determining Asymptomatic Status in COVID-19? *QJM* (2021) ((hcab002).

31. Farzadegan H, Polis MA, Wolinsky SM, Rinaldo Jr. CR, Sninsky JJ, Kwok S, et al. Loss of Human Immunodeficiency Virus Type 1 (HIV-I) Antibodies with Evidence of Viral Infection in Asymptomatic Homosexual Men. *Ann Intern Med* (1988) 108(6):785–90. doi:10.7326/0003-4819-108-6-785
32. Hyland P, Coulter W, Abu-Ruman I, Fulton C, O'Neill H, Coyle P, et al. Asymptomatic Shedding of HSV-1 in Patients Undergoing Oral Surgical Procedures and Attending for Noninvasive Treatment. *Oral Dis* (2007) 13(4): 414–8. doi:10.1111/j.1601-0825.2007.01316.x
33. Tang S, Mao Y, Jones RM, Tan Q, Ji JS, Li N, et al. Aerosol Transmission of SARS-CoV-2? Evidence, Prevention and Control. *Environ Int* (2020) 144: 106039. doi:10.1016/j.envint.2020.106039
34. Chan K-H, Sridhar S, Zhang RR, Chu H, Fung AY-F, Chan G, et al. Factors Affecting Stability and Infectivity of SARS-CoV-2. *J Hosp Infect* (2020) 106(2):226–31. doi:10.1016/j.jhin.2020.07.009
35. Tang JW, Bahnfleth WP, Bluyssen PM, Buonanno G, Jimenez JL, Kurnitski J, et al. Dismantling Myths on the Airborne Transmission of Severe Acute Respiratory Syndrome Coronavirus-2 (SARS-CoV-2). *J Hosp Infect* (2021) 110:89–96. doi:10.1016/j.jhin.2020.12.022
36. van Doremalen N, Bushmaker T, Morris DH, Holbrook MG, Gamble A, Williamson BN, et al. Aerosol and Surface Stability of SARS-CoV-2 as Compared with SARS-CoV-1. *N Engl J Med* (2020) 382(16):1564–7. doi:10.1056/nejmc2004973
37. Fears AC, Klimstra WB, Duprex P, Hartman A, Weaver SC, Plante KC, et al. *Comparative Dynamic Aerosol Efficiencies of Three Emergent Coronaviruses and the Unusual Persistence of SARS-CoV-2 in Aerosol Suspensions*. Cold Spring Harbor, NY: medRxiv [Preprint] (2020).
38. Alonso C, Goede DP, Morrison RB, Davies PR, Rovira A, Marthaler DG, et al. Evidence of Infectivity of Airborne Porcine Epidemic Diarrhea Virus and Detection of Airborne Viral RNA at Long Distances from Infected Herds. *Vet Res* (2014) 45:73. doi:10.1186/s13567-014-0073-z
39. Tellier R, Li Y, Cowling BJ, and Tang JW. Recognition of Aerosol Transmission of Infectious Agents: a Commentary. *BMC Infect Dis* (2019) 19(1):101. doi:10.1186/s12879-019-3707-y
40. Denman AM. Principles of Clinical Immunology. *Practitioner* (1982) 226(1374):1993–2007.
41. Lentz AK, and Feezor RJ. Principles of Immunology. *Nutr Clin Pract* (2003) 18(6):451–60. doi:10.1177/0115426503018006451
42. Mohamed H, Esposito RA, Kutzler MA, Wigdahl B, Krebs FC, and Miller V. Nonthermal Plasma as Part of a Novel Strategy for Vaccination. *Plasma Process Polym* (2020) 17:e2000051. doi:10.1002/ppap.202000051
43. Herzog RW, and Ostrov DA. A Decorated Virus Cannot Hide. *Science* (2012) 338(6108):748–9. doi:10.1126/science.1230342
44. Agol VI. Cytopathic Effects: Virus-Modulated Manifestations of Innate Immunity? *Trends Microbiol* (2012) 20(12):570–6. doi:10.1016/j.tim.2012.09.003
45. Alcami A, and Koszinowski UH. Viral Mechanisms of Immune Evasion. *Trends Microbiol* (2000) 8(9):410–8. doi:10.1016/s0966-842x(00)01830-8
46. Iwasaki M, Saito J, Zhao H, Sakamoto A, Hirota K, and Ma D. Inflammation Triggered by SARS-CoV-2 and ACE2 Augment Drives Multiple Organ Failure of Severe COVID-19: Molecular Mechanisms and Implications. *Inflammation* (2021) 44(1):13–34. doi:10.1007/s10753-020-01337-3
47. Mayer BK, Yang Y, Gerrity DW, and Abbaszadegan M. The Impact of Capsid Proteins on Virus Removal and Inactivation during Water Treatment Processes. *Microbiol Insights* (2015) 8(Suppl 2):15–28. doi:10.4137/MBI.S31441
48. Dietz L, Horve PF, Coil DA, Fretz M, Eisen JA, and Wymelenberg KVD. Novel Coronavirus (COVID-19) Pandemic: Built Environment Considerations to Reduce Transmission. *mSystems* (2019) 5(2):e00245–20.2020
49. Pan M, Lednicky JA, and Wu CY. Collection, Particle Sizing and Detection of Airborne Viruses. *J Appl Microbiol* (2019) 127(6):1596–611. doi:10.1111/jam.14278
50. Viscusi DJ, Bergman MS, Eimer BC, and Shaffer RE. Evaluation of Five Decontamination Methods for Filtering Facepiece Respirators. *Ann Occup Hyg* (2009) 53(8):815–27. doi:10.1093/annhyg/mep070
51. Nardell EA, and Nathavitharana RR. Airborne Spread of SARS-CoV-2 and a Potential Role for Air Disinfection. *JAMA* (2020) 324(2):141–2. doi:10.1001/jama.2020.7603
52. Budowsky EI, Bresler SE, Friedman EA, and Zheleznova NV. Principles of Selective Inactivation of Viral Genome. I. UV-Induced Inactivation of Influenza Virus. *Arch Virol* (1981) 68(3-4):239–47. doi:10.1007/bf01314577
53. De Clercq E. Antiviral Drugs in Current Clinical Use. *J Clin Virol* (2004) 30(2):115–33. doi:10.1016/j.jcv.2004.02.009
54. Leneva IA, Roberts N, Govorkova EA, Goloubeva OG, and Webster RG. The Neuraminidase Inhibitor GS4104 (Oseltamivir Phosphate) Is Efficacious against A/Hong Kong/156/97 (H5N1) and A/Hong Kong/1074/99 (H9N2) Influenza Viruses. *Antiviral Res* (2000) 48(2):101–15. doi:10.1016/s0166-3542(00)00123-6
55. Zepp F. Principles of Vaccine Design-Lessons from Nature. *Vaccine* (2010) 28(Suppl 3):C14–C24. doi:10.1016/j.vaccine.2010.07.020
56. Mocarski ES, Jr., Abenes GB, Manning WC, Sambucetti LC, and Cherrington JM. Molecular Genetic Analysis of Cytomegalovirus Gene Regulation in Growth, Persistence and Latency. *Curr Top Microbiol Immunol* (1990) 154: 47–74. doi:10.1007/978-3-642-74980-3_3
57. Oldstone MBA. Immunotherapy for Virus Infection. *Curr Top Microbiol Immunol* (1987) 134:211–29. doi:10.1007/978-3-642-71726-0_9
58. Hadden JW. Immunotherapy of Human Immunodeficiency Virus Infection. *Trends Pharmacol Sci* (1991) 12(3):107–11. doi:10.1016/0165-6147(91)90517-v
59. Gaens WV, and Bogaerts A. Kinetic Modelling for an Atmospheric Pressure Argon Plasma Jet in Humid Air. *J Phys D: Appl Phys* (2013) 46(27):275201. doi:10.1088/0022-3727/46/27/275201
60. Reuter S, von Woedtke T, and Weltmann K-D. The kINPen-A Review on Physics and Chemistry of the Atmospheric Pressure Plasma Jet and its Applications. *J Phys D: Appl Phys* (2018) 51(23):233001. doi:10.1088/1361-6463/aab3ad
61. Hijnen WAM, Beerendonk EF, and Medema GJ. Inactivation Credit of UV Radiation for Viruses, Bacteria and Protozoan (Oo)cysts in Water: A Review. *Water Res* (2006) 40(1):3–22. doi:10.1016/j.watres.2005.10.030
62. de Roda Husman AM, Bijkerk P, Lodder W, van den Berg H, Pribil W, Cabaj A, et al. Calicivirus Inactivation by Nonionizing (253.7-Nanometer-Wavelength [UV]) and Ionizing (Gamma) Radiation. *Aem* (2004) 70(9): 5089–93. doi:10.1128/aem.70.9.5089-5093.2004
63. Park GW, Linden KG, and Sobsey MD. Inactivation of Murine Norovirus, Feline Calicivirus and Echovirus 12 as Surrogates for Human Norovirus (NoV) and Coliphage (F+) MS2 by Ultraviolet Light (254 Nm) and the Effect of Cell Association on UV Inactivation. *Lett Appl Microbiol* (2011) 52(2): 162–7. doi:10.1111/j.1472-765x.2010.02982.x
64. Thurston-Enriquez JA, Haas CN, Jacangelo J, Riley K, and Gerba CP. Inactivation of Feline Calicivirus and Adenovirus Type 40 by UV Radiation. *Aem* (2003) 69(1):577–82. doi:10.1128/aem.69.1.577-582.2003
65. Barbosa-Cánovas GV, Tapia MS, and Cano MP. *Novel Food Processing Technologies*. 1 ed.. Boca Raton, FL: CRC Press (2004).
66. Guerrero-Beltrán JA, and Barbosa-Cánovas GV. Advantages and Limitations on Processing Foods by UV Light. *Food Sci Tech Int* (2004) 10(3):137–47.
67. Moldgy A, Aboubakr H, Nayak G, Goyal S, and Bruggeman P. Comparative Evaluation of the Virucidal Effect of Remote and Direct Cold Air Plasmas with UV-C. *Plasma Process Polym* (2020) 17(4):1900234. doi:10.1002/ppap.201900234
68. Ross AIV, Griffiths MW, Mittal GS, and Deeth HC. Combining nonthermal technologies to control foodborne microorganisms. International journal of food microbiology. 2003 Dec 31;89(2-3): 125–38. doi:10.1016/S0168-1605(03)00161-2
69. Deeth HC, Datta N, Ross AI, and Dam XT. *Advances in Thermal and Non-Thermal Food Preservation*. Ames, Iowa, USA: Blackwell Publishing (2007). p. 241–69. Pulsed Electric Field Technology: Effect on Milk and Fruit Juices.
70. Grahl T, and Märkl H. Killing of Microorganisms by Pulsed Electric fields. *Appl Microbiol Biotechnol* (1996) 45:148–57. doi:10.1007/s002530050663
71. Sale AJH, and Hamilton WA. Effects of High Electric fields on Micro-organisms. *Biochim Biophys Acta (Bba) - Biomembranes* (1968) 163(1):37–43. doi:10.1016/0005-2736(68)90030-8
72. Tewari G, and Juneja VK. *Advances in thermal and Non-thermal Food Preservation*. Ames, IA: Blackwell Publishing (2007). p. 1–281.
73. Khadre MA, and Yousef AE. Susceptibility of Human Rotavirus to Ozone, High Pressure, and Pulsed Electric Field. *J Food Prot* (2002) 65(9):1441–6. doi:10.4315/0362-028x-65.9.1441
74. Mizuno A, Inoue T, Yamaguchi S, Sakamoto KI, Saeki T, Matsumoto Y, et al. *Conference Record of the 1990*. IEEE Industry Applications Society Annual Meeting (1990). p. 713–9. Inactivation of Viruses Using Pulsed High Electric Field.
75. Todd ECD. *Encyclopedia of Food Safety*. Elsevier (2014). p. 221–42. doi:10.1016/b978-0-12-378612-8.00071-8 Foodborne Diseases: Overview of Biological Hazards and Foodborne Diseases.

76. Barbosa Cánovas GV, Pothakamury UR, Palou E, and Swason BG. *Nonthermal Preservation of Foods*. New York: Marcel Dekker (1997). p. 276.
77. Govaris A, and Pexara A. Inactivation of Foodborne Viruses by High-Pressure Processing (HPP). *Foods* (2021) 10(2):215. doi:10.3390/foods10020215
78. Pereira RN, and Vicente AA. Environmental Impact of Novel thermal and Non-thermal Technologies in Food Processing. *Food Res Int* (2010) 43(7): 1936–43. doi:10.1016/j.foodres.2009.09.013
79. Resurreccion AVA, Galvez FCF, Fletcher SM, and Misra SK. Consumer Attitudes toward Irradiated Food: Results of a New Study. *J Food Prot* (1995) 58(2):193–6. doi:10.4315/0362-028x-58.2.193
80. Hirneisen KA, Black EP, Cascarino JL, Fino VR, Hoover DG, and Kniel KE. Viral Inactivation in Foods: A Review of Traditional and Novel Food-Processing Technologies. *Compr Rev Food Sci Food Saf* (2010) 9(1):3–20. doi:10.1111/j.1541-4337.2009.00092.x
81. World Health Organization (W.H.O). *Surface Decontamination of Fruits and Vegetables Eaten Raw : A Review* (1998). [cited 2021.; Available from: https://apps.who.int/iris/handle/10665/64435.
82. Ramos B, Miller FA, Brandão TRS, Teixeira P, and Silva CLM. Fresh Fruits and Vegetables-An Overview on Applied Methodologies to Improve its Quality and Safety. *Innovative Food Sci Emerging Tech* (2013) 20:1–15. doi:10.1016/j.ifset.2013.07.002
83. Ölmez H, and Kretzschmar U. Potential Alternative Disinfection Methods for Organic Fresh-Cut Industry for Minimizing Water Consumption and Environmental Impact. *LWT - Food Sci Tech* (2009) 42(3):686–93. doi:10.1016/j.lwt.2008.08.001
84. Filipić A, Gutierrez-Aguirre I, Primc G, Mozetič M, and Dobnik D. Cold Plasma, a new hope in the Field of Virus Inactivation. *Trends Biotechnol* (2020) 38(11):1278–91. doi:10.1016/j.tibtech.2020.04.003
85. Graves DB. The Emerging Role of Reactive Oxygen and Nitrogen Species in Redox Biology and Some Implications for Plasma Applications to Medicine and Biology. *J Phys D: Appl Phys* (2012) 45(26):263001. doi:10.1088/0022-3727/45/26/263001
86. Lukes P, Dolezalova E, Sisrova I, and Clupek M. Aqueous-phase Chemistry and Bactericidal Effects from an Air Discharge Plasma in Contact with Water: Evidence for the Formation of Peroxynitrite through a Pseudo-second-order post-discharge Reaction of H2O 2 and HNO2. *Plasma Sourc Sci Tech* (2014) 23(1):015019. doi:10.1088/0963-0252/23/1/015019
87. Van Gils CAJ, Hofmann S, Boekema BK, Brandenburg R, and Bruggeman PJ. Mechanisms of Bacterial Inactivation in the Liquid Phase Induced by a Remote RF Cold Atmospheric Pressure Plasma Jet. *J Phys D: Appl Phys* (2013) 46(7):175203. doi:10.1088/0022-3727/46/17/175203
88. Weltmann KD, Kindel E, von Woedtke T, Hähnel M, Stieber M, and Brandenburg R. Atmospheric-pressure Plasma Sources: Prospective Tools for Plasma Medicine. *Pure Appl Chem* (2010) 82(6):1223–37. doi:10.1351/pac-con-09-10-35
89. Laroussi M, Lu X, and Keidar M. Perspective: The Physics, Diagnostics, and Applications of Atmospheric Pressure Low Temperature Plasma Sources Used in Plasma Medicine. *J Appl Phys* (2017) 122(2):020901. doi:10.1063/1.4993710
90. Laroussi M, and Akan T. Arc-Free Atmospheric Pressure Cold Plasma Jets: A Review. *Plasma Process Polym* (2007) 4(9):777–88. doi:10.1002/ppap.200700066
91. Lu X, Laroussi M, and Puech V. On Atmospheric-Pressure Non-equilibrium Plasma Jets and Plasma Bullets. *Plasma Sourc Sci. Technol.* (2012) 21(3): 034005. doi:10.1088/0963-0252/21/3/034005
92. Guo L, Yao Z, Yang L, Zhang H, Qi Y, Gou L, et al. Plasma-activated Water: An Alternative Disinfectant for S Protein Inactivation to Prevent SARS-CoV-2 Infection. *Chem Eng J* (2020) 127742. doi:10.1016/j.cej.2020.127742
93. Wende K, Williams P, Dalluge J, Van Gaens W, Aboubakr H, Bischof J, et al. Identification of the Biologically Active Liquid Chemistry Induced by a Nonthermal Atmospheric Pressure Plasma Jet. *Biointerphases* (2015) 10(2):029518. doi:10.1116/1.4919710
94. Aboubakr HA, Gangal U, Youssef MM, Goyal SM, and Bruggeman PJ. Inactivation of Virus in Solution by Cold Atmospheric Pressure Plasma: Identification of Chemical Inactivation Pathways. *J Phys D: Appl Phys* (2016) 49(20):204001. doi:10.1088/0022-3727/49/20/204001
95. Moldgy A, Nayak G, Aboubakr HA, Goyal SM, and Bruggeman PJ. Inactivation of Virus and Bacteria Using Cold Atmospheric Pressure Air Plasmas and the Role of Reactive Nitrogen Species. *J Phys D: Appl Phys* (2020) 53(4):434004. doi:10.1088/1361-6463/aba066
96. Zimmermann JL, Dumler K, Shimizu T, Morfill GE, Wolf A, Boxhammer V, et al. Effects of Cold Atmospheric Plasmas on Adenoviruses in Solution. *J Phys D: Appl Phys* (2011) 44(50):505201. doi:10.1088/0022-3727/44/50/505201
97. Schütze A, Jeong JY, Babayan SE, Jaeyoung Park fnm, Selwyn GS, and Hicks RF. The Atmospheric-Pressure Plasma Jet: A Review and Comparison to Other Plasma Sources. *IEEE Trans Plasma Sci* (1998) 26(6):1685–94. doi:10.1109/27.747887
98. Kogelschatz U. Dielectric-barrier Discharges: Their History, Discharge Physics, and Industrial Applications. *Plasma Chem Plasma Process* (2003) 23:1–46. doi:10.1023/a:1022470901385
99. Guo L, Xu R, Gou L, Liu Z, Zhao Y, Liu D, et al. Mechanism of Virus Inactivation by Cold Atmospheric-Pressure Plasma and Plasma-Activated Water. *Appl Environ Microbiol* (2018) 84(15):e00726–18. doi:10.1128/aem.00726-18
100. Aboubakr HA, Nisar M, Nayak G, Nagaraja KV, Collins J, Bruggeman PJ, et al. Bactericidal Efficacy of a Two-Dimensional Array of Integrated, Coaxial, Microhollow, Dielectric Barrier Discharge Plasma against *Salmonella enterica* Serovar Heidelberg. *Foodborne Pathog Dis* (2020) 17(3):157–65. doi:10.1089/fpd.2019.2698
101. Nayak G, Aboubakr HA, Goyal SM, and Bruggeman PJ. Reactive Species Responsible for the Inactivation of Feline Calicivirus by a Two-Dimensional Array of Integrated Coaxial Microhollow Dielectric Barrier Discharges in Air. *Plasma Process Polym* (2018) 15(1): 1700119. doi:10.1002/ppap.201700119
102. Isbary G, Shimizu T, Zimmermann JL, Heinlin J, Al-Zaabi S, Rechfeld M, et al. Randomized Placebo-Controlled Clinical Trial Showed Cold Atmospheric Argon Plasma Relieved Acute Pain and Accelerated Healing in Herpes Zoster. *Clin Plasma Med* (2014) 2(2):50–5. doi:10.1016/j.cpme.2014.07.001
103. Bae S-C, Park SY, Choe W, and Ha S-D. Inactivation of Murine Norovirus-1 and Hepatitis A Virus on Fresh Meats by Atmospheric Pressure Plasma Jets. *Food Res Int* (2015) 76:342–7. doi:10.1016/j.foodres.2015.06.039
104. Lacombe A, Niemira BA, Gurtler JB, Sites J, Boyd G, Kingsley DH, et al. Nonthermal Inactivation of Norovirus Surrogates on Blueberries Using Atmospheric Cold Plasma. *Food Microbiol* (2017) 63:1–5. doi:10.1016/j.fm.2016.10.030
105. Czernichowski A. Gliding Arc: Applications to Engineering and Environment Control. *Pure Appl Chem* (1994) 66(6):1301–10. doi:10.1351/pac199466061301
106. Fridman A, Nester S, Kennedy LA, Saveliev A, and Mutaf-Yardimci O. Gliding Arc Gas Discharge. *Prog Energ Combustion Sci* (1999) 25(2):211–31. doi:10.1016/s0360-1285(98)00021-5
107. Kim HY, Kang SK, Park SM, Jung HY, Choi BH, Sim JY, et al. Characterization and Effects of Ar/air Microwave Plasma on Wound Healing. *Plasma Process Polym* (2015) 12(12):1423–34. doi:10.1002/ppap.201500017
108. Uhm HS, Hong YC, and Shin DH. A Microwave Plasma Torch and its Applications. *Plasma Sourc Sci. Technol.* (2006) 15:S26–S34. doi:10.1088/0963-0252/15/2/s04
109. Laroussi M. Low Temperature Plasma-Based Sterilization: Overview and State-Of-The-Art. *Plasma Process Polym* (2005) 2(5):391–400. doi:10.1002/ppap.200400078
110. Shimizu T, Nosenko T, Morfill GE, Sato T, Schmidt HU, and Urayama T. Characterization of Low-Temperature Microwave Plasma Treatment with and without UV Light for Disinfection. *Plasma Process Polym* (2010) 7(3-4): 288–93. doi:10.1002/ppap.200900085
111. Shimizu T, Steffes B, Pompl R, Jamitzky F, Bunk W, Ramrath K, et al. Characterization of Microwave Plasma Torch for Decontamination. *Plasma Process Polym* (2008) 5(6):577–82. doi:10.1002/ppap.200800021
112. Pexara A, and Govaris A. Foodborne Viruses and Innovative Non-thermal Food-Processing Technologies. *Foods* (2020) 9(11):1520. doi:10.3390/foods9111520
113. Kamgang-Youbi G, Herry J-M, Meylheuc T, Brisset J-L, Bellon-Fontaine M-N, Doubla A, et al. Microbial Inactivation Using Plasma-Activated Water

Obtained by Gliding Electric Discharges. *Lett Appl Microbiol* (2009) 48(1): 13–8. doi:10.1111/j.1472-765x.2008.02476.x
114. Zhang Q, Liang Y, Feng H, Ma R, Tian Y, Zhang J, et al. A Study of Oxidative Stress Induced by Non-thermal Plasma-Activated Water for Bacterial Damage. *Appl Phys Lett* (2013) 102:203701. doi:10.1063/1.4807133
115. Nayak G, Andrews AJ, Marabella I, Aboubakr HA, Goyal SM, Olson BA, et al. Rapid Inactivation of Airborne Porcine Reproductive and Respiratory Syndrome Virus Using an Atmospheric Pressure Air Plasma. *Plasma Process. Polym.* (2020) 17 (10): 1900269. doi:10.1002/ppap.201900269
116. Chen C, Liu DX, Liu ZC, Yang AJ, Chen HL, Shama G, et al. A Model of Plasma-Biofilm and Plasma-Tissue Interactions at Ambient Pressure. *Plasma Chem Plasma Process* (2014) 34:403–41. doi:10.1007/s11090-014-9545-1
117. Oinuma G, Nayak G, Du Y, and Bruggeman PJ. Controlled Plasma-Droplet Interactions: A Quantitative Study of OH Transfer in Plasma-Liquid Interaction. *Plasma Sourc Sci Tech* (2020) 29(9):095002. doi:10.1088/1361-6595/aba988
118. Rumbach P, Bartels DM, Sankaran RM, and Go DB. The Solvation of Electrons by an Atmospheric-Pressure Plasma. *Nat Commun* (2015) 6: 7248. doi:10.1038/ncomms8248
119. Sander R. Compilation of Henry's Law Constants (Version 4.0) for Water as Solvent. *Atmos Chem Phys* (2015) 15(8):4399–981. doi:10.5194/acp-15-4399-2015
120. Pavlovich MJ, Chang H-W, Sakiyama Y, Clark DS, and Graves DB. Ozone Correlates with Antibacterial Effects from Indirect Air Dielectric Barrier Discharge Treatment of Water. *J Phys D: Appl Phys* (2013) 46:145202. doi:10.1088/0022-3727/46/14/145202
121. Aboubakr HA, Williams P, Gangal U, Youssef MM, El-Sohaimy SAA, Bruggeman PJ, et al. Virucidal Effect of Cold Atmospheric Gaseous Plasma on Feline Calicivirus, a Surrogate for Human Norovirus. *Appl Environ Microbiol* (2015) 81(11):3612–22. doi:10.1128/aem.00054-15
122. Alshraiedeh NH, Alkawareek MY, Gorman SP, Graham WG, and Gilmore BF. Atmospheric Pressure, Nonthermal Plasma Inactivation of MS2 Bacteriophage: Effect of Oxygen Concentration on Virucidal Activity. *J Appl Microbiol* (2013) 115(6):1420–6. doi:10.1111/jam.12331
123. Filipić A, Primc G, Zaplotnik R, Mehle N, Gutierrez-Aguirre I, Ravnikar M, et al. Cold Atmospheric Plasma as a Novel Method for Inactivation of Potato Virus Y in Water Samples. *Food Environ Virol* (2019) 11:220–8. doi:10.1007/s12560-019-09388-y
124. Ryan HA, Neuber J, Song S, Beebe SJ, and Jiang C. *38th Annual International Conference of the IEEE Engineering in Medicine and Biology Society*. EMBC). IEEE (2016). p. 537–40. Effects of a Non-thermal Plasma Needle Device on HPV-16 Positive Cervical Cancer Cell Viability In Vitro.
125. Takamatsu T, Uehara K, Sasaki Y, Hidekazu M, Matsumura Y, Iwasawa A, et al. Microbial Inactivation in the Liquid Phase Induced by Multigas Plasma Jet. *PLoS One* (2015) 10(8):e0135546. doi:10.1371/journal.pone.0135546
126. Wang G, Zhu R, Yang L, Wang K, Zhang Q, Su X, et al. Non-thermal Plasma for Inactivated-Vaccine Preparation. *Vaccine* (2016) 34(8):1126–32. doi:10.1016/j.vaccine.2015.10.099
127. Wu Y, Liang Y, Wei K, Li W, Yao M, Zhang J, et al. MS2 Virus Inactivation by Atmospheric-Pressure Cold Plasma Using Different Gas Carriers and Power Levels. *Appl Environ Microbiol* (2015) 81(3):996–1002. doi:10.1128/aem.03322-14
128. Kondeti VSSK, and Bruggeman PJ. The Interaction of an Atmospheric Pressure Plasma Jet with Liquid Water: Dimple Dynamics and its Impact on crystal Violet Decomposition. *J Phys D: Appl Phys* (2021) 54:045204. doi:10.1088/1361-6463/abbeb5
129. Labuza TP. The Properties of Water in Relationship to Water Binding in Foods: a Review2. *J Food Process. Preservation* (1977) 1(2):167–90. doi:10.1111/j.1745-4549.1977.tb00321.x
130. Hoff JC. *Inactivation of Microbial Agents by Chemical Disinfectants*. Cincinnati, Ohio: U. S. Environmental Protection Agency (1986).EPA/600/2-86/067
131. Maslennikov OV, Kontorshchikova CN, and Gribkova IA. *The State Medical Academy of Nizhny Novgorod-Ozone Therapy in Practice Health Manual* (2008). O3 Ministry of Health Service of the Russian Federation.
132. Schwartz A, Martínez Sánchez G, and Sabah F. In: *Madrid Declaration on Ozone Therapy*. 2nd. edition. Madrid, Spain: Official document of ISCO3 (2015).
133. Shmakova IP, and Nazarov EI. *Methods of Application of Ozone in Medicine (Guidelines)*. Kiev, Ukraine: Kiev (2004).
134. Akey DH, and Walton TE. Liquid-phase Study of Ozone Inactivation of Venezuelan Equine Encephalomyelitis Virus. *Appl Environ Microbiol* (1985) 50(4):882–6. doi:10.1128/aem.50.4.882-886.1985
135. Roy D, Wong PK, Engelbrecht RS, and Chian ES. Mechanism of Enteroviral Inactivation by Ozone. *Appl Environ Microbiol* (1981) 41(3):718–23. doi:10.1128/aem.41.3.718-723.1981
136. Hudson JB, Sharma M, and Vimalanathan S. Development of a Practical Method for Using Ozone Gas as a Virus Decontaminating Agent. *Ozone: Sci Eng* (2009) 31(3):216–23. doi:10.1080/01919510902747969
137. Hudson JB, Sharma M, and Petric M. Inactivation of Norovirus by Ozone Gas in Conditions Relevant to Healthcare. *J Hosp Infect* (2007) 66(1):40–5. doi:10.1016/j.jhin.2006.12.021
138. Lin Y-C, and Wu S-C. Effects of Ozone Exposure on Inactivation of Intra- and Extracellular Enterovirus 71. *Antiviral Res* (2006) 70(3):147–53. doi:10.1016/j.antiviral.2005.12.007
139. Tseng C, and Li C. Inactivation of Surface Viruses by Gaseous Ozone. *J Environ Health* (2008) 70(10):56–62.
140. Tseng C-C, and Li C-S. Ozone for Inactivation of Aerosolized Bacteriophages. *Aerosol Sci Tech* (2006) 40(9):683–9. doi:10.1080/02786820600796590
141. Thurston-Enriquez JA, Haas CN, Jacangelo J, and Gerba CP. Inactivation of Enteric Adenovirus and Feline Calicivirus by Ozone. *Water Res* (2005) 39: 3650–6. doi:10.1016/j.watres.2005.06.006
142. Bentley K, Dove BK, Parks SR, Walker JT, and Bennett AM. Hydrogen Peroxide Vapour Decontamination of Surfaces Artificially Contaminated with Norovirus Surrogate Feline Calicivirus. *J Hosp Infect* (2012) 80(2): 116–21. doi:10.1016/j.jhin.2011.10.010
143. Goyal SM, Chander Y, Yezli S, and Otter JA. Evaluating the Virucidal Efficacy of Hydrogen Peroxide Vapour. *J Hosp Infect* (2014) 86:255–9. W.B. Saunders Ltd. doi:10.1016/j.jhin.2014.02.003
144. Heckert RA, Best M, Jordan LT, Dulac GC, Eddington DL, and Sterritt WG. Efficacy of Vaporized Hydrogen Peroxide against Exotic Animal Viruses. *Appl Environ Microbiol* (1997) 63(10):3916–8. doi:10.1128/aem.63.10.3916-3918.1997
145. Pottage T, Richardson C, Parks S, Walker JT, and Bennett AM. Evaluation of Hydrogen Peroxide Gaseous Disinfection Systems to Decontaminate Viruses. *J Hosp Infect* (2010) 74(1):55–61. doi:10.1016/j.jhin.2009.08.020
146. Rudnick SN, McDevitt JJ, First MW, and Spengler JD. Inactivating Influenza Viruses on Surfaces Using Hydrogen Peroxide or Triethylene Glycol at Low Vapor Concentrations. *Am J Infect Control* (2009) 37(10):813–9. doi:10.1016/j.ajic.2009.06.007
147. Pinto AK, Richner JM, Poore EA, Patil PP, Amanna IJ, Slifka MK, et al. A Hydrogen Peroxide-Inactivated Virus Vaccine Elicits Humoral and Cellular Immunity and Protects against Lethal West Nile Virus Infection in Aged Mice. *J Virol* (2013) 87(4):1926–36. doi:10.1128/jvi.02903-12
148. Stief TW. Singlet Oxygen -oxidazable Lipids in the HIV Membrane, New Targets for AIDS Therapy? *Med Hypotheses* (2003) 60(4):575–7. doi:10.1016/s0306-9877(03)00046-x
149. Hamblin MR, and Hasan T. Photodynamic Therapy: A New Antimicrobial Approach to Infectious Disease? *Photochem Photobiol Sci* (2004) 3(5):436–50. doi:10.1039/b311900a
150. Lenard J, Rabson A, and Vanderoef R. Photodynamic Inactivation of Infectivity of Human Immunodeficiency Virus and Other Enveloped Viruses Using Hypericin and Rose Bengal: Inhibition of Fusion and Syncytia Formation. *Proc Natl Acad Sci* (1993) 90(1):158–62. doi:10.1073/pnas.90.1.158
151. Dai T, Huang YY, and Hamblin MR. Photodynamic Therapy for Localized Infections-State of the Art. *Photodiagnosis Photodynamic Ther* (2009) 6(3-4): 170–88. doi:10.1016/j.pdpdt.2009.10.008
152. Wainwright M. Local Treatment of Viral Disease Using Photodynamic Therapy. *Int J Antimicrob Agents* (2003) 21(6):510–20. doi:10.1016/s0924-8579(03)00035-9

153. Kharkwal GB, Sharma SK, Huang Y-Y, Dai T, and Hamblin MR. Photodynamic Therapy for Infections: Clinical Applications. *Lasers Surg Med* (2011) 43(7):755–67. doi:10.1002/lsm.21080
154. Matthews J, Newman J, Sogandares-Bernal F, Judy M, Skiles H, Leveson J, et al. Photodynamic Therapy of Viral Contaminants with Potential for Blood Banking Applications. *Transfusion* (1988) 28(1):81–3. doi:10.1046/j.1537-2995.1988.28188127963.x
155. Mohr H, Lambrecht B, and Selz A. Photodynamic Virus Inactivation of Blood Components. *Immunological Invest* (1995) 24(1-2):73–85. doi:10.3109/08820139509062763
156. Santus R, Grellier P, Schrével J, Mazière JC, and Stoltz JF. Photodecontamination of Blood Components: Advantages and Drawbacks. *Clin Hemorheol Microcirc* (1998) 18(4):299–308.
157. Müller-Breitkreutz K, Mohr H, Briviba K, and Sies H. Inactivation of Viruses by Chemically and Photochemically Generated Singlet Molecular Oxygen. *J Photochem Photobiol B: Biol* (1995) 30(1):63–70. doi:10.1016/1011-1344(95)07150-z
158. Hotze EM, Badireddy AR, Chellam S, and Wiesner MR. Mechanisms of Bacteriophage Inactivation via Singlet Oxygen Generation in UV Illuminated Fullerol Suspensions. *Environ Sci Technol* (2009) 43(17):6639–45. doi:10.1021/es901110m
159. Kohn T, Grandbois M, McNeill K, and Nelson KL. Association with Natural Organic Matter Enhances the Sunlight-Mediated Inactivation of MS2 Coliphage by Singlet Oxygen. *Environ Sci Technol* (2007) 41(13):4626–32. doi:10.1021/es070295h
160. Rule Wigginton K, Menin L, Montoya JP, and Kohn T. Oxidation of Virus Proteins during UV254and Singlet Oxygen Mediated Inactivation. *Environ Sci Technol* (2010) 44(14):5437–43. doi:10.1021/es100435a
161. Kohn T, and Nelson KL. Sunlight-mediated Inactivation of MS2 Coliphage via Exogenous Singlet Oxygen Produced by Sensitizers in Natural Waters. *Environ Sci Technol* (2007) 41(1):192–7. doi:10.1021/es061716i
162. Yamashiro R, Misawa T, and Sakudo A. Key Role of Singlet Oxygen and Peroxynitrite in Viral RNA Damage during Virucidal Effect of Plasma Torch on Feline Calicivirus. *Sci Rep* (2018) 8(1):17947. doi:10.1038/s41598-018-36779-1
163. Su X, Tian Y, Zhou H, Li Y, Zhang Z, Jiang B, et al. Inactivation Efficacy of Nonthermal Plasma-Activated Solutions against Newcastle Disease Virus. *Appl Environ Microbiol* (2018) 84(9):e02836–17. doi:10.1128/aem.02836-17
164. Iseki S, Hashizume H, Jia F, Takeda K, Ishikawa K, Ohta T, et al. Inactivation ofPenicillium digitatumSpores by a High-Density Ground-State Atomic Oxygen-Radical Source Employing an Atmospheric-Pressure Plasma. *Appl Phys Express* (2011) 4(11):116201. doi:10.1143/apex.4.116201
165. Bekeschus S, Wende K, Hefny MM, Rödder K, Jablonowski H, Schmidt A, et al. Oxygen Atoms Are Critical in Rendering THP-1 Leukaemia Cells Susceptible to Cold Physical Plasma-Induced Apoptosis. *Scientific Rep* (2017) 7(2791):1–12. doi:10.1038/s41598-017-03131-y
166. Vujošević D, Cvelbar U, Repnik U, Modic M, Lazović S, ZavašNik-Bergant T, et al. Plasma Effects on the Bacteria *Escherichia coli* via Two Evaluation Methods. *Plasma Sci Tech* (2017) 19(7):075504.
167. Hashizume H, Ohta T, Hori M, and Ito M. Growth Control of *Saccharomyces cerevisiae* through Dose of Oxygen Atoms. *Appl Phys Lett* (2015) 107:093701. doi:10.1063/1.4929952
168. Kondeti VSSK, Phan CQ, Wende K, Jablonowski H, Gangal U, Granick JL, et al. Long-lived and Short-Lived Reactive Species Produced by a Cold Atmospheric Pressure Plasma Jet for the Inactivation of *Pseudomonas aeruginosa* and *Staphylococcus aureus*. *Free Radic Biol Med* (2018) 124(20):275–87. doi:10.1016/j.freeradbiomed.2018.05.083
169. Byczkowski JZ, and Gessner T. Biological Role of Superoxide Ion-Radical. *Int J Biochem* (1988) 20(6):569–80. doi:10.1016/0020-711x(88)90095-x
170. Van Hemmen JJ, and Meuling WJA. Inactivation of *Escherichia coli* by Superoxide Radicals and Their Dismutation Products. *Arch Biochem Biophys* (1977) 182(2):743–8. doi:10.1016/0003-9861(77)90556-2
171. Bisag A, Isabelli P, Laurita R, Bucci C, Capelli F, Dirani G, et al. Cold Atmospheric Plasma Inactivation of Aerosolized Microdroplets Containing Bacteria and Purified SARS-CoV-2 RNA to Contrast Airborne Indoor Transmission. *Plasma Process Polym* (2020) 17(10):2000154. doi:10.1002/ppap.202000154
172. Attri P, Koga K, and Shiratani M. Possible Impact of Plasma Oxidation on the Structure of the C-Terminal Domain of SARS-CoV-2 Spike Protein: a Computational Study. *Appl Phys Express* (2021) 14(2):027002. doi:10.35848/1882-0786/abd717
173. Yasuda H, Miura T, Kurita H, Takashima K, and Mizuno A. Biological Evaluation of DNA Damage in Bacteriophages Inactivated by Atmospheric Pressure Cold Plasma. *Plasma Process Polym* (2010) 7:301–8. doi:10.1002/ppap.200900088
174. Aboubakr HA, Mor SK, Higgins L, Armien A, Youssef MM, Bruggeman PJ, et al. Cold Argon-Oxygen Plasma Species Oxidize and Disintegrate Capsid Protein of Feline Calicivirus. *PLoS One* (2018) 13(3):e0194618. doi:10.1371/journal.pone.0194618
175. Lim ME, Lee Y-l., Zhang Y, and Chu JJH. Photodynamic Inactivation of Viruses Using Upconversion Nanoparticles. *Biomaterials* (2012) 33(6):1912–20. doi:10.1016/j.biomaterials.2011.11.033
176. Kim CK, Gentile DM, and Sproul OJ. Mechanism of Ozone Inactivation of Bacteriophage F2. *Appl Environ Microbiol* (1980) 39(1):210–8. doi:10.1128/aem.39.1.210-218.1980
177. Torrey J, von Gunten U, and Kohn T. Differences in Viral Disinfection Mechanisms as Revealed by Quantitative Transfection of Echovirus 11 Genomes. *Appl Environ Microbiol* (2019) 85(14):e00961–19. doi:10.1128/aem.00961-19
178. Wu Y, Liang Y, Wei K, Li W, Yao M, Zhang J, et al. MS2 Virus Inactivation by Atmospheric-Pressure Cold Plasma Using Different Gas Carriers and Power Levels. *Appl Environ Microbiol* (2015) 81(3):996–1002. doi:10.1128/aem.03322-14
179. Sakudo A, Toyokawa Y, and Imanishi Y. Nitrogen Gas Plasma Generated by a Static Induction Thyristor as a Pulsed Power Supply Inactivates Adenovirus. *PLoS One* (2016) 11(6):e0157922. doi:10.1371/journal.pone.0157922
180. Aboubakr HA, Sampedro Parra F, Collins J, Bruggeman P, and Goyal SM. Ìn Situ Inactivation of Human Norovirus GII.4 by Cold Plasma: Ethidium Monoazide (EMA)-coupled RT-qPCR Underestimates Virus Reduction and Fecal Material Suppresses Inactivation. *Food Microbiol* (2020) 85:103307. doi:10.1016/j.fm.2019.103307
181. Park SY, and Ha S-D. Assessment of Cold Oxygen Plasma Technology for the Inactivation of Major Foodborne Viruses on Stainless Steel. *J Food Eng* (2018) 223:42–5. doi:10.1016/j.jfoodeng.2017.11.041
182. Cimolai N. Environmental and Decontamination Issues for Human Coronaviruses and Their Potential Surrogates. *J Med Virol* (2020) 92(11):2498–510. doi:10.1002/jmv.26170
183. Otter JA, Donskey C, Yezli S, Douthwaite S, Goldenberg SD, and Weber DJ. Transmission of SARS and MERS Coronaviruses and Influenza Virus in Healthcare Settings: The Possible Role of Dry Surface Contamination. *J Hosp Infect* (2016) 92(3):235–50. doi:10.1016/j.jhin.2015.08.027
184. Gill J, and Hyman P. Phage Choice, Isolation, and Preparation for Phage Therapy. *Cpb* (2010) 11(1):2–14. doi:10.2174/138920110790725311
185. McMinn BR, Ashbolt NJ, and Korajkic A. Bacteriophages as Indicators of Faecal Pollution and Enteric Virus Removal. *Lett Appl Microbiol* (2017) 65(1):11–26. doi:10.1111/lam.12736
186. Verreault D, Moineau S, and Duchaine C. *Microbiology and Molecular Biology Reviews*, 72. American Society for Microbiology (ASM) (2008). p. 413–44. doi:10.1128/mmbr.00002-08 Methods for Sampling of Airborne Viruses*Mmbr*.
187. Locke BR, Sato M, Sunka P, Hoffmann MR, and Chang J-S. Electrohydraulic Discharge and Nonthermal Plasma for Water Treatment. *Ind Eng Chem Res* (2006) 45(3):882–905. doi:10.1021/ie050981u
188. Ikawa S, Tani A, Nakashima Y, and Kitano K. Physicochemical Properties of Bactericidal Plasma-Treated Water. *J Phys D: Appl Phys* (2016) 49(42):425401. doi:10.1088/0022-3727/49/42/425401
189. Traylor MJ, Pavlovich MJ, Karim S, Hait P, Sakiyama Y, Clark DS, et al. Long-term Antibacterial Efficacy of Air Plasma-Activated Water. *J Phys D: Appl Phys* (2011) 44(47):472001. doi:10.1088/0022-3727/44/47/472001
190. Oehmigen K, Hähnel M, Brandenburg R, Wilke C, Weltmann KD, Von Woedtke T, et al. The Role of Acidification for Antimicrobial Activity of Atmospheric Pressure Plasma in Liquids. *Plasma Process Polym* (2010) 7(3-4):250–7. doi:10.1002/ppap.200900077
191. Tani A, Ono Y, Fukui S, Ikawa S, and Kitano K. Free Radicals Induced in Aqueous Solution by Non-contact Atmospheric-Pressure Cold Plasma. *Appl Phys Lett* (2012) 100:254103. doi:10.1063/1.4729889

192. Bruggeman P, and Locke B. *Low Temperature Plasma Technology: Methods and Applications*. Boca Raton, FL: CRC Press (2013). p. 367–99. doi:10.1201/b15153-16 Assessment of Potential Applications of Plasma with Liquid Water.
193. Von Keudell A, Awakowicz P, Benedikt J, Raballand V, Yanguas-Gil A, Opretzka J, et al. Inactivation of Bacteria and Biomolecules by Low-Pressure Plasma Discharges. *Plasma Process. Polym* (2010) 7:327–52. doi:10.1002/ppap.200900121
194. Jacobs PT, and Lin S-M. *Hydrogen Peroxide Plasma Sterilization System*. United States Patent (1987).
195. Haertel B, Woedtke Tv., Weltmann K-D, and Lindequist U. Non-thermal Atmospheric-Pressure Plasma Possible Application in Wound Healing. *Biomolecules Ther* (2014) 22(6):477–90. doi:10.4062/biomolther.2014.105
196. Pei X, Lu X, Liu J, Liu D, Yang Y, Ostrikov K, et al. Inactivation of a 25.5 μmEnterococcus Faecalisbiofilm by a Room-Temperature, Battery-Operated, Handheld Air Plasma Jet. *J Phys D: Appl Phys* (2012) 45:165205. doi:10.1088/0022-3727/45/16/165205
197. Alekseev O, Donovan K, Limonnik V, and Azizkhan-Clifford J. Nonthermal Dielectric Barrier Discharge (DBD) Plasma Suppresses Herpes Simplex Virus Type 1 (HSV-1) Replication in Corneal Epithelium. *Trans Vis Sci Tech* (2014) 3(2):2. doi:10.1167/tvst.3.2.2
198. Terrier O, Essere B, Yver M, Barthélémy M, Bouscambert-Duchamp M, Kurtz P, et al. Cold Oxygen Plasma Technology Efficiency against Different Airborne Respiratory Viruses. *J Clin Virol* (2009) 45(2):119–24. doi:10.1016/j.jcv.2009.03.017
199. Chen Z, Garcia G, Arumugaswami V, and Wirz RE. Cold Atmospheric Plasma for SARS-CoV-2 Inactivation. *Phys Fluids (1994)* (1994) 32(11):111702. doi:10.1063/5.0031332
200. Ahlfeld B, Li Y, Boulaaba A, Binder A, Schotte U, Zimmermann JL, et al. Inactivation of a Foodborne Norovirus Outbreak Strain with Nonthermal Atmospheric Pressure Plasma. *mBio* (2015) 6(1):e02300–14. doi:10.1128/mbio.02300-14
201. López M, Calvo T, Prieto M, Múgica-Vidal R, Muro-Fraguas I, Alba-Elías F, et al. A Review on Non-thermal Atmospheric Plasma for Food Preservation: Mode of Action, Determinants of Effectiveness, and Applications. *Front Microbiol* (2019) 10:622. doi:10.3389/fmicb.2019.00622
202. Misra NN, Tiwari BK, Raghavarao KSMS, and Cullen PJ. Nonthermal Plasma Inactivation of Food-Borne Pathogens. *Food Eng Rev* (2011) 3:159–70. doi:10.1007/s12393-011-9041-9
203. Niemira BA. Cold Plasma Decontamination of Foods. *Annu Rev Food Sci Technol* (2012) 3:125–42. doi:10.1146/annurev-food-022811-101132
204. Pankaj SK, Wan Z, and Keener KM. Effects of Cold Plasma on Food Quality: A Review. *Foods* (2018) 7(1):4.
205. Schlüter O, Ehlbeck J, Hertel C, Habermeyer M, Roth A, Engel K-H, et al. Opinion on the Use of Plasma Processes for Treatment of Foods*. *Mol Nutr Food Res* (2013) 57(5):920–7. doi:10.1002/mnfr.201300039
206. Xia T, Kleinheksel A, Lee EM, Qiao Z, Wigginton KR, and Clack HL. Inactivation of Airborne Viruses Using a Packed Bed Non-thermal Plasma Reactor. *J Phys D: Appl Phys* (2019) 52(25):255201. doi:10.1088/1361-6463/ab1466
207. Schiappacasse C, Peng P, Zhou N, Liu X, Zhai J, Cheng Y, et al. Inactivation of Aerosolized Newcastle Disease Virus with Non-thermal Plasma. *Appl Eng Agric* (2020) 36(1):55–60. doi:10.13031/aea.13699
208. Xia T, Yang M, Marabella I, Lee EM, Olson B, Zarling D, et al. Inactivation of Airborne Porcine Reproductive and Respiratory Syndrome Virus (PRRSv) by a Packed Bed Dielectric Barrier Discharge Non-thermal Plasma. *J Hazard Mater* (2020) 393:122266. doi:10.1016/j.jhazmat.2020.122266
209. Kettleson EM, Ramaswami B, Hogan CJ, Lee M-H, Statyukha GA, Biswas P, et al. Airborne Virus Capture and Inactivation by an Electrostatic Particle Collector. *Environ Sci Technol* (2009) 43(15):5940–6. doi:10.1021/es803289w
210. Okubo M, Kuroki T, Kametaka H, and Yamamoto T. Odor Control Using the AC Barrier-type Plasma Reactors. *IEEE Trans Ind Applicat* (2001) 37:1447–55. doi:10.1109/28.952520
211. Zhang R, Yamamoto T, and Bundy DS. Control of Ammonia and Odors in Animal Houses by a Ferroelectric Plasma Reactor. *IEEE Trans Industry Appl* (1996) 32(1):113–7.
212. Lahariya C. Vaccine Epidemiology: A Review. *J Fam Med Prim Care* (2016) 5(1):7–15. doi:10.4103/2249-4863.184616
213. Hongzhuan Z, Ying T, Xia S, Jinsong G, Zhenhua Z, Beiyu J, et al. Preparation of the Inactivated Newcastle Disease Vaccine by Plasma Activated Water and Evaluation of its protection Efficacy. *Appl Microbiol Biotechnol* (2020) 104(1):107–17. doi:10.1007/s00253-019-10106-8
214. Connolly RJ, Chapman T, Hoff AM, Kutzler MA, Jaroszeski MJ, and Ugen KE. Non-contact Helium-Based Plasma for Delivery of DNA Vaccines. *Hum Vaccin Immunother* (2012) 8(11):1729–33. doi:10.4161/hv.21624
215. Khalili M, Daniels L, Lin A, Krebs FC, Snook AE, Bekeschus S, et al. Non-thermal Plasma-Induced Immunogenic Cell Death in Cancer. *J Phys D: Appl Phys* (2019) 52(42):423001. doi:10.1088/1361-6463/ab31c1
216. Busco G, Robert E, Chettouh-Hammas N, Pouvesle J-M, and Grillon C. The Emerging Potential of Cold Atmospheric Plasma in Skin Biology. *Free Radic Biol Med* (2020) 161:290–304. doi:10.1016/j.freeradbiomed.2020.10.004
217. Thompson HW, Dupuy B, Beuerman RW, Hill JM, Rootman DS, and Haruta Y. Neural Activity from the Acutely Infected HSV-1 Rabbit Cornea. *Curr Eye Res* (1988) 7(2):147–55. doi:10.3109/02713688808995744
218. Friedman PC, Miller V, Fridman G, and Fridman A. Use of Cold Atmospheric Pressure Plasma to Treat Warts: a Potential Therapeutic Option. *Clin Exp Dermatol* (2019) 44(4):459–61. doi:10.1111/ced.13790
219. Friedman PC, Fridman G, and Fridman A. Using Cold Plasma to Treat Warts in Children: A Case Series. *Pediatr Dermatol* (2020) 37(4):706–9. doi:10.1111/pde.14180
220. Amiran MR, Sepahi AA, Zabiollahi R, Ghomi H, Momen SB, and Aghasadeghi MR. In Vitro assessment of Antiviral Activity of Cold Atmospheric Pressure Plasma Jet against the Human Immunodeficiency Virus (HIV). *J Med Microbiol Infec Dis* (2016) 4(3-4):62–6.
221. Volotskova O, Dubrovsky L, Keidar M, and Bukrinsky M. Cold Atmospheric Plasma Inhibits HIV-1 Replication in Macrophages by Targeting Both the Virus and the Cells. *PLoS One* (2016) 11(10):e0165322. doi:10.1371/journal.pone.0165322
222. Ramamurthy D, Nundalall T, Cingo S, Mungra N, Karaan M, Naran K, et al. Recent Advances in Immunotherapies against Infectious Diseases. *Immunother Adv* (2020) ltaa007.
223. Mahdikia H, Saadati F, Freund E, Gaipl US, Majidzadeh-a K, Shokri B, et al. Gas Plasma Irradiation of Breast Cancers Promotes Immunogenicity, Tumor Reduction, and an Abscopal Effect In Vivo. *Oncoimmunology* (2020) 10(1):1859731. doi:10.1080/2162402x.2020.1859731
224. Lin A, Truong B, Patel S, Kaushik N, Choi E, Fridman G, et al. Nanosecond-pulsed DBD Plasma-Generated Reactive Oxygen Species Trigger Immunogenic Cell Death in A549 Lung Carcinoma Cells through Intracellular Oxidative Stress. *Ijms* (2017) 18(5):966. doi:10.3390/ijms18050966
225. Hamblin TJ. Ex Vivo activation and Retransfusion of white Blood Cells. The Immunotherapy of Cancer. *Curr Stud Hematol Blood Transfus* (1990)(57)249–66. doi:10.1159/000418564
226. Dubuc A, Monsarrat P, Virard F, Merbahi N, Sarrette JP, Laurencin-Dalicieux S, et al. Use of Cold-Atmospheric Plasma in Oncology: a Concise Systematic Review. *Ther Adv Med Oncol* (2018) 10:1758835918786475. doi:10.1177/1758835918786475
227. Semmler ML, Bekeschus S, Schäfer M, Bernhardt T, Fischer T, Witzke K, et al. Molecular Mechanisms of the Efficacy of Cold Atmospheric Pressure Plasma (CAP) in Cancer Treatment. *Cancers* (2020) 12(2):269. doi:10.3390/cancers12020269
228. Volberding PD. Perspectives on the Use of Antiretroviral Drugs in the Treatment of HIV Infection. *Infect Dis Clin North America* (1994) 8(2):303–17. doi:10.1016/s0891-5520(20)30591-2
229. Akase IE, Musa BOP, Obiako RO, Elfulatiy AA, and Mohammed AA. Immune Dysfunction in HIV: A Possible Role for Pro- and Anti-inflammatory Cytokines in HIV Staging. *J Immunol Res* (2017) 2017:4128398. doi:10.1155/2017/4128398
230. Cha L, Berry CM, Nolan D, Castley A, Fernandez S, and French MA. Interferon-alpha, Immune Activation and Immune Dysfunction in Treated HIV Infection. *Clin Trans Immunol* (2014) 3(2):e10. doi:10.1038/cti.2014.1
231. Kottilil S, Shin K, Jackson JO, Reitano KN, O'Shea MA, Yang J, et al. Innate Immune Dysfunction in HIV Infection: Effect of HIV Envelope-NK Cell Interactions. *J Immunol* (2006) 176(2):1107–14. doi:10.4049/jimmunol.176.2.1107
232. Mohamed H, Clemen R, Freund E, Lackmann J, Wende K, Connors J, et al. Non-thermal Plasma Modulates Cellular Markers Associated with

Immunogenicity in a Model of Latent HIV-1 Infection. *PLoS One* (2021) 16(3):e0247125. doi:10.1371/journal.pone.0247125
233. Ranieri P, Shrivastav R, Wang M, Lin A, Fridman G, Fridman AA, et al. Nanosecond-Pulsed Dielectric Barrier Discharge-Induced Antitumor Effects Propagate through Depth of Tissue via Intracellular Signaling. *Plasma Med* (2017) 7(3):283–97. doi:10.1615/plasmamed.2017019883
234. Collins DR, Gaiha GD, and Walker BD. CD8+ T Cells in HIV Control, Cure and Prevention. *Nat Rev Immunol* (2020) 20(8):471–82. doi:10.1038/s41577-020-0274-9
235. Buhrman JD, and Slansky JE. Improving T Cell Responses to Modified Peptides in Tumor Vaccines. *Immunol Res* (2013) 55(1-3):34–47. doi:10.1007/s12026-012-8348-9
236. Luo GG, and Ou J-h. J. Oncogenic Viruses and Cancer. *Virol Sin* (2015) 30(2):83–4. doi:10.1007/s12250-015-3599-y
237. Friedman PC, Miller V, Fridman G, and Fridman A. Various Cold Plasma Devices for the Treatment of Actinic Keratosis. *J Eur Acad Dermatol Venereol* (2018) 32(12):e445–e446. doi:10.1111/jdv.14969
238. Bauer G, and Graves DB. Mechanisms of Selective Antitumor Action of Cold Atmospheric Plasma-Derived Reactive Oxygen and Nitrogen Species. *Plasma Process Polym* (2016) 13(12):1157–78. doi:10.1002/ppap.201600089
239. Tian W, and Kushner MJ. Atmospheric Pressure Dielectric Barrier Discharges Interacting with Liquid Covered Tissue. *J. Phys. D: Appl. Phys.* (2014) 47 (16): 165201. doi:10.1088/0022-3727/47/16/165201
240. Burleson GR, Murray TM, and Pollard M. Inactivation of Viruses and Bacteria by Ozone, with and without Sonication. *Appl Microbiol* (1975) 29(3):340–4. doi:10.1128/am.29.3.340-344.1975
241. Vickery K., Deva AK, Kumaradeva P, Bissett L, and Cossart YE. Inactivation of duck hepatitis B virus by a hydrogen peroxide gas plasma sterilization system: laboratory and 'in use' testing. *Journal of Hospital Infection* (1999) 1999(41):317–322. doi:10.1053/jhin.1998.0516
242. Kelly-Wintenberg K., Hodge A., Montie T. C., Deleanu L., Sherman D., Reece Roth J., et al. Use of a one atmosphere uniform glow discharge plasma to kill a broad spectrum of microorganisms. *Journal of Vacuum Science & Tech A: Vacuum, Surfaces, and Films* (1999) 17(4):1539–1544. doi:10.1116/1.581849
243. Kelly-Wintenberg K., Sherman D. M., Tsai P. P.-Y., Gadri R. B., Karakaya F., Zhiyu Chen F., et al. Air filter sterilization using a one atmosphere uniform glow discharge plasma (the volfilter). *IEEE Trans. Plasma Sci.* (2000) 28:64–71. doi:10.1109/27.842866
244. Shin G.-A., and Sobsey M. D. Reduction of Norwalk virus, poliovirus 1, and bacteriophage MS2 by ozone disinfection of water. *Aem* (2003) 69(7):3975–3978. doi:10.1128/aem.69.7.3975-3978.2003
245. Roth J.R., Nourgostar S., and Bonds T.A. The One Atmosphere Uniform Glow Discharge Plasma (OAUGDP) — A platform technology for the 21st century. *IEEE Transactions on Plasma Science* (2007) 35(2):233–250.
246. Venezia R. A., Orrico M., Houston E., Yin S.-M., and Naumova Y. Y. Lethal activity of nonthermal plasma sterilization against microorganisms. *Infect. Control Hosp. Epidemiol.* (2008) 29(5):430–436. doi:10.1086/588003
247. Yasuda H., Hashimoto M., Rahman M. M., Takashima K., and Mizuno A. States of biological components in bacteria and bacteriophages during Inactivation by atmospheric dielectric barrier discharges. *Plasma Process. Polym.* (2008) 5(6):615–621. doi:10.1002/ppap.200800036
248. Kalghatgi S., Kelly CM, Cerchar E, Torabi B, Alekseev O, Fridman A, et al. Effects of non-thermal plasma on mammalian cells. *PLoS One* (2011) 6(1):e16270. doi:10.1371/journal.pone.0016270
249. Brun P., Brun P, Vono M, Venier P, Tarricone E, Deligianni V, et al. Disinfection of ocular cells and tissues by atmospheric-pressure cold plasma. *PLoS One* (2012) 7(3):e33245. doi:10.1371/journal.pone.0033245
250. Shi X.-M., Zhang G.-J., Wu X.-L., Peng Z.-Y., Zhang Z.-H., Shao X.-J., et al. Effect of Low-Temperature Plasma on Deactivation of Hepatitis B Virus. *IEEE Trans. Plasma Sci.* (2012) 40(10):2711–2716. doi:10.1109/tps.2012.2210567
251. Min S. C., Roh S. H., Niemira B. A., Sites J. E., Boyd G., and Lacombe A. Dielectric barrier discharge atmospheric cold plasma inhibits *Escherichia coli* O157:H7, Salmonella, Listeria monocytogenes, and Tulane virus in romaine lettuce. *International Journal of Food Microbiology* (2016) 237:114–120. doi:10.1016/j.ijfoodmicro.2016.08.025
252. Sakudo A., Toyokawa Y., Imanishi Y., and Murakami T. Crucial roles of reactive chemical species in modification of respiratory syncytial virus by nitrogen gas plasma. *Materials Science and Engineering: C* (2017) 74:131–136. doi:10.1016/j.msec.2017.02.007
253. Braga E. A., Lopes Filho G. d. J., and Saad S. S. Argon plasma versus electrofulguration in the treatment of anal and perianal condylomata acuminata in patients with acquired immunodeficiency virus. *Acta Cir. Bras.* (2017) 32(6):482–490. doi:10.1590/s0102-865020170060000009
254. Park S. Y., and Ha S.-D. Assessment of cold oxygen plasma technology for the inactivation of major foodborne viruses on stainless steel. *Journal of Food Engineering* (2018) 223:42–45. doi:10.1016/j.jfoodeng.2017.11.041
255. Štěpánová V., Slavicek P, Kelar J, Prasil J, Smekal M, Stupavska M, et al. Atmospheric pressure plasma treatment of agricultural seeds of cucumber (Cucumis sativus L.) and pepper (Capsicum annuum L.) with effect on reduction of diseases and germination improvement. *Plasma Processes and Polymers* (2018) 15(2):1700076.
256. Hanbal S. E., Takashima K., Miyashita S., Ando S., Ito K., Elsharkawy M. M., et al. Atmospheric-pressure Plasma Irradiation Can Disrupt Tobacco Mosaic Virus Particles and RNAs to Inactivate Their Infectivity. *Arch Virol* (2018) 163(10):2835–40. doi:10.1007/s00705-018-3909-4
257. Bunz O, Mese K, Zhang W, Piwowarczyk A, and Ehrhardt A. Effect of Cold Atmospheric Plasma (CAP) on Human Adenoviruses Is Adenovirus Type-dependent. *PLoS One* (2018) 13(10):e0202352. doi:10.1371/journal.pone.0202352
258. Bunz O, Mese K, Funk C, Wulf M, Bailer SM, Piwowarczyk A, et al. Cold Atmospheric Plasma as Antiviral Therapy - Effect on Human Herpes Simplex Virus Type 1. *J Gen Virol* (2020) 101(2):208–15. doi:10.1099/jgv.0.001382
259. Roh SH, Oh YJ, Lee SY, Kang JH, and Min SC. Inactivation of *Escherichia coli* O157:H7, Salmonella, Listeria Monocytogenes, and Tulane Virus in Processed Chicken Breast via Atmospheric In-Package Cold Plasma Treatment. *Lwt* (2020) 127:109429. doi:10.1016/j.lwt.2020.109429

Conflict of Interest: The authors declare that the research was conducted in the absence of any commercial or financial relationships that could be construed as a potential conflict of interest.

frontiers in Physics

ORIGINAL RESEARCH
published: 24 August 2021
doi: 10.3389/fphy.2021.659227

Systematic Safety Evaluation of Cold Plasma-Activated Liquid in Rabbits

Yujing Xu[1], Sansan Peng[1], Bing Li[2], Shuai Wang[2], Hao Zhang[1], Qiaosong Li[1], Zhijie Liu[1], Bo Guo[1], Dingxin Liu[1] and Dehui Xu[1]**

[1]State Key Laboratory of Electrical Insulation and Power Equipment, Centre for Plasma Biomedicine, Xi'an Jiaotong University, Xi'an, China, [2]The School of Life Science and Technology, Xi'an Jiaotong University, Xi'an, China

Plasma-activated liquid (PAL) can effectively and selectively kill various types of cancer cells both in superficial and deeper tumors. As a promising novel approach to oncotherapy, the safety of PAL is essential in the clinic but has not been thoroughly assessed. In myeloma and blood tumors, the pathogenesis is in the bone marrow cavity. We have therefore evaluated the safety of PAL in New Zealand rabbits by intra-bone marrow injection, and provide a basis of further clinical research and application of PALs. In this study, both a plasma jet and plasma surface were used to treat saline solution, phosphate-buffered solution, and cell culture medium, to produce PAL. Then, oscillograms and optical emission spectra were evaluated to characterize the plasma discharge. Acute toxicity tests and safety evaluation studies were conducted by intra-bone marrow injection of PAL into New Zealand rabbits, while control rabbits received saline only. Body weight, vital organ coefficient, organ appearance, organ histopathology, blood cell and hemoglobin parameters, and blood biochemical indicators were tested on the 30th day after injection. We found that there was no mortality or loss of mobility throughout the experimental period. Acute toxicity tests showed that there were no PAL-related side effects in rabbits receiving the maximum dose of 700 μL PAL. PAL treatments did not affect body weight, organ coefficient, organ appearance, organ histopathology, or blood biochemical indicators. However, the percentage of lymphocytes decreased while the percentage of neutrophil granulocytes increased compared with the control group. In summary, our results indicate that PAL can be safely injected into bone marrow of New Zealand rabbits without significant toxicity.

Keywords: cold atmospheric plasma, plasma-activated liquid, New Zealand rabbits, safety evaluation, tumor

OPEN ACCESS

Edited by:
Mounir Laroussi,
Old Dominion University,
United States

Reviewed by:
Hiromasa Tanaka,
Nagoya University, Japan
Alan A. Howling,
École Polytechnique Fédérale de Lausanne, Switzerland
Lenka Zajíčková,
Masaryk University, Czechia

****Correspondence:***
Dingxin Liu
liudingxin@mail.xjtu.edu.cn
Dehui Xu
dehuixu@mail.xjtu.edu.cn

Specialty section:
This article was submitted to Plasma Physics, a section of the journal Frontiers in Physics

Received: *27 January 2021*
Accepted: *10 August 2021*
Published: *24 August 2021*

Citation:
Xu Y, Peng S, Li B, Wang S, Zhang H, Li Q, Liu Z, Guo B, Liu D and Xu D (2021) Systematic Safety Evaluation of Cold Plasma-Activated Liquid in Rabbits. Front. Phys. 9:659227. doi: 10.3389/fphy.2021.659227

INTRODUCTION

The number of cancer cases is increasing in both developed and developing countries, and cancer continues to be a major health problem that has in recent years placed a heavy burden on families and society. According to GLOBOCAN2020 statistics, patients in China account for approximately 23.7% of fresh cancer cases and 30% of malignant tumor-related deaths worldwide [1]. Accumulating evidence has confirmed that cancer relapse and drug resistance are problems that urgently need to be addressed, despite great progress having been made in the field of cancer therapy [2, 3]; thus it is necessary to introduce new therapeutic strategies for cancer treatment.

In this study, we focused on the emerging technology of cold atmospheric plasma (CAP). Plasma is defined as a fourth state of matter in addition to solid, liquid, and gas. Thermal and non-thermal

plasma are ionized gases composed of electrons and ions [4]. CAP is a typical non-thermal plasma, and since it can be produced at atmospheric pressure and near room temperature, it has been used in many medical fields, including wound healing, dentistry, sterilization, dermatology, and oncology, among others [5–8]. Many studies have shown that CAP can efficiently kill various types of tumor cells, including melanoma cells, colorectal cancer, leukemia cancer, multiple myeloma, and others [8–12]. However, the underlying mechanisms by which tumor cells sustain damage remain unclear. Many scholars have proposed that reactive oxygen species (ROS) and reactive nitrogen species (RNS) generated by CAP might play a significant role in the induction of cancer cell death [13, 14].

Depending on its application to biological tissues, CAP can be classified as direct or indirect plasma. Direct plasma, which employs direct application of the CAP device, is more suitable for treating surface diseases like cutaneous carcinoma and wound healing [5, 8]. Nevertheless, penetration of direct plasma into tissue is limited, and results from simulations showed that the active substances produced by plasma only extend into skin or tissues by 1–3 mm [15], which limits its use in clinical applications. Development of indirect plasma addressed this limitation. Indirect plasma, or plasma-activated liquid (PAL), involves treating a liquid with CAP, and the liquid is then applied to cells. Notably, PAL maintains its biological activity for at least 7 days when stored at −80°C or 4°C [16, 17], allowing it to be prepared in advance and later applied to cancer cells and tissues without a CAP device. Moreover, PAL can be used in solid and blood tumors that are not near the surface of the body by injecting it into tumor sites deep in tissue. Previous investigations showed that PAL could inhibit the growth of leukemia, bone cancer, pancreatic adenocarcinoma cells, glioblastoma cells, and other cancer cells *in vitro* [13, 18, 19]. Canal et al. [19] also found that the cytotoxicity of PAL indirect treatment of tumor cells was comparable to that of CAP direct treatment. Consequently, PAL greatly expands the potential application and development of CAP in medicine.

However, the biosafety of PAL in animals has not been systematically studied. Biscop et al. [20] reported that various components of plasma-treated liquid greatly affect cellular cytotoxicity of PAL. Thus, we selected three kinds of liquid in this study–saline, phosphate buffer solution (PBS), and cell culture medium–to evaluate the safety of different PALs in New Zealand rabbits by intra-bone marrow injection, and to provide further support for the safe application of PALs in the clinic.

EXPERIMENTAL SETUP AND METHODS

Plasma Generation Systems

The plasma jet system consisted of a gas flow controller, high-voltage power, oscilloscope, and plasma device. The plasma jet with a gas flow of two slm He (standard liters per minute with helium as the carrier gas) and an additional 0.01 slm of O_2 was excited by a power supply generating a peak-to-peak sinusoidal voltage of 8 kV at a frequency of 10 kHz to generate He + O_2 plasma. The jet length can be up to 1.5–2 cm. **Figures 1A,B** shows a diagram of the plasma jet device and a photograph of the jet itself. The plasma jet source adopted a needle-to-ring electrode structure. And a stainless-steel needle with an inside diameter of 1 mm was used as a high voltage electrode, which was enclosed in a 6 cm long quartz tube and about 15 mm above the top of the quartz tube. Quartz glass tubes with outer diameter of 6 mm and inner diameter of 4 mm were used as the insulating medium. A 10 mm copper ring was placed around the wall of the quartz tube as the ground electrode, 10 mm away from the tube at the bottom.

The plasma surface was generated from ambient air using the same power as that applied to the plasma jet device. **Figures 1C,D** shows a diagram of the device and image of the discharge. The air surface discharge device is a sandwich structure formed by a dielectric layer and two electrodes. The dielectric layer is sandwiched between a high-voltage electrode and a mesh ground electrode. Each mesh element has a hexagonal shape.

The images were captured by a digital camera (Nikon D7200) using an exposure time of 0.5 s. We used an oscilloscope (Tektronix, DPO3000) to record the waveform of the discharge voltage and current detected by a high-voltage probe (Tektronix, P6015A) and a current probe (Tektronix, P6021), respectively (**Figures 2A,B**). It can be seen that for both devices, the positive and negative half-cycle current waveforms were asymmetrical. When the same voltage was applied at 8 kV, the jet device current generated by a positive half period voltage consisting of a series of small pulses typical of glow discharge. For the surface device, the peak current appeared at the rising and falling edges of the voltage waveform, which was composed of a series of small pulses. This is typical of filamentous discharge. Power waveforms of the jet and surface devices are plotted in **Figures 2C,D**, respectively. Average power was calculated by integrating voltage and current across multiple discharge cycles. The average discharge power of the jet device was 1.2 W, while that of the surface device was 4.62 W.

Measurements of Physicochemical Properties of PALs

Plasma discharge was used to treat three types of liquid: stroke-physiological saline solution (0.9% NaCl; SMARBO, Ningbo Yinuo Medical Equipment Co., Ltd., China), 1×PBS (Thermo Fisher Scientific, MA, United States; Cat No. 10010002), and RPMI (Roswell Park Memorial Institute) 1,640 complete medium containing 10% fetal bovine serum and 1% penicillin-streptomycin solution (Corning, NY, United States; Cat No.10-040-CVRC). For plasma jet treatment, 300 μL of liquid were placed in a 24-well plate and treated for 3 min, with a 10 mm distance between the end of plasma jet plume and the liquid surface. The three solutions treated by plasma jet discharge were 0.9% NaCl, 1,640 medium, and 1× PBS, and these treatment groups were abbreviated J-N, J-M, and J-P, respectively. For plasma surface treatment, 3.5 ml of liquid were placed in a 60 mm diameter dish 10 mm away from the plasma surface device and treated for 3 min. The same three solutions were treated by plasma-surface discharge, and the groups were abbreviated S-N, S-M, and S-P.

The pH and oxidation-reduction potential (ORP) of the liquids were measured with a pH meter (METTLER-TOLEDO, FE20) and a

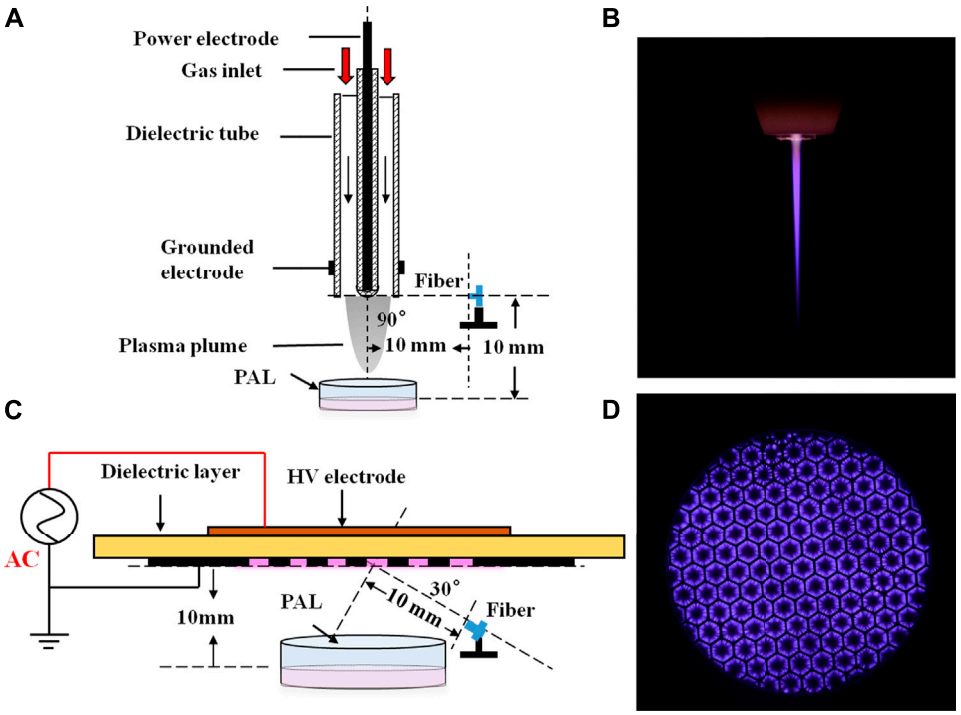

FIGURE 1 | Low temperature plasma jet/surface at atmospheric pressure. **(A)** Structure and **(B)** photograph of the plasma jet device; **(C)** structure and **(D)** photograph of the plasma surface device.

benchtop ORP meter (METTLER-TOLEDO, S210-K), respectively. The concentration of aqueous long-lived reactive oxygen and nitrogen species (RONS) of PALs induced by the plasma jet and surface devices was measured as follows. H_2O_2 was detected using a hydrogen peroxide assay kit (Beyotime, Shanghai, China; Cat No. S0038), NO_2^- was detected using a nitric oxide assay kit (Beyotime, Shanghai, China; Cat No. S0024), and absorbance was measured using a microplate analyzer (Thermo Science, MA, United States).

Optical Emission Spectroscopy

Optical emission spectroscopy (OES) of plasma jets and surfaces was performed using an Andor SR-750i grating monochromator (grating grooving 1,200 lines mm^{-1}) in the presence of liquid. Wavelength ranged from 200 to 800 nm. The locations of the optical probe in the two devices are shown in **Figures 1A,C**. Light emitted by the plasma jet was collected at the nozzle of the quartz tube by an optical fiber perpendicular to the center of a quartz tube, which was focused on the jet plume at a distance of 1 cm from the discharge area. For the surface device, the optical probe was 30° from the horizontal at a distance of 1 cm from the discharge area. When measuring the spectra of different liquids treated by the two devices, OES detected a discharge area of about 2 mm^2.

Animals and PAL Treatment

Healthy New Zealand Rabbits, weighing 2.35 ± 0.35 kg ($p > 0.05$), were raised in the Experimental Animal Center of Xi'an Jiaotong University under an experimental animal production license [SCXK (shaan) 2008-008] and animal use certificate [SYXK (shaan) 2008-002] issued by the Science and Technology department of Shaanxi province. They were housed individually in clean cages and were given water and a diet of pellets ad libitum. The animal house was maintained at a room temperature of about 20°C and 60% relative humidity. Twenty-one rabbits were randomly divided into seven groups of three rabbits each. Before treatment, all rabbits were anesthetized with sodium pentobarbital by slow injection *via* an ear side vein. Then, the surgical area was sterilized with iodine after gently removing hair. The puncture needles were used to inject the preparations at 0.3–0.5 cm below the tip of the third trochanter of the femur. Each of the rabbits was given 0.4 ml of prepared PAL and an equal volume of physiological solution was given to the control rabbits. After surgery, cefuroxime sodium was injected to reduce inflammation. Acute toxicity experiments in response to injection of PAL into bone marrow were performed at a dose of 700 μL saline using the above surgical procedures. During the experimental period (30 days post-injection), the rabbits were observed daily for any adverse effects such as illness or death, including changes in mental, dietary, and diarrhea status. After fasting overnight, all animals were sacrificed to collect blood and organ samples.

Analysis of Blood Biochemical Index and Blood Cell

At 8–9 am 30 days after surgery, blood from each rabbit was drawn from an ear vein. Then 1.5 ml of blood was injected into a vacuum anticoagulant tube containing EDTA that was gently

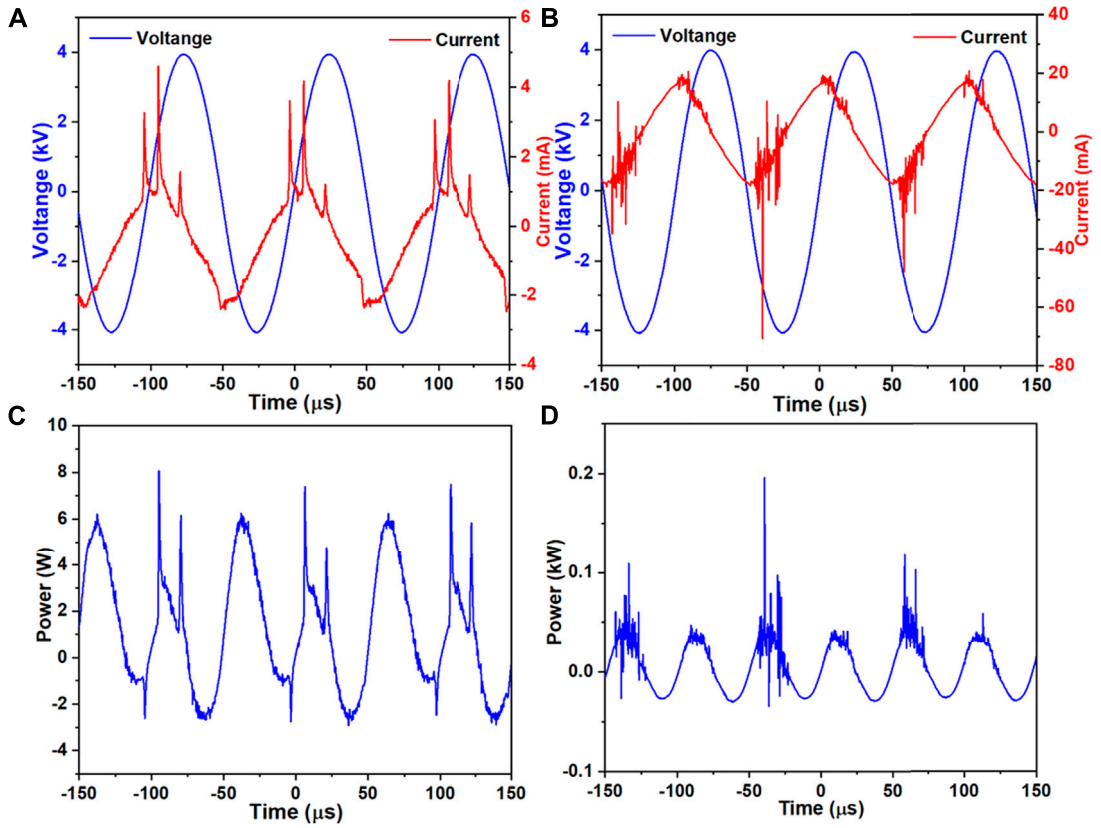

FIGURE 2 | Waveforms of voltage and current **(A, B)** and power **(C, D)** for the jet **(A, C)** and surface **(B, D)** devices.

inverted several times to mix the anticoagulant and blood. Whole blood was used for routine blood testing, which was performed by an automatic blood cell analyzer (Mindray veterinary automatic blood cell analyzer; model: BC-2800vet). The remaining 3.5 ml of blood was injected into a 15 ml EP tube, which was placed on a table at a tilt of 30° for 30 min. Serum, used to test liver and kidney function and other biochemical indicators, was obtained by centrifugation of the whole blood at 3,000 rpm for 10 min. All biochemical indexes were tested by an automatic biochemical analyzer (Shenzhen Rayto life science co. Ltd.; model: Chemray 240).

Coefficients of Vital Organs

The rabbits were weighed on day 30 and sacrificed after blood was taken and the abdomen and chest were opened with a scalpel to assess the organs. The connective tissue around the heart, liver, spleen, kidney, and lung was cut away and these organs were excised and weighed. The coefficient of an organ is expressed as organ index = weight of the organ (g)/weight of the rabbit (g) × 100%.

Histopathological Examination

After photographing each organ, small pieces of tissues from the same part of the same organ (heart, liver, lung, and kidney) were put into 4% paraformaldehyde, which was prepared in advance, and fixed at 4°C for 12 h. Subsequently, they were dehydrated in 30% sucrose and then embedded in OCT (optimal cutting temperature) compound. The tissue specimens were sliced into 5 μm sections with a freezing microtome (Leica CM1950, Leica Biosystems Nussloch GmbH, Germany) and then stained with hematoxylin and eosin (HE), according to standard protocols. After that, tissue slides were processed for histopathological examination under an optical microscope (BX53 and DP73, Olympus, Tokyo, Japan).

Statistical Analysis

In this study, SPSS 23 statistics software was used for statistical analysis. All data are expressed as mean ± standard error of the mean (SEM) for three independent experiments and analyzed by an independent sample *t*-test and one-way analysis of variance (ANOVA), followed by post-hoc multiple comparisons tests such as LSD and Duncan's test. Differences were considered statistically significant when the p value was less than or equal to 0.05 ($p \leq 0.05$) with a confidence interval of 95%.

RESULTS

Physicochemical Properties and Long-Lived RONS of PALs

As shown in **Figures 3A,B**, there were only small differences in the pH and ORP of the 0.9% NaCl solution, PBS and cell culture

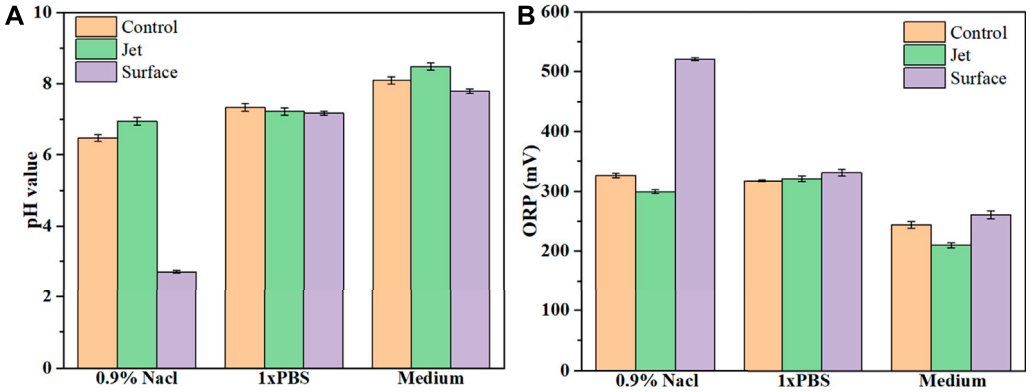

FIGURE 3 | Values of pH **(A)** and ORP **(B)** in control, plasma jet- and surface-treated 0.9% NaCl solution, PBS, and 1,640 medium. Solutions were treated by the plasma jet or surface devices for 3 min.

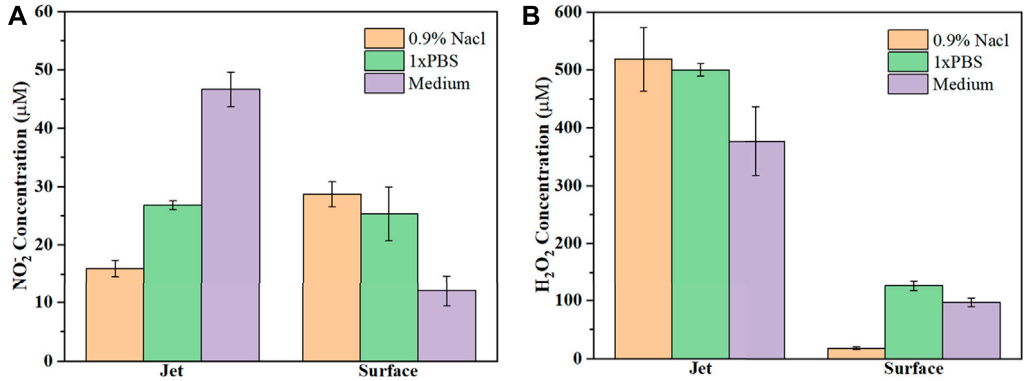

FIGURE 4 | Concentration of **(A)** NO_2^- and **(B)** H_2O_2 in the three types of PALs. All solutions are treated by the plasma jet or surface device for 3 min.

medium for the control group (no plasma treatment), mainly due to different liquid components. When comparing the control and plasma jet groups, we found that pH and ORP in PBS was little affected by jet treatment, however, the pH of the 0.9% NaCl solution and culture medium increased slightly while ORP exhibited a downward trend after jet treatment. In the case of the plasma surface device, the pH of all three solutions decreased when compared with the control and plasma jet groups. In contrast, we found that plasma surface treatment reduced the pH of the 0.9% NaCl solution much more than PBS and culture medium. ORP in PALs exposed to plasma surface treatment was negatively correlated with pH. **Figures 4A,B** shows the concentration of H_2O_2 and NO_2^- in the PALs. We found that the H_2O_2 concentration produced by the jet device was more than twice as high as that produced by the surface device, while there was less difference in the generation of NO_2^- in the liquids exposed to these two devices.

Spectra Characteristics

OES was used to determine the excited products of plasma treatment. Emission spectra were measured for treatment of PBS, 0.9% NaCl solution and RPMI 1640 medium by the He+0.5% O_2 plasma jet (**Figures 5A–C**, respectively) and the plasma surface device (**Figures 5D–F**, respectively). For both the plasma jet and surface devices, the spectral bands were the same regardless of the solution being treated, but the intensity of each band varied slightly. However, the plasma jet and surface devices had quite different emission spectra. The spectrum of the plasma surface device was mainly composed of the first negative band of $N_2^+(B_2\Sigma u^+ \rightarrow X_2\Sigma g^+)$, the second positive band of $N_2(C_3\Pi u \rightarrow B_3\Pi g)$, and the second order diffraction of $N_2(C_3\Pi u \rightarrow B_3\Pi g)$. In addition to the first negative band of $N_2^+(B_2\Sigma u+ \rightarrow X2\Sigma g+)$ and the second positive band of N2(C3Πu→B3Πg), the spectrum of the plasma jet device also contained the band of OH radicals and some excited states of He.

Acute Toxicity Test by Different PAL Injections

Acute toxicity experiments were conducted by injecting PAL into the bone marrow of rabbits. As shown in **Table 1**, no rabbit died after injection of 700 μL plasma jet- or plasma surface-treated PAL. We continuously observed the rabbits for one month after

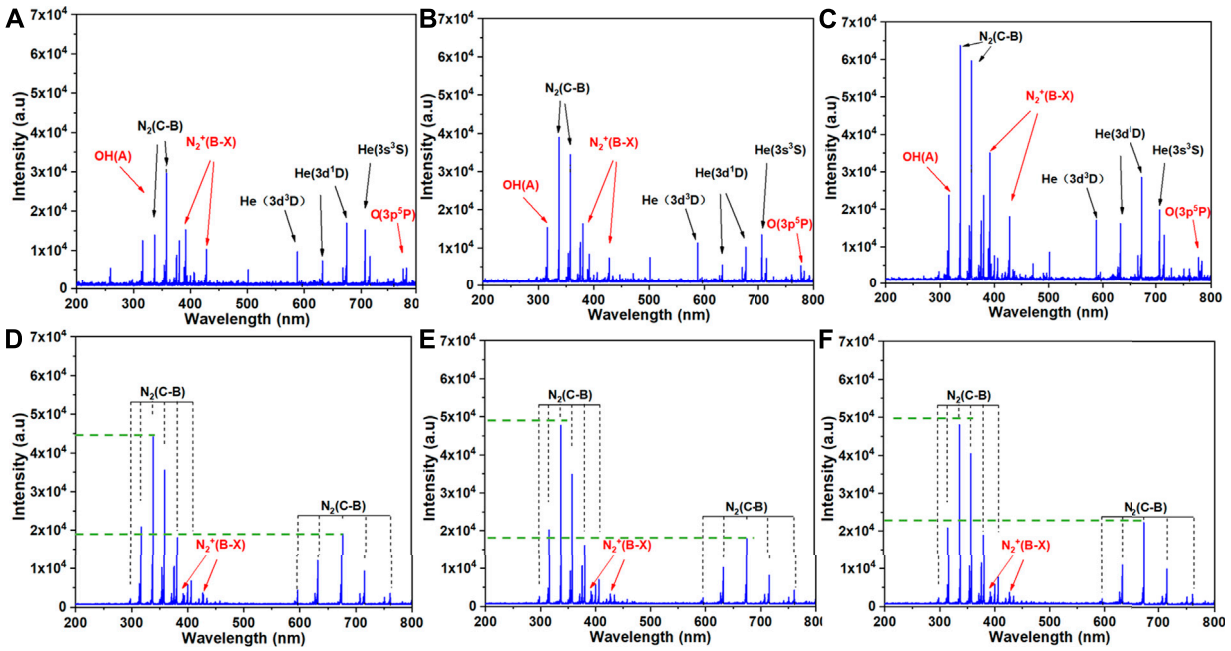

FIGURE 5 | Emission spectra of the two plasma discharge devices in the presence of the three types of solution: **(A)** J-P, **(B)** J-N, **(C)** J-M, **(D)** S-P, **(E)** S-N and **(F)** S-M. The six treatment groups are described in Experimental setup and methods.

TABLE 1 | Acute toxicity tests of PAL treatments of New Zealand rabbits.

Treatment	Plasma dose (μL)	Rabbit numbers	Initial body weight (kg)	Final body weight (kg)	Deaths	MTD (μL)
Jet	700	6	2.5 ± 0.2	3.0 ± 0.3	0	>700
Surface	700	6	2.5 ± 0.3	3.0 ± 0.3	0	>700

PAL injection. For either plasma jet- or plasma surface-treated PALs, body weight of the rabbits after PAL injection was similar to that of the control group ($p > 0.05$). The rabbits showed no abnormal behavior, such as mental state, excretion, food intake, etc. Therefore, the maximum tolerated dose (MTD) of PAL injection in the bone marrow of rabbits is greater than 700 μL.

Changes of Body Weight and Vital Organs After PAL Injection

Throughout the experimental period, no abnormal behavior or symptoms were observed in the rabbits. To evaluate the effect of different PALs, body weight and several vital organs were assessed 30 days after injection. There was no significant change in body weight between groups ($p > 0.05$; **Figure 6A**). After sacrificing the rabbits, organ coefficients were calculated and are shown in **Figure 6B**. No obvious differences in cardiac index, liver index, spleen index, lung index, or kidney index were found among the groups ($p > 0.05$).

Furthermore, post-mortem observations revealed that the heart, liver, spleen, lung, and kidneys of the rabbits in each treatment group had a shiny surface, uniform color, and a compact and flexible texture, as shown in **Figure 6C**, indicating that no abnormal organ morphology and no obvious macroscopic lesions emerged after different PAL treatments. Additionally, it can be seen in the images of **Figure 6C** that there were no visible differences in size, color, appearance, or morphology of each organ between the control group and the different PAL treatment groups.

Histopathological Changes in Vital Organs After PAL Injection

To assess the effect of the different PALs on microscopic tissue structure, frozen sections of the heart, liver, lung, and kidneys were processed for HE staining and visualization by light microscopy. **Figure 7**shows that there were no unusual pathological changes in the heart, liver, lung, and kidney tissue sections of the rabbits in each treatment group.

The images of heart tissue from each group showed that heart structure was intact and myocardial cells were cylindrical. The myocardial fibers were neatly arranged with clear horizontal lines, and no obvious atrophy, degeneration, hypertrophy, or necrosis was observed. In addition, no abnormalities, such as hemorrhage,

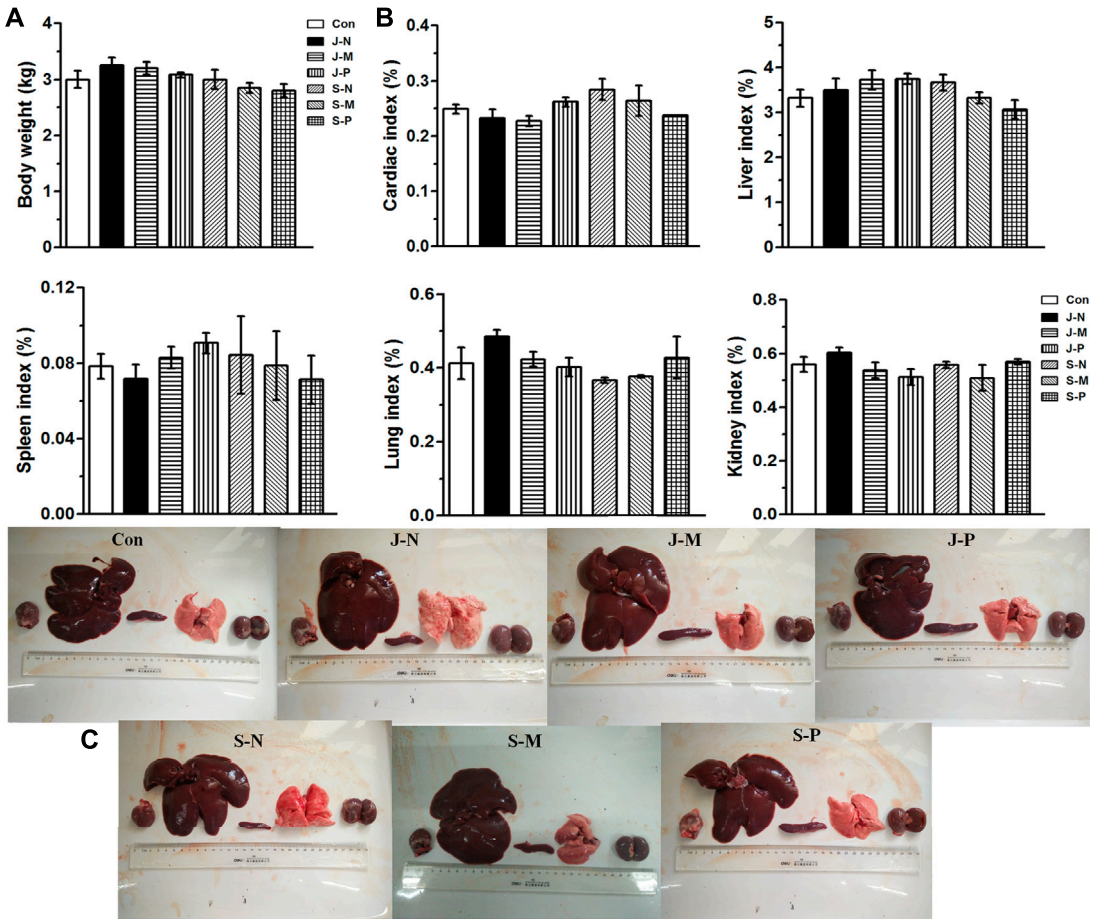

FIGURE 6 | Effects of different PALs at 30 days after injection on **(A)** body weight; **(B)** organ coefficient, including cardiac index, liver index, spleen index, lung index, and kidney index; **(C)** photographs of vital organs (heart, liver, spleen, lungs, and kidneys) in New Zealand rabbits (n = 3 rabbits/group, mean ± SEM). The control and six treatment groups (Con, J-N, J-M, J-P, S-N, S-M, and S-P) are as described in Experimental setup and methods.

were observed in the myocardial interstitium. This illustrated that there was no damage to the heart tissue after different PAL treatments and there were no significant differences when compared with the control group (**Figure 7**).

Liver structure appeared normal, with the central vein, hepatic sinus, hepatic lobule, and portal area clearly visible. Moreover, hepatocytes were arranged tightly and tidily, with the intermediate nucleus and the morphology being clear. No abnormalities, such as necrosis and degeneration, were seen in the liver cells. The liver sections showed no hyperplasia of collagen fibers in the central vein or perisinusoidal space, as well as no infiltration of the inflammatory cells or proliferation of connective tissue in the manifold area after different PAL treatments and no visible difference when compared to the control group (**Figure 7**).

The lung tissue structure was complete and clear, and the lung cells were regularly arranged without inflammatory cell infiltration. The alveoli were uniform in size, and no inflammatory exudates or thrombus were seen in the alveolar cavity or the capillaries of the alveolar wall, respectively. The epithelium of all the levels of bronchioles was intact, and no deformation or dilatation of each bronchiole, as well as no necrosis or degeneration of each bronchiole epithelium, was observed. No pulmonary interstitial inflammation, fibrosis, pulmonary edema, alveolar hemorrhage, emphysema, hyaline membrane formation, alveolar epithelial hyperplasia, etc., occurred after different PAL treatments and there was no difference when compared to the control group.

The structure of the renal tissue was complete and the epithelial cells of the renal tubules were arranged regularly, and the renal cortex, medulla, and nephrons were visible and had normal structure. There was no abnormal change in the shape of the glomerulus and there were no obvious pathological changes in the proximal and distal renal convoluted tubules. Additionally, we observed no infiltration of inflammatory cells in the renal interstitium nor any infiltration of inflammatory cells, fibrinoid necrosis, or thrombosis into the blood vessels of the kidneys. Therefore, we observed no kidney injury in response to the different PAL treatments, and no apparent difference was seen between the PAL treatment and control groups.

Changes of Blood Index After PAL Injection

To check for toxic side effects of the different PAL injections, we assessed several blood parameters in the rabbits, including

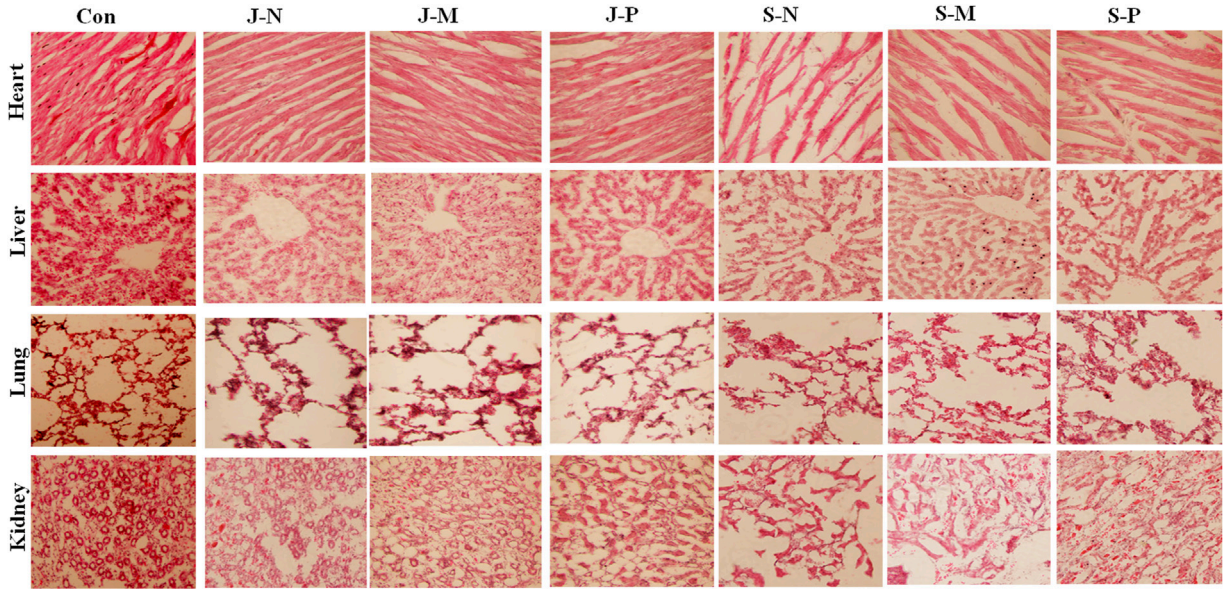

FIGURE 7 | The histomorphological features of New Zealand rabbits after different PAL treatments. HE-stained images showed no pathological changes in heart, liver, lung, or kidney tissue when compared with the control group.

TABLE 2 | Effect of different PALs on blood cell and hemoglobin parameters.

Parameter	Con	J-N	J-M	J-P	S-N	S-M	S-P	*p* Value
WBC (10^9/L)	9.2 ± 0.6	10 ± 1	10 ± 1	11 ± 2	9.0 ± 0.6	10 ± 1	10 ± 3	0.985
Lymph (10^9/L)	6.4 ± 0.7	7.5 ± 0.7	5 ± 1	5 ± 1	4.6 ± 0.5	4.3 ± 0.9	4 ± 2	0.215
Mon (10^9/L)	0.30 ± 0.06	0.3 ± 0.1	0.23 ± 0.09	0.33 ± 0.09	0.27 ± 0.03	0.30 ± 0.06	0.23 ± 0.09	0.954
Gran (10^9/L)	2.6 ± 0.2b	2.2 ± 0.5b	4.2 ± 0.6ab	5.9 ± 0.7a	4.2 ± 0.2ab	5.2 ± 0.3a	6 ± 1a	0.008
Lymph (%)	81.0 ± 0.9a	70 ± 10ab	60 ± 20abc	42 ± 5c	51 ± 2bc	43 ± 5c	38 ± 5c	0.011
Mon (%)	3.9 ± 0.5	6 ± 3	2.4 ± 0.6	3.3 ± 0.7	3.3 ± 0.3	2.8 ± 0.3	2.8 ± 0.2	0.497
Gran (%)	15 ± 1b	22 ± 7b	30 ± 20ab	55 ± 5a	46 ± 2a	54 ± 5a	59 ± 5a	0.005
RBC (10^{12}/L)	5.5 ± 0.1	5.0 ± 0.1	5.5 ± 0.7	5.7 ± 0.1	6.4 ± 0.2	6.0 ± 0.4	5.8 ± 0.5	0.275
HGB (g/L)	103 ± 2	91 ± 4	100 ± 10	109.3 ± 0.3	118 ± 7	119 ± 5	108 ± 5	0.120
HCT (%)	40.7 ± 0.4	39 ± 1	40 ± 4	38.50 ± 0.06	42 ± 2	45 ± 2	40 ± 2	0.447
MCV (fL)	74 ± 1	78.3 ± 0.3	73 ± 3	68 ± 1	69 ± 3	70 ± 2	69 ± 5	0.158
MCH (pg)	18.7 ± 0.5	18.2 ± 0.3	19.0 ± 0.9	19.2 ± 0.3	18.3 ± 0.5	18.7 ± 0.5	19 ± 1	0.948
MCHC (g/L)	276 ± 5	287 ± 7	281 ± 5	283 ± 6	280 ± 5	279 ± 4	277 ± 5	0.836
RDW (%)	15.5 ± 0.7	15.7 ± 0.7	15.8 ± 0.1	16.1 ± 0.5	16.1 ± 0.3	16.2 ± 0.3	16.5 ± 0.5	0.804
PLT (10^9/L)	360 ± 40	520 ± 20	530 ± 20	520 ± 40	510 ± 50	510 ± 40	500 ± 30	0.086
MPV (fL)	7.4 ± 0.2	7.6 ± 0.4	8.2 ± 0.7	7.1 ± 0.4	7.2 ± 0.2	6.6 ± 0.6	7.00 ± 0.06	0.274
PDW (fL)	18.5 ± 0.4	18.0 ± 0.5	18 ± 2	17.8 ± 0.2	18.0 ± 0.4	17.6 ± 0.6	17.9 ± 0.5	0.987
PCT (%)	0.27 ± 0.06	0.33 ± 0.05	0.31 ± 0.09	0.22 ± 0.06	0.21 ± 0.02	0.24 ± 0.02	0.19 ± 0.08	0.640

See Glossary, *for definitions of the parameters in the first column. The mean values of rows with the different superscript (a, b, c) are significantly different from each other (*$p < 0.05$*). Letter ab indicates that the value is not obviously different from either a or b. Letter bc indicates that the value is not obviously different from either b or c. Letter abc indicates that the value is not obviously different from either a, b, or c.*

biochemical indicators of liver and kidney function, electrolyte levels, myocardial enzymes, antioxidant levels, glucose metabolism, and lipid metabolism.

Table 2 shows changes in blood cell and hemoglobin parameters after the injection of different PALs into the bone marrow. We observed that the number of white blood cells (WBC), lymphocytes (Lymph), monocytes (Mon), red blood cells (RBC), the percentage of mononuclear cells (Mon%), hemoglobin (HGB), hematocritg (HCT), mean red blood cell volume (MCV), mean erythrocyte hemoglobin content (MCH), mean erythrocyte hemoglobin concentration (MCHC), erythrocyte distribution width variation coefficient (RDW), mean platelet volume (MPV), platelet distribution width (PDW), and platelet backlog (PCT) were not affected by the different PAL treatments.

There were significant differences in the number of neutrophil granulocytes (Gran) among the groups; however, the values for

TABLE 3 | Analysis of liver function after different PAL treatments.

Parameter	Con	J-N	J-M	J-P	S-N	S-M	S-P	*p* Value
ALT (U/L)	60 ± 10	45 ± 9	46 ± 3	61 ± 6	53 ± 5	54 ± 4	58 ± 8	0.661
AST (U/L)	50 ± 10	48 ± 8	47 ± 7	51 ± 8	54 ± 4	50 ± 4	52 ± 1	0.988
ALB (g/L)	25 ± 2	24.2 ± 0.4	24 ± 1	23.8 ± 0.8	24.0 ± 0.5	24.5 ± 0.5	24 ± 1	0.933
T-BIL (μM/L)	10.1 ± 0.6	10 ± 2	9.3 ± 0.6	9.3 ± 0.4	9.9 ± 0.3	8 ± 1	8.5 ± 0.2	0.606
D-BIL (μM/L)	10 ± 2	10 ± 2	10 ± 1	10.1 ± 0.1	9.7 ± 0.2	10 ± 2	8.8 ± 0.5	0.997
ALP (U/L)	60 ± 10	67 ± 9	67 ± 9	70 ± 10	70 ± 10	68 ± 3	65 ± 8	0.949

See Glossary, *for definitions of the parameters in the first column.*

TABLE 4 | Kidney function and electrolytes after different PAL treatments.

Parameter	Con	J-N	J-M	J-P	S-N	S-M	S-P	p Value
BUN (mg/dl)	15.4 ± 0.1	16 ± 1	16.7 ± 0.6	15.5 ± 0.9	16 ± 2	15.5 ± 0.5	17 ± 3	0.968
UA (μM/L)	160 ± 20	140 ± 30	140 ± 30	119 ± 4	140 ± 20	140 ± 30	140 ± 20	0.962
CR (μM/L)	90 ± 10	91 ± 5	92 ± 2	87 ± 9	91 ± 5	94 ± 2	90 ± 5	0.976
Zn (μM/L)	13.9 ± 0.7	14.1 ± 0.2	14.4 ± 0.4	13.7 ± 0.5	14.1 ± 0.5	13.4 ± 0.5	14.7 ± 0.6	0.599
Fe (μM/L)	41 ± 5	42 ± 1	40.3 ± 0.7	41 ± 4	40 ± 4	41 ± 6	41 ± 3	1.000
Mg (mM/L)	1.05 ± 0.04	1.11 ± 0.01	1.12 ± 0.07	1.03 ± 0.02	1.06 ± 0.02	1.08 ± 0.05	1.08 ± 0.01	0.605
Cl (mM/L)	101 ± 2	100 ± 2	105 ± 3	98 ± 4	99 ± 2	105 ± 4	101 ± 3	0.561
p (mM/L)	2.0 ± 0.2	2.00 ± 0.08	2.0 ± 0.3	2.04 ± 0.05	2.0 ± 0.2	2.1 ± 0.2	1.99 ± 0.02	0.999
Ca (mM/L)	2.6 ± 0.1	2.5 ± 0.2	2.4 ± 0.4	2.5 ± 0.2	2.52 ± 0.09	2.6 ± 0.1	2.4 ± 0.1	0.959

See Glossary, *for definitions of the parameters in the first column.*

each group were within the normal range (2.0–7.5). In addition, the percentage of neutrophil granulocytes (Gran%) and lymphocytes (Lymph%) were clearly affected by the PAL treatments. After performing a *post-hoc* multiple comparisons or independent sample *t*-test, we found that the Lymph% in the control group was significantly higher than in the JP, SN, SM, and SP groups. The Gran% in the control group was clearly lower than in the JM, JP, SN, SM, and SP groups. The platelet count (PLT) tended to be different among the groups ($p = 0.086$), and it was found that PLT was most notably elevated in all PALs with respect to the control group, although they were all within the normal range (100–712).

Alanine transaminase (ALT), aspartate transaminase (AST), albumin (ALB), total bilirubin (T-BIL), direct bilirubin (D-BIL), and alkaline phosphatase (ALP), which are indicators of liver health, did not differ between the different PAL treatments and control group at day 30, indicating that injection of PALs into bone marrow did not cause liver damage (**Table 3**).

Table 4 shows that different PAL treatments did not modify the concentration of nephrotoxicity markers [blood urea nitrogen (BUN), uric acid (UA), creatinine (CR)] and electrolytes (Zn, Fe, Mg, Cl, P, and Ca) when compared to the control group. Therefore, the different PAL injections were not harmful to kidney function and did not interfere with electrolyte balance.

Furthermore, we analyzed myocardial enzyme levels and antioxidant index after different PAL treatments. The analysis showed that different types of PAL did not affect the myocardial enzymes lactate dehydrogenase (LDH) and creatine kinase (CK), nor the antioxidant indexes superoxide dismutase (SOD), malondialdehyde (MAD), and glutathione peroxidase (GPX) (**Table 5**, all p values >0.05). These results indicate that different PAL treatments do not cause myocardial damage or systemic oxidative stress.

Finally, we investigated serum lipid and glucose metabolism after the different PAL injections into the rabbits. The results did not reveal any significant changes in the levels of triglyceride (TG), high-density lipoprotein cholesterol (HDL-C), low-density lipoprotein cholesterol (LDL-C), glycated serum protein (GSP) or glucose (GLU) between the control group and different PAL treatments (**Table 6**). It can be inferred therefore that the PAL treatments did not cause lipid or glucose metabolism disorders.

DISCUSSION

PALs containing various active substances are an area of intense research in the biomedical field, especially in cancer therapy. It has been shown that atmospheric-pressure cold plasma selectively inhibits the growth of cancer cells and causes relatively less or no cytotoxicity in normal cells [10]. As a promising novel approach to cure certain cancers, studies of PAL safety, in assessing the potential side effects, are a basic premise, and it could be classified into three stages: pre-clinical trials, clinical trials *in vivo*, and detection trials of adverse reactions after approval [21]; the present experiments represent a non-clinical study of PALs. A review of PAL safety studies concluded that up to 25% of toxic reactions observed in animal experiments may occur in humans [22]. Therefore, we initiated the current study to test the safety of PALs and to provide a basis for clinical research and applications.

TABLE 5 | Myocardial enzyme and antioxidant index after different PAL treatments.

Parameter	Con	J-N	J-M	J-P	S-N	S-M	S-P	*p* Value
LDH (U/L)	600 ± 100	700 ± 100	600 ± 200	700 ± 200	730 ± 30	680 ± 90	700 ± 200	0.999
CK (U/L)	1,600 ± 900	950 ± 30	960 ± 80	1,000 ± 300	1,000 ± 100	1,000 ± 300	1,000 ± 100	0.887
SOD (U/mL)	300 ± 20	320 ± 3	320 ± 40	330 ± 20	330 ± 20	340 ± 30	340 ± 20	0.913
MDA (nM/ml)	5.1 ± 0.6	4 ± 1	4.4 ± 1.0	4.5 ± 0.8	4.6 ± 0.2	4.4 ± 1.0	4.8 ± 0.5	0.995
GPX (U)	220 ± 10	230 ± 20	240 ± 20	226 ± 9	230 ± 10	250 ± 10	250 ± 20	0.857

See Glossary, *for definitions of the parameters in the first column.*

TABLE 6 | Lipid and glucose metabolism after different PAL treatments.

Parameter	Con	J-N	J-M	J-P	S-N	S-M	S-P	*p* Value
TG (mM/L)	1.7 ± 0.2	1.5 ± 0.1	1.49 ± 0.04	1.52 ± 0.04	1.52 ± 0.09	1.54 ± 0.08	1.57 ± 0.08	0.772
HDL-C (mM/L)	0.5 ± 0.1	0.49 ± 0.06	0.48 ± 0.04	0.52 ± 0.01	0.5 ± 0.2	0.5 ± 0.1	0.5 ± 0.1	0.999
LDL-C (mM/L)	3.3 ± 0.1	2.6 ± 0.3	2.7 ± 0.5	2.6 ± 0.8	2.4 ± 0.3	2.6 ± 0.3	2.4 ± 0.3	0.857
GSP(mM/L)	2.1 ± 0.2	2.2 ± 0.3	2.2 ± 0.2	1.8 ± 0.1	2.1 ± 0.1	2.2 ± 0.3	2.2 ± 0.4	0.903
GLU (mM/L)	6.7 ± 0.8	7.1 ± 0.1	8 ± 1	8 ± 2	8.7 ± 0.9	11 ± 3	7.4 ± 0.2	0.530

See Glossary, *for definitions of the parameters in the first column.*

As mentioned in the literature, saline, cell culture medium, and PBS have been widely used in plasma-activated fluids since culture medium is suited to the study of cancer cells while buffers like saline and PBS have a relatively simple composition [23–26]. Hence, we chose them as plasma-activated liquids in the present work. We analyzed changes in the physicochemical properties of the different solutions after plasma jet/surface treatment and found that different PALs had different pH and ORP values. The PBS used in this study contained a large amount of potassium hydrogen phosphate (weak acid, KH_2PO_4, pH 4.4–4.9) and sodium hydrogen phosphate (weak base, Na_2HPO_4, pH 9.5) that makes it a strong buffer, so the pH and ORP of PBS did not change after the jet treatment when compared with the control group (**Figures 3A,B**). Jirasek et al. [27] reported that 85% hypochlorite in a physiological NaCl solution treated by a plasma jet existed in the form of NaOCl, and as a consequent had a high pH, consistent with our results (**Figure 3A**). As RPMI 1640 medium includes polysaccharides, amino acids, vitamins, and many other compounds, the increased pH of the jet-treated culture medium might be due to reaction of these organic compounds with plasma-generated chemicals (particularly ROS and RNS). Moreover, because of the disparate discharge gases of these two plasma devices and the greater variety of gases in the plasma surface discharge, the rapid decrease of pH in the three kinds of surface-treated solutions might be caused by reaction of the vapor-phase NO_x species with H_2O molecules to produce HNO_3, resulting in the generation of a large number of H^+ ions [28, 29]. The pH of 1,640 medium and PBS after plasma surface treatment did not decrease as significantly as that of saline solution, which was due to the buffering ability of 1,640 medium and PBS. ORP, a concentration-dependent indicator of solution oxidation capacity, is commonly used to evaluate the global level of RONS in PALs. Changes in ORP are often opposite to those in pH, which may result from PALs having a greater oxidizing capacity at lower pH [30].

In this study, the plasma jet was used with He+0.5% O2 and the plasma surface with ambient air, which are considered the most commonly used methods of applying plasma [10, 31]. Our previous results showed that 3 min of PAL treatment with either device could inhibit the growth of cancer cells since they generate various kinds of ROS and RNS, like hydroxyl radical (OH), hydrogen peroxide (H_2O_2), atomic oxygen (O), nitric oxide (NO), and peroxynitrite anion ($ONOO^-$) (**Figure 4**) [10, 31]. **Figure 5** shows the active particles in the gaseous state, and prior studies noted that only small amounts of O_3, H_2O_2, OH, and NO_x could pass through the gas-liquid interface [23, 24], while other ROS/RNS are transferred into liquid via secondary reactions [32]. Unlike H_2O_2, which can penetrate the cell membrane, most other radicals cannot and so may play roles in cell-signal transduction [10]. Furthermore, the addition of 0.5% O2 generated more ROS and caused more cell death compared with He plasma alone [10]. The generation pathway of H_2O_2 is mainly due to the combination reaction of aqueous hydroxide radical (.OH) [33]. As shown in **Figure 5**, bands of OH radicals were observed in the spectra of three different liquids treated by the plasma jet device, but not in the plasma surface device. Therefore, the concentration of H_2O_2 produced by the jet was much higher than that produced by the surface device (**Figure 4B**). Bands of N excitation were found in both devices for treating three different liquids (**Figure 5**), and they had significant effects on the production of NO_2 and NO_3.

PAL is administered *via* intravenous, intra-arterial, intramuscular, oral, intra-luminal injection, and other routes [34, 35]. In the present experiments, we adopted the route of intramedullary injection. Firstly, intramedullary injection is suitable for myeloma and blood tumors, especially since pathogenesis is in the bone marrow cavity, and the drug can

directly act on the tumor site without being affected by the bone marrow-blood barrier. Likewise, many stem cells exist in bone marrow, and the current study provides a basis for further treatment of tumors by intramedullary injection of PAL to kill tumor stem cells [36]. Lastly, the advantage of intramedullary injection is that it can induce both local and systemic effects. Additionally, Wei Zhang et al. [37] found both intravenous and paravertebral dexmedetomidine attenuated independent lung injury.

Generally, we chose a higher dose of material for the acute toxicity test, and our results showed that rabbits injected with 700 μL of PAL did not exhibit any mortality, loss of mobility, or visible signs of toxicity when compared to the control group during the 30-days experimental period.

Changes in body and organ weight are sensitive indicators of the general health of animals [38]. Studies show that a loss of body weight of more than 20% should be considered a serious condition that can also impact organ size and weight [39–41]. Thus, the organ-to-body weight index is regarded as a useful indicator of the toxicity of new compounds. No morbidity or mortality was evident throughout the experimental period, and body weight of the rabbits actually increased similarly in the control and PAL-treated groups by day 30 (**Figure 6A**). Furthermore, in comparison with the control group, PAL treatment caused no lesions in the heart, liver, spleen, lung, or kidney (**Figure 6C**), and there were no significant differences in organ index (**Figure 6B**). Thus, we conclude that the different PALs had no adverse effects on growth of the rabbits.

Changes in histopathology of organs, examined by microscopy, are also considered a basic test of the safety of the materials [42]. No abnormality was observed in histopathological sections of the organs in this study (**Figure 7**), indicating that the different PALs did not induce any toxic symptoms in the major internal organs, including the heart, liver, lung, and kidney.

Hematological analyses are of critical importance in the evaluation of toxic effects induced by materials [43]. Due to blood being the main transporter of many xenobiotics in the body, blood components are exposed to numerous toxic compounds that induce damage or destruction of blood cells and harm normal physiological function [44, 45]. Our analyses of blood biochemistry in the treated rabbits suggested that the three types of PAL did not alter normal liver/hepatic/myocardial function, oxidative stress, and lipid or glucose metabolism. Observations of these blood parameters were consistent with measurements of body weight, organ index, organ appearance, and organ histopathology, further validating the absence of toxicity in response to PALs. Furthermore, our observations of blood parameters normally associated with systemic toxic symptoms showed that most were not affected by PAL treatment. In addition, the increase in the PLT count after PAL treatment revealed that PAL might accelerate blood clotting, as PLTs are small pieces of cytoplasm that detach from the cytoplasm of mature megakaryocytes of the bone marrow and are essential for hemostasis [46]. The findings of other studies also suggest that platelets are important for cold physical plasma-facilitated blood coagulation [47, 48]. However, Gran% increased and Lymph% decreased after PAL treatment, suggesting that PAL treatment might improve the activity of the immune system. Shi et al. [49] took peripheral blood lymphocytes from 20 healthy adults and found that plasma could induce apoptosis of lymphocytes as evidenced by leakage of protein, nucleic acid, and K^+ after treatment, consistent with our observations of lymphocytes. It is worth noting that different immune cells exhibit distinct sensitivities after plasma treatment [50, 51]. Bundscherer et al. [51] observed that the number of $CD4^+$ T helper cells, a kind of lymphocyte, decreased significantly in a time-dependent manner after 60 s of plasma treatment and there was a marked attenuation in monocyte growth after exposure to plasma for 360 s. In our study, 3 min of plasma treatment reduced Lymph% but did not affect Mon%, which was similar to the results of Bundscherer et al. [51]. Therefore, we speculate that the different changes in the levels of lymphocytes and monocytes after plasma treatment may be due to the duration of plasma treatment and the distinct sensitivity of immune cells to plasma. Meanwhile, as white blood cell count was not significantly different among groups, we suggest the increase of Gran% may be due to the reduction of Lymph%. Moreover, Lardner A (2001) reported that extracellular pH affected immune cells and immune function [52], so we suggested that the different pH values of PALs (**Figure 3**) might contribute to the changes of Gran% and Lymph% (**Table 2**).

Although the physicochemical properties and the active substances varied among the three PALs in our study, PAL injection did not cause toxicity, indicating that PAL treatment is safe for New Zealand rabbits when injected into the bone marrow, and therefore has great potential for development of clinical therapeutics. In the future, we will evaluate the safety and efficacy of PAL in humans and principally focus on clinical application of PALs in hematologic tumors such as leukemia and multiple myeloma. Specifically, PAL will be used alone or in association with other conventional chemotherapeutic agents to kill cancer cells and stem cells within the marrow cavities of patients during myeloablative treatments prior to bone marrow transplantation.

CONCLUSION

This work provides a foundation for safety and toxicity studies of PALs. PAL treatment of New Zealand rabbits by intra-bone marrow injection was not lethal and did not lead to any acute toxicity. In addition, PAL treatments did not affect body weight or the coefficient, appearance, or histopathology of the major organs. These results were consistent with blood biochemical indexes showing that PAL treatment had no observable effects on liver/renal/myocardial function, oxidative status, electrolyte and glucose levels, or lipid metabolism. Furthermore, PAL treatment decreased the percentage of lymphocytes while increasing the percentage of neutrophil granulocytes. In conclusion, the results of the present study indicate that PAL treatment can be used safely

on New Zealand rabbits without significant toxicity when injected into bone marrow.

DATA AVAILABILITY STATEMENT

The original contributions presented in the study are included in the article/supplementary material, further inquiries can be directed to the corresponding authors.

ETHICS STATEMENT

The animal study was reviewed and approved by the Experimental Animal Center of Xi'an Jiaotong University which has obtained the experimental animal production license [SCXK (shaan) 2008-008] and animal use certificate [SYXK (shaan) 2008-002] issued by the Science and Technology department of Shaanxi province.

AUTHOR CONTRIBUTIONS

YX and SP performed the experiments and writing the manuscript; DX and DL conceived and supervised the study; BL, SW, and QL participated in the experiment work; HZ, ZL, and BG contributed to the figures of this study. All authors have read and agreed to the published version of the manuscript.

FUNDING

This work is supported by the National Natural Science Foundation of China (Grant No. 51521065 and 51837008), China Postdoctoral Science Foundation (2017M610639) and Special Fund of China Postdoctoral Science Foundation, State Key Laboratory of Electrical Insulation and Power Equipment (EIPE19309) and Special Fund of Shaanxi Postdoctoral Science Foundation (2017BSHTDZZ04).

REFERENCES

1. Global cancer Observatory. *Cancer today*. https://gco.iarc.fr/today/home.
2. Leary M, Heerboth S, Lapinska K, and Sarkar S. Sensitization of Drug Resistant Cancer Cells: A Matter of Combination Therapy. *Cancers* (2018) 10:483. doi:10.3390/cancers10120483
3. Friberg S, and Nyström A. Cancer Metastases: Early Dissemination and Late Recurrences. *Cancer Growth Metastasis* (2015) 8:43–9. doi:10.4137/CGM.S31244
4. Graves D, Hamaguchi S, and O'Connell D. In Focus: Plasma Medicine. *Biointerphases* (2015) 10:029301. doi:10.1116/1.4922357
5. Shome D, von Woedtke T, Riedel K, and Masur K. The HIPPO Transducer YAP and its Targets CTGF and Cyr61 Drive a Paracrine Signalling in Cold Atmospheric Plasma-Mediated Wound Healing. *Oxidative Med Cell Longevity* (2020) 2020:1–14. doi:10.1155/2020/4910280
6. Hoffmann C, Berganza C, and Zhang J. Cold Atmospheric Plasma: methods of production and application in dentistry and oncology. *Med Gas Res* (2013) 3: 21–15. doi:10.1186/2045-9912-3-21
7. Lou B-S, Lai C-H, Chu T-P, Hsieh J-H, Chen C-M, Su Y-M, et al. Parameters Affecting the Antimicrobial Properties of Cold Atmospheric Plasma Jet. *Jcm* (2019) 8:1930. doi:10.3390/jcm8111930
8. Heinlin J, Isbary G, Stolz W, Morfill G, Landthaler M, Shimizu T, et al. Plasma applications in medicine with a special focus on dermatology. *J Eur Acad Dermatol Venereol* (2011) 25:1–11. doi:10.1111/j.1468-3083.2010.03702.x
9. Thiyagarajan M, Waldbeser L, and Whitmill A. THP-1 leukemia cancer treatment using a portable plasma device. *Stud Health Technol Inform* (2012) 173:515–7.
10. Xu D, Xu Y, Cui Q, Liu D, Liu Z, Wang X, et al. Cold atmospheric plasma as a potential tool for multiple myeloma treatment. *Oncotarget* (2018) 9:18002–17. doi:10.18632/oncotarget.24649
11. Schneider C, Arndt S, Zimmermann JL, Li Y, Karrer S, and Bosserhoff AK. Cold atmospheric plasma treatment inhibits growth in colorectal cancer cells. *Biol Chem* (2018) 400:111–22. doi:10.1515/hsz-2018-0193
12. Schneider C, Gebhardt L, Arndt S, Karrer S, Zimmermann JL, Fischer MJM, et al. Acidification is an Essential Process of Cold Atmospheric Plasma and Promotes the Anti-cancer Effect on Malignant Melanoma Cells. *Cancers* (2019) 11:671. doi:10.3390/cancers11050671
13. Griseti E, Merbahi N, and Golzio M. Anti-Cancer Potential of Two Plasma-Activated Liquids: Implication of Long-Lived Reactive Oxygen and Nitrogen Species. *Cancers* (2020) 12:721. doi:10.3390/cancers12030721
14. Hirst AM, Frame FM, Arya M, Maitland NJ, and O'Connell D. Low temperature plasmas as emerging cancer therapeutics: the state of play and thoughts for the future. *Tumor Biol* (2016) 37:7021–31. doi:10.1007/s13277-016-4911-7
15. Xu D, Liu D, Wang B, Chen C, Chen Z, Li D, et al. *In Situ* OH Generation from O2– and H2O2 Plays a Critical Role in Plasma-Induced Cell Death. *PLoS One* (2015) 10:e0128205. doi:10.1371/journal.pone.0128205
16. Judée F, Fongia C, Ducommun B, Yousfi M, Lobjois V, and Merbahi N. Short and long time effects of low temperature Plasma Activated Media on 3D multicellular tumor spheroids. *Sci Rep* (2016) 6:21421. doi:10.1038/srep21421
17. Adachi T, Tanaka H, Nonomura S, Hara H, Kondo S-i., and Hori M. Plasma-activated medium induces A549 cell injury via a spiral apoptotic cascade involving the mitochondrial-nuclear network. *Free Radic Biol Med* (2015) 79: 28–44. doi:10.1016/j.freeradbiomed.2014.11.014
18. Yan D, Cui H, Zhu W, Nourmohammadi N, Milberg J, Zhang LG, et al. The Specific Vulnerabilities of Cancer Cells to the Cold Atmospheric Plasma-Stimulated Solutions. *Sci Rep* (2017) 7:4479. doi:10.1038/s41598-017-04770-x
19. Canal C, Fontelo R, Hamouda I, Guillem-Marti J, Cvelbar U, and Ginebra M-P. Plasma-induced selectivity in bone cancer cells death. *Free Radic Biol Med* (2017) 110:72–80. doi:10.1016/j.freeradbiomed.2017.05.023
20. Biscop E, Lin A, Boxem WV, Loenhout JV, Backer JD, Deben C, et al. Influence of Cell Type and Culture Medium on Determining Cancer Selectivity of Cold Atmospheric Plasma Treatment. *Cancers* (2019) 11:1287. doi:10.3390/cancers11091287
21. Yao B, Zhu L, Jiang Q, and Xia H. Safety monitoring in clinical trials. *Pharmaceutics* (2013) 5:94–106. doi:10.3390/pharmaceutics5010094
22. Fletcher AP. Drug safety tests and subsequent clinical experience. *J R Soc Med* (1978) 71:693–6. doi:10.1177/014107687807100915
23. Bauer G. The synergistic effect between hydrogen peroxide and nitrite, two long-lived molecular species from cold atmospheric plasma, triggers tumor cells to induce their own cell death. *Redox Biol* (2019) 26:101291. doi:10.1016/j.redox.2019.101291
24. Van Boxem W, Van der Paal J, Gorbanev Y, Vanuytsel S, Smits E, Dewilde S, et al. Anti-cancer capacity of plasma-treated PBS: effect of chemical composition on cancer cell cytotoxicity. *Sci Rep* (2017) 7:16478. doi:10.1038/s41598-017-16758-8
25. Mateu-Sanz M, Tornín J, Brulin B, Khlyustova A, Ginebra M-P, Layrolle P, et al. Cold Plasma-Treated Ringer's Saline: A Weapon to Target Osteosarcoma. *Cancers* (2020) 12:227. doi:10.3390/cancers12010227
26. Tanaka H, Mizuno M, Katsumata Y, Ishikawa K, Kondo H, Hashizume H, et al. Oxidative stress-dependent and -independent death of glioblastoma cells induced by non-thermal plasma-exposed solutions. *Sci Rep* (2019) 9:13657. doi:10.1038/s41598-019-50136-w
27. Jirásek V, and Lukeš P. Formation of reactive chlorine species in saline solution treated by non-equilibrium atmospheric pressure He/O2 plasma jet. *Plasma Sourc Sci. Technol.* (2019) 28:035015. doi:10.1088/1361-6595/ab0930
28. Lukes P, Dolezalova E, Sisrova I, and Clupek M. Aqueous-phase chemistry and bactericidal effects from an air discharge plasma in contact with water: evidence for the formation of peroxynitrite through a pseudo-second-order

post-discharge reaction of H2O2and HNO2. *Plasma Sourc Sci. Technol.* (2014) 23:015019. doi:10.1088/0963-0252/23/1/015019
29. Zhang X, Zhou R, Zhou R, Chen M, Li J, Sun Y, et al. Treatment of Ribonucleoside Solution with Atmospheric-Pressure Plasma. *Plasma Process Polym* (2016) 13:429–37. doi:10.1002/ppap.201500088
30. Zhou R, Zhou R, Prasad K, Fang Z, Speight R, Bazaka K, et al. Cold atmospheric plasma activated water as a prospective disinfectant: the crucial role of peroxynitrite. *Green Chem* (2018) 20:5276–84. doi:10.1039/c8gc02800a
31. Zhong SY, Dong YY, Liu DX, Xu DH, Xiao SX, Chen HL, et al. Surface air plasma-induced cell death and cytokine release of human keratinocytes in the context of psoriasis. *Br J Dermatol* (2016) 174:542–52. doi:10.1111/bjd.14236
32. Tornin J, Mateu-Sanz M, Rodríguez A, Labay C, Rodríguez R, and Canal C. Pyruvate Plays a Main Role in the Antitumoral Selectivity of Cold Atmospheric Plasma in Osteosarcoma. *Sci Rep* (2019) 9:10681. doi:10.1038/s41598-019-47128-1
33. Chen Z, Liu D, Chen C, Xu D, Liu Z, Xia W, et al. Analysis of the production mechanism of H2O2 in water treated by helium DC plasma jets. *J Phys D: Appl Phys* (2018) 51:325201. doi:10.1088/1361-6463/aad0eb
34. Shim J, Kwak BK, Jung J, and Park S. Evaluation of engraftment of superparamagnetic iron oxide-labeled mesenchymal stem cells using three-dimensional reconstruction of magnetic resonance imaging in photothrombotic cerebral infarction models of rats. *Korean J Radiol* (2015) 16:575–85. doi:10.3348/kjr.2015.16.3.575
35. Shi Y, Peng D, Wang D, Zhao Z, Chen B, He B, et al. Biodistribution Survey of Oxidized Single-Wall Carbon Nanohorns Following Different Administration Routes by Using Label-free Multispectral Optoacoustic Tomography. *Ijn* (2019) Vol. 14:9809–21. doi:10.2147/ijn.s215648
36. Feng R, Ning N, Tian M, Peng S, Wang S, Li B, et al. Evaluation of the anticancer effects induced by cold atmospheric plasma on leukemia stem cells. *Plasma Res Express* (2020) 2:024001. doi:10.1088/2516-1067/ab9154
37. Zhang W, Zhang S, Li B, Sun M, and Zhang J. Paravertebral dexmedetomidine as an adjuvant to ropivacaine protects against independent lung injury during one-lung ventilation: a preliminary randomized clinical trial. *BMC Anesthesiol* (2018) 18:67. doi:10.1186/s12871-018-0532-6
38. Chitra B, Ramaswamy RS, and Suba V. Toxicity Evaluation of Pūrṇa Cantirotaya Centūram, a Siddha Medicine in Wistar Rats. *Int scholarly Res notices* (2015) 2015:1–10. doi:10.1155/2015/473296
39. William S. *Guidance Document on the Recognition, Assessment, and Use of Clinical Signs as Humane Endpoints for Experimental Animals Used in Safety Evaluations* ***2000***.
40. Olfert E, Bhasin J, Latt R, Macallum E, Mccutcheon K, Rainnie D, et al. CCAC Guidelines on: Choosing an Appropriate Endpoint in Experiments Using Animals for Research. *Teaching and Testing* (1998). Ottawa, Canada: Canadian Council on AnimalCare.
41. Lazic SE, Semenova E, and Williams DP. Determining organ weight toxicity with Bayesian causal models: Improving on the analysis of relative organ weights. *Sci Rep* (2020) 10:6625. doi:10.1038/s41598-020-63465-y
42. Wolf JC, and Maack G. Evaluating the credibility of histopathology data in environmental endocrine toxicity studies. *Environ Toxicol Chem* (2017) 36: 601–11. doi:10.1002/etc.3695
43. Petterino C, and Argentino-Storino A. Clinical chemistry and haematology historical data in control Sprague-Dawley rats from pre-clinical toxicity studies. *Exp Toxicologic Pathol* (2006) 57:213–9. doi:10.1016/j.etp.2005.10.002
44. Abotsi W, Ainooson G, and Boakye-Gyasi E. Acute and Sub-acute Toxicity Studies of the Ethanolic Extract of the Aerial Parts of Hilleria Latifolia (Lam.) H. Walt.(Phytolaccaceae) in Rodents. *West Afr J Pharm* (2011) 22:27–35.
45. Olson H, Betton G, Robinson D, Thomas K, Monro A, Kolaja G, et al. Concordance of the toxicity of pharmaceuticals in humans and in animals. *Regul Toxicol Pharmacol* (2000) 32:56–67. doi:10.1006/rtph.2000.1399
46. Baccini V, Geneviève F, Jacqmin H, Chatelain B, Girard S, Wuilleme S, et al. Platelet Counting: Ugly Traps and Good Advice. Proposals from the French-Speaking Cellular Hematology Group (GFHC). *Jcm* (2020) 9:808. doi:10.3390/jcm9030808
47. Bekeschus S, Brüggemeier J, Hackbarth C, von Woedtke T, Partecke L-I, and van der Linde J. Platelets are key in cold physical plasma-facilitated blood coagulation in mice. *Clin Plasma Med* (2017) 7-8:58–65. doi:10.1016/j.cpme.2017.10.001
48. Bekeschus S, Brüggemeier J, Hackbarth C, Weltmann K-D, von Woedtke T, Partecke L-I, et al. The feed gas composition determines the degree of physical plasma-induced platelet activation for blood coagulation. *Plasma Sourc Sci. Technol.* (2018) 27:034001. doi:10.1088/1361-6595/aaaf0e
49. Shi X, Zhang G, Yuan Y, Ma Y, Xu G, and Yang Y. Effects of low-temperature atmospheric air plasmas on the activity and function of human lymphocytes. *Plasma Process Polym* (2010) 5:482–8.
50. Haertel B, Volkmann F, von Woedtke T, and Lindequist U. Differential sensitivity of lymphocyte subpopulations to non-thermal atmospheric-pressure plasma. *Immunobiology* (2012) 217:628–33. doi:10.1016/j.imbio.2011.10.017
51. Bundscherer L, Wende K, Ottmüller K, Barton A, Schmidt A, Bekeschus S, et al. Impact of non-thermal plasma treatment on MAPK signaling pathways of human immune cell lines. *Immunobiology* (2013) 218:1248–55. doi:10.1016/j.imbio.2013.04.015
52. Lardner A. The effects of extracellular pH on immune function. *J Leukoc Biol* (2001) 69:522–30.

Conflict of Interest: The authors declare that the research was conducted in the absence of any commercial or financial relationships that could be construed as a potential conflict of interest.

Publisher's Note: All claims expressed in this article are solely those of the authors and do not necessarily represent those of their affiliated organizations, or those of the publisher, the editors and the reviewers. Any product that may be evaluated in this article, or claim that may be made by its manufacturer, is not guaranteed or endorsed by the publisher.

GLOSSARY

ALB albumin
ALP alkaline phosphatase
ALT alanine transaminase
ANOVA analysis of variance
AST aspartate transaminase
BUN blood urea nitrogen
CAP cold atmospheric plasma
CK creatine kinase
CR creatinine
D-BIL direct bilirubin
GLU glucose
GPX glutathione peroxidase
Gran number of neutrophil granulocyte
Gran% percentage of neutrophil granulocyte
GSP glycated serum protein
HCT hematocritg
HDL-C high-density lipoprotein cholesterol
HE hematoxylin and eosin
HGB hemoglobin
H_2O_2 Hydrogen peroxide
LDH lactate dehydrogenase
LDL-C low-density lipoprotein cholesterol
Lymph number of lymphocytes
Lymph% percentage of lymphocytes
MAD malondialdehyde
MCH mean erythrocyte hemoglobin content
MCHC mean erythrocyte hemoglobin concentration
MCV mean red blood cell volume
Mon number of monocytes
Mon% percentage of mononuclear cells
MPV mean platelet volume
MTD maximum tolerated dose
NO nitric oxide
O atomic oxygen
OCT optimal cutting temperature
OES optical emission spectroscopy
OH hydroxyl radical
$ONOO^-$ peroxynitrite anion.
ORP oxidation-reduction potential
PAL plasma-activated liquid
PBS phosphate buffer solution
PCT platelet backlog
PDW platelet distribution width
PLT platelet count
RBC number of red blood cells
RDW erythrocyte distribution width variation coefficient
RNS nitrogen-based reactive species
RONS reactive oxygen and nitrogen species
ROS oxygen-based reactive species
RPMI Roswell Park Memorial Institute
SEM standard error of the mean
SOD superoxide dismutase
T-BIL total bilirubin
TG triglyceride
UA uric acid
WBC white blood cells

frontiers in Physics

ORIGINAL RESEARCH
published: 14 December 2021
doi: 10.3389/fphy.2021.759005

Radiation Driven Chemistry in Biomolecules—is (V)UV Involved in the Bioactivity of Argon Jet Plasmas?

G. Bruno[1,2], *S. Wenske*[1], *H. Mahdikia*[3], *T. Gerling*[1], *T. von Woedtke*[3,4] *and K. Wende*[1]*

[1]ZIK Plasmatis, Leibniz Institute for Plasma Science and Technology (INP), Greifswald, Germany, [2]Metabolomics Facility, Berlin Institute of Health (BIH) at Max Delbrück Center for Molecular Medicine, Berlin, Germany, [3]Leibniz Institute for Plasma Science and Technology (INP), Greifswald, Germany, [4]Institute for Hygiene and Environmental Medicine, University Medicine Greifswald, Greifswald, Germany

Cold physical plasmas, especially noble gas driven plasma jets, emit considerable amounts of ultraviolet radiation (UV). Given that a noble gas channel is present, even the energetic vacuum UV can reach the treated target. The relevance of UV radiation for antimicrobial effects is generally accepted. It remains to be clarified if this radiation is relevant for other biomedical application of plasmas, e.g., in wound care or cancer remediation. In this work, the role of (vacuum) ultraviolet radiation generated by the argon plasma jet kINPen for cysteine modifications was investigated in aqueous solutions and porcine skin. To differentiate the effects of photons of different wavelength and complete plasma discharge, a micro chamber equipped with a MgF_2, Suprasil, or Borosilicate glass window was used. In liquid phase, plasma-derived VUV radiation was effective and led to the formation of cysteine oxidation products and molecule breakdown products, yielding sulfite, sulfate, and hydrogen sulfide. At the boundary layer, the impact of VUV photons led to water molecule photolysis and formation of hydroxyl radicals and hydrogen peroxide. In addition, photolytic cleavage of the weak carbon-sulfur bond initiated the formation of sulfur oxy ions. In the intact skin model, protein thiol modification was rare even if a VUV transparent MgF_2 window was used. Presumably, the plasma-derived VUV radiation played a limited role since reactions at the boundary layer are less frequent and the dense biomolecules layers block it effectively, inhibiting significant penetration. This result further emphasizes the safety of physical plasmas in biomedical applications.

Keywords: cold physical plasma, redox signaling, porcine skin model, VUV radiation, tape stripping model, kINpen

OPEN ACCESS

Edited by:
Vladimir I. Kolobov,
CFD Research Corporation,
United States

Reviewed by:
Anna Khlyustova,
Institute of Solution Chemistry (RAS),
Russia
Zdenko Machala,
Comenius University, Slovakia

***Correspondence:**
K. Wende
kristian.wende@inp-greifswald.de

Specialty section:
This article was submitted to Plasma Physics, a section of the journal Frontiers in Physics

Received: *15 August 2021*
Accepted: *09 November 2021*
Published: *14 December 2021*

Citation:
Bruno G, Wenske S, Mahdikia H, Gerling T, von Woedtke T and Wende K (2021) Radiation Driven Chemistry in Biomolecules—is (V)UV Involved in the Bioactivity of Argon Jet Plasmas? Front. Phys. 9:759005. doi: 10.3389/fphy.2021.759005

1 INTRODUCTION

Emerging therapies for the treatment of chronic wounds and cancerous lesions involve the administration of exogenous reactive species directly delivered on the target (e.g., cold physical plasmas) [1–4]; or produced *in situ* by administration of specific drugs (e.g., nanoprodrugs) [5,6]. For example, the formation of singlet oxygen by irradiation (600–800 nm) of a photosensitizer, is the molecular mechanism behind the effectiveness of the photodynamic therapy in use for cancer regression [7]. Among the emerging therapies, cold physical plasmas are multi-function tools comprising of reactive species, ions, metastables, electrons, magnetic fields, and photons [8,9]. These, synergistically acting on the target, are effective in cancer regression [10–12]; and wound healing

[13–15]. Furthermore, the use of plasmas is considered in other fields, such as sterilization [16–18]; and dentistry [19–21].

While downstream effects have been detected [11,22], many are the open questions regarding the working mechanism of plasmas on biological target. Therefore, the variable production of plasma elements has been studied, with focus on reactive species, at date considered the predominant responsible of plasma effectiveness [23]. In particular, their amounts on the target can be regulated by tuning the plasma parameters (e.g., treatment duration, distance, working gases) [2,24], achieving bivalent aims such as promoting cell proliferation and migration in would healing, or inducing cell death and apoptosis for cancer treatment and biological decontamination. Cold plasmas can be generated by a multitude of different designs, yielding differences in species output and biomedical impact [25]; [26].

One plasma source is the kINPen, an argon-driven jet which gas phase has been already well characterized. The production of primary reactive species such as excited states of argon (e.g., metastables, excimers) were observed in the effluent area (or gas phase). Those reactive species react with others gases (e.g., N_2, O_2, H_2) present in the surrounding atmosphere or in the core gas to generate secondary species, such as atomic oxygen (·O), singlet oxygen ($^1O_2$), ozone (O_3), hydroxyl radicals (·OH), superoxide anions radicals (O_2^-), hydrogen peroxide (H_2O_2), nitric oxide radicals (·NO_x), acids containing nitrogen (HNO_x). Finally, a tertiary chemistry is stimulated directly in the target. Using biochemical models, covalent modification of biomolecules were predicted and observed, especially in amino acids and proteins [27–30]; and lipids [31–33].

In the cellular environment, plasma-induced biomolecules modifications could be the responsible event for the deregulation of redox signaling pathways. Indeed, it was shown that kINPen plasmas led to an abnormal production/functioning of e.g., transcription factors (e.g., Nrf2 and p53), which modulates differentially gene expressions, cellular organization and apoptosis processes [15,34–36]. Together with reactive species, radiation generated by cold plasmas could cover important synergistic effects in stimulating these processes.

In kINPen plasmas, their relevance in inducing oxidative stress must be considered, since the emission region goes from the vacuum UV region (105 nm) (emitted by argon excimers) to the near infrared (1,000 nm) [9,37]. The ultraviolet radiation (100–400 nm) emitted by kinpen plasmas could have a synergistic role in their effectiveness, e.g., for antibacterial purposes as shown also for other plasma sources [38–41].

Radiation can be generally classified in ionizing (10–125 nm), which have short wavelength, high frequency and energy, and non-ionizing (>125 nm), which oppositely are longer wavelengths with lower frequency and energy. Therefore, even if measured in low levels [42,43], vacuum UV radiation (100–200 nm) emitted by argon metastable produced by kINPen plasmas could have enough energy to impact strongly on the biological matter, leading to DNA damage, protein denaturation and cell death. Indeed, it is well known that high levels of ionizing radiation can be harmful for the living matter, generally disrupting and damaging molecular structures (e.g., lipids, proteins, nucleic acids, carbohydrates) [44–48]. However, in relation to the quantity and time of exposure, UV radiation (mostly UV-C and UV-B, 200–315 nm) can also increase the general oxidative stress, induce indirectly or directly structural changes in biomolecules, and consequentially modulate redox signaling pathways [49,50]. The mechanism of action of radiation is still under clarification in biology, but generally they can generate biomolecules modifications by being directly absorbed (e.g., amino acids cysteine, tyrosine, tryptophan), or by stimulating sensitizing compounds (e.g., exogenous or endogenous). In both cases, excited forms will be generated, which starts photo-oxidation reactions. Indeed, radicals can be formed by hydrogen abstraction or one electron oxidation (Type I mechanism) and reactive species can be formed by energy transfer to molecular oxygen, which forms singlet oxygen (Type II mechanism) [50,51]. Generally, an increased release of reactive species from mitochondria was measured after radiation exposure, as well as the activation of a calcium dependent NOS-1 with increase of peroxynitrite levels. The chain reaction induced by photo-oxidation can be harmful in long and intense exposure, but for short and not severe exposure a transitory effect was observed, leading to a cytoprotective response mediated by MAPK1/2 activation [51]. The UV and vacuum UV light produced by different plasma sources has been considered as essential elements for the antimicrobial activity [38–41,52,53].

In this work, the role of ultraviolet radiation generated by the argon plasma jet kINPen for cysteine modifications was investigated. Cysteine is easily oxidized, and served to investigate plasma chemistry in liquids before [24,54–56]. Modifications occurring on cysteine in aqueous solutions or porcine epithelium were identified via mass spectrometry and major derivatives were quantified using it coupled to high-pressure liquid chromatography. To isolate the effects of photons from complete plasma discharge, a micro chamber equipped with VUV, UV-C, and UV-A windows was used. Alongside, optical emission spectrometry and aqueous chemistry was applied to characterize reactive species formation in the gas and liquid phase. A significant contribution of plasma derived UV radiation on cysteine chemistry was observed if water molecules were present.

2 MATERIALS AND METHODS

2.1 Sample Preparation

Crystalline cysteine (Sigma Aldrich) was solubilized in double distilled water (ddH_2O) to a final concentration of 2 mM on a daily basis. For short-term storage, blue ice was used to avoid pH value distortions during freeze-thawing cycles [57]. After respective plasma or irradiation treatments, solutions were immediately subjected to high-resolution mass spectrometry, multiple reaction monitoring mass spectrometry, or ion chromatography. Fresh porcine ears were received from Landmetzgerei Urich (Bad Koenig, Germany) on blue ice, serving as a well-accepted replacement model for human skin [58]. The ears were washed carefully, shaved, and the superficial

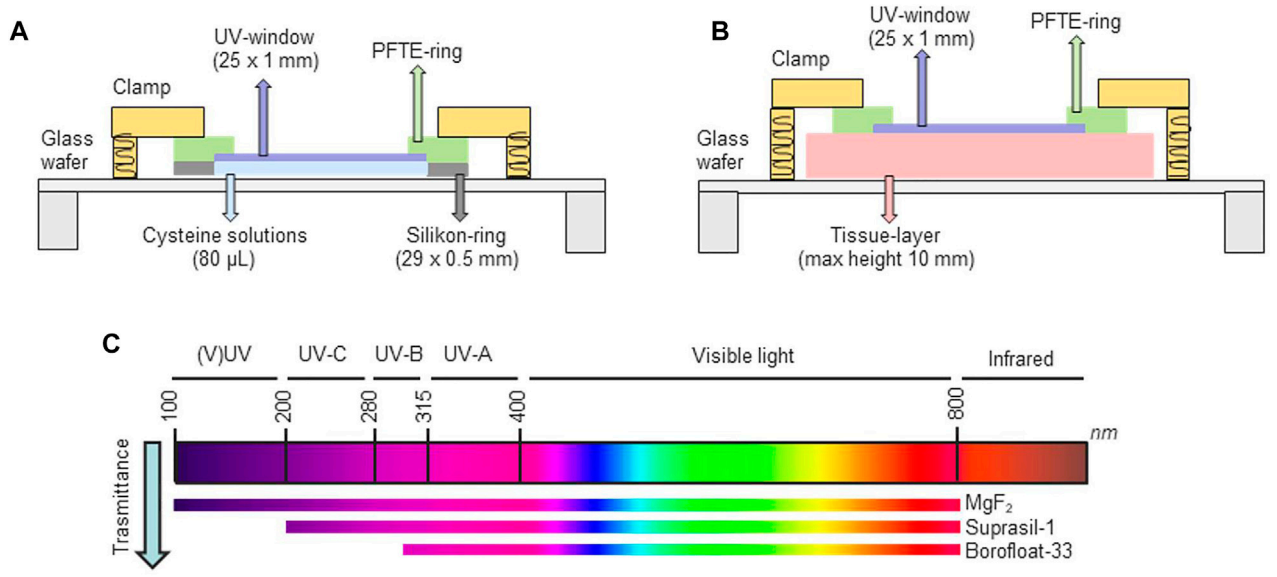

FIGURE 1 | Micro-chamber used to apply UV radiation emitted kINPen plasmas **(A, B)**. Cysteine solutions **(A)** or porcine skin sections **(B)** were introduced into the chamber. The light transmission of the three windows is indicated in **(C)**.

corneocyte layer was removed with a single CorneoFix strip (Courage and Khazaka electronic GmbH, Cologne, Germany) to increase homogenicity. Plasma treatment was performed in selected clean and homogenous areas of a 2 cm × 2 cm dimension.

2.2 Plasma Treatments

The kINPen, an argon-driven (99.999%, Air Liquide) dielectric barrier plasma jet with a flow rate of 3 standard liters per minute (slm) served as plasma source. If desired, the working gas was modified by 1% admixture of molecular oxygen (99.998, Air Liquide). Its central electrode is powered by an alternating current with a sinusoidal waveform, 2–6 kV peak–peak voltage, and a frequency of around 1 MHz. The outer electrode is insulated by a ceramic tube. The dissipated electrical power is around 1.1 W. For most experiments, a gas curtain created by a nozzle and 5 slm nitrogen (99.999%, Air Liquide) shielded the effluent from the ambient air. For details about the design and working principle of the jet, refer to Reuter and colleagues [9] and citations therein. To investigate the plasma-derived products and emitted radiation by optical emission spectroscopy, the plasma jet was positioned on axis at a distance of 9 mm to the front of a spectrometer (AvaSpec-2048; Avantes, Germany) allowing the observation of both UV and VIS/NIR range (195–980 nm) with a spectral resolution of 0.7 nm. For the VUV spectral measurements, a single grating monochromator (Acton VM-502, grating 1200 g/ mm) was used. This system was set to a spectral resolution of 0.2 nm and the spectral range of 100–200 nm was observed. Furthermore, the system was under low pressure ($2.2*10^{-6}$ mbar) and connected via an MgF_2 window for VUV transmissions down to 100 nm. The kINPen was placed at 9 mm distance in front of the MgF_2 window.

The distance between the nozzle and the target was kept at 9 mm. Targets were either 750 µL aqueous solution in a 24 well-plate, fresh porcine skin prepared as described in 2.1, or a 25 mm diameter radiation chamber. The chamber could be equipped with windows that transmit different parts of the VUV/UV radiation and was filled with 80 µL solution forming a 500 µm thick layer or sections of porcine skin (**Figure 1A,B**). After treatments (20 s–180 s) samples were submitted to reactive species analysis (**Section 2.3**). Liquids containing the tracer molecule cysteine were also analyzed via liquid chromatography coupled to mass spectrometry for the detection of oxidative modifications (**Section 2.4**). The first 3 layers of treated porcine skin tissues were sampled using three consecutive CorneoFix strips that were immediately deposited in a protein solubilization buffer and subjected to shotgun proteomics (as described in **Section 2.5**). Each experiment was performed in triplicate.

2.3 OH and H_2O_2 Quantification via Colorimetric Assays in Liquids

For the quantification of plasma-generated, short-lived ROS (hydroxyl radicals, atomic oxygen) solution of 5 mM terephthalic acid in 25 mM phosphate buffer, pH 7.4 was used despite the limited selectivity [59]. The reaction yield to the fluorescent compound 2-hydroxyterephthalic acid (HTPA) that could be quantified at 318 nm excitation and 426 nm emission using an external calibration curve. Hydrogen peroxide deposited in treated liquids was determined using the ferrous oxidation–xylenol orange (FOX) assay according to the manufacturer's protocol (Thermo Scientific, Dreieich, Germany). The reaction yield to a purple product, which absorbance at 595 nm was

measured in a spectrophotometer (Tecan M200 multi-plate reader, Männedorf, Switzerland).

2.4 Characterization of Plasma-Induced Sulfur Chemistry in Liquids

2.4.1 Cysteine Derivatives.

Cysteine, cystine, cysteine sulfonic acid, cysteine sulfinic acid, alanine, cysteine-*S*-sulfonate were quantified by coupling a chromatographic separation (Agilent 1,290 Infinity II, Waldbronn, Germany) to targeted mass spectrometry (Q-Trap 5500, Sciex, Darmstadt, Germany). Analytes were separated on a 2.1 mm × 100 mm Acquity Amide Column with 130 Å pore size and 1.7 µm particle size and a corresponding VanGuard precolumn (Waters, Manchester, England) at a column temperature of 35°C. Mobile phase A consisted of 10 mM ammonium formate in water plus 0.15% formic acid while B consisted of 10 mM ammonium formate in acetonitrile plus 0.15% formic acid. The flow rate was 0.8 ml/min. A linear gradient was applied (0.0 min–99% B; 4.0 min–85% B; 7.0 min–30% B; 7.1 min–99% B; 9.0 min–99% B). Prior to injection, samples were diluted 1:5 in mobile phase B. Compounds were determined via multiple reaction monitoring in positive mode. The electrospray (ESI) source parameters were the following: curtain gas 35 psi, gas 1 20 psi, gas 2 25 psi, temperature 150°C, 5.5 kV probe voltage, 50 V declustering potential. The transitions and the correspondent collisional energies (CE) used for each compounds were for cysteine 122 → 76 m/z, CE 20; cystine 241 → 152 m/z, CE 10; cysteine sulfinic acid 154 → 74 m/z, CE 20; cysteine sulfonic acid 170 → 124 m/z, CE 10; cysteine-*S*-sulfonate 202 → 120 m/z, CE 10; alanine 90.1 → 44.1 m/z, CE 8. External calibration curves allowed the absolute quantification of the listed compounds in plasma-treated or irradiated samples.

2.4.2 Hydrogen Sulfide.

To quantify the formation of hydrogen sulfide (H_2S) from cysteine, the monobromobimane (mBB) assay was optimized [60]. A solution of 100 mM MBB in acetonitrile was freshly prepared. First, 25 µL of analyte solutions was mixed with 2 µL MBB and 65 µL of 100 mM phosphate buffer at pH 7.8. After vigorous mixing, samples were incubated at 37°C for 10, 30, or 60 min using a thermomixer, yielding sulfodibimane (SDB) in the presence of H_2S. The reaction was stopped by adding 5 µL formic acid 50% and cleared by centrifugation. SDB was quantified by targeted mass spectrometry. Analytes were separated on a 2.1 × 50 mm Zorbax RRHD Eclipse Plus C18 column (Waters, 95 Å pore size, 1.8 µm particle size) and corresponding guard column. Mobile phases were water (A; Th. Geyer, Renningen, Germany) and acetonitrile (B; ibid). A linear gradient was applied (0 min–5% B; 2.1 min–40% B; 5 min–40% B; 5.1 min–98% B; 6 min–98% B; 6.1 min–5% B; 8 min–5% B). The flow rate was of 0.8 ml/min. Atmospheric pressure chemical ionization (APCI) was applied with the following source parameters: curtain gas 20 psi, gas 1 50 psi, temperature 500°C, 3 kV needle current, 100 V declustering potential, 32 V collision energy. The transitions used for the analyzed compounds were for MBB 272 → 193 m/z; SDB 415.1 → 193.3 m/z.

2.4.3 Sulfite and Sulfate.

Ion chromatography (ICS-5000, Dionex Corp., Sunnyvale, United States) was used for the quantification of sulfite (SO_3^-) and sulfate (SO_4^-) anions. These were separated on a IonPac® AS23 pre-column (2 × 50 mm) coupled to an IonPac® AS23 anion exchange column (2 × 250 mm, Thermo Fisher Scientific Inc., Waltham, United States). Isocratic separation was achieved using a carbonate buffer (4.5 mM Na_2CO_3/0.8 mM $NaHCO_3$) and the flow rate of 0.25 ml/ min.

2.5 Investigation of Protein Modifications in Tissues

2.5.1 Protein sample preparation.

After sampling via tape stripping controls and plasma treated porcine skin layers, proteins were solubilized by introducing the tape strip in 500 µL of SDS-based lysis buffer (5% SDS, 50 mM TEAB pH 7.55) and by vortexing the vials for 2 min at room temperature. A S-Trap midi spin column digestion protocol from ProtiFi was applied according to the manufacturers protocol. The solutions were sonicated to disrupt cells, dissolve proteins, and shear DNA and clarified by centrifugation at 4000g for 10 min at 4°C. The supernatant was transferred to a clean vial. The reduction and alkylation of sulfhydryl groups was performed by incubating respectively with 5 mM tris(2-carboxyethyl) phosphine (TCEP, 55°C, 15 min) and subsequently with 20 mM methyl methanethiosulfonate (MMTS) at RT for 10 min. The reaction was stopped by adding 12% phosphoric acid. Next, 300 µL S-Trap buffer (90% methanol, 100 mM TEAB, pH 7.1) was added, and samples were transferred to the spin column. After centrifugation (2 min × 4000 g), the column was washed with 300 µL S-Trap buffer three times. Protein digestion was achieved in column by adding 1:25 wt:wt sequencing grade trypsin (Promega, Madison, United States) in 50 mM TEAB and incubating for 1 hour at 47°C. In this case, the columns were sealed with a lid to avoid solution evaporation. Finally, peptides were eluted with 500 µL of acetonitrile containing 0.2% formic acid. The solutions were dried using a SpeedVac and resuspended in 10 µL of water containing 0.1% formic acid before nanoLC-MS analysis.

2.5.2 LC-MS analysis.

The proteomes and the oxidative modifications occurring in porcine skin layers after treatments were analyzed by nanoflow liquid chromatography, using an UltiMate 300 RSLCnano coupled to a QExactive Hybrid-Quadrupol-Orbitrap from Thermo Fisher Scientific, Dreieich/Germany. The technical details of the separation and detection are described in Wenske et al., 2021. Raw data were analyzed with the Proteome Discoverer 2.4 (Thermo Fischer Scientific) and the Byonic 3.6.0 node (Protein Metrics) for searching protein modifications. A list of 15 modifications previously identified for gas plasma treatments of thiol moieties was used to reduce

TABLE 1 | Analyzed thiols oxidative modifications occurring in the proteome of plasma treated porcine skin samples.

Mass shift (Da)	Composition	Modification	Acronym	Label
−2.02	−2H	Dehydrogenation	Didehydro	A
+15.99	+O	Oxidation	Oxidation	B_1
+21.98	+2O	Dioxidation	Dioxidation	B_2
+47.98	+3O	Trioxidation	Trioxidation	B_3
+28.99	+N + O -H	Nitrosylation	Nitrosyl	C1
+44.98	+N +2O -H	Nitration	Nitro + O	C2
−15.01	−N −H	Deamination	−NH	D_1
−17.03	−N −3H	Deamination + Dehydrogenation	−NH3	D_2
−31.97	−S	Sulphur loss	−S (alanine)	E_1
+31.97	+S	Sulphur addition	+S	E_2
+79.96	+S +3O	Sulfonylation	+SO3	E_3
+119.00	+S +3C +5H + N +2O	Cysteine addition	+S2R	F_1
+150.99	+S +3C +5H + N +4O	Cysteine addition + Dioxidation	+S2O4R	F_2

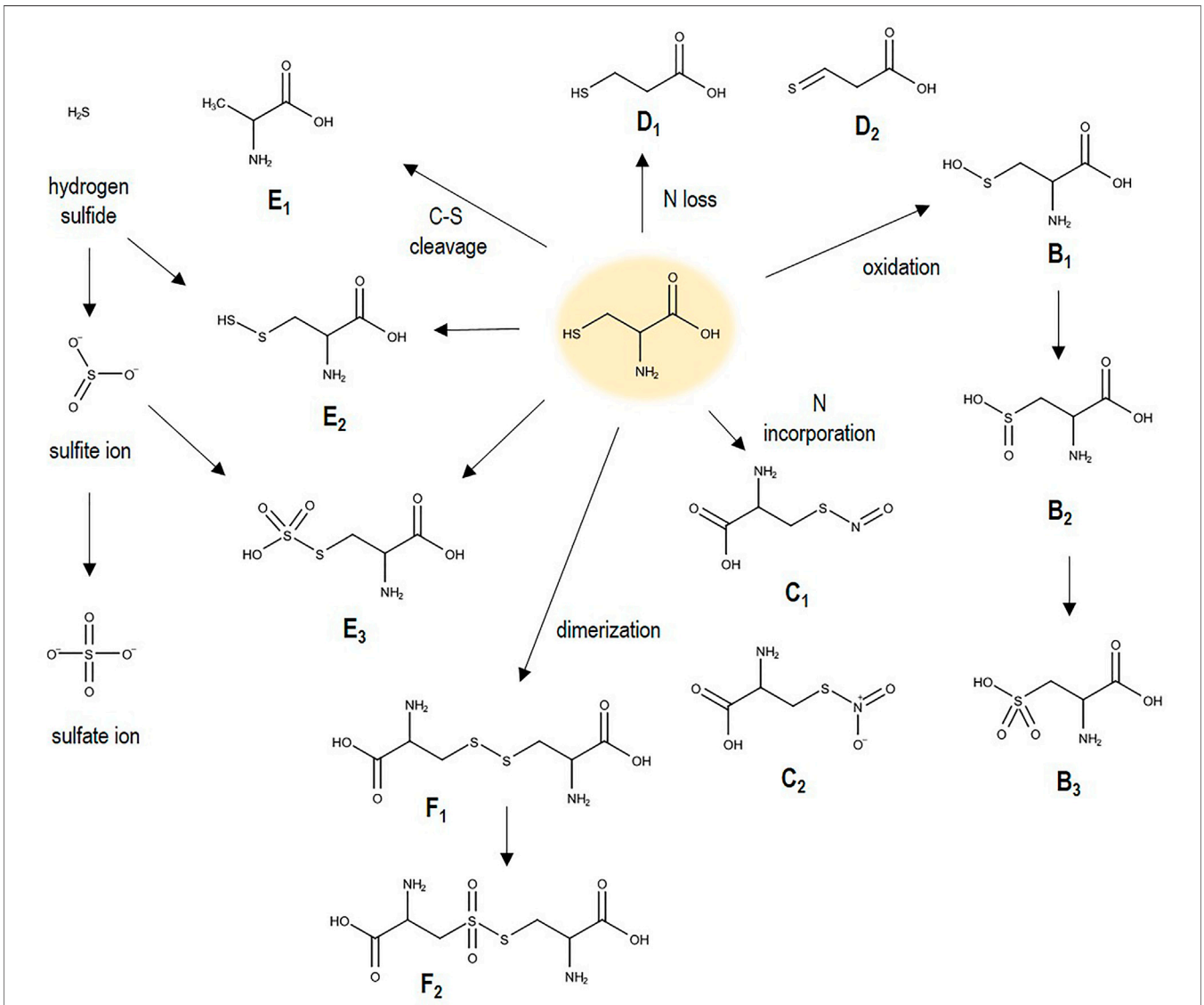

FIGURE 2 | Cysteine oxidation and cleavage products (see **Tables 1**, **2**). When incorporated into a protein, the carboxyl and amino group are incorporated in the peptide bond.

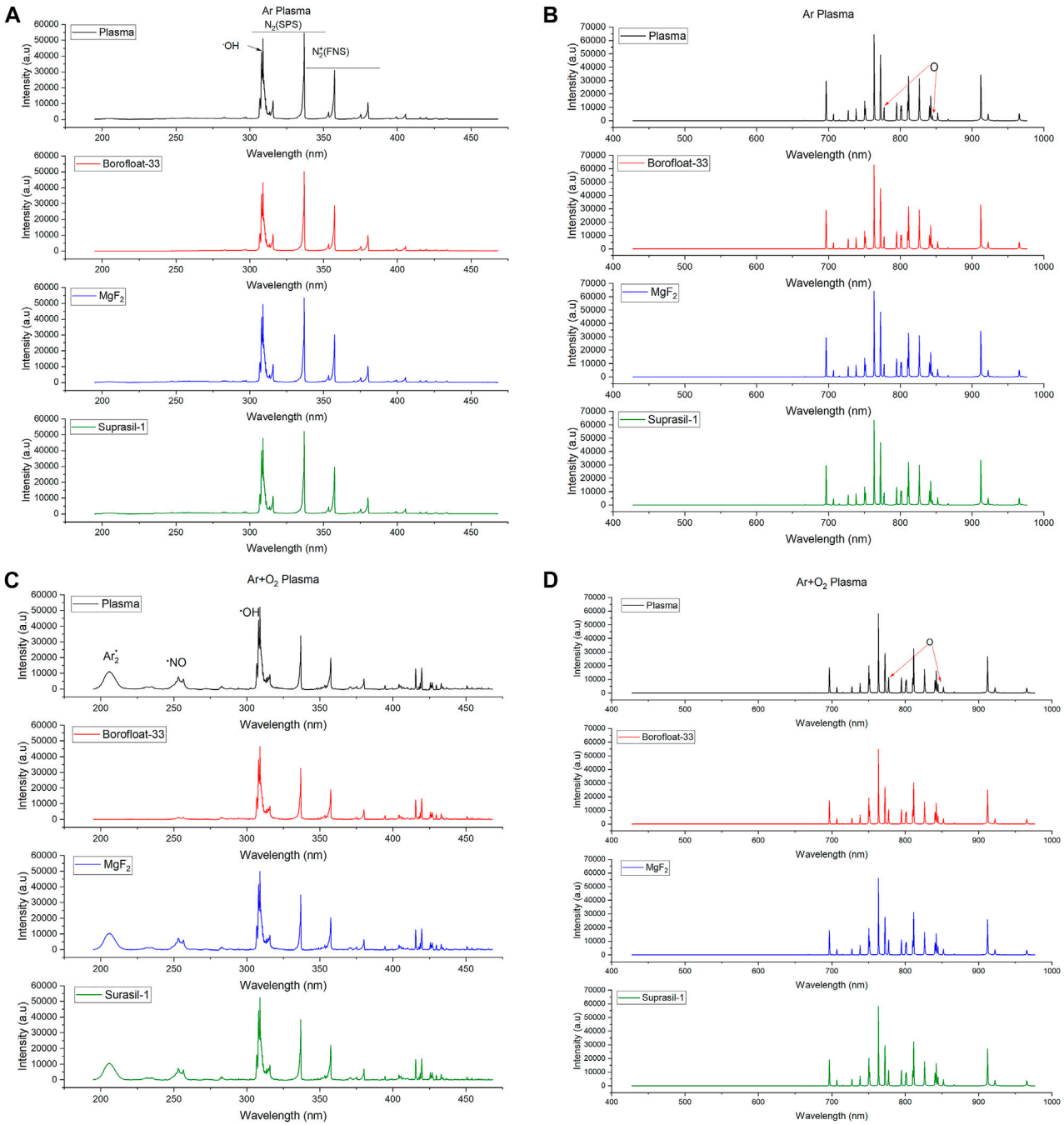

FIGURE 3 | OES spectra registered at 9 mm distance from jet nozzle in the range 195–465 nm (UV range, **(A and C)** and 430–980 nm (VIS/NIR range, **(B and D)**. **(A and B)**: kINPen09, 3 slm Ar, **(C and D)**: kINPen09/3slm Ar + 0.5% oxygen. Free plasma jet, and radiation filtered through MgF_2 (transparent >125 nm), Suprasil (quartz based, > 195 nm), and Borofloat glass (>300 nm) were compared (see legend in spectra). Due to limitations in setup (no measurements <195 nm), only slight changes between 200 and 300 nm were observed. The VIS/NIR region remained unchanged by the different windows except for a minor reduction in intensity.

calculation times (**Table 1**) [24,55]. A maximum of three modifications per peptide was set, and to ensure result validity, only peptides with a Byonic score >250 and a Delta Mod score of >5 were accepted for downstream data analysis. A normalization on the total peptides containing cysteine was performed, yielding a percentage of modified thiols on the total proteome. Furthermore, the oxidative modifications found in controls were subtracted as background from all other samples and data are shown as difference from the control. One-way ANOVA statistical test was performed in order to detect significant modifications, allowing a comparison between different conditions.

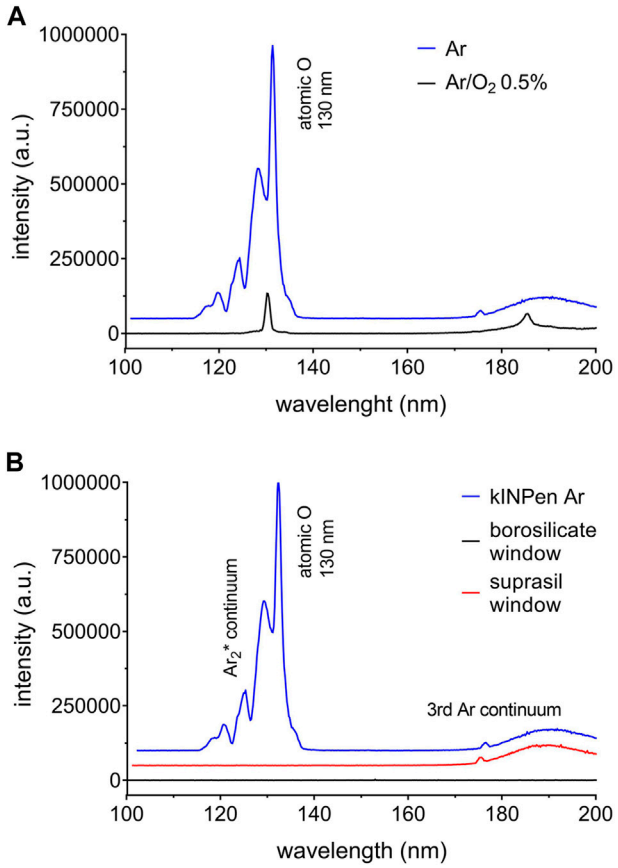

FIGURE 4 | OES spectra registered at 9 mm distance from kINPen09 jet nozzle in the range 100–200 nm. Argon excimer lines were observed around 120–130 nm and 180–200 nm. A significant reduction of these emissions lines was observed for 0.5% oxygen admixture to the argon working gas **(A)**. The VUV range was blocked for some experiments using borosilicate or suprasil windows **(B)**, or allowed to access the target (MgF_2 window).

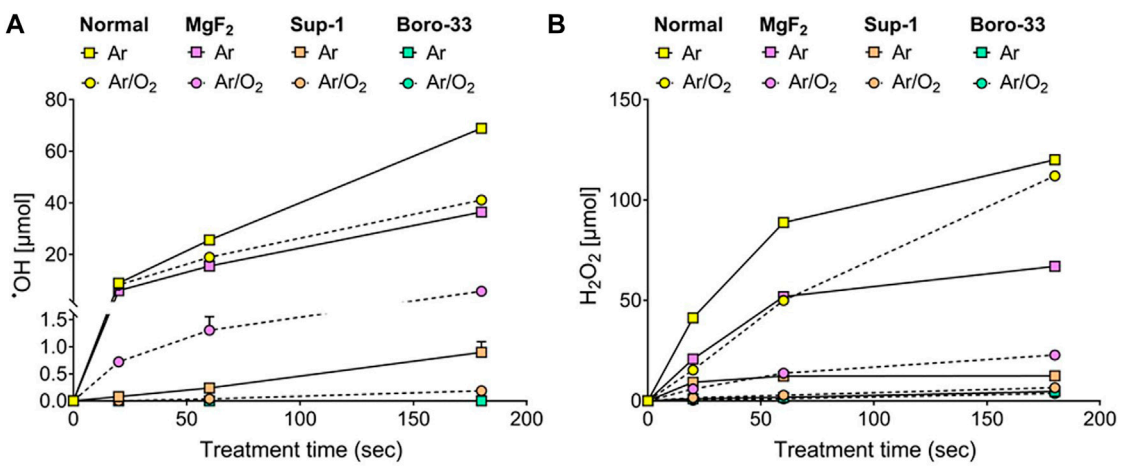

FIGURE 5 | Formation of hydroxyl radicals **(A)**, and hydrogen peroxide **(B)** after plasma treatments using 3 slm Ar ± O_2 and 5 slm shielding gas (N_2). Solutions were treated in either 24 well plates or radiation chamber (see **Figure 1**) with different volumes due to technical constraints (see text). Quantification performed *via* colorimetric assays [$^{\bullet}$OH according to [72]]; experiment performed in triplicates. Error bars (range) are in some cases smaller than data points and not visible.

TABLE 2 | Analyzed cysteine derivatives, acronyms, formulas, quantification method and responsible plasma element.

Name	Acronym	Hill notation	Analysis	Plasma element
Cysteine	RSH	$C_3H_6NO_2S$	HILIC-MRM	None
Cystine	RSSR	$C_6H_{12}N_2O_4S_2$	HILIC-MRM	Radicals
Alanine	RH	$C_3H_7NO_2$	HILIC-MRM	(V)UV
Sulfonic acid	RSO_3H	$C_3H_7NO_5S$	HILIC-MRM	·OH, $^1O_2$, Ȯ
Sulfinic acid	RSO_2H	$C_3H_7NO_4S$	HILIC-MRM	·OH, $^1O_2$, Ȯ
S-sulfonate	$RSSO_3H$	$C_3H_7NO_5S_2$	HILIC-MRM	·OH, Ȯ (indirect)
Sulfite	SO_3^-	O_3S	IC	(V)UV, ·OH, $^1O_2$, Ȯ
Sulfate	SO_4^-	O_4S	IC	(V)UV, ·OH, $^1O_2$, Ȯ
Hydrogen sulfide	H_2S	H_2S	MBB, RP-MRM	(V)UV

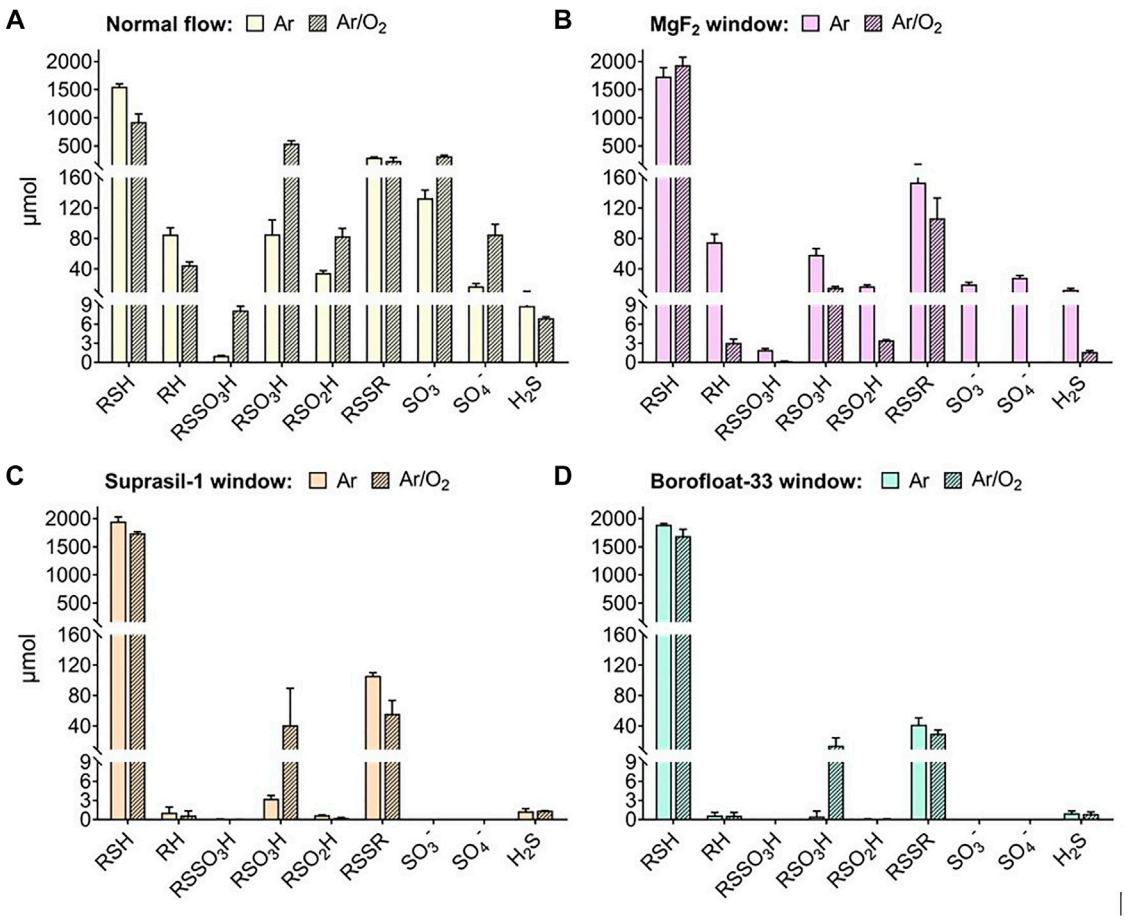

FIGURE 6 | Plasma-induced formation of cysteine derivatives (1 min treatments), using a 3 slm Ar ± O_2 and 5 slm N_2 shielding gas. Solutions treated in 24 well plates (750 µL, free plasma, **(A)** or radiation micro-chamber (80 µL, see **Figure 1**, **(B–D)**). Quantification performed using derivatization with monobromobimane and RP-SRM for H_2S (according to [60]), using IC for SO_4^{2-} and SO_3^{2-} and HILIC-MRM for the other compounds; experiment performed in triplicates.

3 RESULTS AND DISCUSSION

3.1 Fingerprinting the kINPen Plasma Radiation

The kINPen spectra of emission goes from the vacuum UV (100 nm) to the near infrared (1,000 nm) [61]. The intensity of the UV irradiation was determined to be around 100 µJ cm^{-2}. Optical emission spectroscopy was performed in order to characterize the emission spectra of the applied plasma treatment conditions (**Figure 1**). In this case, the emission spectra were measured applying the three different windows filtering various radiation ranges (**Figure 2**). Additionally, the vacuum UV range was recorded using a vacuum setup (**Figure 3**) [9,37]. In pure argon, emission lines from impurities of •OH and

N_2 were measured between 300 and 350 nm, and small atomic oxygen lines at 777 and 844 nm. The infrared region was dominated by argon emission lines, while between the range 400–700 nm no emission was observed. In the vacuum UV region (<195 nm), a dominant continuum centered at 126 nm can be measured for argon excimer (Ar_2^*), which includes also small absorption lines from ozone and O_2. The modulation of working or shielding gases, induced changes in the emission spectra, e.g., the addition of molecular oxygen in the working gas leads to a reduction of Ar_2^* emission lines and increase those oxygen-based [9,37]; (**Figure 2**). The presence of molecular O_2 in the working gas interfered with the gas phase chemistry and UV emission of various species, such as $^{\bullet}$OH, N, $^{\bullet}$NO, and Ar_2^*. Suprasil and Borofloat-33 scavenged the emission of argon excimers, while in the range between 195 and 465 more subtle changes were observed, reflecting the characteristics of normal glass (**Figure 2**). Particularly in conditions with pure argon, which are certified for medical applications with kINPen MED, the role of vacuum UV radiation was dominant (**Figure 3**). As discussed previously, this event could be due to the lower formation of gaseous reactive species and therefore less reactions of argon metastable and excimers with surrounding gases to form further species, e.g., ozone, atomic oxygen, singlet oxygen, etc. [9,37]; (**Figures 2**, **4**).

3.2 Vacuum UV as Source of Water-Derived $^{\bullet}$OH and H_2O_2 Production

The formation of $^{\bullet}$OH and H_2O_2 in water was compared using full plasma treatments (3 slm Ar and Ar + 1% O_2) and treatments using windows filtering different radiation ranges (**Figure 5**). The dissociation of water yielding OH radicals was favored in full argon plasma treatments and when VUV radiation was admitted (MgF_2-window). For short treatments only small differences in $^{\bullet}$OH production was observed, but enlarging with treatment time. Full argon plasma produced around 30 μmol of $^{\bullet}$OH more than Ar plasma/MgF_2-window. It may be argued that either OH radicals from the gas phase contributed here or atomic oxygen generated from impurities. A recent report showed the sensitivity of terephatalic acid to this reactive short-lived species. Also liquid dynamic effects increasing the contact area between emitted radiation and target in contrast to the static treatments performed in the micro-chamber can contribute. Upon addition of molecular oxygen to the working gas, a decrease in $^{\bullet}$OH and H_2O_2 production was observed, especially when the MgF_2-window was used, blocking interphase chemistry. In the near-complete absence of VUV radiation from the argon excimers, water dissociation did not occur. Corroborating this observation, almost no OH/H_2O_2 formation was sparked by the longer UV ranges (UV-C and B and UV-A, respectively Suprasil-1 and Borofloat 33). Therefore, oxygen-base emission lines (atomic oxygen in NIR, ozone and O_2 in VUV), which increases in presence of molecular oxygen in the working gas, did not led to water dissociation. However, their potential direct impact on cysteine structures was investigated [55]. Overall, being highly energetic, VUV radiation emitted by Ar_2^* were able to induce water ionization, in contrast to the other UV ranges. Therefore, the direct and indirect (e.g., water-derived species production) impact of VUV radiation resulted as predominant responsible of the effects induced on the liquid target. In the presence of oxygen in the gas phase, species derived from interphase chemistry and/or chemistry in liquid bulk are dominant, while VUV radiation is eliminated (**Figure 3A**).

3.2 Direct and Liquid-Mediated Effects of Radiation on Cysteine Solutions

The impact of full plasma treatments and plasma-generated UV/VIS/NIR light on cysteine molecules is shown in **Figure 6**. **Table 2** shows the structures, the quantification methods, and the major plasma components involved in the generation of each cysteine derivative. As discussed, argon plasma conditions stimulated predominantly pathways in liquid via impact of VUV radiation emitted by argon excimers, leading to $^{\bullet}$OH and H_2O_2 production. The same experiments were performed with cysteine containing solutions. The formation of products that derive from the loss of the thiol group in cysteine (alanine, cysteine-*S*-sulfonate, sulfite ions, sulfate ions, and hydrogen sulfide) was almost identical in treatments with full argon plasmas and filtered VUV radiation of argon plasmas (MgF_2). In contrast, these products almost disappeared when VUV-impermeable oxygen was introduced to the working gas and gas–liquid phase chemistry was blocked by an MgF_2-window. This confirmed the key role of VUV radiation, leading to a cleavage of the carbon-sulfur bond [63], that was not observed by using other windows/radiation ranges. The energy of this bond is 272 kJ mol^{-1}, weaker than other bonds in cysteine or water (H-O 465 kJ mol^{-1}, C-C 347 kJ mol^{-1}, S-H 347 kJ mol^{-1}). The energy of the impinging UV photons of the argon excimer lines is much higher, 949 kJ mol^{-1} (126 nm), allowing the cleavage of all bonds present in the target, including the oxygen-hydrogen bond in water molecules. Accordingly, it might be argued that OH radical formation is the first step ultimately yielding in thiol moiety abstraction. However, the presence of hydrogen sulfide (H_2S) clearly indicates that a direct cleavage of the C-S bond contributes significantly or is even dominant considering the weaker bond energy compared to the H-O bond. Interestingly, no indications of a C-C bond breakage in cysteine, leading e.g. to the formation formic acid, was observed. Summarizing, conditions with pure argon showed a significant contribution of the VUV radiation, stimulating i) the production of OH radicals, and ii) C-S bond breakages. Under VUV radiation, derivatives such as cystine and cysteine acids were also produced in consistent amounts in relation to full argon plasmas. The origin of the oxygen incorporated in structures such as sulfite, sulfate, cysteine acids and *S*-sulfonate, in this case, are water-derived species [55].

As previously discussed, due to the controlled pH (7.2), only low amounts of thiolate were available to react with H_2O_2 since the pKa of the cysteine thiol group is 8.18—allowing less than 5% deprotonation. Therefore, a minimal role in thiol oxidation could be attributed to hydrogen peroxide. Furthermore, a two-step reaction would be needed to form cystine: a first reaction of H_2O_2 with thiolate, with formation of cysteine sulfenic acid, and a second reaction of RSOH with another thiolate [63]; [64]. More

TABLE 3 | Cysteine focused protein modifications observed in porcine epidermis model (ANOVA and Post-hoc analysis Fisher's LSD, p-value and FDR ≤0.05).

	$p < 0.05$ (n)	Type of modification
Overall	5	sulphur loss (-S), Trioxidation, Sulfonylation (+SO3), Cysteine addition (+S2R), Didehydrogenation (didehydro)
Layer I	5	Sulphur loss (-S), Trioxidation, Sulfonylation (+SO3), Cysteine addition (+2SR), Didehydrogenation (didehydro)
Layer II	3	Cysteine addition (+S2R), Nitrosylation (nitrosyl), Sulphur loss (-S)
Layer III	3	Sulphur loss (-S), Cysteine addition (+S2R), Trioxidation
Ar/O2 plasma	5	Nitrosylation (nitrosyl), Sulphur loss (-S), Sulfonylation (+SO3), Trioxidation, Didehydrogenation (didehydro)
Ar plasma	4	Cysteine addition (+S2R), Sulfonylation (+SO3), Didehydrogenation (didehydro), Sulphur loss (-S)
Ar MgF2 window	1	Nitrosylation (nitrosyl)
Ar Borofloat window	1	Cysteine addition (+S2R)

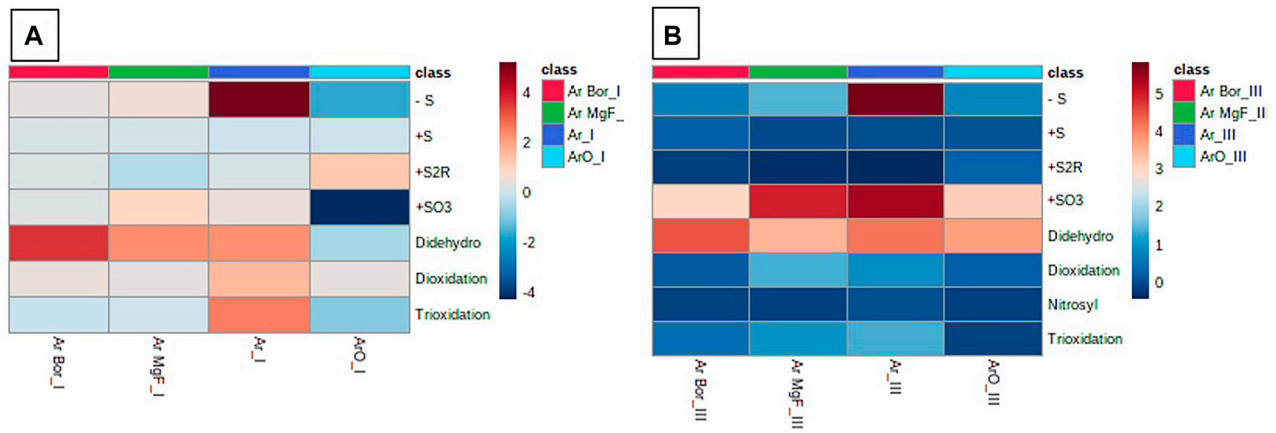

FIGURE 7 | Comparison of major modifications observed in epidermis model (layer I/A and III/B). Conditions with free plasma or trough borofloat (Bor)/MgF_2 window treatments for 1 min cm^{-2} are compared. Layer III is clearly less affected than layer I and direct plasma is more effective than (UV) light irradiation. VUV treatment (MgF) is more effective than UVB (Bor). Further, see text and **Table 3**. Relative changes in modified cysteine moieties shown via two-color gradient. Roman numbers indicate the layer with layer I the outer and laver III the inner layer investigated. Experiment performed in triplicates.

likely, the reaction of $^{\bullet}OH$ with cysteine generates cystine by first formation of thiyl radicals ($RS^{\bullet}$), which rapidly recombine to form cystine. The formation of cysteinyl radicals was detected using BMPO/EPR spectroscopy earlier [54].

The reaction of $RS^{\bullet}$ with $^{\bullet}OH$ would lead to cysteine sulfenic acid, which immediately is oxidized into sulfinic and further to sulfonic acid by $^{\bullet}OH$ or H_2O_2 [65–67]. The production of S-sulfonate ($RSSO_3H$), in absence of atomic oxygen, could be promoted by first cystine oxidation by two $^{\bullet}OH$, with following C-S breakage promoted by VUV and final incorporation of another oxygen. Sulfite can be generated by cut of the C-S bond in cysteine sulfonic acids, or most likely, cysteine S-sulfonate (S-S bond dissociation energy 414.6 kJ mol^{-1}) [68]. Supplementary experiments have been performed by treating cysteine sulfonic acid in the radiation chamber, as shown in the supplementary material (**Supplementary Figure S1**). Despite the high concentration of the reference compound cysteine sulfonic acid, only small amounts of sulfite and sulfate ions are formed, indicating that the majority of C-S bond cleavages takes place at the cysteine or cystine level. With that, most sulfite and sulfate ions were generated by the oxidation of H_2S. This pathway is favored in the presence of reactive oxygen species produced by the cleavage water molecules (e.g. H_2O_2, $^{\bullet}OH$). Clearly, a number of chemical pathways were active in liquids under the influence of vacuum UV radiation, in contrast to radiation >195 nm (UV-C).

The cysteine products generated by UV-C (Suprasil) or UVB/UVA (Borofloat) were clearly different. In these cases, almost no production of the water-derived species OH/H_2O_2 (**Figure 5**) and cysteine derivatives generated by C-S bond cleavage (SO_4^{2-}, SO_3^{2-}, alanine/RH; **Figure 6**) were observed.

The formation of cystine via hydrogen abstraction in cysteine (type I photo-oxidation mechanisms) and $RS^{\bullet}$ recombination [50,51]; was observed independent from the window, but with lower extent when vacuum UV is blocked (Borofloat/Suprasil). The production of sulfonic acid (RSO_3H, **Figure 6**) was measured in conditions with oxygen in the working gas, suggesting the potential role of radiation emitted in the near infrared and depending by the presence of O_2. The origin of oxygen incorporated by sulfonic acid, in this case, could be due to the reaction of thiyl radical with water, generating $^{\bullet}OH$ by hydrogen abstraction. Even though the radiation emitted in these ranges are not ionizing, due to the lower energy, it was shown that also the UV radiation >200 nm can induce oxidative stress in cellular compartments in relation to the exposure time, with increase in the cellular production of reactive species [49,50].

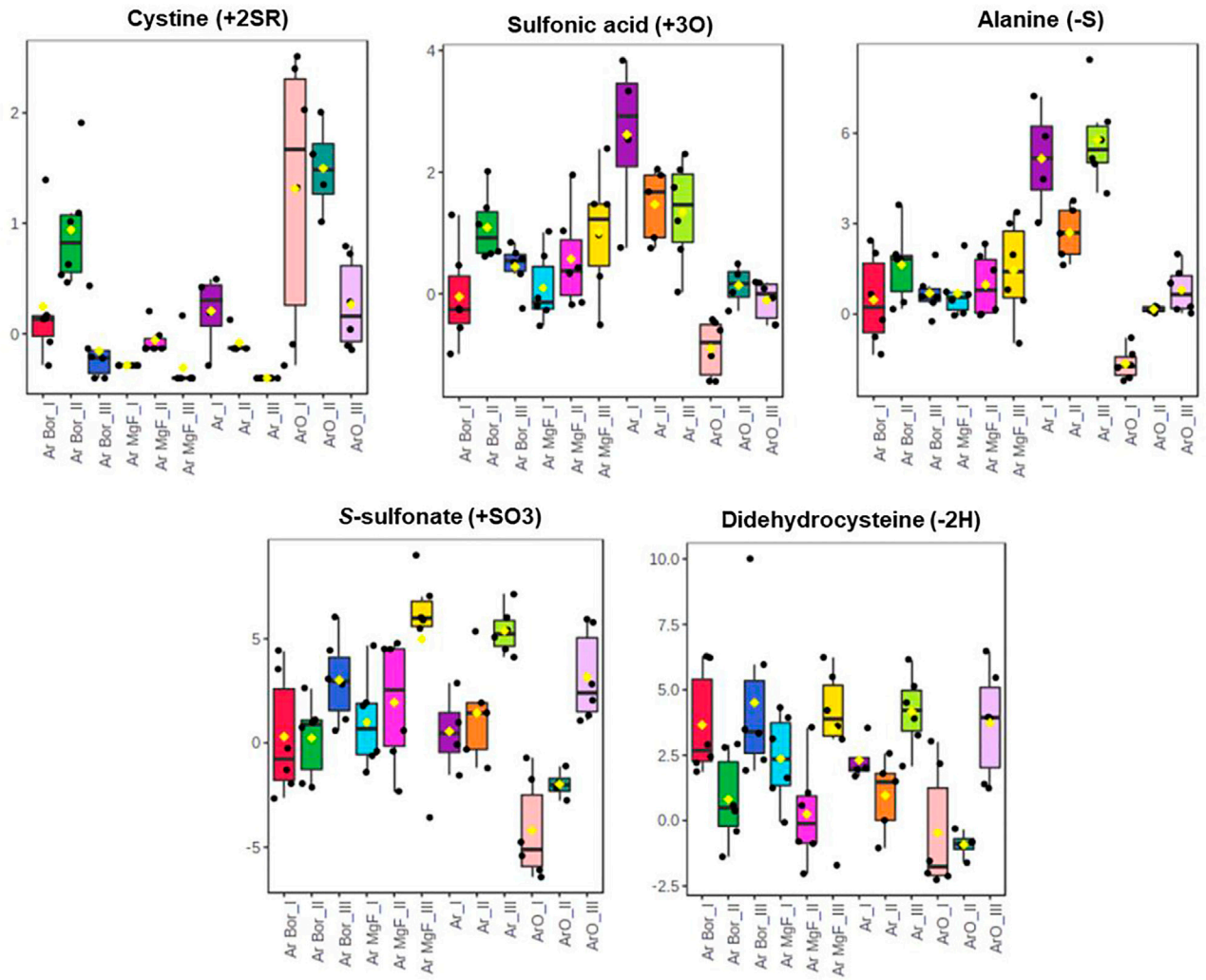

FIGURE 8 | Major oxidative modifications induced in cysteine residues of porcine epidermis proteins. While overall introduction of modifications remain low, free plasma treatment is more effective than VUV treatment (MgF_2 window) or UVB (borofloat window, Bor). Layer I is more affected than layers II/III, indicating a limited penetration of reactive species/VUV radiation. See text. Plasma treatments for 1 min cm^{-2}, using a 3 slm Ar ± O_2 and 5 slm N_2 shielding gas. Experiment performed in triplicates. Percentage of modified cysteines shown. Modification selected by ANOVA, p-value < 0.05.

3.3 Plasma Radiation Impact on Epidermal Protein Structures

The analysis of the oxidative modifications of cysteine belonging to the porcine epidermal proteome was performed via tape stripping assay in combination with high-resolution mass spectrometry. The oxidation was monitored in the first three stratum corneum layers of the porcine epidermis, reflecting a penetration depth of 5–7 µm. **Table 3** and **Figure 7** give an overview of the detected modifications, while **Figure 8** shows a quantitative comparison of the most relevant oxidative modifications. Unstable oxidative modifications, such as S-nitrosylation, may have been underestimated. According to proteomics standard procedures, thiols were reduced and alkylated during sample workup. Some losses to the plasma chemistry on protein thiols (e.g., sulfenic acids, *S*-nitrosylation) cannot be excluded although stable modifications (e.g., cysteine sulfonic acid, cysteine-S-sulfonate) were retained. Overall, five types of modifications were found to be introduced into the epidermal proteins with a statistical significance. These are the apparent replacement of cysteine by alanine (sulphur loss), the formation of cysteine sulfonic acid (trioxidation), the formation of cysteine-S-sulfonate (sulfonylation), the formation of a disulfide with other cysteine moieties (+S2R), and the loss of two hydrogen atoms forming an unsaturated cysteine molecule (didehydrogenation) (**Table 3**). Alongside depth in the epidermis, the intensity and number of detected modifications decrease (**Figure 7**). The impact of plasma-derived UV or VUV light was lower than expected from the *in vitro* experiments (**Table 3**). Only nitrosylation was found to be significantly elevated by MgF_2 filtered kINPen irradiation, pointing at a limited role of (V)UV photons *in vivo*.

The conversion of cysteine in cysteine *S*-sulfonate (+SO_3) and dehydrogenated cysteine (-2H) (**Figure 8**), was promoted especially in the third skin epidermis layer, regardless of the applied treatment condition. The results indicate that protein modifications result from complex dynamics and are not corresponding to the action of only one plasma components produced in specific conditions.

Some modifications appear in special conditions only. For example, the conversion of cysteine into cystine was observed in treatment with Ar/O_2 full plasmas, with a maximum in the first layer and a progressive decrease in the second and third. In this condition, the effluent contains significant amounts of singlet oxygen and atomic oxygen, especially at short distances from the nozzle. Atomic oxygen is able to form thyil radicals by hydrogen abstraction to the protein cysteines, which rapidly may recombine forming a disulfide bond. This event causes conformational changes of the protein, alongside a potential gain or loss of function. The oxidation of cysteine into sulfonic acid by the incorporation of three oxygen atoms, and the breakage of the C-S bond with conversion of cysteine to alanine were events observed predominantly in treatments with full argon plasma in the first layer of the skin. When using windows, even in case of the VUV-transmitting MgF_2 and more prominent in suprasil and Borofloat-33 windows, only few such modifications were detected. This indicates that the VUV radiation, although most prominent in Ar plasma, does in soft targets not contribute in the same manner to biomolecule modification than in liquid targets. In this case, the direct impact of argon metastables and other gas phase species and the subsequent formation of secondary reactive species is more prominent. This is in line with a report investigating the oxidation of human skin lipids that showed a limited impact of the argon plasma on lipid side chain oxidation in the absence of water [33]. Obviously, the highly energetic VUV radiation is unable to penetrate deeper into layers of biomolecules such as the model described here or the sebum lipids, limiting its ability to contribute significantly to the plasma chemistry *in situ*.

4 CONCLUSION

In aqueous targets (**Sections 3.2, 3.3**), plasma-derived VUV radiation is an effective component in plasma-liquid chemistry. The liquid phase acts as compartment amplifying the plasma chemistry by the *de novo* formation of secondary water-derived reactive species (e.g., hydroxyl radicals, hydrogen peroxide) at the gas-liquid interphase, that subsequently allow the modification of sensitive targets such as thiol moieties. In contrast, in complex targets like the intact skin the plasma-derived VUV radiation is blocked effectively by the dense biomolecules layers and plays a limited role only. While this might be disappointing from the scientific viewpoint it emphasizes the safety of physical plasmas which has been a significant concern for years. Corroborating a number of reports proofing the safety [69]; [70]; [71], our results further support the safe application of physical plasmas. Even in humid wounds where resident water molecules allow the formation of secondary species by the UV radiation increasing the effectiveness of plasma while the protein layer in the wound bed protects the local tissue.

Proteomics Data

The proteomics data connected to this paper have been uploaded to the ProteomeXchange servers under the project name "Gas plasma and (V)UV impact on porcine epidermis using a tape strip assay approach" (Project accession: PXD028915, username: reviewer_pxd028915@ebi.ac.uk/Password: OPKS8hii).

DATA AVAILABILITY STATEMENT

The datasets presented in this study can be found in online repositories. The names of the repository/repositories and accession number(s) can be found below: ProteomeXchange with accession PXD028915.

AUTHOR CONTRIBUTIONS

GB, KW, and TvW devised the experiments, wrote an corrected the manuscript HM and TG performed OES measurements and discussed the data GB, SW, and KW performed mass spectrometry analysis and discussed the data/incorporated it into the manuscript.

FUNDING

Funding from the German Federal Ministry of Education and Research (grant number 03Z22DN12 to KW) supported this work.

ACKNOWLEDGMENTS

The authors like to thank Steffen Franke for contributing the VUV spectrometer setup.

SUPPLEMENTARY MATERIAL

The Supplementary Material for this article can be found online at: https://www.frontiersin.org/articles/10.3389/fphy.2021.759005/full#supplementary-material

REFERENCES

1. Weltmann K-D, Von Woedtke T Plasma Medicine-Current State of Research and Medical Application. *Plasma Phys Control Fusion* (2017) 59:014031–41. doi:10.1088/0741-3335/59/1/014031
2. Khlyustova A, Labay C, Machala Z, Ginebra M-P, Canal C Important Parameters in Plasma Jets for the Production of RONS in Liquids for Plasma Medicine: A Brief Review. *Front Chem Sci Eng* (2019) 13:238–52. doi:10.1007/s11705-019-1801-8
3. Von Woedtke T, Schmidt A, Bekeschus S, Wende K, Weltmann K-D Plasma Medicine: A Field of Applied Redox Biology. *In Vivo* (2019) 33:1011–26. doi:10.21873/invivo.11570
4. Stratmann B, Costea T-C, Nolte C, Hiller J, Schmidt J, Reindel J, et al. Effect of Cold Atmospheric Plasma Therapy vs Standard Therapy Placebo on Wound Healing in Patients with Diabetic Foot Ulcers. *JAMA Netw Open* (2020) 3: e2010411. doi:10.1001/jamanetworkopen.2020.10411
5. Zhang W, Hu X, Shen Q, Xing D Mitochondria-specific Drug Release and Reactive Oxygen Species Burst Induced by Polyprodrug Nanoreactors Can Enhance Chemotherapy. *Nat Commun* (2019) 10:1704. doi:10.1038/s41467-019-09566-3
6. Tang ZM, Liu YY, Ni DL, Zhou JJ, Zhang M, Zhao PR, et al. Biodegradable Nanoprodrugs: "Delivering" ROS to Cancer Cells for Molecular Dynamic Therapy. *Adv Mater* (2020) 32:e1904011. doi:10.1002/adma.201904011
7. Agostinis P, Berg K, Cengel KA, Foster TH, Girotti AW, Gollnick SO, et al. Photodynamic Therapy of Cancer: an Update. *CA: A Cancer J Clinicians* (2011) 61:250–81. doi:10.3322/caac.20114
8. Graves DB Mechanisms of Plasma Medicine: Coupling Plasma Physics, Biochemistry, and Biology. *IEEE Trans Radiat Plasma Med Sci* (2017) 1: 281–92. doi:10.1109/trpms.2017.2710880
9. Reuter S, Von Woedtke T, Weltmann KD The kINPen-A Review on Physics and Chemistry of the Atmospheric Pressure Plasma Jet and its Applications. *J Phys D-Applied Phys* (2018) 51. doi:10.1088/1361-6463/aab3ad
10. Gay-Mimbrera J, García MC, Isla-Tejera B, Rodero-Serrano A, García-Nieto AV, Ruano J Clinical and Biological Principles of Cold Atmospheric Plasma Application in Skin Cancer. *Adv Ther* (2016) 33:894–909. doi:10.1007/s12325-016-0338-1
11. Liedtke KR, Bekeschus S, Kaeding A, Hackbarth C, Kuehn J-P, Heidecke C-D, et al. Non-thermal Plasma-Treated Solution Demonstrates Antitumor Activity against Pancreatic Cancer Cells *In Vitro* and *In Vivo*. *Sci Rep* (2017) 7:8319. doi:10.1038/s41598-017-08560-3
12. Liedtke KR, Freund E, Hackbarth C, Heidecke C-D, Partecke L-I, Bekeschus S A Myeloid and Lymphoid Infiltrate in Murine Pancreatic Tumors Exposed to Plasma-Treated Medium. *Clin Plasma Med* (2018) 11:10–7. doi:10.1016/j.cpme.2018.07.001
13. Bekeschus S, Schmidt A, Weltmann K-D, Von Woedtke T The Plasma Jet kINPen - A Powerful Tool for Wound Healing. *Clin Plasma Med* (2016) 4: 19–28. doi:10.1016/j.cpme.2016.01.001
14. Bernhardt T, Semmler ML, Schäfer M, Bekeschus S, Emmert S, Boeckmann L. Plasma Medicine: Applications of Cold Atmospheric Pressure Plasma in Dermatology. *Oxid Med Cel Longev* (2019) 2019:3873928. doi:10.1155/2019/3873928
15. Schmidt A, Von Woedtke T, Vollmar B, Hasse S, Bekeschus S Nrf2 Signaling and Inflammation Are Key Events in Physical Plasma-Spurred Wound Healing. *Theranostics* (2019) 9:1066–84. doi:10.7150/thno.29754
16. Lackmann J-W, Bandow JE Inactivation of Microbes and Macromolecules by Atmospheric-Pressure Plasma Jets. *Appl Microbiol Biotechnol* (2014) 98: 6205–13. doi:10.1007/s00253-014-5781-9
17. Jablonowski H, Hänsch MAC, Dünnbier M, Wende K, Hammer MU, Weltmann K-D, et al. Plasma Jet's Shielding Gas Impact on Bacterial Inactivation. *Biointerphases* (2015) 10:029506. doi:10.1116/1.4916533
18. Matthes R, Jablonowski L, Koban I, Quade A, Hübner N-O, Schlueter R, et al. *In Vitro* treatment of Candida Albicans Biofilms on Denture Base Material with Volume Dielectric Barrier Discharge Plasma (VDBD) Compared with Common Chemical Antiseptics. *Clin Oral Invest* (2015) 19:2319–26. doi:10.1007/s00784-015-1463-y
19. Duske K, Koban I, Kindel E, Schröder K, Nebe B, Holtfreter B, et al. Atmospheric Plasma Enhances Wettability and Cell Spreading on Dental Implant Metals. *J Clin Periodontol* (2012) 39:400–7. doi:10.1111/j.1600-051x.2012.01853.x
20. Jablonowski L, Koban I, Berg MH, Kindel E, Duske K, Schröder K, et al. Elimination of E. Faecalis by a New Non-Thermal Atmospheric Pressure Plasma Handheld Device for Endodontic Treatment. A Preliminary Investigation. *Plasma Process. Polym* (2013) 10:499–505. doi:10.1002/ppap.201200156
21. Duske K, Jablonowski L, Koban I, Matthes R, Holtfreter B, Sckell A, et al. Cold Atmospheric Plasma in Combination with Mechanical Treatment Improves Osteoblast Growth on Biofilm Covered Titanium Discs. *Biomaterials* (2015) 52:327–34. doi:10.1016/j.biomaterials.2015.02.035
22. Hartwig S, Doll C, Voss JO, Hertel M, Preissner S, Raguse JD Treatment of Wound Healing Disorders of Radial Forearm Free Flap Donor Sites Using Cold Atmospheric Plasma: A Proof of Concept. *J Oral Maxillofac Surg* (2017) 75:429–35. doi:10.1016/j.joms.2016.08.011
23. Bruggeman PJ, Kushner MJ, Locke BR, Gardeniers JGE, Graham WG, Graves DB, et al. Plasma-liquid Interactions: a Review and Roadmap. *Plasma Sourc Sci. Technol.* (2016) 25:053002. doi:10.1088/0963-0252/25/5/053002
24. Bruno G, Heusler T, Lackmann J-W, Von Woedtke T, Weltmann K-D, Wende K Cold Physical Plasma-Induced Oxidation of Cysteine Yields Reactive Sulfur Species (RSS). *Clin Plasma Med* (2019) 14:100083. doi:10.1016/j.cpme.2019.100083
25. Brandenburg R Dielectric Barrier Discharges: Progress on Plasma Sources and on the Understanding of Regimes and Single Filaments. *Plasma Sourc Sci. Technol.* (2017) 26:053001. doi:10.1088/1361-6595/aa6426
26. Bruggeman PJ, Iza F, Brandenburg R Foundations of Atmospheric Pressure Non-equilibrium Plasmas. *Plasma Sourc Sci. Technol.* (2017) 26:123002. doi:10.1088/1361-6595/aa97af
27. Takai E, Kitamura T, Kuwabara J, Ikawa S, Yoshizawa S, Shiraki K, et al. Chemical Modification of Amino Acids by Atmospheric-Pressure Cold Plasma in Aqueous Solution. *J Phys D: Appl Phys* (2014) 47:285403. doi:10.1088/0022-3727/47/28/285403
28. Lackmann JW, Baldus S, Steinborn E, Edengeiser E, Kogelheide F, Langklotz S, et al. A Dielectric Barrier Discharge Terminally Inactivates RNase A by Oxidizing Sulfur-Containing Amino Acids and Breaking Structural Disulfide Bonds. *J Phys D-Applied Phys* (2015) 48. doi:10.1088/0022-3727/48/49/494003
29. Verlackt CCW, Van Boxem W, Dewaele D, Lemière F, Sobott F, Benedikt J, et al. Mechanisms of Peptide Oxidation by Hydroxyl Radicals: Insight at the Molecular Scale. *J Phys Chem C* (2017) 121:5787–99. doi:10.1021/acs.jpcc.6b12278
30. Nasri Z, Memari S, Wenske S, Clemen R, Martens U, Delcea M, et al. Singlet Oxygen-Induced Phospholipase A2 Inhibition: a Major Role for Interfacial Tryptophan Dioxidation. *Eur Chem J* (2021) 27(59):14702–10. doi:10.1002/chem.202102306
31. Maheux S, Frache G, Thomann JS, Clément F, Penny C, Belmonte T, et al. Small Unilamellar Liposomes as a Membrane Model for Cell Inactivation by Cold Atmospheric Plasma Treatment. *J Phys D: Appl Phys* (2016) 49:344001. doi:10.1088/0022-3727/49/34/344001
32. Yusupov M, Wende K, Kupsch S, Neyts EC, Reuter S, Bogaerts A Effect of Head Group and Lipid Tail Oxidation in the Cell Membrane Revealed through Integrated Simulations and Experiments. *Sci Rep* (2017) 7:5761. doi:10.1038/s41598-017-06412-8
33. Striesow J, Lackmann J-W, Ni Z, Wenske S, Weltmann K-D, Fedorova M, et al. Oxidative Modification of Skin Lipids by Cold Atmospheric Plasma (CAP): A Standardizable Approach Using RP-LC/MS2 and DI-ESI/MS2. *Chem Phys Lipids* (2020) 226:104786. doi:10.1016/j.chemphyslip.2019.104786
34. Schmidt A, Bekeschus S Redox for Repair: Cold Physical Plasmas and Nrf2 Signaling Promoting Wound Healing. *Antioxidants (Basel)* (2018) 7. doi:10.3390/antiox7100146
35. Muzumdar S, Hiebert H, Haertel E, Ben-Yehuda Greenwald M, Bloch W, Werner S, et al. Nrf2-Mediated Expansion of Pilosebaceous Cells Accelerates Cutaneous Wound Healing. *Am J Pathol* (2019) 189:568–79. doi:10.1016/j.ajpath.2018.11.017
36. Schmidt A, Bekeschus S, Jarick K, Hasse S, Von Woedtke T, Wende K. Cold Physical Plasma Modulates P53 and Mitogen-Activated Protein Kinase Signaling in Keratinocytes. *Oxid Med Cel Longev* (2019) 2019:7017363. doi:10.1155/2019/7017363

37. Jablonowski H, Bussiahn R, Hammer MU, Weltmann K-D, Von Woedtke T, Reuter S Impact of Plasma Jet Vacuum Ultraviolet Radiation on Reactive Oxygen Species Generation in Bio-Relevant Liquids. *Phys Plasmas* (2015) 22: 122008. doi:10.1063/1.4934989
38. Laroussi M, Dobbs FC, Wei Z, Doblin MA, Ball LG, Moreira KR, et al. Decontamination of Water by Excimer UV Radiation. *IEEE Trans Plasma Sci* (2002) 30:1501–3. doi:10.1109/tps.2002.804208
39. Brandenburg R, Lange H, Von Woedtke T, Stieber M, Kindel E, Ehlbeck J, et al. Antimicrobial Effects of UV and VUV Radiation of Nonthermal Plasma Jets. *IEEE Trans Plasma Sci* (2009) 37:877–83. doi:10.1109/tps.2009.2019657
40. Schneider S, Lackmann J-W, Ellerweg D, Denis B, Narberhaus F, Bandow JE, et al. The Role of VUV Radiation in the Inactivation of Bacteria with an Atmospheric Pressure Plasma Jet. *Plasma Process. Polym* (2012) 9:561–8. doi:10.1002/ppap.201100102
41. Judée F, Wattieaux G, Merbahi N, Mansour M, Castanié-Cornet MP The Antibacterial Activity of a Microwave Argon Plasma Jet at Atmospheric Pressure Relies Mainly on UV-C Radiations. *J Phys D: Appl Phys* (2014) 47:405201. doi:10.1088/0022-3727/47/40/405201
42. Lange H, Foest R, Schafer J, Weltmann K-D Vacuum UV Radiation of a Plasma Jet Operated with Rare Gases at Atmospheric Pressure. *IEEE Trans Plasma Sci* (2009) 37:859–65. doi:10.1109/tps.2009.2019982
43. Bahre H, Lange H, Schulz-Von Der Gathen V, Foest R. Vacuum Ultraviolet (VUV) Emission of an Atmospheric Pressure Plasma Jet (M-APPJ) Operated in Helium-Oxygen Mixtures in Ambient Air. *Acta Technica* (2011) 56.
44. Yurkova I, Shadyro O, Kisel M, Brede O, Arnhold J Radiation-induced Free-Radical Transformation of Phospholipids: MALDI-TOF MS Study. *Chem Phys Lipids* (2004) 132:235–46. doi:10.1016/j.chemphyslip.2004.08.006
45. Corre I, Niaudet C, Paris F Plasma Membrane Signaling Induced by Ionizing Radiation. *Mutat Research/Reviews Mutat Res* (2010) 704:61–7. doi:10.1016/j.mrrev.2010.01.014
46. Rastogi RP, RichaKumar A, Kumar A, Tyagi MB, Sinha RP. Molecular Mechanisms of Ultraviolet Radiation-Induced DNA Damage and Repair. *J Nucleic Acids* (2010) 2010:592980. doi:10.4061/2010/592980
47. Islam MT Radiation Interactions with Biological Systems. *Int J Radiat Biol* (2017) 93:487–93. doi:10.1080/09553002.2017.1286050
48. Lalande M, Schwob L, Vizcaino V, Chirot F, Dugourd P, Schlathölter T, et al. Direct Radiation Effects on the Structure and Stability of Collagen and Other Proteins. *Chembiochem* (2019) 20:2972–80. doi:10.1002/cbic.201900202
49. Mikkelsen RB, Wardman P Biological Chemistry of Reactive Oxygen and Nitrogen and Radiation-Induced Signal Transduction Mechanisms. *Oncogene* (2003) 22:5734–54. doi:10.1038/sj.onc.1206663
50. Pattison DI, Davies MJ *Actions of Ultraviolet Light on Cellular Structures*. Birkhaeuser, Basel: EXS (2006). p. 131–57.
51. Pattison DI, Rahmanto AS, Davies MJ Photo-oxidation of Proteins. *Photochem Photobiol Sci* (2012) 11:38–53. doi:10.1039/c1pp05164d
52. Von Woedtke T, Jülich W-D, Thal S, Diederich M, Stieber M, Kindel E Antimicrobial Efficacy and Potential Application of a Newly Developed Plasma-Based Ultraviolet Irradiation Facility. *J Hosp Infect* (2003) 55: 204–11. doi:10.1016/s0195-6701(03)00290-1
53. Laroussi M, Leipold F Evaluation of the Roles of Reactive Species, Heat, and UV Radiation in the Inactivation of Bacterial Cells by Air Plasmas at Atmospheric Pressure. *Int J Mass Spectrom* (2004) 233:81–6. doi:10.1016/j.ijms.2003.11.016
54. Lackmann J-W, Bruno G, Jablonowski H, Kogelheide F, Offerhaus B, Held J, et al. Nitrosylation vs. Oxidation - How to Modulate Cold Physical Plasmas for Biological Applications. *PLoS One* (2019) 14:e0216606. doi:10.1371/journal.pone.0216606
55. Wende K, Bruno G, Lalk M, Weltmann K-D, Von Woedtke T, Bekeschus S, et al. On a Heavy Path - Determining Cold Plasma-Derived Short-Lived Species Chemistry Using Isotopic Labelling. *RSC Adv* (2020) 10:11598–607. doi:10.1039/c9ra08745a
56. Sremački I, Bruno G, Jablonowski H, Leys C, Nikiforov AY, Wende K Influence of Aerosol Injection on the Liquid Chemistry Induced by an RF Argon Plasma Jet. *Plasma Sources Sci. Technol.* (2021) 30(9). doi:10.1088/1361-6595/abe176
57. Pikal-Cleland KA, Cleland JL, Anchordoquy TJ, Carpenter JF. Effect of glycine on pH Changes and Protein Stability during Freeze-Thawing in Phosphate Buffer Systems. *J Pharm Sci* (2002) 91:1969–79. doi:10.1002/jps.10184
58. Jacobi U, Kaiser M, Toll R, Mangelsdorf S, Audring H, Otberg N, et al. Porcine Ear Skin: an *In Vitro* Model for Human Skin. *Skin Res Technol* (2007) 13: 19–24. doi:10.1111/j.1600-0846.2006.00179.x
59. Myers B, Ranieri P, Smirnova T, Hewitt P, Peterson D, Quesada MH, et al. Measuring Plasma-Generated center Dot OH and O Atoms in Liquid Using EPR Spectroscopy and the Non-selectivity of the HTA Assay. *J Phys D-Applied Phys* (2021) 54. doi:10.1088/1361-6463/abd9a6
60. Shen X, Kolluru GK, Yuan S, Kevil CG Measurement of H2S *In Vivo* and *In Vitro* by the Monobromobimane Method. *Methods Enzymol* (2015) 554:31–45. doi:10.1016/bs.mie.2014.11.039
61. Foest R, Kindel E, Lange H, Ohl A, Stieber M, Weltmann K-D RF Capillary Jet - a Tool for Localized Surface Treatment. *Contrib Plasma Phys* (2007) 47: 119–28. doi:10.1002/ctpp.200710017
62. Reuter S, Winter J, Schmidt-Bleker A, Schroeder D, Lange H, Knake N, et al. Atomic Oxygen in a Cold Argon Plasma Jet: TALIF Spectroscopy in Ambient Air with Modelling and Measurements of Ambient Species Diffusion. *Plasma Sourc Sci Tech* (2012) 21:024005.%&
63. Abedinzadeh Z, Gardes-Albert M, Ferradini C Kinetic Study of the Oxidation Mechanism of Glutathione by Hydrogen Peroxide in Neutral Aqueous Medium. *Can J Chem* (1989) 67:1247–55. doi:10.1139/v89-190
64. Luo D, Smith SW, Anderson BD Kinetics and Mechanism of the Reaction of Cysteine and Hydrogen Peroxide in Aqueous Solution. *J Pharm Sci* (2005) 94: 304–16. doi:10.1002/jps.20253
65. Enescu M, Cardey B Mechanism of Cysteine Oxidation by a Hydroxyl Radical: a Theoretical Study. *Chem Eur J Chem Phys* (2006) 7:912–9. doi:10.1002/cphc.200500585
66. Gupta V, Carroll KS Sulfenic Acid Chemistry, Detection and Cellular Lifetime. *Biochim Biophys Acta (Bba) - Gen Subjects* (2014) 1840:847–75. doi:10.1016/j.bbagen.2013.05.040
67. Chauvin J-PR, Pratt DA On the Reactions of Thiols, Sulfenic Acids, and Sulfinic Acids with Hydrogen Peroxide. *Angew Chem Int Ed* (2017) 56:6255–9. doi:10.1002/anie.201610402
68. Stans MH *Bond Dissociation Energies in Simple Molecules*NIST Special Publication 1 %6, 58 %& (1970).
69. Wende K, Bekeschus S, Schmidt A, Jatsch L, Hasse S, Weltmann KD, et al. Risk Assessment of a Cold Argon Plasma Jet in Respect to its Mutagenicity. *Mutat Research/Genetic Toxicol Environ Mutagenesis* (2016) 798-799:48–54. doi:10.1016/j.mrgentox.2016.02.003
70. Schmidt A, Woedtke TV, Stenzel J, Lindner T, Polei S, Vollmar B, et al. One Year Follow-Up Risk Assessment in SKH-1 Mice and Wounds Treated with an Argon Plasma Jet. *Int J Mol Sci* (2017) 18. doi:10.3390/ijms18040868
71. Bekeschus S, Schmidt A, Kramer A, Metelmann H-R, Adler F, Von Woedtke T, et al. High Throughput Image Cytometry Micronucleus Assay to Investigate the Presence or Absence of Mutagenic Effects of Cold Physical Plasma. *Environ Mol Mutagen* (2018) 59:268–77. doi:10.1002/em.22172
72. Linxiang L, Abe Y, Nagasawa Y, Kudo R, Usui N, Imai K, et al. An HPLC Assay of Hydroxyl Radicals by the Hydroxylation Reaction of Terephthalic Acid. *Biomed Chromatogr* (2004) 18:470–4. doi:10.1002/bmc.339

Conflict of Interest: The authors declare that the research was conducted in the absence of any commercial or financial relationships that could be construed as a potential conflict of interest.

Frontiers in Physics

Investigates complex questions in physics to understand the nature of the physical world

Addresses the biggest questions in physics, from macro to micro, and from theoretical to experimental and applied physics.

Discover the latest Research Topics

See more →

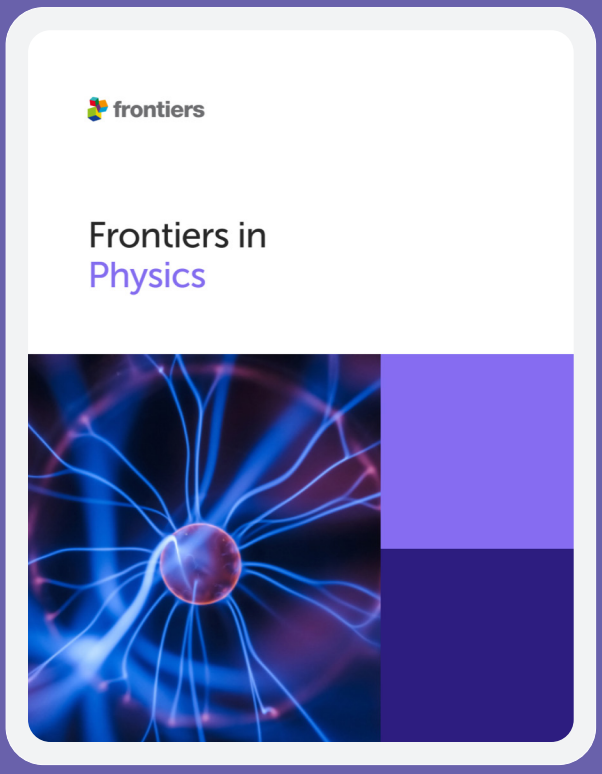

Frontiers

Avenue du Tribunal-Fédéral 34
1005 Lausanne, Switzerland
frontiersin.org

Contact us

+41 (0)21 510 17 00
frontiersin.org/about/contact